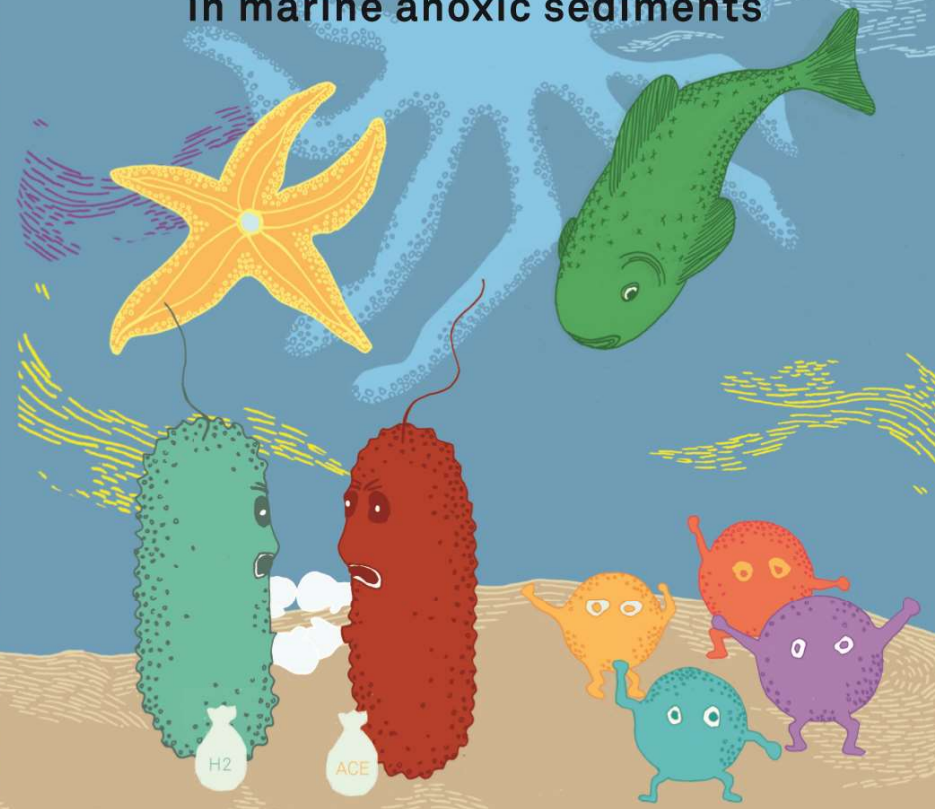


Ecophysiology of sulfate-reducing bacteria and syntrophic communities in marine anoxic sediments

Ecophysiology of sulfate-reducing bacteria and syntrophic communities in marine anoxic sediments

Derya Özüölmez, 2017



Derya Özüölmez

Propositions

1. Prolonged incubation is a key strategy toward the enrichment of marine syntrophs.
(this thesis)
2. Hydrogen-consuming methanogens can effectively compete with hydrogen-consuming sulfate reducers even at high sulfate concentration.
(this thesis)
3. The plastic-eating wax worm, *Galleria mellonella*, can help cleaning up existing plastic mass (Bombelli et al. 2017, Current Biology 27(8): 292-293), but the real solution to environmental pollution still relies on shifting from disposable plastics to reusable and biodegradable materials.
4. With the discovery of abundant molecular hydrogen in Enceladus' salty ocean (Waite et al. (2017) Science 356:6334, 155-159) extraterrestrial life in our solar system has become highly probable, and should shift our life-hunting focus from distant stars to our nearby neighbors.
5. With the "Help me to do it myself" motto, the Montessori education leads children to grow into mature, creative and self-confident adults.
6. Nothing is impossible as long as the dream is held close to the heart and patience and persistence are applied for the accomplishment.

Propositions belonging to the PhD thesis entitled:

"Ecophysiology of sulfate-reducing bacteria and syntrophic communities in marine anoxic sediments"

Derya Özüölmez

Wageningen, 12 September 2017

Ecophysiology of sulfate-reducing bacteria and syntrophic communities in marine anoxic sediments

Derya Özüölmez

Thesis committee

Promotor

Prof. Dr Alfons J.M. Stams
Personal chair at the Laboratory of Microbiology
Wageningen University & Research

Co-promotor

Dr Caroline M. Plugge
Associate professor, Laboratory of Microbiology
Wageningen University & Research

Other members

Prof. Dr Tinka Murk, Wageningen University & Research
Prof. Dr Gerard Muyzer, University of Amsterdam, The Netherlands
Prof. Dr Stefan Schouten, Utrecht University and Netherlands Institute for Sea Research,
Texel, The Netherlands
Dr Verona Vandieken, University of Oldenburg, Germany

This research was conducted under the auspices of the Graduate School for SocioEconomic and Natural Sciences of the Environment (SENSE).

Ecophysiology of sulfate-reducing bacteria and syntrophic communities in marine anoxic sediments

Derya Özüölmez

Thesis

submitted in fulfilment of the requirements for the degree of doctor

at Wageningen University

by the authority of the Rector Magnificus,

Prof. Dr A.P.J. Mol,

in the presence of the

Thesis Committee appointed by the Academic Board

to be defended in public

on Tuesday 12 September 2017

at 4 p.m. in the Aula.

Derya Özüölmez

Ecophysiology of sulfate-reducing bacteria and syntrophic communities in marine anoxic sediments,

231 pages.

PhD thesis, Wageningen University, Wageningen, the Netherlands (2017)

With references, with summary in English and Dutch

ISBN: 978-94-6343-654-0

DOI: 10.18174/420757

Table of Contents

Chapter 1	General Introduction	1
Chapter 2	Methanogenic archaea and sulfate reducing bacteria co-cultured on acetate: teamwork or coexistence?	19
Chapter 3	Butyrate degradation by sulfate-reducing and methanogenic communities in anoxic sediments of Aarhus Bay, Denmark	45
Chapter 4	Propionate conversion under sulfidogenic and methanogenic conditions in different biogeochemical zones of Aarhus Bay, Denmark	85
Chapter 5	Membrane lipid composition in enrichments from the sulfate and methane zones of Aarhus Bay, Denmark	119
Chapter 6	Physiological and molecular characterization of anaerobic marine propionate- and butyrate-converting syntrophic cultures	139
Chapter 7	General Discussion	167
Appendices		182
	References	184
	Summary	212
	Samenvatting	214
	Author affiliations	217
	Acknowledgements	218
	About the author	221
	List of publications	222
	SENSE Diploma	223

Chapter 1

General Introduction

Derya Özüölmez

1.1 Global carbon cycle

Carbon is the major element of all life forms, and it is actively cycled in the biosphere. The carbon cycle reflects the flow and exchange of carbon among living organisms and the environment through a series of chemical, physical and biological reactions (Figure 1). Inorganic carbon that is formed from organic matter or weathered from limestone enters the atmosphere as CO_2 or in aquatic environments mostly as HCO_3^- . Atmospheric CO_2 is in equilibrium with the carbonate system of the oceans (Takahashi *et al.*, 1997; Fasham *et al.*, 2001). Atmospheric CO_2 or $\text{CO}_2/\text{HCO}_3^-$ in the oceans or lakes can be fixed by autotrophic or photolithotrophic organisms (e.g. plants, phytoplankton and marine algae) to synthesize organic carbon. By decay of these organisms, organic carbon is converted back to inorganic carbon through hydrolysis, fermentation and mineralization by the combined action of different organisms (Canfield, 1993; Kristensen and Holmer, 2001).

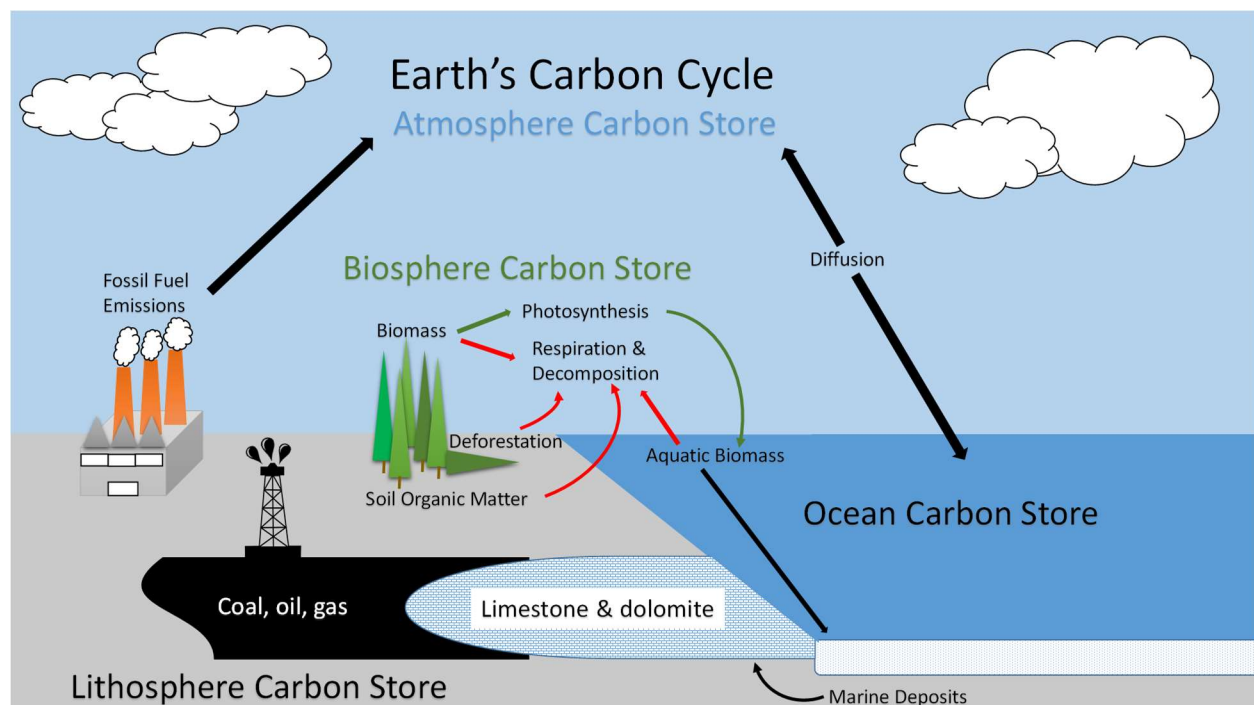


Figure 1. Global carbon cycle. Figure is adapted from Pidwirny, 2012.

Carbon is stored in our planet (a) as living and dead biomass in the biosphere; (b) as carbon dioxide gas in the atmosphere, (c) as organic matter in soils and sediments, (d) in the lithosphere as fossil fuels like coal, oil, and natural gas, and as carbonate-based sedimentary rock deposits such as limestone and dolomite; and (e) in the oceans as dissolved atmospheric carbon dioxide and as

calcium carbonate shells in marine organisms (Figure 1) (Pidwirny, 2012). The majority of the carbon is fixed as inorganic carbon in limestone or in fossil organic pools, largely as CO_2 , whereas organic carbon represents only about 0.1% of the total carbon cycles through the active pool on Earth (Harvey, 2006). Soils represent the largest pool within this active cycle. This is followed by land biota, dissolved organic matter in seawater, and surficial marine sediments with decreasing amounts of organic matter. The smallest fraction includes marine biota and particulate pools (Harvey, 2006). Although the particulate organic carbon reservoir is small, it is dynamic and plays a central role in both amount and composition of organic matter which reaches underlying sediments (Harvey, 2006).

1.2 Degradation of organic matter in marine sediments

Coastal marine ecosystems receive regular inputs of organic matter and nutrients from primary production of phytoplankton, rivers, coastal erosion, and the atmosphere (Jørgensen, 1982). Mineralization of the particulate organic matter starts already in the water column. On the other hand, the organic matter that is not decomposed in the water column rapidly sinks down to the sediment in coastal shelf sediments and part of it gets buried in the sediment (Jørgensen, 1983). It is shown that 10 – 50 % of carbon from primary production was deposited on the bottom in coastal shelf sediments (0-200 m depth), whereas this fraction decreases to about 1% in pelagic sediments (5000-6000 m) (Jørgensen, 1983). The coastal shelves comprise 8.6% of the total area of the oceans, and it is estimated that 83% of the mineralization in the sea bottom takes place in these shelf areas (Jørgensen, 1983). This reflects the importance of coastal and shelf areas in the carbon cycle.

High microbial activity in the upper sediment layers leads the formation of distinct biogeochemical zones. The depth range of each zone varies strongly depending on the supply of organic matter from overlying seawater and the sedimentation rate which have an effect on accumulation of organic matter (Jørgensen, 1983). In coastal marine sediments, the oxic surface layer constitutes a thin layer due to the rapid consumption of oxygen for aerobic mineralization. Therefore, the remaining organic matter will be degraded by anaerobic microbes and part of it will be buried in the sediment where mineralization continues albeit slow. In the anoxic part of the sediment, nitrate, manganese, iron, sulfate and carbon dioxide serve as terminal electron acceptors for the mineralization processes (Figure 2). The depth sequence of electron acceptors reflects a gradual decrease in redox potential and thus a decrease in the free energy available by respiration.

It is estimated that 25-50% of the organic carbon is mineralized through sulfate reduction, which makes sulfate an important electron acceptor in anoxic part of the sediments (Jørgensen, 1982).

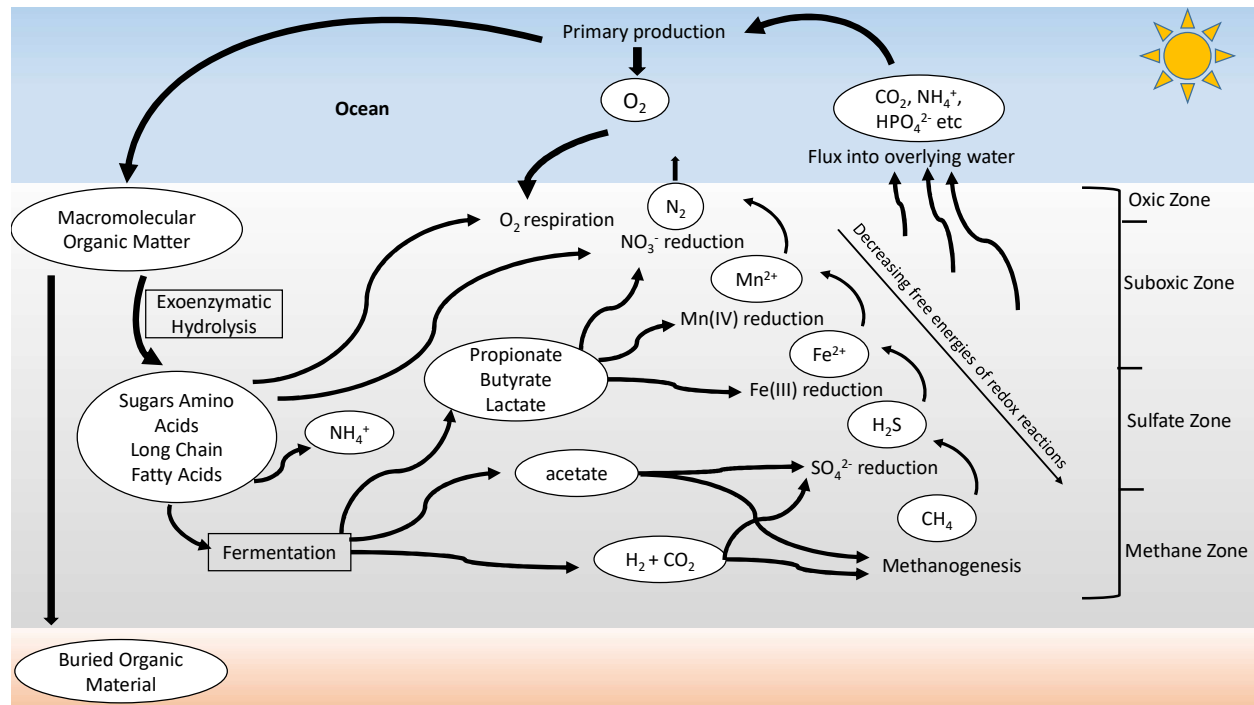


Figure 2. Organic carbon degradation pathways in marine sediments and their relation to the biological redox zonation. Figure is adapted from Parkes et al., 2014 and Jørgensen, 2006.

Anaerobic degradation of organic matter in marine sediments is a complex sequential process in which a variety of physiologically different microorganisms takes part. The first step is an extracellular hydrolysis of polymers (polysaccharides, proteins, nucleic acids and lipids) (Fig 2, Fig 3). Primary fermenting bacteria ferment the monomers and oligomers to fatty acids, branched-chain fatty acids, alcohols, aromatic acids, H_2 and CO_2 . Some of these fermentation products, such as acetate, H_2 , CO_2 , and other one-carbon compounds, can be converted directly to methane and carbon dioxide by methanogens. In methanogenic environments, secondary fermenters or proton reducers convert alcohols, long-chain, branched-chain and aromatic fatty acids to acetate, formate, H_2 and CO_2 which are then used by the methanogens (Figure 3b) (Schink and Stams, 2013). The conversion of polymers in sulfate-rich anoxic habitats such as marine sediments is slightly different. Polymers are degraded by primary fermenting bacteria and fermentation products are formed. Different from methanogens, sulfate-reducing bacteria can use all products of primary fermentations, and oxidize them to carbon dioxide, while reducing sulfate to sulfide (Figure 3a) (Widdel 1988).

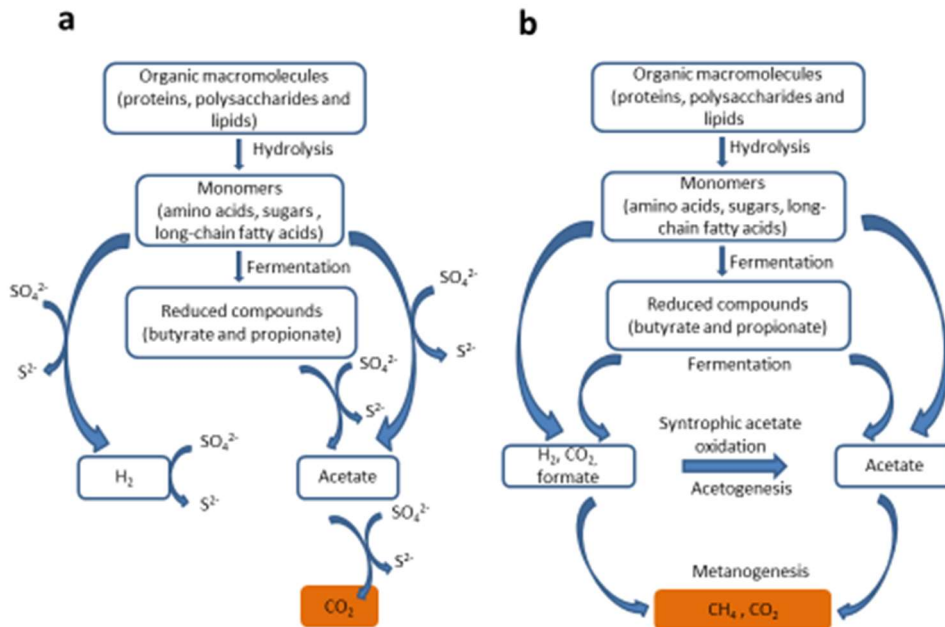


Figure 3. Mineralization of organic matter in the presence (a) and absence (b) of sulfate in anoxic marine sediments. Figure is adapted from Muyzer and Stams, 2008.

Sulfate reduction and methanogenesis are the terminal steps in the degradation process (Jørgensen, 1982; Schink and Stams, 2013; Muyzer and Stams, 2008; Stams and Plugge, 2009). They are thought to be mutually exclusive in most environmental settings and controlled mainly by the amount of available sulfate (Reeburgh and Heggie, 1977; Winfrey and Zeikus, 1977).

1.3 Microbial interactions shaping biogeochemical zonation

Previous studies on marine sediments have explained the biological redox zonation by competition among different physiological groups (Martens and Berner 1974; Lovley and Goodwin 1988; Chapelle and Lovley 1992; Hoehler et al., 1998). Accordingly, methanogenesis and sulfate reduction were suggested to be temporally or spatially separated (Cappenberg, 1974; Mountfort and Asher, 1979) and methanogenesis is typically dominant in deeper sulfate-depleted sediment parts that are below the active sulfate reduction zone. Thus, when different physiological groups compete for a common substrate, the microbes using the energetically most favorable electron acceptor available will outcompete the ones using energetically less favorable electron acceptors. For instance, methanogenic *Archaea* do not utilize large organic molecules but can use only a narrow spectrum of substrates. Most methanogens produce methane either by reducing CO_2 , with H_2 as the primary

electron donor, or by cleaving acetate. However, sulfate reducers outcompete methanogens for the common substrates, H_2 and acetate, due to their higher affinity and lower threshold values for these substrates (Stams, 1994; Hoehler et al., 1998; Muyzer and Stams, 2008) (Table 1). Consequently, significant methane generation in marine sediments occurs at deeper sediment zones, after almost all sulfate has been reduced to sulfide (Jørgensen and Kasten, 2006). The third substrate group for methanogens includes methylated compounds such as methanol, methylated amines (mono-, di-, and trimethylamine, and tetramethylammonium), and methylated sulfides (e.g., dimethyl sulfide and methanethiol). These compounds are known as non-competitive substrates since they are not commonly utilized by sulfate reducers, but mainly by methylotrophic methanogens (Liu and Whitman, 2008). The consumption of non-competitive substrates by methanogens allow simultaneous methanogenesis and sulfate reduction within sulfate containing anoxic sediments, as demonstrated in several investigations (Oremland and Taylor, 1978; Oremland and Polcin, 1982; Oremland et al., 1982a, 1982b, 1987; Kiene et al., 1986; Oremland et al., 1988; Wang and Lee, 1995). On the other hand, methanogenesis from H_2 and acetate was also observed within the sulfate zones (Wellsbury et al., 2002; Parkes et al., 2005). Therefore, there is no distinct separation of sulfate reducers and methanogens along the sediment, and the absence of methane in sulfate zones might indicate the occurrence of active anaerobic oxidation of methane (AOM) (Parkes et al., 2014).

The sulfate-methane transition zone (SMTZ) corresponds to the sedimentary interval characterized by a mutual depletion of methane and sulfate due to the microbial anaerobic oxidation of methane (Sultan et al., 2016; Iversen and Jørgensen, 1985). Previously, it was postulated that sulfate and methane profiles at this specific part of the sediment were formed due to competition of sulfate reducers and methanogens for common substrates (Martens and Berner, 1974). After several studies, however, it was demonstrated that methane, which diffuses upwards from the deeper sediment, is oxidized by anaerobic methanotrophic archaea (ANME) coupled to sulfate reduction (Barnes and Goldberg, 1976; Martens and Berner, 1977; Murray et al., 1978; Reeburgh, 1980; Alperin et al., 1988; Hinrichs et al., 1999; Krüger et al. 2003; Nauhaus et al. 2005). Later, *in vitro* studies showed that AOM and sulfate reduction are directly coupled and this is a syntrophic processes involving ANME and SRB that are metabolically interdependent on each other (Nauhaus et al., 2002; Nauhaus et al., 2005). The depth of the transition zone varies depending on the organic matter supply, the depth of the methane production zone, and the transport and consumption rates of methane and sulfate (Claypool and Kvenvolden, 1983; Borowski et al., 1999; Claypool, 2004; Jørgensen and Kasten, 2006; Knittel and Boetius, 2009).

1.4 Syntrophy

Methanogenic degradation of organic matter in sulfate-depleted marine sediments is carried out by the cooperation of physiologically different microorganisms. This relationship is called 'syntrophy' and involves the consumption of degradation end products, usually hydrogen, formate and acetate, by the partner organisms. Syntrophic bacteria perform secondary fermentation of small organic molecules such as lactate, propionate, butyrate and produce acetate, formate, H_2 and CO_2 (Morris et al., 2013; Schink and Stams, 2013). However, these reactions are endergonic under standard conditions and thus not possible unless a H_2 /formate scavenging partner organism keeps the concentration of these intermediates low (Schink and Stams, 2013). Hydrogenotrophic methanogens act as syntrophic partners of syntrophs by utilizing H_2 and formate to form CH_4 (Morris et al., 2013; Sieber et al., 2014) (Figure 4). This anaerobic metabolism, especially when methanogenesis is the terminal electron accepting process, involves consortia with tightly coupled syntrophic partnerships (Schink and Stams, 2013; McNerney et al., 2008). Syntrophic interactions are not restricted to the methanogenic environments but also occur in sulfate-reducing environments as evidenced by sulfate-reducing consortia involved in anaerobic oxidation of methane (AOM) (Nauhaus et al., 2005) (Figure 4).

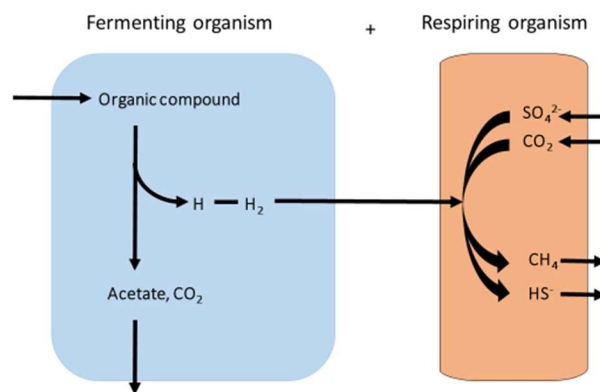


Figure 4. Schematic diagram of interspecies hydrogen transfer between fermenting and respiring organism.

It has also been demonstrated that syntrophic consortia of acetogens and hydrogen-/formate-consuming sulfate reducers catalyze propionate and butyrate degradation in sulfate-reducing environments (Stams et al., 2005; Elferink et al., 1998; Visser et al., 1993). It is not surprising that hydrogen-/formate-consuming sulfate reducers are commonly used as the syntrophic partner to

isolate syntrophic propionate- and butyrate-converting microorganisms in co-cultures (Dong et al., 1994; Boone and Bryant, 1980; McInerney et al., 1979).

Interspecies electron transfer plays a key role in the functioning of methanogenic microbial communities, which have a significant impact on the global carbon cycle (Stams and Plugge, 2009; Sieber et al., 2012). Therefore, it is crucial to study the syntrophic cooperations to understand methanogenic conversions in different environments (McInerney et al., 2008). The most difficult step in the methanogenic degradation is the second fermentation step in which short-chain fatty acids such as propionate and butyrate are converted. The oxidation of propionate and butyrate to H_2 , formate and acetate are endergonic reactions under standard conditions (P_{H_2} of 1 atm, substrate and product concentrations of 1 M, temperature 298°K, pH 7) (Table 1).

Table 1. Equations and standard free energy changes for acetate and hydrogen producing and methanogenic reactions at standard conditions (at 1 M, pH 7.0, 1 atm and $T = 25^\circ\text{C}$). ΔG° values taken from Thauer et al., 1977.

Equation		ΔG° (kJ/reaction)
Sulfate-reducing reactions		
Butyrate ⁻ + 0.5 SO ₄ ²⁻	→ 2 Acetate ⁻ + 0.5 HS ⁻ + 0.5 H ⁺	-27.8
Propionate ⁻ + 0.75	→ Acetate ⁻ + 0.75 HS ⁻ + HCO ₃ ⁻ + 0.25 H ⁺	-37.8
Acetate ⁻ + SO ₄ ²⁻	→ 2 HCO ₃ ⁻ + HS ⁻	-47.6
4 H ₂ + SO ₄ ²⁻ + H ⁺	→ HS ⁻ + 4 H ₂ O	-151.9
Formate ⁻ + SO ₄ ²⁻ + H ⁺	→ 4 HCO ₃ ⁻ + HS ⁻	-146.7
Hydrogen-producing reactions		
Propionate ⁻ + 2 H ₂ O	→ Acetate ⁻ + CO ₂ + 3 H ₂	+76.0
Propionate ⁻ + 2 H ₂ O + 2 CO ₂	→ Acetate ⁻ + 3 HCOO ⁻ + 3 H ⁺	+65.3
Butyrate ⁻ + 2 H ₂ O	→ 2 Acetate ⁻ + H ⁺ + 2 H ₂	+48.3
Butyrate ⁻ + 2 H ₂ O + 2 CO ₂	→ 2 Acetate ⁻ + 2 HCOO ⁻ + 2 H ⁺	+38.5
Acetate ⁻ + 4 H ₂ O	→ 4 H ₂ + 2 HCO ₃ ⁻ + H ⁺	+104.6
Formate ⁻ + H ₂ O	→ HCO ₃ ⁻ + H ₂	+1.3
Methanogenic reactions		
4 H ₂ + HCO ₃ ⁻ + H ⁺	→ CH ₄ + 3 H ₂ O	-135.6
Acetate ⁻ + H ₂ O	→ CH ₄ + HCO ₃ ⁻	-31.0
Formate ⁻ + H ⁺ + 3 H ₂	→ CH ₄ + 2 H ₂ O	-134.3

1.5 Syntrophic butyrate conversion

All known syntrophic butyrate-degrading bacteria belong to the phyla *Firmicutes* and *Proteobacteria* (Table 2). Besides oxidation of saturated fatty acids in coculture with methanogens, most butyrate degraders can grow axenically only by fermenting unsaturated fatty acids such as

crotonate (Schink, 1997). Butyrate degraders use the beta-oxidation pathway to oxidize butyrate (Schink, 1997) (Figure 5A). Thermodynamically the most difficult step in butyrate oxidation is the oxidation of butyryl-CoA to crotonyl-CoA. Hydrogen (at 1 Pa H_2) and formate (at 1 mM formate) (the minimum level that can be maintained by methanogens) production from electrons generated in the oxidation of butyryl-CoA to crotonyl-CoA is endergonic. Therefore, a process called 'reversed electron transport' is required to use part of the gained ATP to drive these redox reactions (Sieber et al., 2012; McInerney et al., 2009). Genomic analysis indicates that several different gene clusters are involved in syntrophic reverse electron transfer (Sieber et al., 2012). Müller et al. (2009) partially purified an NADH:acceptor oxidoreductase from syntrophically grown *S. wolfei* cells and proposed that this enzyme complex is homologue of the *Thermotoga maritima* bifurcating [FeFe]-hydrogenase and are involved in the thermodynamically favorable production of hydrogen from reduced ferredoxin to drive the unfavorable production of hydrogen from NADH by a process called electron confurcation (Müller et al. 2010; Schut and Adams, 2009). Since this enzyme complex has subunits predicted to function as an NADH-linked formate dehydrogenase and an NADH-linked hydrogenase, interspecies electron transfer may occur via either hydrogen and/or formate, depending on the environmental conditions (Müller et al. 2009; Müller et al. 2010). However, it needs to be verified if the hydrogenase acts in a bifurcating manner as observed in *T. maritima*. A possible mechanism for reverse electron transfer is electron bifurcation by butyryl-CoA dehydrogenase:electron transfer flavoprotein (bcd/etfAB) complex of *Clostridium kluyveri* (Li et al., 2008). *Syntrophomonas wolfei* has a gene cluster homologous to the bcd/etfAB complex from *C. kluyveri* (Sieber et al., 2010). Previous studies showed that bifurcation of electrons from NADH with crotonyl-CoA and oxidized ferredoxin by the bcd/etfAB complex of *C. kluyveri* is not involved in butyrate oxidation by *S. wolfei*, as Bcd of *S. wolfei* is not associated with etfAB (Sieber et al., 2012; Müller et al. 2010; Müller et al. 2009). Ion gradients can also drive the reverse electron transfer during syntrophic metabolism (McInerney et al., 2009). The ferredoxin:NAD⁺ oxidoreductase may function as a reverse electron transfer complex, using the ion gradient to drive the unfavorable reduction of ferredoxin with NADH (Sieber et al., 2012). The genome of *S. wolfei* contains a gene for a membrane-bound iron-sulfur (FeS) oxidoreductase that is adjacent to the two genes for electron transfer flavoprotein (etfAB) (Callaghan et al., 2011; Sieber et al., 2010; McInerney et al., 2007). The FeS complex could funnel electrons from β -oxidation to membrane redox carriers (Sieber et al., 2010; McInerney et al., 2007).

Table 2. Butyrate and propionate degrading syntrophs and the substrates that they utilize in pure culture and in syntrophic cultures. Adapted from Schink and Stams, 2013 and Sieber et al., 2012.

Organism	pH range	Temperature range (°C)	Substrates used		Phylogenetic affiliation	References
			Pure culture	Syntrophic coculture		
Butyrate degraders						
<i>Syntrophomonas wolfei</i>	ND	35-37	Crotonate	C4-C8 ^a	Firmicutes	McInerney et al. (1979, 1981)
<i>Syntrophomonas sapovorans</i>	6.3-8.1	25-45	None	C4-C18	Firmicutes	Roy et al. (1986)
<i>Syntrophomonas</i> (<i>Syntrophospora</i>) <i>bryantii</i>	6.5–7.5	28-34	Crotonate	C4–C11, 2-methyl valerate	Firmicutes	Stieb and Schink (1985); Zhao et al. (1989)
<i>Syntrophomonas curvata</i>	6.3–8.4	20–42	Crotonate	C4–C18, C18:1	Firmicutes	Zhang et al. (2004)
<i>Syntrophomonas erecta</i>	6.0-8.8	25-47	Crotonate	C4-C8	Firmicutes	Zhang et al. (2005)
<i>Syntrophomonas zehnderi</i>	7.0	25-40	None	C4-C18, C16:1, C18:1, C18:2	Firmicutes	Sousa et al. (2007a)
<i>Thermosyntropha lipolytica</i>	7.15-9.5	52-70	Crotonate, yeast extract, tryptone, casamino acids, betaine, pyruvate, ribose, xylose	C4–C18, C18:1, C18:2; triglycerides	Firmicutes	Svetlitshnyi et al. (1996)
<i>Syntrophothermus lipocalidus</i>	5.8-7.5	45-60	Crotonate	C4–C10, isobutyrate	Firmicutes	Sekiguchi et al (2000)
<i>Syntrophus aciditrophicus</i>	ND	25-42	Crotonate	Butyrate, benzoate, alicyclic compounds, fatty acids	δ-Proteobacteria	Jackson et al., 1999
<i>Algorimarina butyrica</i>	6.2-7.1	10-25	None	C4, isobutyrate	δ-Proteobacteria	Kendall et al. (2006)
Propionate degraders						
<i>Syntrophobacter wolinii</i>	ND	ND	Propionate with sulfate; fumarate	Propionate	δ-Proteobacteria	Boone and Bryant (1980), Wallrabenstein et al. (1994)
<i>Syntrophobacter fumaroxidans</i>	6.0–8.0	20–40	Propionate, formate, hydrogen with sulfate and fumarate; Succinate with sulfate; fumarate, malate, aspartate, pyruvate,	Propionate	δ-Proteobacteria	Harmsen et al. (1998)
<i>Syntrophobacter pfennigii</i>	6.2–8.0	30–37	Propionate, lactate with sulfate, sulfite, thiosulfate	Propionate, lactate, propanol	δ-Proteobacteria	Wallrabenstein et al. (1995)
<i>Syntrophobacter sulfatireducens</i>	6.2–8.8	20–48	Propionate with sulfate or thiosulfate; pyruvate	Propionate	δ-Proteobacteria	Chen et al. (2005)
<i>Pelotomaculum thermopropionicum</i>	6.7-7.5	45-65	Pyruvate, fumarate; propionate, ethanol or lactate with fumarate	Propionate, ethanol, lactate, ethylene glycol, 1-butanol, 1-propanol, 1-pentanol and 1,3-propanediol	Firmicutes	Imachi et al. (2002)

<i>Pelotomaculum schinkii</i>	ND	ND	None	Propionate	Firmicutes	de Bok et al. (2002a)
<i>Smithella propionica</i>	ND	ND	Crotonate	Propionate	δ -Proteobacteria	Liu et al. (1999)
<i>Desulfotomaculum thermobenzoicum</i> subsp. <i>thermosyntrophicum</i>	6.0–8.0	45–62	propionate, lactate, pyruvate and H ₂ /CO ₂ with sulfate; Pyruvate, lactate, fumarate, glycine, benzoate	Propionate	Firmicutes	Plugge et al. (2002)

^a The number of carbons in the fatty acid is indicated. When a range is given, this means that the organism can use compounds within the indicated range of carbon numbers, but not all possibilities were tested. ND = Not determined.

Recently, Schmidt et al. (2013) confirmed the constitutive expression of a membrane-bound, internally oriented iron-sulfur oxidoreductase (DUF224) and electron-transfer flavoproteins (etfAB) during syntrophic butyrate oxidation by *S. wolfei*. According to Schmidt et al. (2013), electrons released in the butyryl-CoA dehydrogenase reaction are transferred through a membrane-bound EtfAB:quinone oxidoreductase (DUF224) to a menaquinone and further via a b-type cytochrome to an externally oriented formate dehydrogenase. Hence, an ATP hydrolysis driven proton-motive force across the cytoplasmatic membrane would provide the energy input for the electron potential shift necessary for formate formation (Schmidt et al., 2013). Thus, formate would be the preferential electron carrier in syntrophic butyrate oxidation by *S. wolfei*, or could be exchanged into hydrogen as electron carrier at the hydrogenase/formate dehydrogenase (HYD-1/FDH-1) complex (Schmidt et al., 2013). In the 3-hydroxybutyryl-CoA dehydrogenase reaction, the second reaction that generates electrons (NADH), electrons are transferred to NAD⁺ to form NADH. The NADH can then be used to reduce either protons to molecular hydrogen, or CO₂ to formate (Schmidt et al., 2013).

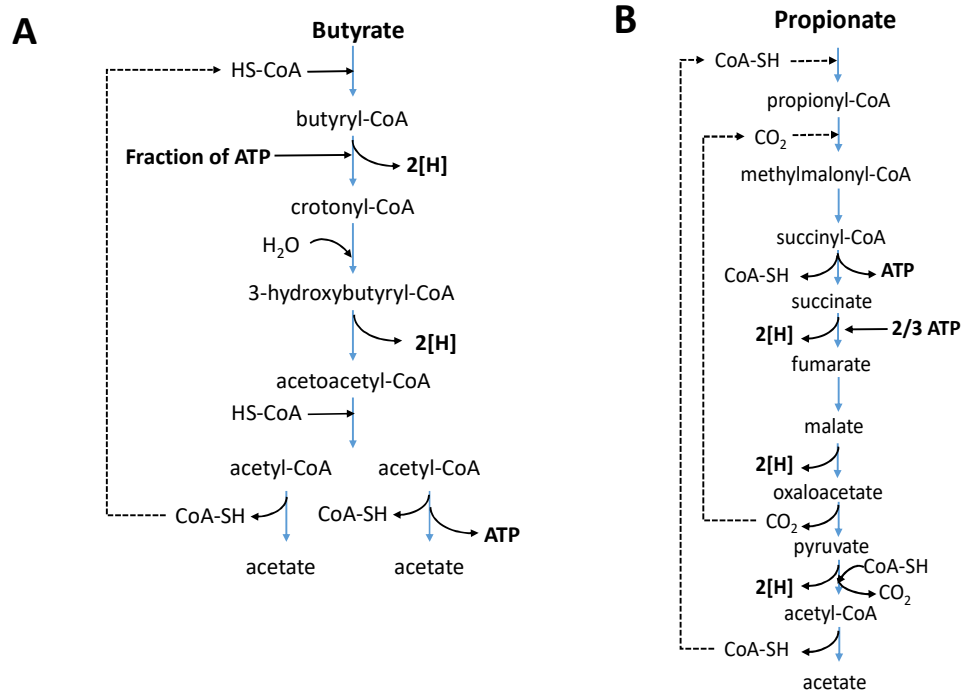


Figure 5. Metabolic pathways of butyrate (A) and propionate (B) conversion by bacteria that can grow in syntrophy with methanogens.

1.6 Syntrophic propionate conversion

Syntrophic propionate degraders are affiliated with the classes of *Deltaproteobacteria* and *Clostridia* (Imachi et al., 2002; Plugge et al., 2002) (Table 2). Different from syntrophic butyrate degraders, some syntrophic propionate degraders, such as *Syntrophobacter sp.*, can grow in pure culture by using sulfate as electron acceptor for propionate oxidation (McInerney et al., 2005). Additionally, some can grow by fermenting pyruvate or fumarate in pure culture. *Smithella propionica* ferments propionate via dismutating pathway to acetate and butyrate, and butyrate is subsequently oxidized to acetate (de Bok et al., 2001). All other known syntrophic propionate degraders use methylmalonyl-CoA pathway to oxidize propionate to acetate and CO₂ (Figure 5B). The key redox reactions are the oxidation of succinate to fumarate, malate to oxaloacetate and the conversion of pyruvate to acetyl-CoA and CO₂ (Schink, 1997). Oxidation of succinate and malate are highly endergonic reactions and thus require an energy input via reverse electron transfer. The reverse electron transport for the oxidation of succinate during syntrophic propionate metabolism involves coupling menaquinone reduction with the oxidation of succinate to fumarate by succinate dehydrogenase. In *Syntrophobacter fumaroxidans* and *Pelotomaculum thermopropionicum*, menaquinone oxidation is linked to a membrane-bound hydrogenase or formate dehydrogenase

(Sieber et al., 2012). *S. fumaroxidans* has a membrane-bound succinate dehydrogenase, two cytoplasmic succinate dehydrogenases, and several periplasmic and cytoplasmic hydrogenases and formate dehydrogenases (Müller et al., 2010; Worm et al., 2011; de Bok et al., 2002a, 2003). Significantly higher expression of the confurcating hydrogenase, a periplasmic formate dehydrogenase, and the hydrogen-formate lyase was observed during syntrophic growth versus monoculture growth of *S. fumaroxidans* (Worm et al., 2011). *P. thermopropionicum* also contains a similar system with a membrane-associated succinate dehydrogenase, which was transcribed highly during coculture growth on propionate (Kato et al., 2009). Malate oxidation to oxaloacetate and pyruvate to acetyl-CoA and CO₂ also generates each two electrons (NADH) (van Kuijk et al., 1996; Chabrière et al., 1999). Genome analysis suggests that NADH generated from malate oxidation and reduced ferredoxin generated from pyruvate oxidation could be coupled to formate or hydrogen production by confurcating formate dehydrogenases and hydrogenases (Müller et al., 2010). Such a mechanism would use the energy that remains from ferredoxin oxidation with protons to allow the endergonic coupling of NADH oxidation to proton reduction.

Among multiple routes that have been suggested for reverse electron transfer mechanism during syntrophic metabolism, the presence of confurcating-type hydrogenase genes and a gene for novel membrane-bound FeS oxidoreductase and adjacent to *etfAB* were found to be common in almost all microorganisms capable of syntrophic metabolism, despite the distinctly different phylogenetic lineages of these organisms (Sieber et al., 2012).

1.7 Do sulfate reducers and syntrophs coexist throughout the sediment?

In anoxic marine environments where the amount of organic carbon is high, both sulfate reduction and methanogenesis were reported to occur simultaneously (Oremland and Taylor, 1978; Oremland et al., 1982b; Senior et al., 1982; Holmer et al., 1994). There are several studies supporting the coexistence of both microbial groups using competitive substrates, H₂ and acetate, in sulfate-rich sediments (Oremland and Taylor, 1978; Senior et al., 1982).

The zonation of mineralization processes may be kinetically or energetically controlled based on the abilities of the physiological groups to compete for common substrates. The H₂ concentration in anaerobic sedimentary environments is an important factor in determining the predominant terminal electron-accepting process and consequently the biological redox zonation observed in sediments. According to Lovley and Goodwin (1988), each terminal electron-accepting process requires different minimum H₂ concentrations in order to conserve energy and to grow.

They reported the H_2 concentration range for methanogenesis as 7 – 10 nM, for sulfate reduction as 1 – 1.5 nM, for Fe (III) reduction as 0.2 nM, and for Mn(IV)/nitrate reduction as less than 0.05 nM (Lovley and Goodwin, 1988). Hence, sulfate reducers will maintain H_2 concentrations at very low levels (1 – 1.5 nM) in sulfate zones, and H_2 -dependent methanogenesis will then be thermodynamically unfavorable. The regulation of the ambient H_2 by sulfate-reducing bacteria or methanogenic archaea at a minimum concentration constitutes a clear example of thermodynamic control which still enables these organisms to maintain the required energy yield of ≤ -10 to -20 kJ mol⁻¹ (Hoehler et al., 2001). Acetate is another important and common substrate for sulfate reduction and methanogenesis in marine anoxic sediments. As compared to H_2 concentrations, measured pore water concentrations of acetate in marine sediments have been reported to be 10 μ M or more. This concentration is enough to support both sulfate reduction and methanogenesis. Almost all acetate in the sulfate zone is converted to CO_2 instead of CH_4 (King et al., 1983). This phenomenon has been explained by the ability of acetoclastic methanogens to grow in syntrophy with sulfate reducers which results in shifting from producing methane from acetate to feeding the sulfate reducers with H_2 (Finke et al., 2007b). The competitive and potential syntrophic relationships between these two phylogenetic groups of microorganisms may therefore be more complex than has so far been recognized.

Similar to the fact that methanogens reside in the upper sulfate-rich sediments, recent data on the relative distribution of sulfate-reducing bacteria in Black Sea and Aarhus Bay sediments shows that SRB are present within the methane zone at similar high numbers as in the sulfate zone (Leloup et al., 2007, 2009). According to the study of Leloup et al. (2007), sulfate- and methane-rich sediment layers showed the dominance of similar, novel cluster of *dsrAB* sequences. *dsrAB* are the functional marker genes encoding alpha- and beta-subunits of dissimilatory (bi)sulfite reductase that is used by sulfate-reducing microorganisms for energy conservation (Pester et al., 2012). Considering that the phylogenetic position of the novel *dsrAB* cluster is in close vicinity of some sulfate-reducing microorganisms that have the ability to grow syntrophically (Leloup et al. 2007), it becomes obvious that the ability of sulfate reducers to perform both sulfidogenic and syntrophic lifestyle enables them to thrive in high- and low-sulfate environments in high numbers. On the other hand, Holmkvist et al. (2011) proposed that the sulfate reducers inhabiting the methane zone of Aarhus Bay live by reducing sulfate. They showed an immediate 10- to 40-fold increase in sulfate reduction after addition of both sulfate and organic substrates into the sediment and concluded that the low background sulfate concentration in the sediment is generated from

the chemical reaction of downwards diffusing sulfide with deeply buried Fe(III) species and perhaps to a low diffusive flux of sulfate from above. Despite the occurrence of sulfate reduction in the methane zone, Holmkvist et al. (2011) also reported that sulfate reduction in the methane zone was only a fraction of ongoing methanogenesis and it corresponded to 0.1% of the total sulfate reduction in the sulfate zone. Therefore, it is relevant to understand how sulfate reducers interact with methanogenic communities when the sulfate is insufficient for complete oxidation of organic compounds.

1.8 Outline of the thesis

Sulfate reduction and methanogenesis are important terminal electron accepting processes in many anaerobic ecosystems including marine sediments, freshwater sediments, digesters, and propionate, butyrate, acetate, hydrogen and formate are the major end-products of fermentation during organic matter degradation in these ecosystems. Acetate, H_2 and formate are key intermediates and serve as primary substrates for several terminal processes, such as sulfate reduction and methanogenesis. Sørensen et al. (1981) reported that acetate oxidation contributes for 40-50 % to sulfate reduction in marine sediments while the contribution of H_2 consumption is 5 - 10 %, propionate and butyrate oxidations are 10 - 20 %, in case of complete oxidation of propionate and butyrate. The conversion of propionate and butyrate is critical in deep sulfate-depleted sediments since they can be converted only by the combined action of several different physiological groups of bacteria and archaea. Despite the importance of these compounds in sulfate-rich and sulfate-depleted parts of marine sediments, it is often unclear what populations of microorganisms are involved in their degradation in the upper and lower parts of the sediment column. Therefore, we aimed to gain more insight into the propionate- and butyrate-degrading microbial communities residing at different depths of marine sediments and to better understand the factors affecting their growth, such as substrate and sulfate availability, and temperature. We also targeted to isolate butyrate and propionate-degrading syntrophic communities from different parts of the sediment. The sources of organic matter and the degradation of organic matter, the biogeochemical zones and the role of microorganisms in shaping these zones are discussed. The focus is brought on the butyrate and propionate conversions since they are considered as rate limiting steps in anaerobic degradation of organic matter.

Chapter 2 evaluates interspecies hydrogen transfer between and coexistence of marine methanogens and sulfate reducers using acetate as sole electron and carbon source in mixed pure

cultures. To test interspecies hydrogen transfer, acetoclastic *Methanosaeta* (*Methanotrix*) *concilii* was cocultured with either hydrogenotrophic sulfate reducer, *Desulfovibrio vulgaris*, or hydrogenotrophic methanogen, *Methanococcus maripaludis*. Coexistence of *M. concilii* and *Desulfobacter latus* on acetate was investigated under sulfidogenic conditions in mixed pure cultures. The concentrations of substrates, intermediates, and electron acceptor were quantified by analytical methods at different time intervals. The total number of 16S rRNA gene copies was determined regularly by quantitative PCR in order to define the growth curve of each microorganism during experiment. Gibbs free energies per reaction were calculated to determine the possibility of each reaction to occur under given culture conditions and with partner organism.

Chapter 3 aims to investigate butyrate-degrading sulfate-reducing and syntrophic communities in the sulfate, sulfate-methane transition and methane zone of Aarhus Bay, Denmark. In order to enrich for sulfate-reducing, syntrophic bacteria and methanogenic archaea, batch slurry incubations were prepared using the sediment retrieved from different zones. Some of these slurries were amended with 20 mM sulfate to stimulate growth of sulfate-reducing communities. Some of the slurries were amended with 3 mM sulfate to examine the growth behavior of sulfate-reducing and syntrophic communities, and some were incubated without sulfate to stimulate syntrophic communities. Two different temperatures were used for incubation; one is the in situ temperature and the other is a higher temperature to investigate its effect on the conversion rates and the possible change in ultimate community structure. The change in the bacterial and archaeal community structure was analyzed by DGGE using the genomic DNA sampled at different time points. The ultimate microbial community in each batch slurry was determined by pyrosequencing and Illumina MiSeq sequencing of the extracted DNA from the samples taken at the last incubation day.

Chapter 4 is similar to Chapter 3 and investigates the propionate-degrading sulfate-reducing and syntrophic communities inhabiting different biogeochemical zones of Aarhus Bay. The propionate degradation and the product formation was followed by regular gas and liquid sampling. The change in the bacterial and archaeal community structure was analyzed by DGGE using the genomic DNA sampled at different time points. The ultimate microbial community in each batch slurry was determined by pyrosequencing and Illumina MiSeq sequencing of the extracted DNA from the samples taken at the last incubation day. The investigations performed in Chapters 3 and 4 are intended to test the hypothesis that syntrophs are not easily out-competed by sulfate reducers,

rather both physiological groups can coexist throughout the sediment at different sulfate concentrations. Furthermore, the demonstration of simultaneous sulfate reduction and methanogenesis during propionate and butyrate conversion throughout the sediment is important to understand the capabilities of the microbes involved.

Chapter 5 monitors intact polar membrane lipids (IPL) content of all the enrichment slurries studied in Chapters 3 & 4 and constitutes a complementary tool to the molecular analysis conducted in these chapters. IPL analysis was performed by high performance liquid chromatography-electrospray ionization-mass spectrometry (HPLC/ESI/MS) on the original sediment samples and the enrichment slurry samples taken at the end of the incubation period. By comparing the IPL composition of both samples, we aimed to understand the factors shaping microbial community such as amended substrates, availability of sulfate, incubation temperature and the depth of the sediment.

Chapter 6 presents the further enrichment of propionate- and butyrate-degrading slurries to get more defined cultures and aims to take steps further for the isolation of new marine syntrophs. The enrichment slurries obtained in Chapters 3 & 4 were subcultured four times and the obtained microbial community was identified by cloning of bacterial and archaeal 16S rRNA gene analysis. The FISH method was used to visualize the syntrophic interactions and to capture the live microbes.

In **Chapter 7**, results obtained in this thesis are summarized and discussed with the knowledge presented in the literature. Additionally, future perspectives for research are presented.

Chapter 2

Methanogenic archaea and sulfate reducing bacteria co-cultured on acetate: teamwork or coexistence?

This chapter has been published as:

Ozuolmez, D., Na, H., Lever, M.A., Kjeldsen, K.U., Jørgensen, B.B. and Plugge, C.M., (2015) Methanogenic archaea and sulfate reducing bacteria co-cultured on acetate: teamwork or coexistence? *Frontiers in microbiology*, 6(492): 1-12.

Abstract

Acetate is a major product of fermentation processes and an important substrate for sulfate reducing bacteria and methanogenic archaea. Most studies on acetate catabolism by sulfate reducers and methanogens have used pure cultures. Less is known about acetate conversion by mixed pure cultures and the interactions between both groups. We tested interspecies hydrogen transfer and coexistence between marine methanogens and sulfate reducers using mixed pure cultures of two types of microorganisms. First, *Desulfovibrio vulgaris* subsp. *vulgaris* (DSM 1744), a hydrogenotrophic sulfate reducer, was cocultured together with the obligate aceticlastic methanogen *Methanosaeta concilii* using acetate as carbon and energy source. Next, *Methanococcus maripaludis* S2, an obligate H₂- and formate-utilizing methanogen, was used as a partner organism to *M. concilii* in the presence of acetate. Finally, we performed a coexistence experiment between *M. concilii* and an acetotrophic sulfate reducer *Desulfobacter latus* AcSR2. Our results showed that *D. vulgaris* was able to reduce sulfate and grow from hydrogen leaked by *M. concilii*. In the other coculture, *M. maripaludis* was sustained by hydrogen leaked by *M. concilii* as revealed by qPCR. The growth of the two aceticlastic microbes indicated co-existence rather than competition. Altogether, our results indicate that H₂ leaking from *M. concilii* could be used by efficient H₂-scavengers. This metabolic trait, revealed from coculture studies, brings new insight to the metabolic flexibility of methanogens and sulfate reducers residing in marine environments in response to changing environmental conditions and community compositions. Using dedicated physiological studies we were able to unravel the occurrence of less obvious interactions between marine methanogens and sulfate-reducing bacteria.

2.1 Introduction

Marine coastal and shelf sediments are important sites for mineralization of organic matter deposited from land and from the marine photic zones (Jørgensen 1983). It is well established that under anoxic conditions, mineralization of complex organic matter requires cooperation between at least three trophic guilds (Schink and Stams, 2013). The first step in the degradation of organic matter is the hydrolysis of complex molecules into their oligomers or monomers. This step is followed by fermentation involving the degradation of these substrates to reduced organic compounds such as short chain fatty acids, and alcohols. In sulfate-rich sediments, sulfate-reducing bacteria (SRB) can use the products of primary fermentations and oxidize them to CO_2 . However, in sulfate-depleted methanogenic sediments, short chain fatty acids and alcohols are converted by secondary fermenters to acetate, formate, H_2 and CO_2 , which are subsequently utilized by methanogenic archaea (MA) to produce CH_4 (Muyzer and Stams, 2008; McInerney et al., 2008; Stams and Plugge, 2009; Schink and Stams, 2013).

Acetate is a key intermediate in marine sediments as it is one of the major end-products of fermentation and serves as a primary substrate for several terminal electron accepting processes, like sulfate reduction and methanogenesis (Thamdrup et al. 2000; Sørensen et al., 1981; Christensen 1984; Parkes et al., 1989). There are two possible processes for methanogens to produce methane from acetate. In the first process acetate is cleaved to CH_4 and CO_2 . This process is called aceticlastic methanogenesis and it is an energy-yielding reaction under standard conditions (Table 1, reaction 2). The second process, syntrophic acetate oxidation, was first proposed by Barker (Barker 1936), but attracted attention much later by Zinder and Koch (1984). Syntrophic acetate oxidation is a two-step process. In the first step, acetate is oxidized to CO_2 by an aceticlastic microorganism with the generation of reducing equivalents, often as hydrogen. This step is endergonic and requires a hydrogenotrophic microorganism for the consumption of produced hydrogen (Table 1, reaction 1). In the second step, hydrogenotrophic methanogens scavenge that hydrogen and the overall reaction becomes thermodynamically favorable (Table 1, the sum of reactions 1 and 5). Hydrogenotrophic sulfate reducers can also be involved in the second step and in case of SRB as the partner organism, the overall reaction is the same as if a sulfate reducer would oxidize acetate completely without a syntrophic partner (Table 1, the sum of reactions 1 and 3). It has been shown in previous studies that not only aceticlastic bacteria but also aceticlastic methanogens can carry out the first step of syntrophic acetate oxidation (Phelps et al., 1985). In a syntrophic relationship,

the chemical energy is shared via interspecies hydrogen transfer, so that not only sulfate reducers but also the aceticlastic methanogens would be able to grow in the sulfate zone of marine sediments. It is noteworthy that the energy yield from syntrophic acetate oxidation to sulfate is greater than the energy yield from aceticlastic methanogenesis (Table 1, the sum of reactions 1 and 3).

Interspecies H_2 transfer has been studied using mixed pure cultures of the aceticlastic methanogen *Methanosarcina barkeri* and the hydrogenotrophic sulfate reducer *Desulfovibrio vulgaris* (Phelps et al., 1985). Phelps and colleagues co-cultivated *M. barkeri* with *D. vulgaris* and reported that CO_2 production from acetate increased and CH_4 production decreased in cocultures compared to pure cultures of *M. barkeri*, demonstrating interspecies hydrogen transfer. Syntrophic acetate oxidation by aceticlastic methanogens and hydrogenotrophic sulfate reducers was demonstrated for anoxic paddy soils (Achnich et al. 1995) but has not been demonstrated for marine sediments so far.

Acetate concentrations in pore water of marine sediments are reported to be relatively high (typically $>10 \mu M$ (Finke et al; 2007a)) and they are likely not under thermodynamic limitation in marine sediments, which makes acetate conversion by methanogens thermodynamically feasible even in the sulfate zone (Finke et al., 2007b). However, almost all acetate in the sulfate zone is converted to CO_2 , not to CH_4 (Jørgensen and Parkes, 2010), suggesting the predominance of aceticlastic sulfate reduction. Thermodynamic mechanisms to explain the biogeochemical zonation in marine sediments in the presence of acetate are unclear. Finke and colleagues (2007b) suggested that acetate oxidation might proceed via interspecies H_2 transfer. According to their hypothesis, aceticlastic methanogenesis is exergonic as long as acetate concentrations stay above $0.05 \mu M$. Many studies have shown the existence of methanogens in sulfate-rich marine sediments (Wilms et al. 2007; Beck et al. 2011; Schippers et al. 2012). *Methanosaeta* sp. have been detected in marine sediments (Mori et al., 2012), with unknown identities, and the marine “*Methanosaeta pelagica*” has been recently isolated (Mori et al., 2012). Aceticlastic methanogens, specifically *Methanosaeta* species, may be important in contributing to acetate degradation in marine sediments, in particular the tidal flat sediments, which have an abundant supply of organic matter.

In this study, we investigated interspecies hydrogen transfer between aceticlastic *Methanosaeta concilii* and two hydrogenotrophic microorganisms, either a sulfate reducer, *Desulfovibrio vulgaris*, or a methanogen, *Methanococcus maripaludis*. We hypothesized that the existence of interspecies hydrogen transfer between aceticlastic methanogens and

hydrogenotrophic sulfate reducers/methanogens in marine sediments would help to understand what controls the distribution of methanogens in sediments. Additionally, we tested coexistence between *Methanosaeta concilii* and *Desulfobacter latus* on acetate under sulfidogenic conditions in mixed pure cultures.

Table 1: Overview of reactions examined in this study. 1: Acetate oxidation, 2: Aceticlastic methanogenesis, 3: Hydrogenotrophic sulfate reduction, 4: Acetotrophic sulfate reduction, 5: Hydrogenotrophic methanogenesis, the sum of the reactions of 1 and 3 (reaction 4): Syntrophic acetate oxidation by an aceticlastic methanogen and a hydrogenotrophic sulfate-reducer, the sum of the reactions of 1 and 5 (reaction 2): Syntrophic acetate oxidation by an aceticlastic methanogen and a hydrogenotrophic methanogen. The calculations for standard conditions (298K, 1 atm, 1M reactants) were done with thermodynamic data from Lever (2012). The ΔG_r° values of the reactions shown in this table are different from the ΔG_r° values of the same reactions shown in other chapters. The reason is the difference in Gibbs free energies of formation (ΔG_f°) values for H_2 and CH_4 in aqueous state (used in this chapter) and in the gaseous state (used in other chapters).

Reaction number	Reactions	ΔG_r° (kJ mol ⁻¹)
1	$CH_3COO^- + 4H_2O \rightarrow 4H_2 + 2HCO_3^- + H^+$	214.70
2	$CH_3COO^- + H_2O \rightarrow CH_4 + HCO_3^-$	-14.74
3	$4H_2 + SO_4^{2-} + H^+ \rightarrow HS^- + 4H_2O$	-262.06
4	$CH_3COO^- + SO_4^{2-} \rightarrow HS^- + 2HCO_3^-$	-47.36
5	$HCO_3^- + 4H_2 + H^+ \rightarrow CH_4 + 3H_2O$	-229.44

2.2 Materials and methods

2.2.1 Strains and cultivation

Methanosaeta concilii strain (DSM 2139) was adapted to 2% NaCl conditions and maintained routinely on 10 mM acetate. *Desulfovibrio vulgaris* subsp. *vulgaris* (DSM 1744), *Desulfobacter latus* AcRS2 (DSM 3381) and *Methanococcus maripaludis* S2 (DSM 14266) were obtained from the German

Collection of Microorganisms and Cell Cultures (DSMZ, Braunschweig, Germany) and maintained routinely on H_2/CO_2 (80:20%, v/v) plus 10 mM sulfate, 10 mM acetate plus 10 mM sulfate and H_2/CO_2 (80:20%, v/v) respectively. All strains were grown in the same mineral salts medium (described below). Methanogenic archaea and sulfate-reducing bacteria were cultured routinely at 37°C and/or 30°C, respectively.

2.2.2 Media and growth conditions

For the preparation of cocultures and maintaining the pure cultures, a marine, bicarbonate-buffered mineral salts medium was used. The anoxic medium contained the following components (grams/liter): KH_2PO_4 (0.41), $\text{Na}_2\text{HPO}_4 \cdot 2\text{H}_2\text{O}$ (0.53), NH_4Cl (0.3), NaCl (0.3), $\text{CaCl}_2 \cdot 2\text{H}_2\text{O}$ (0.11), $\text{MgCl}_2 \cdot 6\text{H}_2\text{O}$ (0.1), NaHCO_3 (4), $\text{Na}_2\text{S}_9\text{H}_2\text{O}$ (0.024) and 0.05% (w/v) yeast extract (YE) (added only to the pure and cocultures of *D. vulgaris* strain). The medium was supplemented with 1 ml/liter of acid and alkaline trace element solution (Stams et al., 1992). The medium was boiled and cooled to room temperature under an oxygen-free N_2 flow. The medium was dispensed into 120 ml serum bottles. The bottles were sealed with butyl rubber stoppers and crimp caps and the gas headspace was replaced with 1.7 atm. N_2/CO_2 (80:20% v/v) and autoclaved.

Acetate from a concentrated sterile stock solution was added to the medium to a final concentration of 10 mM. Besides the substrate, vitamins (1 ml/liter) (Stams et al., 1992) were added from sterile stock solution to the medium. In order to reach the desired salt concentration (2%, w/v), sterile anoxic artificial seawater, containing (in grams/liter) NaCl (40), $\text{MgCl}_2 \cdot 6\text{H}_2\text{O}$ (10.8), KCl (0.7), $\text{CaCl}_2 \cdot 2\text{H}_2\text{O}$ (1) was added to serum bottles in same volume as the medium volume. The pH of the medium was set to 7.

2.2.3 Experimental design

Microorganisms were cultivated in duplicate in 120 ml serum vials with a final volume of 50 ml. Complete medium (30 ml) was inoculated with 20% (v/v) of each microorganism to prepare cocultures. Final concentrations of acetate and sulfate in bacterial-archaeal cocultures were 10 mM, whereas archaeal-archaeal coculture contained only 10 mM acetate. The flasks were flushed with N_2/CO_2 immediately after inoculation of each strain to remove residual H_2 and CH_4 , leaving 1.7 bar of N_2/CO_2 (80:20% v/v) as the headspace. All inoculations were done aseptically and all cocultures were incubated under static conditions in the dark. Cocultures of methanogenic archaea were

incubated at 37°C while bacterial-archaeal cocultures were incubated at 30°C. Incubations lasted for 41 days for *M. concilii*-*D. vulgaris* and *M. concilii*-*M. maripaludis* cocultures and 21 days for *M. concilii*-*D. latus* cocultures. Gas and liquid samples were taken at different time intervals and analyzed for H₂, CH₄, acetate, sulfate, sulfide, dissolved inorganic carbon and biomass increase.

Pure cultures of respective microorganisms were cultivated in the presence of the required electron donor and acceptor as control. The culture conditions of pure cultures were explained in section 2.1. *D. vulgaris* was incubated at two different conditions in addition to its original culture condition; one was without H₂/CO₂ but with yeast extract addition (0.05%, w/v) and the other was without H₂/CO₂ but with YE (0.05%, w/v) and 10 mM acetate. These controls were made to check for the ability of the strain to grow and reduce sulfate with YE and/or acetate in the absence of H₂/CO₂.

2.2.4 Analytical methods

CH₄ was analyzed by gas chromatography with a Shimadzu GC-14B (Shimadzu, Kyoto, Japan) equipped with a packed column (Molsieve 13X, 60-80 mesh, 2 m length, 3 mm internal diameter) (Varian, Middelburg, The Netherlands) and a thermal conductivity detector set at 70 mA. The injection volume was 0.2 ml. The oven temperature and the injector temperatures were both 100°C. The detector temperature was 150°C. Argon was the carrier gas at a flow rate of 30 ml/min.

H₂ was measured using a gas chromatograph equipped with pulsed discharge detector (PDD) (Trace Analytical, Bester, Amstelveen). The GC had Carboxen 1010 column, 3 m x 0.32 mm followed by a Molsieve 5A column, 25 m x 0.32 mm. The injection volume was 0.5 ml. The carrier gas was helium with a flow rate of 20 ml/min. The column oven temperature was 90°C, the injection oven temperature was 80°C and the detector temperature was 110°C. The pressure was 200 kPa and the input range was 64 nA.

Acetate from centrifuged (10,000 x g, 10 min) samples of the culture media was analyzed by Thermo Scientific Spectrasystem HPLC system equipped with a Varian Metacarb 67H 300 x 6.5 mm column kept at 30°C and running with 0.005 M sulfuric acid as eluent. The eluent had a flow of 0.8 ml/min. The detector was a refractive index detector.

Sulfate concentrations were analyzed by Thermo Scientific Dionex HPLC equipped with an AS22 column (Thermo Scientific Dionex, Massachusetts, USA) with eluents of 0.235 g/l NaHCO₃ and 2.576 g/l Na₂CO₃ at a flow rate of 1.2 ml/min. The column temperature was 30°C and pressure was 130-160 bar.

Sulfide measurements were done using the methylene blue method (Cline, 1969). Samples were diluted 1:1 with 5% ZnAc solution directly after sampling, to precipitate all sulfide. The solution was stored at room temperature for at least 20 minutes in order to promote the precipitation of zinc sulfide. After color development, the concentration was measured on a MERCK Spectroquant® Multy at 670 nm. Demi-water was used as a blank.

The pH was measured using Proline B210 pH electrode.

2.2.5 DIC measurements

For dissolved inorganic carbon (DIC) analysis, a 1 ml glass vial containing glass beads was filled with culture sample till the liquid became convex on top and the vial was sealed with a screw cap. The vials were stored at 4°C until analysis. Total DIC concentrations were measured as gaseous CO₂ after acidification of the liquid using a gas chromatograph (SRI 310C GC, SRI Instruments Europe GmbH) equipped with a thermal conductivity detector (TCD).

2.2.6 DNA extraction

Biomass was harvested at selected time points by sampling 1 mL of culture after homogenization by vortexing, and centrifugation at 13,000 g for 20 min. Genomic DNA was extracted from the pellet, using the PowerSoil^R DNA Isolation kit (MoBio), following the manufacturer's instructions.

2.2.7 Quantification of 16S rRNA genes by quantitative PCR

The total number of 16S rRNA gene copies was quantified by SYBR Green assay, on the CFX96 TouchTM Real-time PCR Detection System (Bio-Rad). The primers used for amplifying bacterial 16S rRNA genes were Bac8F and Bac338Rabc (Juretschko et al. 1998; Daims et al. 1999). For Archaea, Arch806F and Arch958R were used (Takai and Horikoshi, 2000; DeLong, 1992). For the coculture of *Methanosaeta concilii* and *Methanococcus maripaludis*, *Methanosaeta*-specific primers (MS1b 585F and Sae 835R; Conklin et al. 2006) and *Methanococcales*-specific primers (MCC495F and MCC832R; Yu et al. 2005) were used.

Prior to qPCR, the primers were tested by end-point PCR (annealing temperature gradient from 56°C to 65°C, 40 PCR cycles) on DNA extracts from pure cultures of the respective strains to ensure the specificity of the qPCR assays. None of the primer pairs used showed any unspecific amplification of non-target groups. All primers are shown in Supplementary Table 1.

Per PCR reaction, a total volume of 10 μL mixture contained 5 μL of iQ SYBR Green Supermix (Bio-Rad), 10 μM of each primer and 1 μL of $\sim 5 \text{ ng}/\mu\text{L}$ template DNA. The amplification program consisted of an initial activation step at 95°C for 3 min, 45 cycles of: denaturation at 95 °C for 15 s, annealing at 55°C for 30 s and elongation at 72°C for 30 s, and a final extension step at 60°C for 31 s. For reactions involving *Methanosaeta*- and *Methanococcales*-specific primer sets, the annealing temperature was adjusted to 60°C. Melting curves were analyzed using the CFX Manager™ software. The results were expressed as the number of cells per μL of sample, after calculating the number of 16S rRNA genes per genome from reference strains with completely sequenced genomes, using Genbank (<http://www.ncbi.nlm.nih.gov/genbank>) and the RNAmmer 1.2 Server (<http://www.cbs.dtu.dk/services/RNAmmer/>) (Lagesen et al., 2007). The calculated number of 16S rRNA gene copies and the corresponding reference strains were: 2 for *Methanosaeta concilii* GP6, 5 for *Desulfovibrio vulgaris* subsp. *vulgaris* Hildenborough^T, 4 for *Desulfobacter postgatei* 2ac9, and 3 for *Methanococcus maripaludis* (strains C5, C6, C7, and S2).

2.2.8 Calculation of Gibbs free energy (ΔG)

Gibbs free energies per reaction were calculated for the reactions shown in Table 1. For each reaction, the thermodynamic data for ΔG_f° , ΔH_f° , ΔV_f° (Table S2) were used to calculate ΔG_r° (standard Gibbs free energy of reaction), ΔH_r° (standard enthalpy of reaction), ΔV_r° (standard volume of reaction) (Table S3) by subtracting the sum of products from the sum of reactants.

ΔG values of reactions are dependent on temperature, pressure and chemical concentrations. Thus, ΔG_r° values were corrected taking into account the temperature, pressure and concentrations of reactants and products (Wang et al. 2010).

Standard Gibbs free energies of reactions were corrected for different temperatures using the integrated Gibbs-Helmholz equation:

$$\Delta G^\circ(T) = T * \left(\frac{\Delta G^\circ}{298K} + \left(\frac{\Delta H^\circ}{T} - \frac{\Delta H^\circ}{298K} \right) \right)$$

The effect of pressure on ΔG° value was calculated using the equation:

$$\Delta G^\circ(P) = \Delta G^\circ(T) + \Delta V_f^\circ * \frac{(P - 1)}{9869}$$

As last, Gibbs free energies per reaction were calculated using the measured products and reactants via the equation:

$$\Delta G = \Delta G^\circ + RT \ln K$$

where ΔG° was calculated under standard conditions (Table S3), R is the gas constant (0.008314 kJ mol⁻¹ K⁻¹), and T is the absolute temperature (298.15K). The activity coefficient values for bicarbonate and acetate (0.532), for water and H⁺ (1), for H₂ and CH₄ (1.24), for sulfate (0.104) and sulfide (0.41) were taken from Millero and Schreiber (1982) and Lever (2012).

2.3 Results

2.3.1 *M. concilii* in coculture with *D. vulgaris*

Methane formation started directly and increased with time (Figure 1A). 10 mM acetate was fully converted into CH₄. In 41 days, 0.9 mM sulfate was consumed and sulfide accumulated to a concentration of 0.8 mM. The bulk of sulfate was reduced in the first 6 days where H₂ concentration sharply decreased. After that point, there were only slight fluctuations in sulfate concentration. The H₂ pressure in the cocultures was 3.5 Pa when measured on day 1, presumably as a result of carryover from the *D. vulgaris* inocula. Hydrogen levels sharply decreased to 1.08 Pa in a week and then slowly dropped to 0.83 Pa until day 20. Later on, it slowly increased and reached to 1.21 Pa by the last day of the experiment. Pure cultures of *M. concilii* had pressures of 1.03 Pa H₂ on average throughout the incubation period (Figure S1A, S1B). H₂ concentration in pure culture controls of *D. vulgaris* incubated with YE and acetate without H₂ addition was 19.5 Pa and was 8 Pa when incubated with YE only (Figure S2A, S2B). The pressures dropped to 0.92 Pa in both controls by the end of 8th day and remained constant during the rest of the incubation period. H₂ concentration in control bottles did not change any further and same concentration was observed in cocultures. Thus 0.92 Pa H₂ (equivalent to 7.12 nM) was assumed to be the threshold H₂ concentration for the *D. vulgaris* subsp. *vulgaris* strain. Gibbs free-energy changes in the coculture ranged between -36.2 and -20.9 kJ/mol for the conversion of acetate into methane and bicarbonate and between -168.6 and -152.3 kJ/mol H₂ for hydrogenotrophic sulfate reduction (Figure 1B). These results showed that both reactions were favorable throughout the experiment. The most negative Gibbs free-energy values for both reactions were obtained in the beginning of experiment where acetate and hydrogen concentrations were at the highest levels. The highest Gibbs free-energy value for hydrogenotrophic

sulfate reduction was -152.3 kJ/mol, showing that the growth of *D. vulgaris* was thermodynamically feasible at the determined H_2 concentrations.

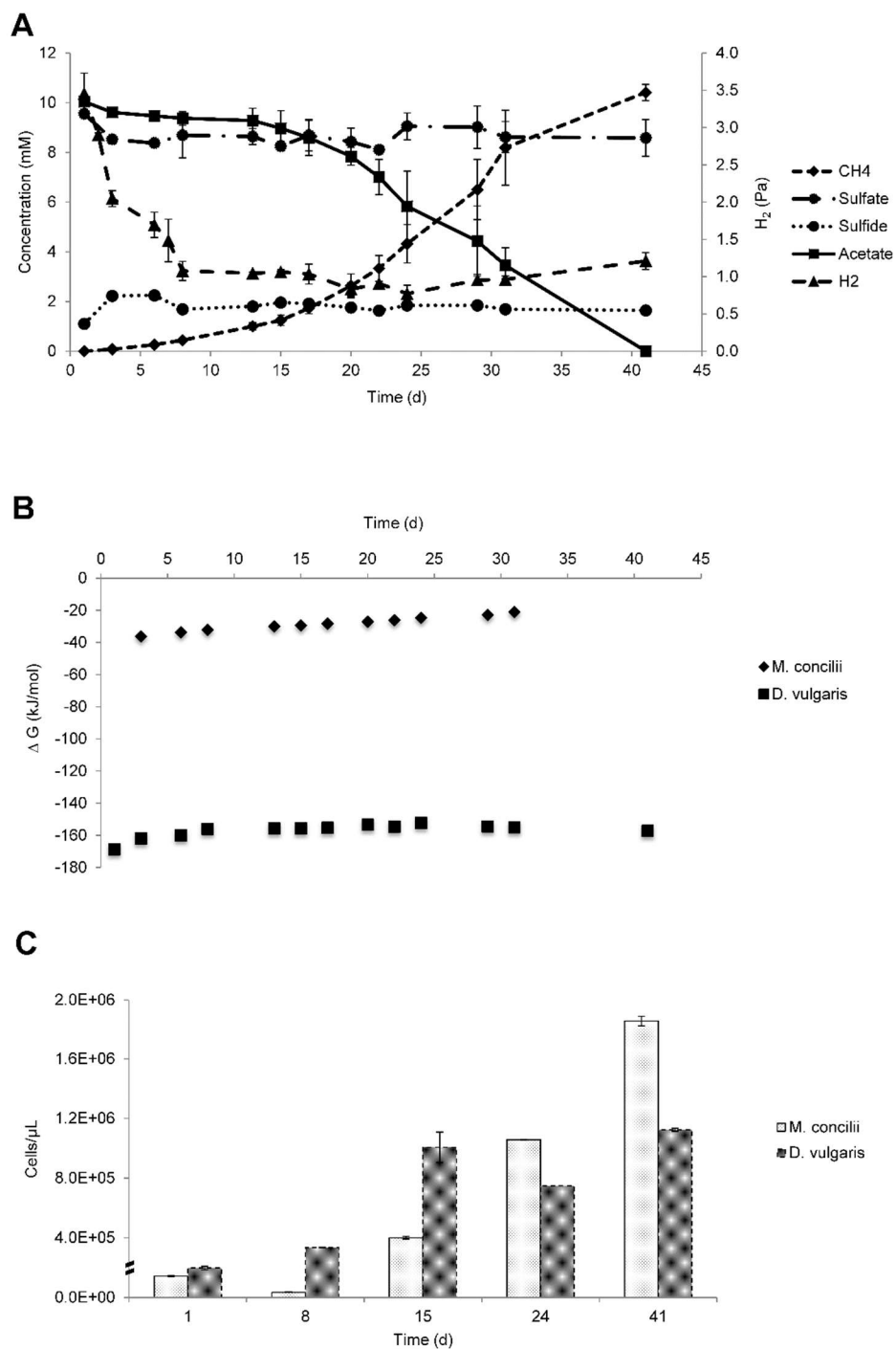


Figure 1. Growth on acetate by coculture of *M. concilii* and *D. vulgaris* subsp. *vulgaris*. (A) Changes in acetate, sulfate, sulfide, methane and hydrogen. (B) Actual Gibbs free-energy changes for acetate degradation to sulfide and bicarbonate and methane formation from acetate. (C) Growth quantified by qPCR in cells/ μ L. All data is average of 2 replicate incubations.

qPCR results showed an increase in cell numbers of both organisms during the experiment (Figure 1C). The decrease in the cell numbers of *M. concilii* in the first 8 days coincided with a lag phase of acetate consumption. *D. vulgaris* cell numbers increased 2-fold in the same period with H₂ consumption coupled to sulfate reduction. Between days 8 and 15, both *M. concilii* and *D. vulgaris* had the highest increase in their cell numbers with 11- and 3-fold increase, respectively. From day 15 until day 24, cell numbers of *M. concilii* increased 2.6-fold whereas *D. vulgaris* cell numbers decreased. In the last period of the incubation, both *M. concilii* and *D. vulgaris* showed growth with 1.8- and 1.5-fold increase in cell numbers, respectively. These results showed that *D. vulgaris* grew after consuming initial hydrogen to the threshold H₂ value.

qPCR analysis of *D. vulgaris* pure culture controls showed growth during the experiment (Figure S3). *D. vulgaris* with YE and acetate showed the highest increase in cell numbers within the first 8 days. However, *D. vulgaris* in coculture grew to the highest cell density and showed a 5-fold increase in numbers after 15 days compared to day 1.

2.3.2 *M. concilii* in coculture with *M. maripaludis*

Acetate conversion started upon the start of the experiment. CH₄ was produced from acetate and increased rapidly after 8 days of incubation (Figure 2A). As the first acetate addition was depleted by day 22, a second feed of acetate was given to the coculture. During the course of the experiment, 27 mM acetate was consumed and 28 mM CH₄ produced.

H₂ level increased from 1.4 Pa to a peak concentration of 1.9 Pa during the first 15 days. This increase was concomitant to acetate consumption and CH₄ production, which suggested H₂ leakage from *M. concilii* cells during growth. After H₂ reached the highest level, it was consumed by *M. maripaludis* to the lowest level which was 1.17 Pa. During the rest of the experiment, there were slight fluctuations in H₂ level, apparent changes were not observed. In pure culture controls of *M. concilii*, average H₂ levels were around 1.2 Pa and stayed constant throughout the experiment (Figure S1).

Gibbs free energies calculated for the conversion of acetate to methane and bicarbonate ranged between -36.2 and -18.4 kJ/mol and Gibbs free energies for hydrogenotrophic methanogenesis ranged between -12.7 and -1.5 kJ/mol H₂ (Figure 2B). ΔG values showed that acetoclastic methanogenesis was favorable throughout the experiment. The Gibbs free energies for hydrogenotrophic methanogenesis were close to the biological energy quantum value.

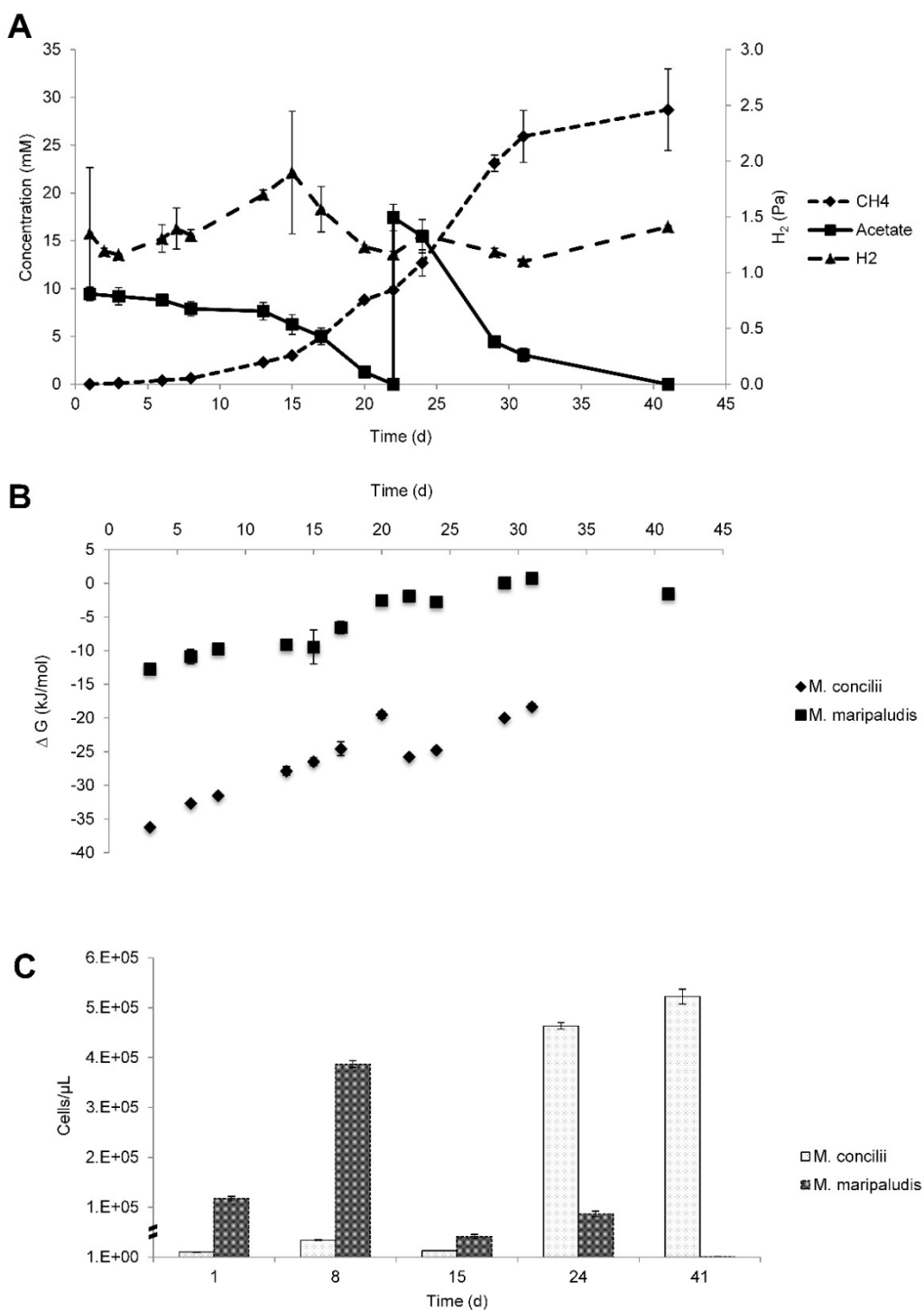


Figure 2. Growth on acetate by coculture of *M. concilii* and *M. maripaludis*. (A) Changes in acetate, methane and hydrogen. (B) Actual Gibbs free-energy changes for acetate degradation to methane formation from acetate. (C) Growth quantified by qPCR in cells/μl expressed. All data is average of 2 replicate incubations.

According to the qPCR results, both organisms showed growth during the course of the study (Figure 2C). As a result of acetate consumption starting in the beginning of the experiment, cell numbers of *M. concilii* increased 3-fold until 8 days. Similarly, *M. maripaludis* cell numbers increased 3-fold in the first week. A decline was detected in both *M. concilii* and *M. maripaludis* cell numbers between days 8 and 15, followed by an increase simultaneous to the consumption of acetate and hydrogen. Between days 15 and 24, *M. concilii* and *M. maripaludis* cell numbers increased 36- and 2-fold, respectively. After day 24, only 1-fold increase detected in *M. concilii* cell numbers whereas a decline in *M. maripaludis* cell numbers was observed.

2.3.3 *M. concilii* in coculture with *D. latus*

Acetate conversion coupled to sulfate reduction started by the initiation of the experiment while CH₄ production from acetate conversion was observed after a 2 day lag period (Figure 3A). Both *M. concilii* and *D. latus* contributed to acetate conversion during the experiment. *D. latus* reduced 16 mM sulfate by the oxidation of acetate, whereas *M. concilii* contributed to the acetate oxidation by producing 1.4 mM CH₄ on average in 21 days.

Under these conditions, Gibbs free energies ranged between -44 and -54 kJ/mol for the conversion of acetate into sulfide and bicarbonate and Gibbs free energies for acetate-driven methanogenesis ranged between -23 and -35 kJ/mol (Figure 3B). ΔG values showed that both reactions were favorable during the course of the experiment.

qPCR results indicate an increase in cell numbers of both organisms during the experiment (Figure 3C). Between day 7 and 14, both *M. concilii* and *D. latus* increased their cell numbers 3.7- and 2.4-fold, respectively. The highest cell increase was observed in the last week of the experiment. Increase in cell numbers of *M. concilii* was 36-fold whereas cell numbers of *D. latus* increased 14.6-fold.

In an additional experiment where we used the same coculture combination, CH₄ production started after few days of incubation when sulfate reduction was already ongoing (Figure S4). This coculture yielded 0.7 mM CH₄ until all sulfate was reduced by *D. latus*, after which *M. concilii* consumed the rest of the acetate coupled to CH₄ formation. After 53 days, 6 mM acetate was consumed by *M. concilii* stoichiometrically, which was much slower than *D. latus* (37 days).

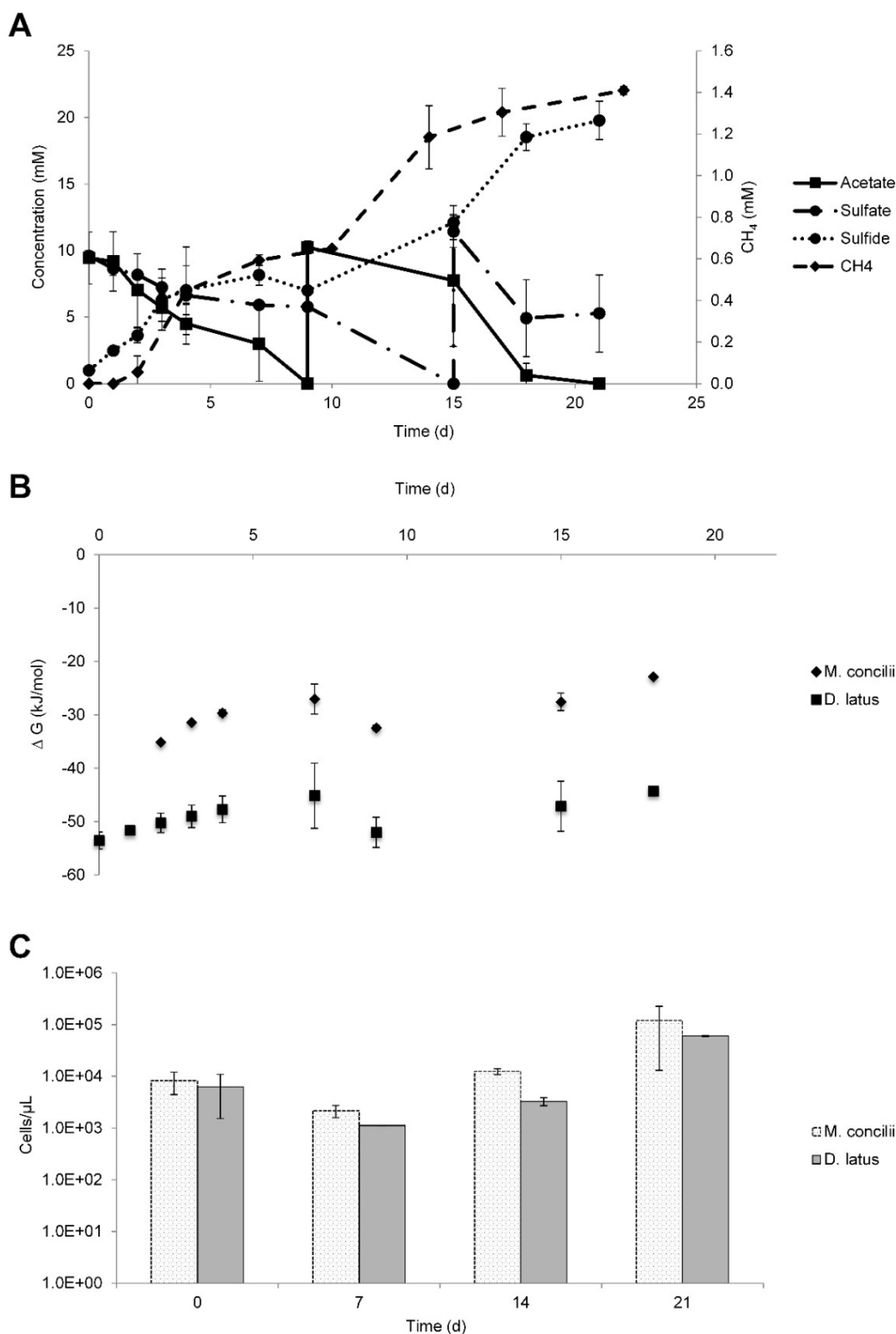


Figure 3. Growth on acetate by coculture of *M. concilii* and *D. latus*. (A) Changes in acetate, sulfate, sulfide and methane. (B) Actual Gibbs free-energy changes for acetate degradation to sulfide and bicarbonate and methane formation from acetate. (C) Growth quantified by qPCR in cells/ μ L. All data is average of 2 replicate incubations.

2.4 Discussion

In this study, we tested interspecies hydrogen transfer in two different coculture combinations. We cocultured an obligate acetoclastic methanogen, *Methanosaeta concilii* together with a hydrogenotrophic sulfate reducer, *Desulfovibrio vulgaris* or a hydrogenotrophic methanogen *Methanococcus maripaludis*. We aimed to investigate whether hydrogen leakage from *Methanosaeta* is possible under conditions where the hydrogen is efficiently scavenged by hydrogenotrophic sulfate reducers or methanogens and whether such a hydrogen leakage enables the growth of the consuming organisms. Additionally, we tested coexistence between *Methanosaeta concilii* and *Desulfobacter latus* on acetate under sulfidogenic conditions in mixed pure cultures.

2.4.1 *M. concilii* in coculture with *D. vulgaris* or *M. maripaludis*

In the cocultures of *M. concilii* and *D. vulgaris*, acetate was converted into CH₄ and CO₂ in 1:1 stoichiometry during the incubation period. In case of syntrophic acetate oxidation by an acetoclastic methanogen and a hydrogenotrophic sulfate reducer couple, the expected overall reaction is exactly the same as if the sulfate reducer oxidized acetate completely without a syntrophic partner (Table 1, reaction 4). Taking this into account, our data on the stoichiometry of the reaction do not point directly toward such a relationship.

Sulfate reduction occurred especially in the beginning of the experiment coupled to the oxidation of residual hydrogen from the inoculum. As a result of sulfate reduction, sulfide production occurred within the same time period. A minor discrepancy between sulfide produced and sulfate consumed may be attributed to chemical oxidation of HS⁻ to polysulfide by trace levels of oxygen.

H₂ measurements were of critical importance in our study to evaluate whether *Methanosaeta* was leaking hydrogen in coculture with a hydrogenotrophic partner. Results showed that *D. vulgaris* could couple hydrogen consumption to sulfate reduction in the first 8 days of the experiment and brought hydrogen levels to threshold concentrations and hydrogen concentrations remained at a constant low level similar to the level observed in *M. concilii* mono cultures (Fig. S1). Many H₂ measurement studies were performed in different ecosystems and in pure cultures to determine threshold H₂ concentrations for different terminal electron accepting reactions. (Lovley, 1985; Cord-Ruwisch et al., 1988; Lovley and Godwin, 1988; Conrad, 1996; Hoehler et al., 1998).

According to these studies, threshold H_2 concentrations for sulfate reduction were found in range between 5-95 nM. Our results show an average of 7 nM hydrogen in mono- and cocultures, which was in line with these observations. Taking into account that different threshold concentrations exist for growth and substrate degradation, *D. vulgaris* could benefit from traces of H_2 leaked by *M. concilii* and coupled this to its growth. The calculated Gibbs free energy values show that the hydrogenotrophic sulfate reduction reaction was thermodynamically feasible with the hydrogen concentrations in the cocultures throughout the study (Fig. 1B). Apparently, *D. vulgaris* was extremely efficient, and needed only a very little amount of hydrogen to produce sufficient energy for growth (Fig. 1C). Moreover, comparing pure culture with the coculture, hydrogen levels in *Methanosaeta* suggested that cocultivation can deviate electrons towards hydrogen production (Fig. 1B, Fig. S1).

Thus, this result supports our hypothesis that a minor part of the acetate was converted via the production of hydrogen.

In the other coculture combination, we used *Methanococcus maripaludis*, a methanogen that can use formate and/or H_2/CO_2 as carbon and energy source (Jones et al., 1983), as partner organism with *M. concilii*. In the presence of the methanogen as partner organism in syntrophic acetate oxidation, the net reaction is exactly the same as if acetate was cleaved by an aceticlastic methanogen (Table 1, reaction 2). In our study, the overall stoichiometry of the reaction, with slightly higher methane production, fits with both possibilities of acetate oxidation.

The trend in hydrogen concentration was different from that the trend in hydrogen concentration in the *M. concilii* and *D. vulgaris* coculture. The initial hydrogen concentration in the coculture was lower and an increase in hydrogen production was observed between day 3 and day 15. This increase was concomitant to acetate consumption and CH_4 production, which suggests H_2 leakage from *M. concilii* cells during growth. In the *M. concilii* control monoculture at 37°C, there was no evidence for H_2 accumulation as H_2 level remained constant around 1.2 Pa throughout the experiment (Fig. S1). Therefore we speculated that *M. maripaludis* induced divergence of electrons from *M. concilii* and scavenged hydrogen leaked by *M. concilii*.

Comparing both cocultures, the H_2 concentration in *M. concilii*-*M. maripaludis* coculture was higher than in *M. concilii*-*D. vulgaris* coculture, which can be attributed to the ability of *D. vulgaris* to reduce H_2 concentrations to lower levels than *M. maripaludis*. Our data on threshold H_2 concentrations determined for *M. maripaludis* (~10 nM) fit with the finding of Hoehler and

colleagues (1998) where threshold H_2 concentrations for methanogens were reported to be around 13 nM.

ΔG values showed that acetoclastic methanogenesis was favorable throughout the experiment. On the other hand, ΔG values for hydrogenotrophic methanogenesis were close to the minimum biological energy quantum that permit organisms to grow (Hoehler et al., 2001). We used batch cultures to demonstrate the growth of both organisms. However accumulating methane in the bottles had a negative effect on the overall Gibbs free energy. If we calculate the Gibbs free energy using 1 mM of methane, a value that is more realistic in marine sediments, the energy ranges from -7 to -14 kJ/mol. Likewise, it was reported that methanogen yields may be -10 to -15 kJ/mol in marine sediments (Hoehler et al., 2001; Finke et al., 2007b; Jørgensen and Parkes, 2010). The decline in *M. marilaudis* cell numbers after day 24 can be explained by the decay rates of *M. maripaludis*. It is known that hydrogenotrophic methanogens have a high decay rate when left without substrate and stabilized in iron sulfide precipitates (Stams et al., 1992).

Taken together, we can speculate that the hydrogenotrophic methanogen benefited from the hydrogen leaked during the growth of the acetoclastic methanogen. Our findings on growth trend, ΔG values and aforementioned reference studies showed the capability of *M. maripaludis* to metabolize and grow on H_2 leaked by *M. concilii*. In this context it could be speculated that the hydrogen scavengers may act as parasites, as they benefit from the leakage of hydrogen by *Methanosaeta*.

There are several studies that demonstrated interspecies hydrogen transfer in defined cocultures (McInerney and Bryant, 1981; Phelps et al., 1985; de Bok et al., 2002b). In one of those studies, mixed pure cultures of *Methanosarcina barkeri* and *Desulfovibrio vulgaris* were tested for interspecies hydrogen transfer under high sulfate conditions using methanol and acetate as carbon and energy sources (Phelps et al., 1985). It is known that *M. barkeri* can produce trace amounts of H_2 during growth on acetate in pure culture and use some of the substrate for growth (Phelps et al., 1985; Valentine et al., 2000). They reported decreased CH_4 production and doubled CO_2 formation when acetate was oxidized in coculture. Lower hydrogen concentrations were measured in coculture compared to the pure cultures of the methanogen, meaning that *D. vulgaris* consumed hydrogen produced by *M. barkeri*. The authors claimed that *D. vulgaris* caused a decrease in methanogenesis by means of linking interspecies hydrogen transfer to sulfate reduction.

Methanosarcina species are known to be generalists, they have low affinity for acetate and have a minimum threshold for acetate of around 0.2 – 1.2 mM (Jetten et al., 1992). On the other

hand, *Methanosaeta* species are specialists, they consume only acetate as carbon and energy source and their minimum threshold for acetate is 7 – 70 μM (Jetten et al., 1992). As acetate concentrations in the pore water of marine sediments are usually less than 20 μM (between 8-45 μM) (Christensen and Blackburn 1982; Wellsbury and Parkes 1995; Finke et al. 2007a), conditions appear to be suitable for *Methanosaeta* rather than for *Methanosarcina*. Many clones closely related to *Methanosaeta* have been detected in marine sediments (Mori et al., 2012), with unknown identities, however *Methanosaeta pelagica* has been recently isolated (Mori et al., 2012). Undoubtedly, *Methanosaeta* is one of the most recalcitrant methanogens and is difficult to enrich and isolate primarily because of slow growth. Hydrogen production from *Methanosaeta* was demonstrated for *Methanosaeta thermophila* when growing on acetate (Valentine et al., 2000), and here we reported for the first time hydrogen leakage from a mesophilic halotolerant *Methanosaeta*.

2.4.2 *M. concilii* in coculture with *D. latus*

M. concilii and *D. latus* grew well in coculture (Figure 3). Methane production occurred even in the presence of high sulfate concentrations (7 mM). In the presence of non-limiting acetate concentrations, there was only minor competition for acetate between *M. concilii* and *D. latus*, as it was indicated by the concomitant sulfate reduction and methane production starting from the beginning of the experiment. qPCR data showed that *M. concilii* had an efficient biomass production at the end of the experiment. Additional data showed the same results, with slow, but steady production of methane after depletion of sulfate (Figure S4). Taken together, it is obvious that acetate conversion by aceticlastic methanogens in the presence of high sulfate and active aceticlastic sulfate reducers is possible. The concept of SRB and methanogen predominance in high-sulfate and low-sulfate environments, respectively, was established through the accumulation of results from a vast number of studies since 1980s (Ward and Winfrey, 1985; Widdel, 1988). Later, the coexistence of methanogens and SRB was observed in the presence of non-limiting sulfate concentrations in different environments (Dar et al., 2008). Coexistence of SRB and MA has been determined in organic-rich sediments with methane production rates accounting for <10% of the sulfate reduction rates (Crill and Martens, 1986). This provides a possible explanation for the coexistence of SRB and MA in this sulfate-rich medium as the concentration of acetate either exceeds the competition level or it is used noncompetitively.

2.4.3 New insights in metabolic flexibility

Interspecies hydrogen transfer has been studied in different anoxic environments (e.g., freshwater and marine sediments, flooded soil, landfills and sewage digesters) for long time and its importance and mechanism in complete mineralization of organic matter has been well documented (McInerney et al., 2008; Stams and Plugge, 2009). Moreover, interspecies formate transfer has been put forward as an alternative way of syntrophy and equally important for electron transfer between microorganisms (Boone et al., 1989; de Bok et al., 2002b; de Bok et al., 2004). Recent studies have described a new concept, direct interspecies electron transfer (DIET), where two *Geobacter* species form large, electrically conductive aggregates and establish electrical connections via the pili of both species to transfer electrons (Summers et al., 2010). In addition, DIET has been reported to occur in coculture of aceticlastic *Methanosaeta harundinacea* and exoelectrogen *Geobacter metallireducens*. In this coculture, *M. harundinacea* was found to convert acetate produced from ethanol metabolism and accept additional electrons *via* DIET for the reduction of carbon dioxide to methane; thus ethanol was converted to methane stoichiometrically (Rotaru et al., 2014). The authors have reported that transcript abundance of the genes for the enzymes necessary for the reduction of carbon to methane was high in the aggregates (Rotaru et al., 2014). Similar findings were reported previously in comparative genome analysis study of *Methanosarcina mazei* and *Methanosaeta thermophila* (Smith and Ingram-Smith, 2007). In this study, it was shown that the two genera use different enzymes to catalyze the first step of aceticlastic methanogenesis, but the majority of the core steps of the pathway were similar, except for the differences in electron transfer and energy conservation. Additionally, they identified the genes required for enzymes to catalyze CO₂ reduction to CH₄ in *Methanosaeta thermophila* genome (Smith and Ingram-Smith, 2007).

Given that *Methanosaeta* genus members are unable to use hydrogen directly to reduce CO₂, these findings become important to exhibit different metabolic capabilities of *Methanosaeta* species to survive under hydrogen and acetate deficient conditions and thrive in methanogenic environments. In another recent study, it was found that both wild type and hydrogenase-deletion mutant of *Methanococcus maripaludis* could produce methane by uptake of cathodic electrons from a graphite electrode, which serves another model to direct electron uptake by methanogens (Lohner et al., 2014). These newly proposed properties of *Methanosaeta* and *Methanococcus* indicate a variety of mechanisms for microbial electron uptake, and suggest that these methanogens may thrive in marine sediments in close contact with each other for the ultimate metabolism of substrates and that they are capable of responding to changes in environmental

conditions. Future experiments on environments with fluctuating sulfate levels could apply individual based technologies to reveal the *in situ* metabolism of the microorganisms present.

2.5 Conclusions

In conclusion, we show that an obligate acetoclastic methanogen, *Methanosaeta concilii*, leaked sufficient hydrogen to support the growth of a hydrogenotrophic sulfate reducer, *D. vulgaris*, or a hydrogenotrophic methanogen, *M. maripaludis*, when cultured together. The other important outcome of this study was the coexistence of the acetoclastic methanogen and an acetoclastic sulfate reducer in the presence of high sulfate concentration. These results bring more insights into the metabolic flexibility of methanogens and sulfate reducers residing in marine environments to adapt to changing environmental conditions and community.

Acknowledgements

We thank Prof. Dr. Fons Stams for helpful discussions, Ton van Gelder and Karina Bomholt Henriksen for technical assistance and Jan Gerritse (Deltares, The Netherlands) for his help with the hydrogen measurements. This work has been funded by the Wimek Graduate School of Wageningen University, Darwin Center for Biogeosciences (the Netherlands), the Danish National Research Foundation and the Max Planck Society (Germany). We also thank the funding support from the European Research Council (ERC) Advanced Grant ‘Microbial life under extreme energy limitation (MICROENERGY)’ awarded to Bo Barker Jørgensen under the European Union’s Seventh Framework Program.

Supplementary data

Table S1. PCR primers used in the study.

Primer Name	Sequence (5' – 3')	Reference
Bac8F	AGAGTTTGATYMTGGCTCAG	Juretschko et al., 1998
Bac338Rabc	GCWGCCWCCCGTAGGWGT	Daims et al., 1999
Arch806F	ATTAGATACCCSBGTAGTCC	Takai & Horikoshi, 2000
Arch958R	YCCGGCGTTGAMTCCAATT	DeLong, 1992
MS1b 585F	CCGGCCGGATAAGTCTCTT GA	Conklin et al., 2006
Sae 835R	GACAACGGTCGCACCGTGGCC	Conklin et al., 2006
MCC495F	TAAGG GCTGG GCAAGT	Yu et al., 2005
MCC832R	CACCT AGTTC GCAGAGTTTA	Yu et al., 2005

Table S2. Thermodynamic data of aqueous educts and products under standard conditions.

Compound	ΔG_f° (kJ mol ⁻¹)	ΔH_f° (kJ mol ⁻¹)	ΔV_f° (cm ³ mol ⁻¹)	Reference
CH ₃ COO ⁻	-369.4	-486.4	40.5	Shock and Helgeson (1990)
HCO ₃ ⁻	-586.9	-692.0	24.6	Wagman et al. (1982), Shock et al. (1997)
H ₂ O	-237.18	-285.83	18.02	Amend and Shock 2001
H ⁺	0.0	0.0	0.0	Shock et al. (1997)
H ₂	17.6	-4.2	25.2	Wagman et al. (1982), Shock and Helgeson (1990)
CH ₄	-34.47	-87.96	37.3	Shock and Helgeson (1990)
SO ₄ ²⁻	-744.96	-910.21	13.88	Shock et al. (1997)
HS ⁻	11.97	-16.12	20.65	Shock et al. (1997)

Table S3. Standard free energy of reaction (ΔG_r°), standard enthalpy of reaction (ΔH_r°) and standard volume of reaction (ΔV_r°) data of aqueous educts and products under standard conditions.

Reactions	ΔG_r° (kJ mol ⁻¹)	ΔH_r° (kJ mol ⁻¹)	ΔV_r° (mol ⁻¹)
CH ₃ COO ⁻ + 4 H ₂ O → 4 H ₂ + 2 HCO ₃ ⁻ + H ⁺	214.70	229.12	37.42
CH ₃ COO ⁻ + H ₂ O → CH ₄ + HCO ₃ ⁻	-14.74	-7.70	3.38
4 H ₂ + SO ₄ ²⁻ + H ⁺ → HS ⁻ + 4 H ₂ O	-262.06	-232.59	-21.95
CH ₃ COO ⁻ + SO ₄ ²⁻ → HS ⁻ + 2 HCO ₃ ⁻	-47.36	-3.47	15.47
HCO ₃ ⁻ + 4 H ₂ + H ⁺ → CH ₄ + 3 H ₂ O	-229.44	-236.82	-34.04

Figure S1. Monocultures of *Methanosaeta concilii* at 30°C (A) and 37°C (B).

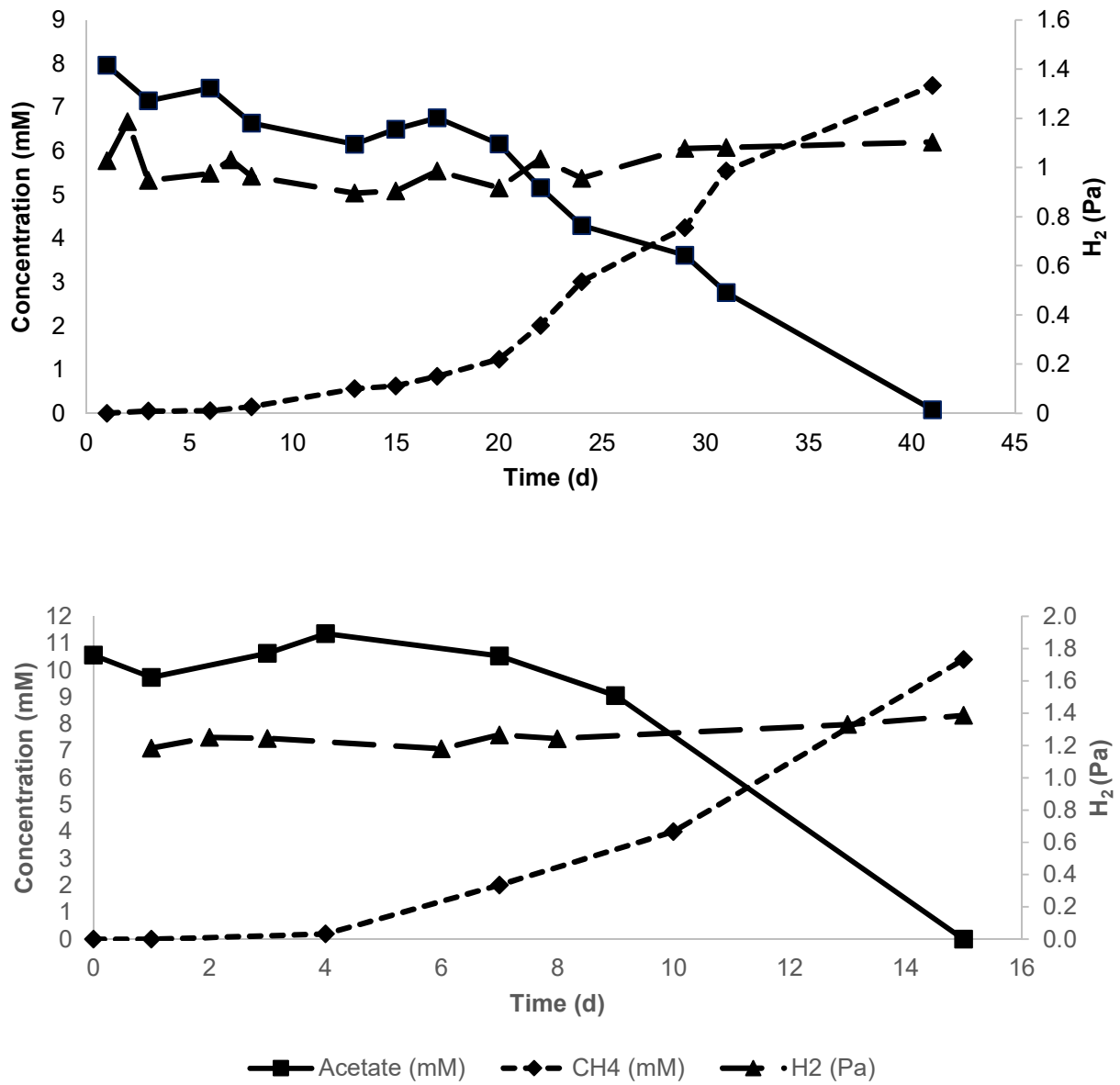


Figure S2. Monocultures of *Desulfovibrio vulgaris* without addition of H_2/CO_2 , with yeast extract only (A), with yeast extract and acetate (B).

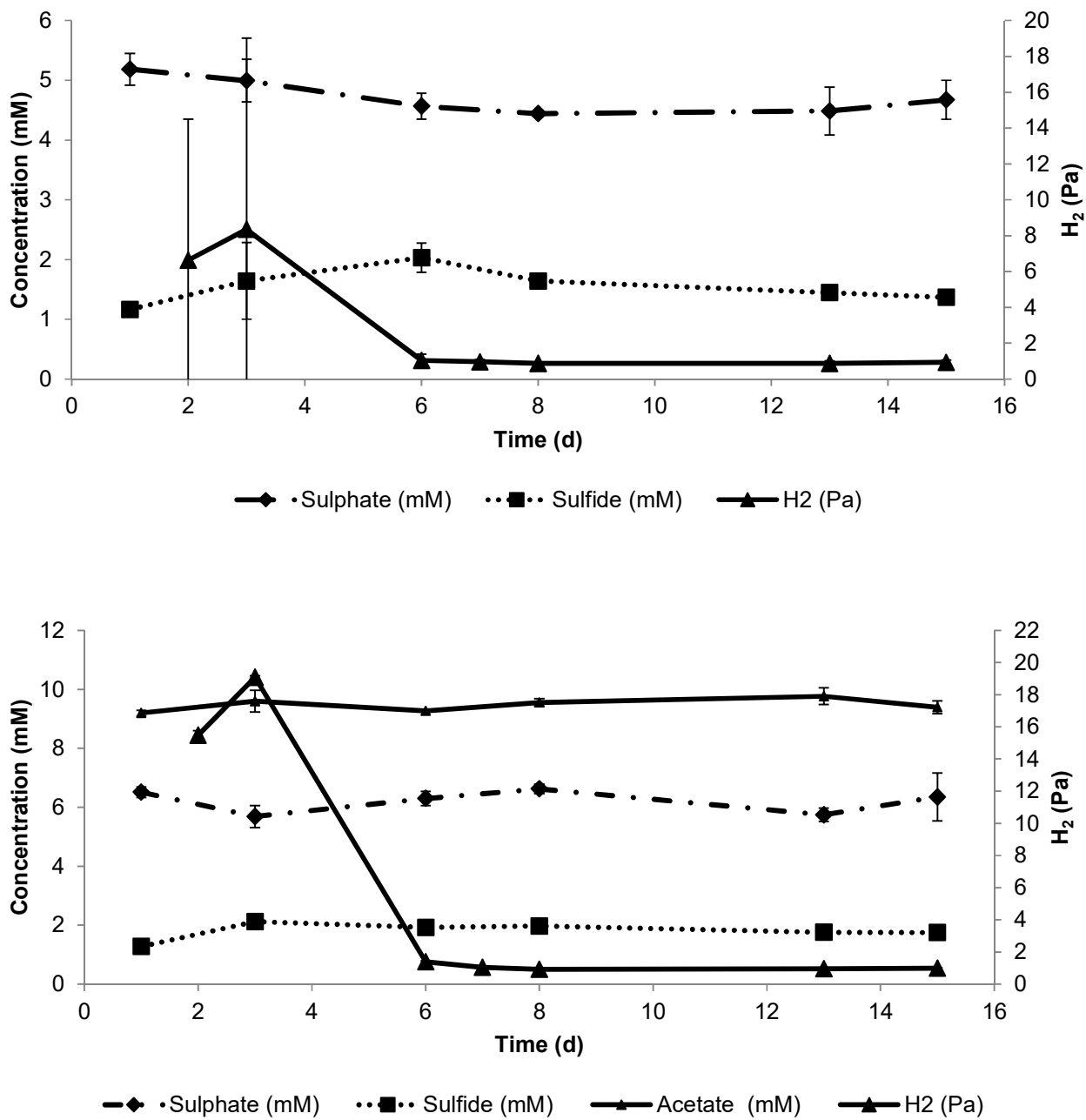


Figure S3. Growth in monocultures of *D. vulgaris* without addition of H_2/CO_2 but with yeast extract, without H_2/CO_2 , but with yeast extract plus acetate and *D. vulgaris* in coculture, quantified by qPCR.

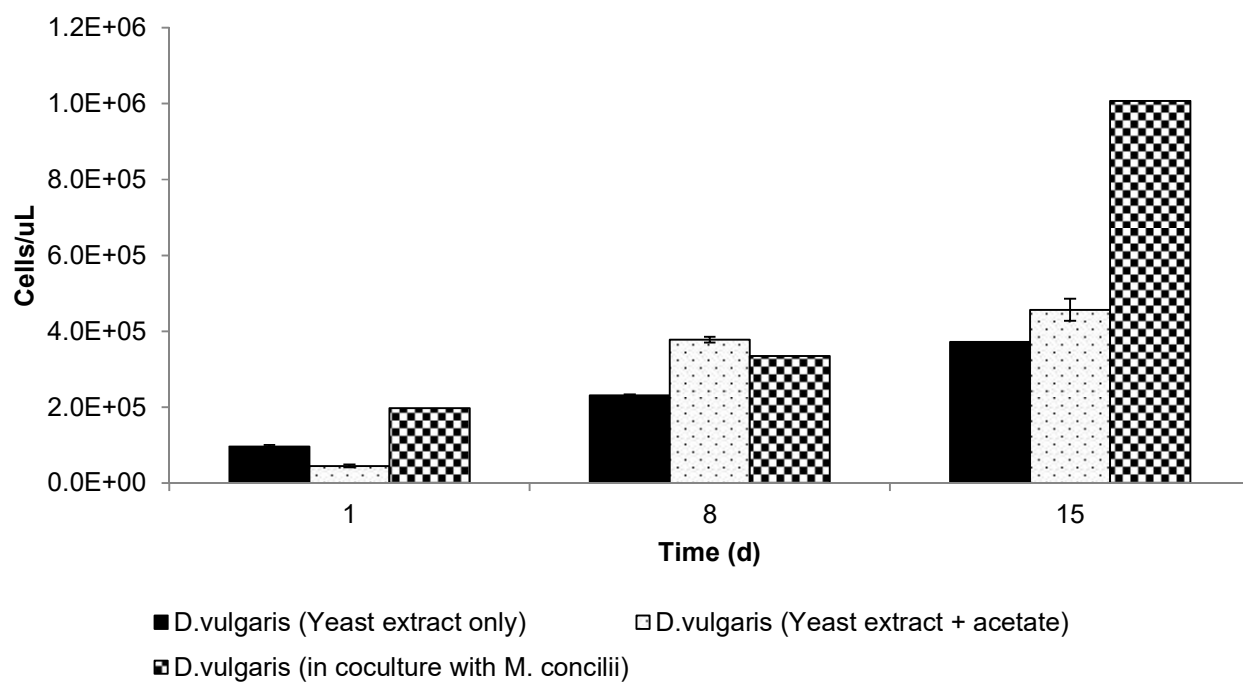
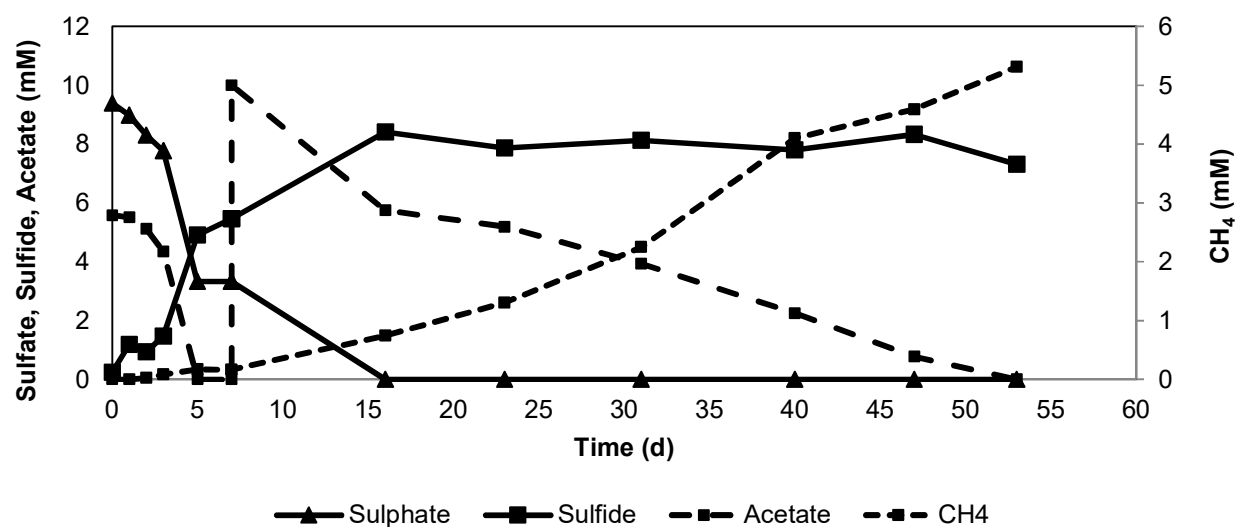


Figure S3. Growth of *Methanosaeta concilii* and *Desulfobacter latus* on acetate.



Chapter 3

Butyrate degradation by sulfate-reducing and methanogenic communities in anoxic sediments of Aarhus Bay, Denmark

Derya Ozuolmez, Alfons J.M. Stams, Caroline M. Plugge

-Manuscript in preparation for publication-

Abstract

The bacterial and archaeal communities enriched with butyrate in sediment slurries taken from different biogeochemical zones of Aarhus Bay, Denmark were analyzed. Sulfate was added at different concentrations (0, 3, 20 mM) to the sediment slurries and the slurries were incubated at 25°C and at 10°C. An immediate start of methanogenesis in sulfate zone slurries and sulfate reduction in methane zone slurries was observed. During butyrate conversion, sulfate reduction and methanogenesis occurred simultaneously. *Desulfobacteraceae*, *Desulfovibrionaceae*, *Desulfobulbaceae*, *Syntrophomonadaceae* and *Clostridiales* members involved in sulfate-dependent butyrate conversion in 25°C slurries. The obligate syntroph *Syntrophomonas* was enriched both in sulfate-amended and sulfate-free slurries indicating the co-occurrence of sulfate-dependent and syntrophic butyrate conversion. The low temperature sulfate-amended slurries contained mainly *Desulfobacteraceae* and uncultured *Firmicutes*, whereas sulfate-free slurries consisted of sequences related to uncultured *Firmicutes* and *Desulfobulbaceae*. Archaeal community analysis revealed the dominance of *Methanomicrobiaceae* in the slurries. *Methanosaetaceae* reached high abundance in the absence of sulfate, whereas the presence of *Methanosarcinaceae* was independent of the sulfate concentration, temperature and the origin of sediment. This study shows that sulfate reducers, syntrophs and methanogens are present together in the upper and lower parts of marine sediments and cooperate in the conversion of butyrate.

3.1 Introduction

Coastal marine ecosystems receive regular input of organic matter and nutrients from primary production of plankton, macroalgae and vascular plants, influx of rivers and remineralization of organic carbon (Jørgensen, 2006; Canfield et al., 2006). Most particulate organic matter is rapidly deposited on the coastal shelf (Jørgensen, 1983). High microbial activity in the sediment layers leads to the formation of distinct biogeochemical zones. The depth range of each zone varies strongly depending on chemical changes in the sediment pore water, the rates of sediment accumulation and replenishment of electron acceptors from overlying seawater (Jørgensen, 1983; Mitterer, 2010). In coastal marine sediments, the thickness of the oxic surface layer is can be just a few mm (Canfield et al., 2006). Where oxygen is depleted, the sediment becomes anoxic. In the anoxic part of the sediment, nitrate, iron, manganese, sulfate and carbon dioxide, in an order of decreasing energy gain, serve as terminal electron acceptors for the mineralization processes. In marine sediments, sulfate reduction is the predominant pathway, while methanogenesis becomes important in zones where sulfate is depleted (Jørgensen, 1982; Holmkvist et al., 2011; Bowles et al., 2014).

Anaerobic degradation of organic matter in sediments is a complex, sequential process involving a variety of physiologically different microorganisms (Jørgensen, 2006). The first step is an extracellular hydrolytic conversion of polymers, followed by fermentation of the monomers and oligomers to reduced organic compounds such as short chain fatty acids, alcohols, formate, H_2 and CO_2 . Organic acids and alcohols are further degraded to acetate, formate, H_2 and CO_2 . In general, sulfate reduction and methanogenesis are the terminal steps in the overall anaerobic degradation process (Schink and Stams, 2013; Muyzer and Stams, 2008; Stams and Plugge, 2009). Both sulfate reduction and methanogenesis are considered to be mutually exclusive in most environmental settings and controlled mainly by the amount of available sulfate (Roussel et al., 2015; O'Sullivan et al., 2013). When the concentration of sulfate is high, which is the case for marine environments, sulfate reducers are the main utilizers of hydrogen, formate and acetate (Hoehler et al., 1998; Bowles et al., 2014). They outcompete methanogens due to their higher affinity and lower threshold values for common substrates.

In sulfate-limited or sulfate-depleted sediments, organic matter is degraded through methanogenesis. In this case, hydrogen, formate and acetate that are released as end products of organic carbon degradation are converted to CH_4 and CO_2 by methanogens. In this way, a syntrophic relationship is established between microorganisms that degrade organic compounds and methanogens (Schink and Stams, 2013; McNerney et al., 2008). Syntrophic fatty acids

degradation is known as a rate limiting step of organic carbon degradation (Schink and Stams, 2013).

In the past, methanogenesis and sulfate reduction were considered to be separated in marine sediments based on sulfate availability (Cappenberg, 1974; Mountfort and Asher, 1981). Later, both sulfate reduction and methanogenesis were reported to occur simultaneously in anoxic marine environments where input of organic carbon is high (Maltby et al., 2016; Mitterer, 2010; Jørgensen and Parkes, 2010; Oremland, 1982; Senior et al., 1982; Holmer and Kristensen, 1994). In such environments, the use of non-competitive methylated substrates by methanogens was suggested to enable co-habitation of both functional groups of microbes (Visscher et al., 2003; Oremland and Polcin, 1982). However, several studies demonstrated the consumption of common substrates, H_2 and acetate, by both microbial groups in sulfate-rich sediments (Oremland and Taylor, 1978; Senior et al., 1982; Finke et al., 2007b). Sulfate reducers were detected in the methane zone in comparable numbers to the sulfate zone of Black Sea and Aarhus Bay (Leloup et al., 2007, 2009). The niche differentiation of the two groups of microbes is not fully understood. Thus far, syntrophic degradation of fatty acids in marine environments has received little attention.

Butyrate can be metabolized by direct sulfate reduction to acetate and CO_2 (Widdel, 1988; Muyzer and Stams, 2008) or by syntrophic associations of butyrate degrading bacteria with H_2 and/or acetate consuming sulfate reducer or methanogen (Table 1). Butyrate degradation coupled to sulfate reduction occurs in anaerobic ecosystems containing high sulfate, such as marine sediments, anaerobic digesters and aquifers (Jørgensen, 1982; Banat and Nedwell, 1983; Alphenaar et al., 1993; Visser et al., 1993; Kleikemper et al., 2002; Roest et al., 2005; Struchtemeyer et al., 2011). Syntrophic butyrate degraders were detected in similar quantities in the presence and absence of sulfate in anaerobic bioreactors (Roest et al., 2005) and others reported that syntrophic butyrate degraders were efficiently able to compete with sulfate reducers even in excess sulfate (Visser et al., 1993; Rebac et al., 1996). Methanogenesis has been observed in sulfate zones of marine sediments (Parkes et al., 1990; Kendall et al., 2006). Kendall and colleagues (2006) detected marine butyrate-degrading syntrophs in the sulfate zone and suggested that syntrophic interactions constitute an enormous methane source in marine sediments. Similarly, high methane concentrations were observed under high sulfate conditions in a hydrocarbon-contaminated aquifer where the investigators concluded that butyrate was metabolized mainly syntrophically (Kleikemper et al., 2002). Several other studies reported the existence of *Syntrophus* and *Syntrophomonas* genera in

different sulfate containing environments as a proof of syntrophic butyrate degradation (Dar et al., 2005; Winderl et al., 2008).

Table 1. Overview of reactions examined in this study. ΔG values were obtained from Thauer et al., 1977.

Reaction	Equation	ΔG° (kJ/reaction)*
Acetogenic reactions		
1	$\text{Butyrate}^- + 2 \text{H}_2\text{O} \rightarrow 2 \text{Acetate}^- + \text{H}^+ + 2 \text{H}_2$	+48.3
Sulfate-reducing reactions		
2	$\text{Butyrate}^- + 0.5 \text{SO}_4^{2-} \rightarrow 2 \text{Acetate}^- + 0.5 \text{HS}^- + 0.5 \text{H}^+$	-27.8
3	$4 \text{H}_2 + \text{SO}_4^{2-} + \text{H}^+ \rightarrow \text{HS}^- + 4 \text{H}_2\text{O}$	-151.9
4	$\text{Acetate}^- + \text{SO}_4^{2-} \rightarrow 2 \text{HCO}_3^- + \text{HS}^-$	-47.6
Methanogenic reactions		
5	$4 \text{H}_2 + \text{HCO}_3^- + \text{H}^+ \rightarrow \text{CH}_4 + 3 \text{H}_2\text{O}$	-135.6
6	$\text{Acetate}^- + \text{H}_2\text{O} \rightarrow \text{CH}_4 + \text{HCO}_3^-$	-31.0
Syntrophic butyrate conversion		
7	$\text{Butyrate}^- + 0.5 \text{HCO}_3^- + 0.5 \text{H}_2\text{O} \rightarrow 2 \text{Acetate}^- + 0.5 \text{CH}_4 + 0.5 \text{H}^+$	-19.5

It is obvious that the ability of some sulfate reducers to perform a syntrophic type of lifestyle enables them to thrive in high- and low-sulfate environments (Van Kuijk and Stams, 1995; McInerney et al., 2008). Thus, it is important to understand how sulfate reducers/syntrophs interact with methanogens in the presence and absence of sulfate.

In this study, we investigated butyrate-degrading communities from sediment of the sulfate, sulfate-methane transition and methane zone of Aarhus Bay, Denmark. We established batch slurry incubations and applied different sulfate concentrations (0, 3, 20 mM) to see if and which methanogens would contribute to butyrate degradation in the presence or absence of sulfate. Another objective was to investigate which butyrate-utilizing sulfate reducers/syntrophs become dominant in response to different sulfate concentrations in sulfate, sulfate-methane transition and methane zone slurries.

3.2 Materials and methods

3.2.1 Sediment sampling

Sediment was collected during a research cruise in May 2011, in Aarhus Bay, Denmark. The studied site, Station M1, is located in the central part of the Bay, at position 56°07'066"N, 10°20'793"E. The *in situ* temperature was ~9°C and the water depth was 15 m. Two 3-m-long gravity cores were retrieved; one of them was sectioned in 10 cm depth intervals for physical, chemical and molecular analyses and the other one was kept intact in the core liners, in sealed gas-tight plastic bags containing AnaeroGen sackets (Oxoid xx) at 4°C until further processed.

3.2.2 Sediment pore water analysis

Methane, sulfate and sulfide analysis from sediment pore water were performed on the sampling day at the laboratories of Center for Geomicrobiology, Aarhus University. Methane concentration was determined in a sediment sample of 2.5 cm³. The sample was taken immediately after retrieval of the sediment core and transferred to a 25 ml serum vial with 4 ml 2.5% NaOH, immediately capped with a butyl rubber stopper, crimp-sealed, shaken vigorously and stored upside down until measurement. After equilibration (~an hour), the headspace composition was analyzed on a gas chromatograph (5890A, Hewlett Packard) equipped with a packed stainless steel Porapak-Q column (6 ft., 0.125 in., 80/100 mesh, Agilent Technology) and a flame ionization detector. Helium was used as a carrier gas at a flow rate of 30 ml/min.

Sulfate and sulfide were quantified in pore water extracted directly from sediment. Rhizon samplers (Rhizosphere Research Products, Wageningen, Netherlands) were inserted into the core at 10 cm intervals through holes that were drilled in the plastic corer and pore water was collected in 5 ml vacuumed plastic syringe connected to Rhizon samplers. For sulfate analysis, subsamples of pore water was degassed with oxygen-free CO₂ to lower the pH and remove hydrogen sulfide. Sulfate measurement was done using Dionex (Sunnyvale, CA) ion chromatography system 50 equipped with AS18 column. The eluent was 20-32 mM KOH at a flow rate of 1 ml/min. For sulfide analysis, subsamples were mixed 1:1 (v/v) with 5% (w/v) zinc acetate. Samples were diluted in MiliQ water and diamine reagent was added. After color development, sulfide concentration was measured by microplate reader at 670 nm.

3.2.3 Sediment slurry incubations

Sediments from three different biogeochemical zones were used to establish replicate sediment slurries. Zones were defined based on sulfate and methane concentrations determined using pore water extracted from sediment during sampling cruise. The sulfate concentration decreased from 18.5 mM at 15 cm of the core to a low background value at 170 cm. Methane increased steeply with depth below 120 cm and reached a plateau of 2 mM at 225 cm (Fig S1). The sediment core was divided into three pieces representing the sulfate zone (SR) (15-120 cm), the sulfate-methane transition zone (SMTZ) (120-170 cm) and the methane zone (MZ) (170-300 cm).

Stored sediment cores were processed under aseptic and anaerobic conditions in the laboratory. Subsamples representing a particular biogeochemical zone were mixed in an anaerobic chamber and used as inoculum for sediment slurry enrichments. 100 ml of the homogenized sediment from each zone was mixed with 300 ml of anaerobic mineral salts medium in 1L serum bottles. The medium composition was as followed (g/L): KH_2PO_4 (0.41), $\text{Na}_2\text{HPO}_4 \cdot 2\text{H}_2\text{O}$ (0.53), NH_4Cl (0.3), $\text{CaCl}_2 \cdot 2\text{H}_2\text{O}$ (0.11), $\text{MgCl}_2 \cdot 6\text{H}_2\text{O}$ (3), NaHCO_3 (4), $\text{Na}_2\text{S} \cdot 9\text{H}_2\text{O}$ (0.024), KCL (0.5), NaCl (25). The medium was supplemented with 1 ml/liter of acid trace element solution (50 mM HCl, 1 mM H_3BO_3 , 0.5 mM MnCl_2 , 7.5 mM FeCl_2 , 0.5 mM CoCl_2 , 0.1 mM NiCl_2 , 0.5 mM ZnCl_2), 1 ml/liter of alkaline trace element solution (10 mM NaOH, 0.1 mM Na_2SeO_3 , 0.1 mM Na_2WO_4 , 0.1 mM Na_2MoO_4) and 10 ml/liter vitamin solution (Biotin 20 mg/l, Nicotinamid 200 mg/l, p-Aminobenzoic acid 100 mg/l, Thiamin 200 mg/l, Panthotenic acid 100 mg/l, Pyridoxamine 500 mg/l, Cyanocobalamine 100 mg/l, Riboflavin 100 mg/l). Bottles were closed with butyl rubber stoppers and the headspace was exchanged with N_2/CO_2 (80:20%, v/v). 10 mM butyrate was used as carbon source with and without 20 mM sulfate in sulfate zone and methane zone slurries, and with 3 mM and 20 mM sulfate for sulfate-methane transition zone slurries as electron acceptor. Control bottles were prepared in the same manner, without addition of butyrate. One set of the bottles representing each condition in duplicate was incubated at 10°C to mimic *in situ* temperature (Dale et al., 2008) and the other set was kept at 25°C statically throughout the experiment. Regular liquid and gas sampling was performed to monitor substrate consumption, product formation and to carry out molecular analysis. Regular additions of butyrate and/or sulfate were done as soon as they were depleted to maintain the slurry conditions same.

3.2.4 Analytical methods

CH₄ in the headspace of slurries was analyzed by gas chromatography with a Shimadzu GC-14B (Shimadzu, Kyoto, Japan) equipped with a packed column (Molsieve 13X, 60-80 mesh, 2 m length, 3 mm internal diameter; Varian, Middelburg, The Netherlands) and a thermal conductivity detector set at 70mA. The oven temperature and the injector temperatures were both 100°C. The detector temperature was 150°C. Argon was the carrier gas at a flow rate of 30 ml min⁻¹.

Volatile fatty acids from centrifuged (10,000 X *g*, 10 min) samples of the sediment slurries were analyzed by HPLC system equipped with a Varian column (Metacarb 67H 300x6.5 mm, Middelburg, The Netherlands) connected to a UV and Refractive Index (RI) detector. 10 mM sulfuric acid was used as eluent and sodium crotonate as internal standard. The flow rate was 0.8 ml min⁻¹ and analyses were carried out at 30°C. Data analyses were performed using ChromQuest (Thermo Scientific, Waltham, MA, USA) and Chromeleon software (Thermo Scientific, Waltham, MA).

Sulfate concentrations were analyzed by Ion Chromatography system equipped with an AS22 column (4x250 mm) and ED 40 electrochemical detector (Dionex, Sunnyvale, CA). The eluents were 1.7 mM NaHCO₃ and 1.8 mM Na₂CO₃. The analyses were conducted with a flow rate of 1.2 ml min⁻¹ at 35°C. Sodium bromide was used as internal standard.

Sulfide measurements were done using methylene blue method (Cline, 1969). Samples were 1:1 diluted with 5% (w/v) zinc acetate solution, directly after sampling, to precipitate all sulfide. 4.45 ml of deionized water, 500 µl of reagent A (2 g/l dimethylparaphenylenediamine and 200 ml/l H₂SO₄) and 50 µl of reagent B (1 g/l Fe((NH₄)(SO₄))₂·12 H₂O and 0.2 ml/l H₂SO₄) was added concurrently and mixed. The solution was stored for at least 10 minutes at room temperature. After color development, the concentration was measured on a MERCK Spectroquant® Multy colorimeter (Merck Millipore, Darmstadt, Germany) at 670nm. Demi-water was used as a blank.

3.2.5 DNA extraction

Genomic DNA was extracted from the sediment and enrichment slurry samples that were taken at different time points using the FastDNA SPIN Kit for Soil (MP Biomedicals, OH) according to manufacturer's protocol. Adaptation of the commercial protocol was carried out to increase the DNA yield. 5 ml sediment or slurry sample were suspended in 10 ml of phosphate-buffered saline (PBS), sonicated at low power to detach cells from the solid phase and was centrifuged at 4700 *g*

for 20 min. The supernatant was discarded and remaining pellet was re-suspended in 10 ml 0.5 M EDTA, pH 8, and incubated overnight at 4°C to dissolve humic substances. After incubation, the suspension was centrifuged at 4700 *g* for 10 min., washed with PBS and DNA extraction procedures were applied to the pellet. The DNA was quantified with a Nanodrop ND-1000 spectrophotometer (Nanodrop Technologies, Wilmington, DE).

3.2.6 DGGE analysis

DNA from one replicate of all the slurries was used for DGGE analysis. Amplification of the V6-V8 region of the bacterial 16S rRNA was performed using the primer pair F-968-GC (5'-AACGCGAAGAACCTTAC-3') and R-1401 (5'-CGGTGTGTACAAGACCC-3') (Nübel et al., 1996). PCR was performed using GoTaq DNA Polymerase Kit (Promega, Madison, WI). The 50 µl reaction mixture contained 10 µl GoTaq buffer, 10 µM of each primer, 1 µl of dNTP solution and 1 µl of genomic DNA. PCR was carried out by using an initial denaturation step at 95°C for 5 min, followed by 35 cycles of denaturation step at 95°C for 30 s, annealing step at 52°C for 40 s, elongation step at 72°C for 60 s., and a final elongation step at 72°C for 10 min. The V3 region of the archaeal 16S rRNA gene fragments was amplified with primers ARC344f-GC (5'-ACGGGGYGCAGCAGGCGCGA-3') and ARC519r (5'-GWATTACCGCGGCKGCTG-3') (Yu et al., 2008) using the GoTaq DNA Polymerase Kit (Promega, Madison, WI). PCR conditions were as followed: an initial denaturation step at 95°C for 5 min; followed by 10 cycles of denaturation step at 95°C for 30 s, annealing step at 61°C for 40 s (-0.5 °C /cycle), elongation step at 72°C for 45 s; 25 cycles of denaturation step at 95°C for 30 s, annealing step at 56°C for 40 s, elongation step at 72°C for 45 s; and final elongation step at 72°C for 10 min. Forward primers had a GC clamp of 40 bp attached to the 5' end (Yu et al., 2008). The presence and sizes of the amplification products were determined by agarose (1%) gel electrophoresis using the Smart Ladder (Eurogentec) as molecular weight marker. SYBR Safe®-stained gel pictures were digitally recorded.

DGGE was performed as described by Muyzer et al. (1993) using the DCode system (BioRad Laboratories, Hercules, CA). A denaturing gradient of 30-60% for bacteria and 40-60% for archaea were used as recommended by Yu et al (2008). Gels were initially run at 200 V for 10 min to facilitate the access of PCR products into the denaturing gradient gel, and then at a constant voltage of 100 V for 16 h at 60°C in 1X TAE buffer. After electrophoresis, the gels were stained with AgNO₃ according to Sanguinetti et al. (1994). DGGE gels were scanned with a BioRad GS-800 Calibrated Densitometer and analyzed using the BioNumerics® software version 4.6 (Applied

Maths, Sint-Martens-Latem, Belgium). The Dice coefficient was used to determine the similarity between DGGE fingerprints by calculating the similarity indices of the densitometric curves of the profiles and dendrograms for bacterial and archaeal DGGE profiles were created using Unweighted Pair Group Method Analysis (UPGMA).

3.2.7 16S rRNA gene amplicon pyrosequencing

Bacterial 16S rRNA gene fragments were amplified using barcoded primers covering the V₁-V₂ region of the bacterial 16S rRNA gene. The forward primer consisted of the 27F-DegS primer (5'- GTTYGATYMTGGCTCAG- 3') (van den Bogert et al., 2011) appended with the titanium sequencing adaptor A (5'- CCATCTCATCCCTGCGTGTCTCCGACTCAG- 3') and an 8 nucleotide sample specific barcode (Hamady et al., 2008) at the 5' end. An equimolar mix of two reverse primers was used i.e. 338RI (5'- GCWGCCTCCCGTAGGAGT- 3') and 338RII (5'- GCWGCCACCCGTAGG TGT- 3') (Daims et al., 1999) that carried the titanium adaptor B (5'- CCTATCCCCTGTGTGCCTTGGCAG TCTCAG- 3') at the 5' end. Sequences of both titanium adaptors were purchased from GATC Biotech (Konstanz, Germany).

Genomic DNA was diluted to a concentration of 20 ng/μl based on Qubit® 2.0 fluorometer readings. PCR was performed using a G5000 thermocycler (Gene Technologies, Braintree, United Kingdom). 100μl PCR mixture contained 20 μl of 5× HF buffer (Finnzymes, Vantaa, Finland), 2μl PCR Grade Nucleotide Mix (Roche Diagnostic GmbH, Mannheim, Germany), 1μl of Phusion hot start II High-Fidelity DNA polymerase (2U/μl; Finnzymes), 500 nM of the reverse primer mix and the forward primer (Biolegio BV, Nijmegen, The Netherlands), 2 μl (40 ng) template, and 65 μl nuclease free water. PCR was performed using the following conditions: 98°C for 30 s to activate the polymerase, followed by 30 cycles of denaturation at 98°C for 10 s, annealing at 56°C for 20 s, elongation at 72°C for 20 s, and a final extension at 72°C for 10 min. Five μl of the PCR products (approximately 450 bp) were analyzed by 1% (w/v) agarose gel electrophoresis, containing 1× SYBR Safe (Invitrogen, Carlsbad, CA) to verify the right length of the amplicons. PCR products were purified using High Pure PCR Cleanup Micro Kit (Roche Diagnostics, Germany) according to the manufacturer's instructions and DNA concentration of gel-purified amplicons was measured by Qubit® 2.0 Fluorometer (Life Technologies, Germany). Purified PCR products were mixed in equimolar amounts and run again on an agarose gel. This was followed by excision of bands and purification using a DNA gel extraction kit (Millipore, Massachusetts, 01821). DNA concentration was measured using Qubit and 1 μl purified equimolar pool of PCR product was analyzed on 1%

agarose gel. Samples were analyzed by pyrosequencing using an FLX genome sequencer in combination with titanium chemistry (GATC Biotech AG, Konstanz, Germany).

3.2.8 Analysis and interpretation of the pyrosequencing data

Pyrosequencing data was analyzed using the Quantitative Insights Into Microbial Ecology (QIIME) 1.8.0 pipeline (Caporaso et al., 2010). Sequence reads were initially filtered using default parameters and denoised (Bragg et al., 2012) for removing low quality reads. UCHIME was used to remove chimeric sequences from pre-processed data from the dataset (Edgar, 2010). From the remaining set of high quality 16S rRNA gene sequences, operational taxonomic units (OTUs) were defined at a 97% identity level. A representative sequence from each OTU was aligned using PyNAST (DeSantis et al., 2006). The taxonomic affiliation of each OTU was determined at an identity threshold of 97% using UCLUST algorithm (Edgar, 2010) and SILVA database as a reference (Pruesse et al., 2007). The relative amount of reads of every OTU to the total amount of reads per sample was quantified and the average relative amount of reads per representative OTU of each slurry sample was calculated.

3.2.9 Illumina MiSeq analysis of archaeal community

Extracted DNA from the samples taken on the last incubation day from all slurries was used for archaeal community analysis. Barcoded amplicons were generated using a two-step PCR method that was shown to reduce the impact of barcoded primers on the outcome of microbial profiling (Berry et al., 2011). First amplification of archaeal 16S rRNA gene fragments was done using primers 518F (5'-CAGCMGCCGCGGTAA-3') (Wang and Qian, 2009) and 905R (5'-CCCGCCAATTCTTTAAGTTTC-3') (Kvist et al., 2007). PCRs were performed using a SensoQuest Labcycler (Göttingen, Germany). PCR amplification was performed in a total volume of 50 µl containing 500 nM of each forward and reverse primer (Biolegio BV), 1 unit of Phusion DNA polymerase (Thermo Scientific), 10 µl of HF-buffer, 200 µM dNTP mix, made to a total volume of 50 µl with nuclease free sterile water. The PCR program was as followed: denaturing at 98°C for 30 s, followed by 25 cycles of denaturing at 98°C for 10 s, annealing at 60°C for 20 s, extension at 72°C for 20 s, followed by a final extension step at 72°C for 10 min. PCR products were confirmed by agarose gel electrophoresis containing 1× SYBR Safe (Invitrogen, Carlsbad, CA). A second PCR was employed to add an 8 nucleotide sample-specific barcode to the 5'- and 3'-end of PCR products

(Ramiro-Garcia et al., 2016). Each PCR reaction with a final volume of 100 μ L contained 5 μ L of the first PCR product, 5 μ L each of 10 μ M barcoded forward and reverse primers (Biolegio BV), 200 μ M PCR Grade dNTP mix (Roche Diagnostics), 2 units of Phusion[®] Hot Start II High-Fidelity DNA polymerase (Thermo Scientific) and 20 μ L of HF buffer (Finnzymes, Vantaa, Finland). Amplification consisted of an initial denaturation at 98 °C for 30 s; 5 cycles of denaturation at 98 °C for 10 s, annealing at 52 °C for 20 s, and elongation at 72 °C for 20 s; and a final extension at 72 °C for 10 min. PCR products were purified using the HighPrep[™] PCR clean-up system (MagBio Genomics Inc., Gaithersburg, MD). Amplicons were quantified using Qubit (Invitrogen, Bleiswijk, The Netherlands). Afterwards, barcoded samples were pooled in equimolar quantities, purified using the MagBio HighPrep PCR- 96 well protocol and then quantified using Qubit. Samples were sequenced at GATC Biotech AG (Konstanz, Germany) by Illumina Miseq sequencing.

16S rRNA gene sequencing data was analysed using NG-Tax, an in-house pipeline (Ramiro-Garcia et al., 2016). Paired-end libraries were filtered to contain only read pairs with perfectly matching barcodes, and those barcodes were used to demultiplex reads by sample. Finally operational taxonomic units (OTUs) were defined using an open reference approach, and taxonomy was assigned to those OTUs using the SILVA 16S rRNA gene reference database (Quast et al., 2013). Microbial composition plots were generated using a workflow based on Quantitative Insights Into Microbial Ecology (QIIME) v1.2 (Caporaso et al., 2010).

3.2.10 Statistical analysis

Redundancy analysis was performed as implemented in the CANOCO 5 software package (Biometris, Wageningen, The Netherlands) in order to assess to what extent experimental variables influenced the microbial community composition. The experimental variables tested were the incubation temperature, total concentrations of sulfate, butyrate, acetate and methane consumed/produced by the end of the incubations. A Monte Carlo permutation test based on 499 random permutations were used to determine which of the experimental variables significantly contributed to the observed variance in the composition of microbial communities at the order (for Bacteria) and family level (for Archaea). Orders and families of at least 5% relative abundance in any sample were included in the analysis. The community structure was visualized via ordination triplots with scaling focused on intersample differences.

Correlations between bacterial and archaeal groups and experimental parameters were determined by means of the two-tailed Spearman's Rank Order Correlation test using the statistical

software SPSS Statistics (IBM SPSS Statistics, Version 22, IBM Corp., Armonk, NY). A statistical significance level of 5% was applied.

3.3 Results

3.3.1 Sampling site geochemistry

Aarhus Bay is a shallow semi-enclosed embayment on the transition between the North Sea and Baltic Sea and characterized by elevated primary production during the summer months (Glud et al., 2003). Two 3-m-long gravity cores were retrieved and one of the cores was used to carry out pore water analysis to measure methane, sulfate and sulfide throughout the core on the same day. According to the pore water analysis results, the sulfate zone was determined to be located between 0 cm and 120 cm, sulfate-methane transition zone (SMTZ) between 120 cm and 170 cm and methane zone between 170 cm and 300 cm (Fig S1).

3.3.2 Sediment slurry enrichments

Sediment slurries consisting of the sediment sample taken from the sulfate, sulfate-methane transition and methane zones were analyzed for substrate consumption and product formation at different time points throughout the incubation period. Total amounts of the butyrate and sulfate consumed and acetate, sulfide and methane produced in all slurries were listed in Table S1.

3.3.2.1 Sulfate zone sediment slurries

Sulfate zone sediment slurries were incubated for 514 days at 25°C and 10°C (Fig 1). Conversion of butyrate in sulfate-containing slurries started after 12 days of incubation (Fig 1B, 1D). Repeated additions of butyrate and sulfate caused a steady increase in acetate and sulfide. Methane formation was observed after 309 days at 25°C and after 260 days at 10°C, and increased with time (Fig 1B, 1D).

In the methanogenic slurries, where no additional sulfate was added, about 1 mM sulfate was measured at the start of the incubation, which presumably originated from the sediment (Fig 1A, 1C). In the first 40 days of incubation at 25°C, conversion of butyrate coupled to sulfate reduction occurred. Methane formation started on day 50, after sulfate had been depleted, indicating syntrophic butyrate conversion. Repeated additions of butyrate yielded high methane and acetate accumulation. Acetate was gradually consumed after day 203 at 25°C, and decreased to 2359

$\mu\text{mol}/\text{bottle}$ from 24752 $\mu\text{mol}/\text{bottle}$ on day 430 (Fig 1A). Butyrate conversion in the 10°C slurry was rather slow (Fig 1C).

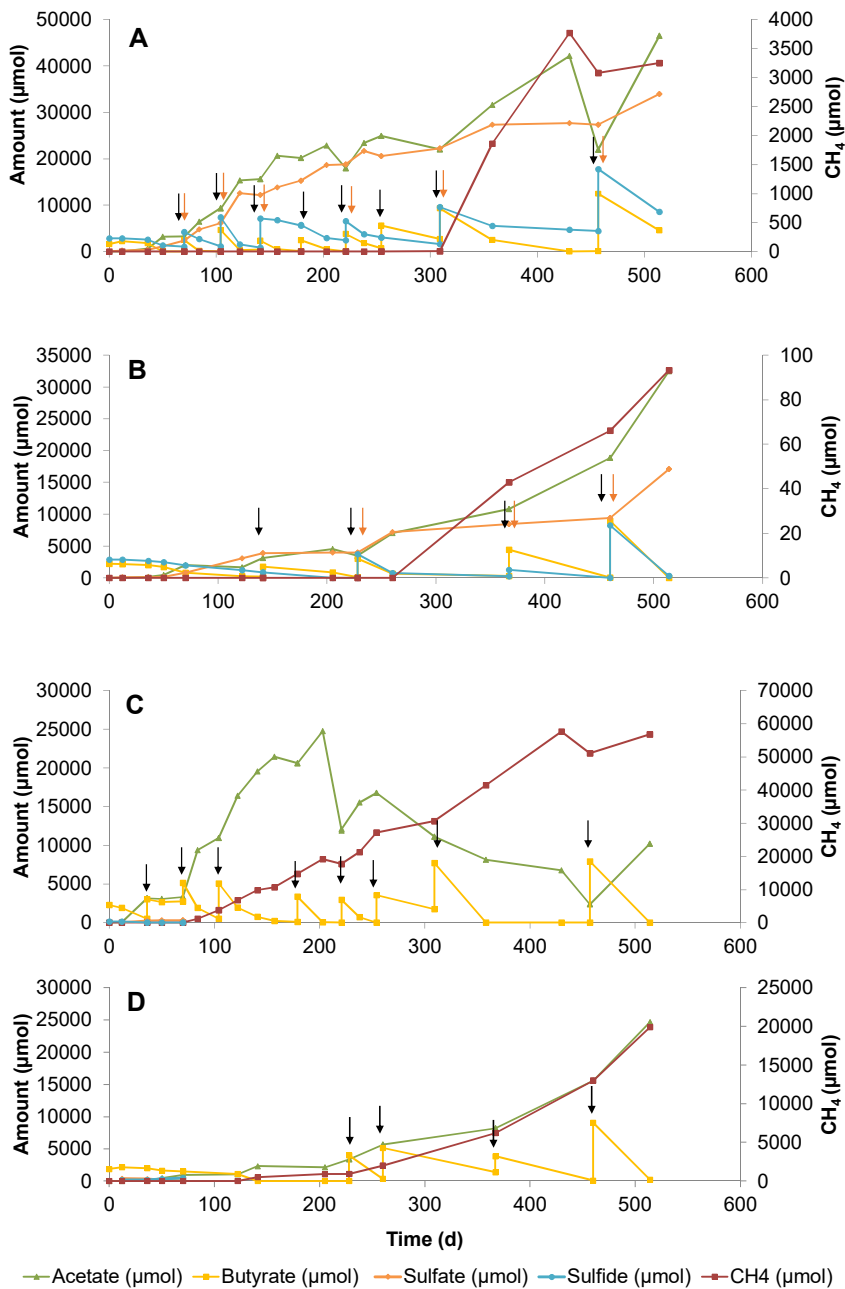


Figure 1. Changes in butyrate, sulfate, acetate, sulfide and methane concentrations during 514 days of incubation in sediment slurry enrichments constituted of sulfate zone sediment (A) Slurry B4, with sulfate addition at 25°C, (B) Slurry B7, with sulfate addition at 10°C, (C) Slurry B1, without sulfate addition at 25°C, (D) Slurry B5, without sulfate addition at 10°C. Arrows denote the time points for the additions of sulfate (red) and butyrate (black).

Trace amounts of sulfate that originated from the sediment depleted within 70 days and methane formation started on day 122. The methane concentration measured in the 10°C slurry at the end of the incubation period was three times less than in the 25°C slurry.

3.3.2.2 Sulfate-methane transition zone sediment slurries

Slurries of SMTZ sediments with low (3 mM) and high (20 mM) sulfate were incubated for 571 days at 25°C and 10°C (Fig 2). Butyrate was converted in high sulfate slurries similarly at both temperatures (Fig 2B, 2D). Acetate and sulfide concentrations increased by repeated butyrate and sulfate re-feeds. Methane production started on day 120 at 25°C (Fig 2B) and on day 229 at 10°C (Fig 2D) and increased slowly. The amount of methane ranged between 8 and 48 µmol/bottle at both temperatures until 500 days. However it rapidly reached to 4183 µmol/bottle after 500 days in slurry at 25°C.

Concerning low-sulfate containing slurries, the total butyrate concentration converted in the 25°C slurry was slightly higher as in the 10°C slurry (Fig 2A, 2C). Two times higher methane amount was measured in the 25°C slurry compared to the 10°C slurry. Acetate accumulated in the 10°C slurry (Fig 2C), whereas no acetate was observed in the 25°C slurry (Fig 2A), especially after 300 days of incubation.

3.3.2.3 Methanogenic zone sediment slurries

Methanogenic zone sediment slurries were incubated for 570 days at 25°C and 10°C with and without sulfate (20mM) (Fig 3). In the 25°C slurries, conversion of butyrate started directly (Fig 3A, 3B). Repeated additions of butyrate and/or sulfate led to a steady increase in acetate and sulfide. Methane formation in the sulfidogenic slurry was observed after 90 days at 25°C (Fig 3A) and increased with time, whereas no methane was detected at 10°C (Fig 3C) during the whole incubation period.

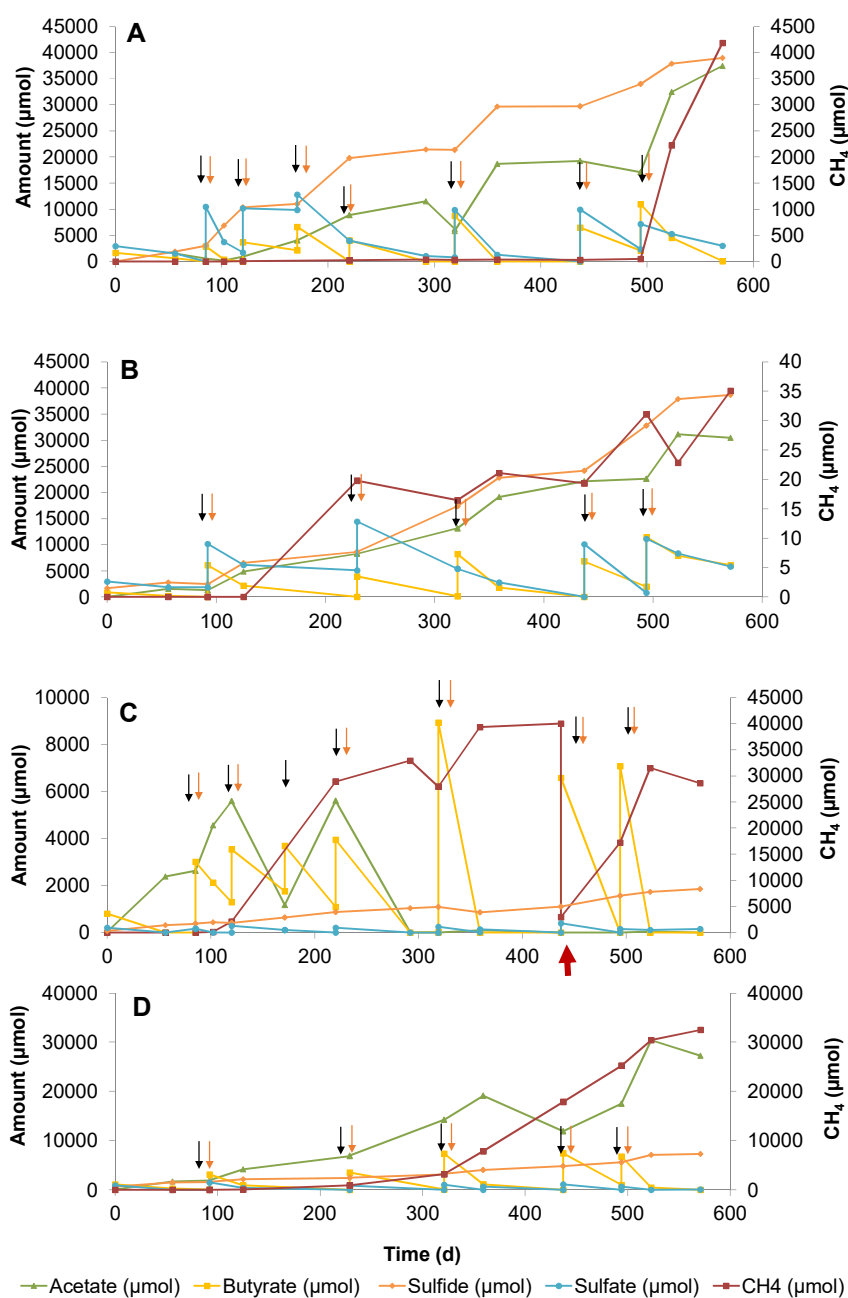


Figure 2. Changes in butyrate, sulfate, acetate, sulfide and methane concentrations during 571 days of incubation in sediment slurry enrichments constituted of sulfate-methane transition zone sediment (A) Slurry B₃, with 20mM sulfate addition at 25°C, (B) Slurry B₇, with 20mM sulfate addition at 10°C, (C) Slurry B₁, with 3mM sulfate addition at 25°C, (D) Slurry B₆ with 3mM sulfate addition at 10°C. Arrows denote the time points for the additions of sulfate (red) and butyrate (black). The red arrow in figure 2C indicates the time point that the excess amount of gas was exhausted from the headspace.

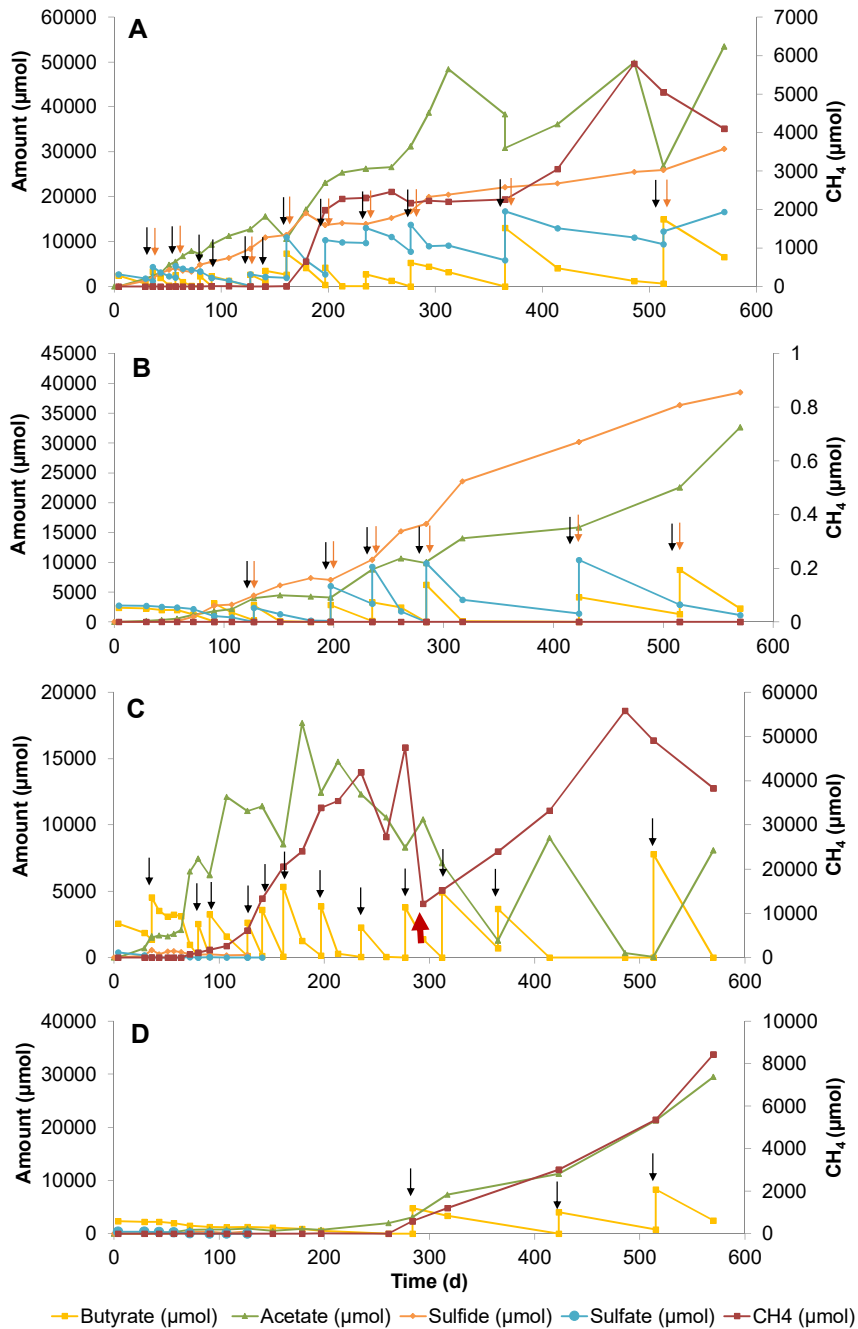


Figure 3. Changes in butyrate, sulfate, acetate, sulfide and methane concentrations during 570 days of incubation in sediment slurry enrichments constituted of methane zone sediment (A) Slurry B3, with 20mM sulfate addition at 25°C, (B) Slurry B2, with 20mM sulfate addition at 10°C, (C) Slurry B5, without sulfate addition at 25°C. (D) Slurry B8, without sulfate addition at 10°C. Arrows denote the time points for the additions of sulfate (red) and butyrate (black). The red arrow in figure 3C indicates the time point that the excess amount of gas was exhausted from the headspace.

Sulfate reduction and methanogenesis co-occurred in the sulfidogenic slurry incubated at 25°C (Fig 3A). The fastest butyrate conversion was observed in the methanogenic slurry at 25°C (Fig 3B). Trace amounts of sulfate detected in the slurry at the beginning of incubation were reduced during butyrate conversion within the first 40 days. Methane was detected at day 64 and increased rapidly due to fast conversion of butyrate. Hence, acetate and methane amounts ascended steeply within 200 days. A steady acetate consumption occurred after day 214. Even though produced after butyrate feeds, acetate was consumed again almost totally after 500 days of incubation. Since the methane pressure in this slurry reached a very high amount at day 277, excess headspace gas was exhausted (Fig 3B). Butyrate conversion in the methanogenic slurry at 10°C proceeded much slower. Methane production started at day 200 and increased gradually. In total, 11 times less methane was produced in the methanogenic slurry incubated at 10°C compared to the one incubated at 25°C within 570 days.

3.3.3 Cluster analysis of DGGE banding pattern

The bacterial DGGE profiles of enrichment slurries revealed that each sample taken at different time points harbored a characteristic community, illustrated by the different banding patterns. However, archaeal DGGE banding patterns of slurries were mostly similar along the incubation period except for some bands which appeared in methanogenic slurries toward the end of experiment. These bands possibly represented the dominant archaeal fractions in the enrichment slurries.

Cluster analysis of the DGGE patterns showed that all bacterial profiles corresponding to a certain sediment depth were grouped into closely related clusters and were separated from the profiles belonging to the other sediment depths (Fig S2). Each cluster representing each depth zone had several sub-clusters with less than 90% similarity which revealed that different bacterial groups were enriched in slurries incubated under different conditions along the experiment.

Archaeal DGGE cluster analysis revealed a different clustering pattern compared to the bacterial clustering analysis (Fig S3). SZ slurry samples taken within the first 140 days of the experiment grouped together with the similarity ranging between 80% and 90%. As the incubation continued, the archaeal community changed and several sub-clusters consisting of mostly two different time samples were formed, where their similarities to each other were around 70%. SMTZ slurry samples grouped together except for the samples taken at the last sampling time indicating that the microbial communities in each slurry differentiated by the end of the experiment. MZ

slurry samples gathered in several sub-clusters exhibiting variety in community compositions at different incubation phases. The samples belonging to the last sampling time of all MZ slurries and SMTZ B3 and B6 slurries were grouped in the same sub-cluster, giving an indication that the enriched archaeal community in different slurries was similar.

3.3.4 Bacterial community composition and structure

To get insight into the microbial composition in the original sediment belonging to each zone and in slurry samples, PCR amplified partial 16S rRNA gene fragments obtained from the sediment and from the slurries at the last incubation day were sequenced. After filtering and trimming, between 3202 and 18687 high quality sequences were found per sample (Table S2) and these clustered in 62–133 operational taxonomic units (OTUs; average 95 ± 24) at the family level per sample.

OTUs were classified into 33 phyla, with 96% of the OTUs belonging to 6 phyla, namely *Proteobacteria* (45.9%), *Chloroflexi* (23.6%), *Firmicutes* (17.7%), *Bacteroidetes* (5.3%), *Spirochaetes* (2.7%) and Candidate division OP9 (1.1%). Different phylotypes were abundant in different zones. Sulfate zone sediment contained *Gammaproteobacteria* (64%), *Chloroflexi* (9%) and *Bacteroidetes* (4%) and methane zone sediment was composed of sequences belonging to *Gammaproteobacteria* (54%) and *Epsilonproteobacteria* (27%). On the other hand, SMTZ sediment was dominated by the sequences related to *Desulfobacteraceae* (79%) belonging to the class *Deltaproteobacteria* (Fig S4).

Within the *Proteobacteria* phylum, *Desulfobacteraceae* was the main family that contained 61% of the reads, which is followed by *Helicobacteraceae* and *Desulfobulbaceae* having 9.4% and 4.1% of the reads, respectively (Fig S4). A similar dominance of the *Anaerolinaceae* family with 89.2% reads was observed in the *Chloroflexi* phylum. The *Syntrophomonadaceae* family covered 39.9% of the reads, while 50.9% of the reads belonged to uncultured *Firmicutes*. One of the families *Desulfobacteraceae*, *Anaerolinaceae*, *Syntrophomonadaceae* and uncultured *Clostridiales* dominated at least one slurry sample. Despite the overall dominance of these families, a high degree of variation was seen in relative abundance of them between different slurry samples.

The most abundant OTUs belonged to *Desulfobacterium* in the phyla *Proteobacteria*, uncultured *Anaerolinaceae* in the phylum *Chloroflexi*, *Syntrophomonas* in the phyla *Firmicutes*, uncultured *Desulfobacteraceae* in the phyla *Proteobacteria*, and uncultured *Clostridiales* in the phylum *Firmicutes* (Fig 4).

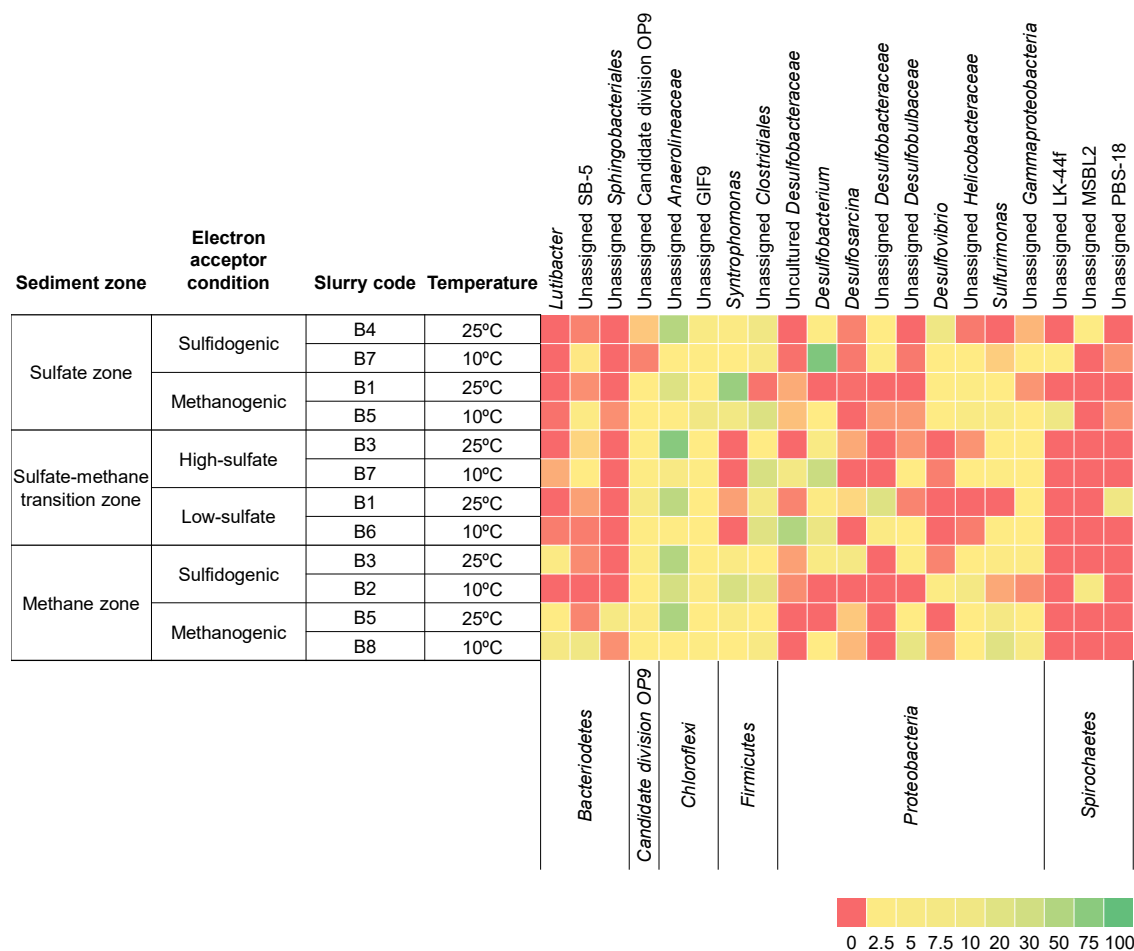


Figure 4. The heatmap depicts the relative percentage of the most common (>5%) bacterial 16S rRNA gene sequences across the 12 slurries analyzed. The heatmap colors represent the relative percentage of the bacterial assignments within each sample. Colors shifted towards dark green indicate higher abundance. Taxonomy is shown at the genus level (unless unassigned) above and at the phylum level below the heatmap.

Redundancy analysis separated bacterial orders by their associations to the incubation conditions (Fig 5). The order *Anaerolineales* (OTU 15) had the highest read abundance among all bacterial orders and showed a strong positive correlation to the temperature and butyrate (Fig 5, S5). *Anaerolineales* had positive associations with the other environmental parameters sulfate, acetate and methane. The slurries in which this order dominated were plotted on the left portion of the RDA graph. Another prevalent bacterial order *Desulfobacteriales* (OTU 27) was observed to be associated with the slurries SZB7, SMTZB6 and SMTZB7. The order *Clostridiales* (OTU 22) was plotted between the slurries SZB1, SZB5 and MZB2 in which they had the highest read abundance. The slurries SZB5 and MZB8 were negatively correlated with temperature and sulfate, and was

plotted toward the upper right portion of the RDA triplot. These slurries were associated most strongly with the orders *Clostridiales* (OTU 22), *Campylobacteriales* (OTU 31) and *Desulfobacteriales* (OTU 27) (Fig 5).

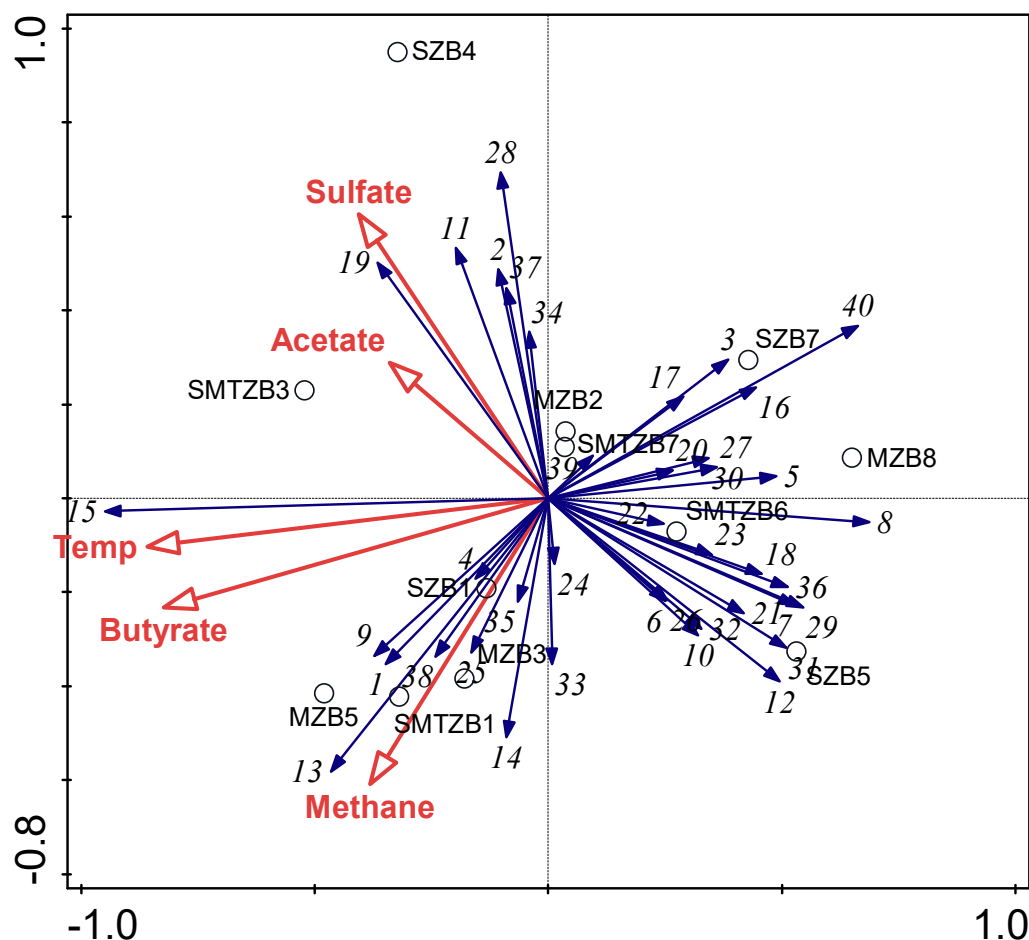


Figure 5. Redundancy Analysis Triplot showing relationship between Bacterial community composition at order level and environmental parameters. Environmental variables are given as red vectors. Blue vectors represent bacterial orders. Orders were included with a relative abundance of at least 1% in any sample. Vector length gives the variance that can be explained by a particular environmental parameter. Perpendicular distance reflects association, with smaller distances indicating a larger association. Temp: Temperature.

OTU numbers and corresponding taxa is as followed: (1)Bacteria-Other, (2)OPB41, (3)BD2-2, (4)Bacteroidales, (5)Cytophagales, (6)Flavobacteriales, (7)SB-1, (8)B-5, (9)Sphingobacteriales, (10)VC2.1.Bac22, (11)vadinHA17, (12)vadinHA17-uncultured bacterium, (13)Candidate division OP9, (14)Anaerolineae, (15)Anaerolineales, (16) GIF9, (17)MSBL5, (18)vadinBA26, (19)Chloroplast, (20)LCP-89, (21)Lineage_IV, (22)Clostridiales, (23)Nitrospirales, (24)Burkholderiales, (25)Hydrogenophilales, (26)Desulfarculales, (27)Desulfobacteriales, (28)Desulfovibrionales, (29)Desulfuromonadales, (30)Svao485, (31)Campylobacteriales, (32)Gammaproteobacteria, (33)Alteromonadales, (34)Pseudomonadales, (35)Thiotrichales, (36)LK-44f, (37)MSBL2, (38)PBS-18, (39)Spirochaetaceae, (40)Acholeplasmatales. A detailed correlation matrix is provided in Table S5.

3.3.5 Archaeal community composition and structure

PCR amplified partial 16S rRNA gene fragments obtained from the last day sampling of all slurries and environmental samples were sequenced. After filtering and trimming, between 9120 and 136909 high quality sequences were found per sample.

In all slurry samples, the highest average percentage of 16S rRNA reads for Archaea clustered within the families *Methanomicrobiaceae* (60.8%), *Methanosarcinaceae* (16.3%) and *Methanosaetaeaceae* (9.3%) (Fig S6). *Methanomicrobiaceae* dominated each slurry sample with read percentages ranging between 26%-98%, except for one slurry incubated at 10°C with high sulfate in which *Methanosarcinaceae* became the most dominant family representing 39% of all the reads. *Methanogenium* belonging to the family *Methanomicrobiaceae* was the most dominant genus among the slurries, followed by the genus *Methanosarcina* from the family *Methanosarcinaceae*, having lower abundance (Fig 6). *Methanosaetaeaceae* was observed only in two slurry samples incubated with low and without sulfate at 25°C, with 43% and 67% of the reads (Fig S6). These reads belonged to *Methanosaeta* and unclassified *Methanosaetaceae* (Fig 6). The other Archaeal groups observed in different slurries were the Marine Benthic Group D/Deep Hydrothermal Vent Euryarchaeotal Group 1 (MBG-D and DHVEG-1), Miscellaneous Crenarchaeotic Group (MCG) and ANME-1b with read percentages 3.7%, 2.5% and 2.1%, respectively (Fig 6, S6).

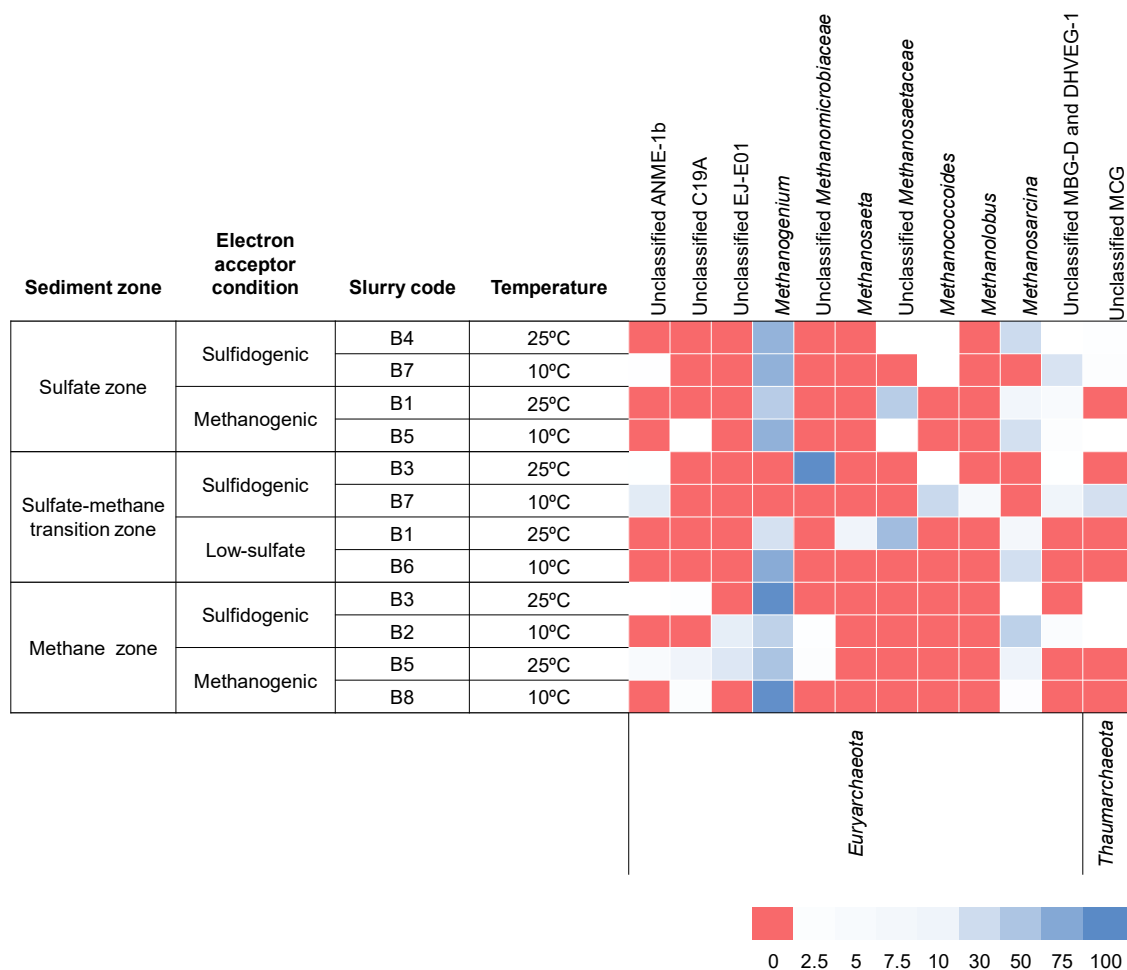


Figure 6. The heatmap depicts the relative abundance of the most common (>5 %) archaeal 16S rRNA gene sequences (unless unclassified) across the 12 slurries analysed. The heatmap colors represent the relative percentage of the archaeal assignments within each sample. Colors shifted towards bright blue indicate higher abundance.

Archaeal community composition at family level in each slurry was plotted on RDA (Fig 7). The slurries which had high methane were plotted toward the upper left quadrant of the graph. An efficient acetate consumption was observed in these slurries, SZB₁, SMTZB₁ and MZB₅, which was confirmed by the negative association to the acetate. *Methanosaetaceae* was observed to be positively correlated with temperature and negatively correlated with sulfate. The slurries SZB₅, SZB₄, SZB₇, MZB₃, MZB₈, SMTZB₃ in which acetate accumulated to very high concentrations showed close clustering toward the bottom middle part of the graph and were associated with acetate and the family *Methanomicrobiaceae* (Fig 7, Fig 1, 2, 3). The slurries that represented less Archaeal diversity and abundance were together in the bottom right portion of the RDA plot.

Methanosarcinaceae was plotted adjacent to the slurries SMTZB6, SMTZB7 and MZB2 in which they were enriched (Fig 7, Fig 2, 3).

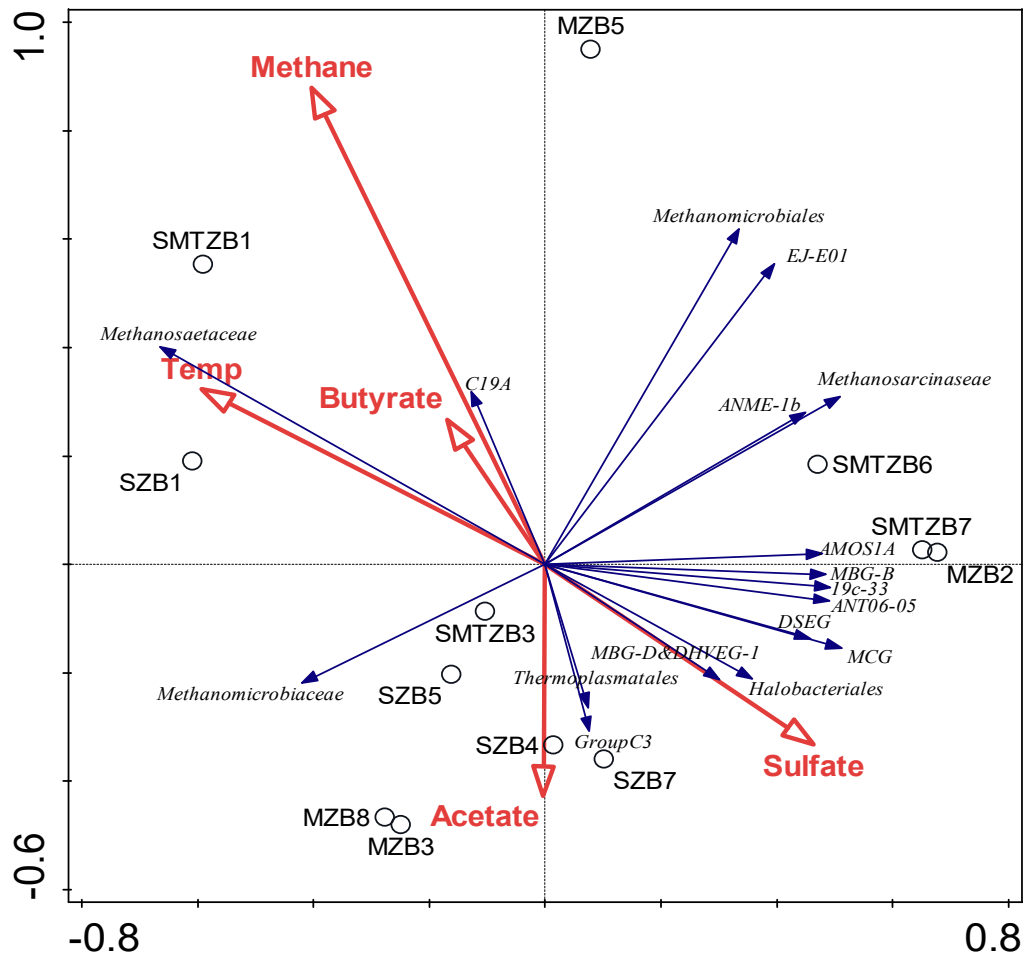


Figure 7. Redundancy Analysis Triplot showing relationship between Archaeal community composition at family level and environmental parameters. Environmental variables are given as red vectors. Blue vectors represent Archaeal families. Families were included with a relative abundance of at least 1% in any sample. Vector length gives the variance that can be explained by a particular environmental parameter. Perpendicular distance reflects association, with smaller distances indicating a larger association. Temp: Temperature.

3.3.6 Correlation between the microbial community and between the microbial community and environmental parameters

To investigate the relationship between the microbial community structure and incubation conditions, sequence data were correlated to environmental parameters data. Correlation analysis of the sequencing data revealed both positive and negative relations between bacterial orders (Fig S5). *Anaerolineales*, the most dominant order in the slurries, was observed to be negatively

correlated to the other two dominant orders *Desulfobacterales* and *Clostridiales*, but positively correlated to all environmental parameters, with a strong correlation to temperature ($P < 0.01$), butyrate ($P < 0.01$) and acetate ($P < 0.05$). *Desulfobacterales* was negatively correlated to the orders *Sphingobacteriales* ($P < 0.01$), *Desulfovibrionales* ($P < 0.05$), *Spirochaetaceae* ($P < 0.05$), *Clostridiales* and all environmental parameters except for sulfate, and positively correlated to candidate division OP9 and *Thiotrichales*. *Clostridiales* order was observed to be positively correlated to *Desulfovibrionales* ($P < 0.05$), *Sphingobacteriales*, GIF9 belonging the phylum *Chloroflexi* and negatively correlated to all environmental parameters except for a weak positive correlation to sulfate. The order *Campylobacterales* was positively correlated to the orders *Desulfuromonadales* ($P < 0.01$), SB-1 ($P < 0.05$) and SB-5 ($P < 0.05$) from the phylum *Bacteroidetes* and unclassified *Gammaproteobacteria* ($P < 0.05$) and negatively correlated to *Desulfobacterales*, PBS-18 from the phylum *Spirochaetes* and to all environmental parameters except for methane.

The two aceticlastic methanogenic families *Methanosaetaceae* and *Methanosarcinaceae* did not positively correlated to each other and showed differences in their correlation to the other taxonomic groups and environmental parameters, in like manner to the difference in their absolute abundances in slurries (Fig S7 and Fig 6). Both families were negatively correlated to the hydrogenotrophic methanogenic family *Methanomicrobiaceae*, among which *Methanosarcinaceae* showed significant negative correlation ($P < 0.05$). *Methanosaetaceae* showed positive correlation to methane and temperature, whereas *Methanosarcinaceae* did not show any significant positive correlation to any of the environmental parameters. Hydrogenotrophic methanogenic families were negatively correlated with most of the other taxonomic groups. Unclassified *Methanomicrobiales* and EJ-Eo1 were positively correlated to methane, whereas *Methanomicrobiaceae* was positively correlated only to acetate.

3.4 Discussion

3.4.1 Butyrate conversion in Aarhus Bay sediment

Our results show that butyrate conversion in Aarhus Bay sediments is coupled to sulfate reduction and methane production. Previous studies indicated that sulfate reduction is an important terminal electron-accepting process in marine sediments (Jørgensen, 1982; Holmkvist et al., 2011; Bowles et al., 2014). The rapid consumption of added sulfate in sulfate-amended and sediment-originated sulfate in sulfate-free slurries suggests that sulfate reduction is the dominant pathway of butyrate

conversion in Aarhus Bay sediment (Fig 1B, 2B, 3B). This is most likely due to the fact that sulfate reduction is energetically more favourable than methanogenic conversion (Muyzer and Stams, 2008). The accumulation of acetate in all slurries indicates incomplete butyrate conversion (Fig 1B, 2A, 2B, 3B). It is remarkable to observe methane production in the presence of sulfate in SZ slurries although late in time (Fig 1B). The decrease in acetate coinciding methane production suggests the occurrence of methanogenesis in the sulfate zone of Aarhus Bay, even though methanogenesis is less favourable in the presence of sulfate (Table 1). Many studies have shown the occurrence of methanogenesis in sulfate-rich marine sediments (Mori et al., 2012; Wilms et al., 2007; Beck et al., 2011; Schippers et al., 2012). Although CH₄ concentrations in many sub-seafloor sediments increase only when sulfate is depleted with depth, active methanogenesis is often detected in the presence of sulfate (e.g. Woodlark Basin, Wellsbury et al., 2002 and Peru Margin, Parkes et al., 2005).

In the absence of sulfate, conversion of butyrate to acetate plus H₂ is an endergonic reaction under standard conditions and becomes feasible by methanogenic partners that keep the H₂ partial pressure low (Table 1) (Schink and Stams, 2013; McInerney et al., 2008). Butyrate conversion trend in sulfate-free SZ and MZ slurries incubated at 25°C was similar in terms of early methane production and complete acetate consumption (Fig 1A, Fig 3A). (Table 1). Apparently, the syntrophic conversion of butyrate under sulfate-free conditions is possible both in the sulfate and methane zones of Aarhus Bay sediments.

3.4.2 The effect of sulfate concentration on conversion dynamics

Significant differences in terms of product formation and consumption in high (20 mM) and low (3 mM) sulfate amended SMTZ slurries at 25°C suggests that the sulfate concentration is an important environmental factor in butyrate conversion in Aarhus Bay sediments. Low and delayed CH₄ production in high sulfate amended slurries indicates possible sulfide inhibition on methanogenesis. Inhibitory effect of high sulphide concentrations on methanogens was reported previously (Pender et al., 2004; O'Flaherty et al., 1998; Shin et al., 1995). Rapid methane production after day 523 in high sulfate containing slurries might be related to the adaptation capacity of hydrogenotrophic methanogens to the slurry conditions and involvement in syntrophic butyrate conversion which caused simultaneous increase in acetate. This suggests that methanogenesis could still occur despite the on-going sulfate-reduction process and sulfide level. On the other hand, high methane production with concomitant acetate consumption in low sulfate amended SMTZ slurries indicates an efficient syntrophic butyrate conversion involving acetate- and

hydrogen-dependent sulfate reduction and methanogenesis processes along the incubation. Apparently, low amounts of sulfate enhanced the whole microbiome, resulting in fast and dedicated population performing both sulfate reduction and methanogenesis.

3.4.3 The effect of temperature on metabolic processes

Different temperatures have an impact on conversion of butyrate in Aarhus Bay sediments. Lower temperatures caused lower sulfate consumption and higher acetate accumulation in SZ slurries. Similarly, below 25°C, reduced sulfate reduction with organic acid accumulation was observed in sulfate-amended marine sediments (Weston and Joye, 2005). In contrast, the produced acetate was efficiently consumed at 25°C especially in sulfate-free slurries. Roussel and colleagues (2015) reported increased acetate fermentation with increasing temperatures (from 12°C to 30°C) in marine sediment slurries. The high-sulfate amended SMTZ slurry at 10°C exhibited the lowest and constantly fluctuating CH₄ amounts (Fig 2B). This trend points to the existence of anaerobic oxidation of methane (AOM) in sulfate-methane transition zone of Aarhus Bay (Thomsen et al., 2001; Dale et al., 2008). Almost all the methane produced in marine sediments is consumed with concomitant sulfate removal within the SMTZ (Knittel and Boetius, 2009; Boetius et al., 2000). Therefore, despite the amounts of substrates and products did not differ significantly, low incubation temperature in SMTZ slurry favoured for a different microbial community which causes a difference in eventual metabolic process.

3.4.4 Enriched microbial community in the presence of sulfate

In sulfate amended slurries, enrichment of *Desulfobacteraceae*, *Desulfovibrionaceae*, *Desulfobulbaceae*, *Syntrophomonadaceae* and *Clostridiales* suggests that the members of these taxa are associated with butyrate conversion. Especially, *Desulfobacterium*, *Desulfonema*, *Desulfosarcina*, *Desulfoarculus* belonging to *Desulfobacteraceae* are known to couple butyrate degradation to sulfate reduction (Kuever et al., 2014b). The increase in the relative abundance of these genera both in the upper and the lower sediment slurries suggests the existence of sulfate reducers both in the sulfate, sulfate-methane transition and methane zones of the sediment. Leloup and colleagues (2009) showed that the sulfate-reducing bacteria in Aarhus Bay sediments are present and active within the methane zone, and have as high bacterial numbers as in the sulfate zone. Similar findings were also reported in coastal marine sediments (Limfjorden, Denmark;

Jørgensen, 1978; Aarhus Bay, Station 6; Thomsen et al., 2001) and in deep-sea sediment (Black Sea; Leloup et al., 2007). Apparently, the ability of some SRB to grow fermentatively may explain their abundant presence in sulfate-depleted sediments and the sudden increase in their relative abundance in sulfate-amended MZ slurries. On the other hand, the increased relative abundance of *Desulfovibrio* in sulfate-amended slurries might be linked to the consumption of H_2 produced by fermentative microorganisms. The ability of *Desulfovibrio* species to use H_2 as electron donor and to assimilate acetate and CO_2 as carbon sources supports this hypothesis (Kuever et al., 2014a). *Syntrophomonas* is a butyrate-degrading syntrophic specialist that grow in close association with methanogens and other hydrogen- and/or formate-using microorganisms (Plugge et al., 2011; Sousa et al., 2009; Oude Elferink et al., 1994). Sulfate-reducing bacteria that directly couple butyrate oxidation to sulfate reduction grow faster than syntrophic butyrate degraders. However, the growth rates of some syntrophic butyrate degraders were reported to be higher than some butyrate-oxidizing sulfate reducers (Oude Elferink et al., 1994). In contrary, the effect of sulfate absence on the microbial community change is the increase in the relative abundance of *Syntrophomonas* especially in the upper sediment slurries. This result clearly shows that sulfate can decelerate the abundance of *Syntrophomonas* species, but does not inhibit the butyrate conversion by *Syntrophomonas*. On the other hand, *Desulfobacteraceae* and *Clostridiales* involved in butyrate conversion rather in SMTZ slurries. Apparently, methanogenic conditions gives *Syntrophomonas* a competitive advantage in the upper sediment zone over other bacteria whereas in deeper sediments niche specific or fast growing bacteria take over butyrate conversion.

3.4.5 The effect of temperature on the enriched bacterial community

Low temperatures have a negative effect on the relative abundance of *Anaerolineaceae* in the Aarhus Bay sediments. At higher temperatures (25°C), *Anaerolineaceae* became dominant and limited the butyrate conversion due to their ability to degrade dead biomass (Kleinstüber et al., 2012) and acetate in marine sediment slurries (Webster et al., 2011). Considering that the slurries in our study were incubated for long period, the *Anaerolineaceae* might have degraded the dead cells forming syntrophic relationship with hydrogenotrophic methanogens (Yamada and Sekiguchi, 2009). The higher relative abundance of *Anaerolineaceae* is known in the organic-rich subsurface marine sediments (Webster et al., 2004, 2006; Teske, 2006; Fry et al., 2008; Biddle et al., 2008).

Lower temperatures (10°C) favours the abundance of *Clostridiales*. The members of the phylum *Firmicutes* are commonly found in surface and deep marine sediments, soils and

methanogenic environments (Fry et al., 2008; Parkes et al., 2014). Sequences related to uncultured *Firmicutes* were previously found in MPN dilution cultures of hydrocarbon-contaminated sediments containing butyrate in the presence and absence of sulfate (Struchtemeyer et al., 2011). These findings point out that the *Firmicutes* might have played a role in syntrophic butyrate conversion in 10°C slurries.

Although temperature did not have a significant effect on the relative abundance of *Desulfobacteraceae*, they were rather abundant at 10°C. In addition, the members of *Desulfobacteraceae* were abundant in most of the slurries regardless of the sulfate concentration and the origin of the sediment. Pyrosequencing of 16S rRNA gene amplicons retrieved from the original sediment confirmed the dominance of *Desulfobacteraceae* in sulfate-methane transition zone of Aarhus Bay (Fig S4). This indicates that the bacterial community at the SMTZ is distinct from other zones (Wagner et al., 2005) and this might be associated with the syntrophic interaction between *Desulfobacteraceae* members and methane-oxidizing archaea involving in AOM (Fig S6) (Knittel and Boetius, 2009; Boetius et al., 2000). As the incubation temperature resembles the in situ condition (Dale et al., 2008), *Desulfobacteraceae* members would be more successful in butyrate conversion at 10°C in the upper sediment slurries.

3.4.6 Archaeal community structure in the slurries

Methanomicrobiaceae is responsible for the consumption of H₂/formate produced by the incomplete conversion of butyrate as its members are specialists on H₂- and formate-utilization and acts as syntrophic partners (Garcia et al., 2006). In our study, *Methanogenium*, belonging to *Methanomicrobiaceae*, dominated all enrichment slurries regardless of the origin of the sediment and the incubation temperature, except for one slurry (SMTZ B7) (Fig 6, S6). This supports the finding of Garcia and colleagues (2006) considering that incomplete butyrate conversion occurred in all slurries. It is known that hydrogenotrophic methanogenesis is dominated in near-surface marine sediments (Parkes et al., 2014; Whiticar, 1999; Kendall and Boone, 2006a; Kendall et al., 2006) and that SRB and methanogenic archaea may coexist and reach equal rates of H₂ consumption at high hydrogen pressures (Kristjansson et al. 1982; Parkes et al., 1990). Therefore, the absence of CH₄ in sulfate-containing zones might be due to the anaerobic oxidation of methane (AOM) (Knittel and Boetius, 2009) or the adaptive mechanisms of methanogens or persistence at extremely low rates of activity even in the presence of sulfate-reducing bacteria.

Methanosarcina is known to consume acetate and methylated compounds and some strains can reduce CO₂ with H₂ (Kendall and Boone, 2006b). *Methanosarcina* is detected in many sulfate-amended and sulfate-free slurries comprised of the upper and the lower parts of the sediment in which acetate consumption occurs. Hence, *Methanosarcina* might be syntrophic partners of incomplete butyrate degraders and responsible for acetate consumption in those slurries. Finke et al. (2007b) suggested that acetate oxidation via interspecies H₂ transfer might be a possible reason for aceticlastic methanogens to occur in sulfate-rich marine sediments. Accordingly, aceticlastic methanogens can carry out the first step of syntrophic acetate oxidation where acetate is oxidized to 2 moles of CO₂ with the generation of reducing equivalents, often as hydrogen (Phelps et al., 1985). In the second step, hydrogenotrophic methanogens or sulfate reducers scavenge that hydrogen and the overall reaction becomes thermodynamically favourable. Hence, not only sulfate reducers but also the aceticlastic methanogens could grow in the sulfate zone of marine sediments (Ozuolmez et al., 2015).

The *Methanosaetaceae* is a specialist that uses only acetate as substrate for methanogenesis (Jetten et al., 1992). The possible reason for the predominance of *Methanosaetaceae* over *Methanosarcinaceae* in the low-sulfate SMTZ and sulfate-free SZ slurries at 25°C might be related to higher acetate affinity of *Methanosaetaceae* over *Methanosarcinaceae* (Jetten et al., 1992). Interestingly, the predominance of *Methanosaetaceae* in low-sulfate SMTZ slurry can be associated with the competition with acetate-degrading *Desulfobacteraceae* which is highly abundant in the original sediment (Fig S4). Although acetate is mainly consumed by sulfate reducers in marine sediments (Schönheit et al., 1982), some acetate-degrading sulfate reducers have slightly better growth kinetics than *Methanosaeta* (Stams et al., 2005). Similar observations were reported by Struchtemeyer et al., (2005) and speculated that low sulfate level may allow *Methanosaetaceae* to compete with sulfate reducers for acetate.

ANME-1 sequences have been found to be the dominant ANME type in the SMTZ of Aarhus Bay (Fig S6) (Thomsen et al., 2001; Aquilina et al., 2010; Webster et al., 2011). Timmers et al. (2015) reported that ANME-1 is more successful in low-methane, low-sulfate and high-sulfide conditions in batch incubations of Baltic Sea sediment which also resembles the characteristic of SMT zone. Low methane and high sulfide amounts in SMTZ B7 slurry supports the findings of Timmers et al. (2015) where ANME-1 was selected over ANME-2 clades under low-sulfate and high-sulfide conditions. The enrichment of both ANME-1 and *Desulfobacteraceae* in low temperature SMTZ slurry is in accordance with previous findings documenting that SMTZ sediments are dominated

by the members of *Desulfobacteraceae* and ANME clusters, forming close associations and involving in anaerobic oxidation of methane (Fig 4, 6) (Harrison et al., 2009; Knittel and Boetius, 2009). The other methane-oxidizing archaeal genera enriched in this slurry were *Methanococcoides* and *Methanolobus* which are defined as ANME-3 *Archaea* (Fig 6) (Knittel and Boetius 2009, Lösekann et al 2007, Niemann et al 2006). Lösekann et al. (2007) reported that ANME-3 cells could live syntrophically with *Desulfobulbus*. Apparently, the incubation condition, inhabiting microbial community and the amounts of sulfate, sulfide and methane in the slurry favoured the enrichment of ANME-3 group.

3.5 Conclusion

This study demonstrates that methanogenic archaea and sulfate-reducing bacteria are present and active in sulfate, sulfate-methane transition and methane zone sediments of Aarhus Bay and there is no vertical separation of both groups in the sediment. Butyrate conversion could occur both under sulfate-reducing and methanogenic conditions regardless of the incubation temperature and the sediment depth. The conversion of butyrate by syntrophic communities throughout the sediment column suggests that continuous supply of available carbon might stimulate syntrophic butyrate degraders in the upper sulfate-rich sediment zone. On the other hand, sulfate reducers in the deeper sulfate-depleted sediment could contribute to the butyrate conversion even in the presence of low concentration of sulfate. We suggest that both groups of microbes can survive at very low activity rates in the sediment and both sulfate reduction and methanogenesis with the same substrate can proceed simultaneously. The results indicate that H_2 and CO_2 may be major substrates for methanogens, as H_2 was never detected throughout the experiments and the members of hydrogenotrophic methanogenic family *Methanomicrobiaceae* were the dominant *Archaea* in the slurries. On the other hand, there is only limited competition between SRB and methanogens for acetate, as the acetoclastic methanogens could also be enriched in sulfate-containing slurries. The enrichment of ANME-1 especially in SMTZ slurries together with ANME-3 suggests the possibility that these *Archaea* might take part in AOM interacting with other responsible microbial groups. Therefore, butyrate is converted in team work of sulfate reducers, syntrophs and methanogens throughout the anoxic marine sediment.

Acknowledgements

We gratefully acknowledge Mark Lever (Eidgenössische Technische Hochschule, Zurich, Switzerland), Kasper Kjeldsen, Hans Røy (Aarhus University, Aarhus, Denmark) for skillful technical assistance and the captains and crews of sailing vessel Marieje and research vessel Tyra for their help during different cruises. We thank Peer Timmers and Martin Liebensteiner (Wageningen University & Research) and Kivanc Ozuolmez for assistance during sampling and Ton van Gelder (Wageningen University & Research) for technical assistance. This work has been funded by the Wimek Graduate School of Wageningen University & Research and the Darwin Center for Biogeosciences (the Netherlands). Research of Alfons Stams is supported by ERC grant (project 323009) Gravitation grant (project 024.002.002) of the Netherlands Ministry of Education, Culture and Science and the Netherlands Science Foundation (NWO).

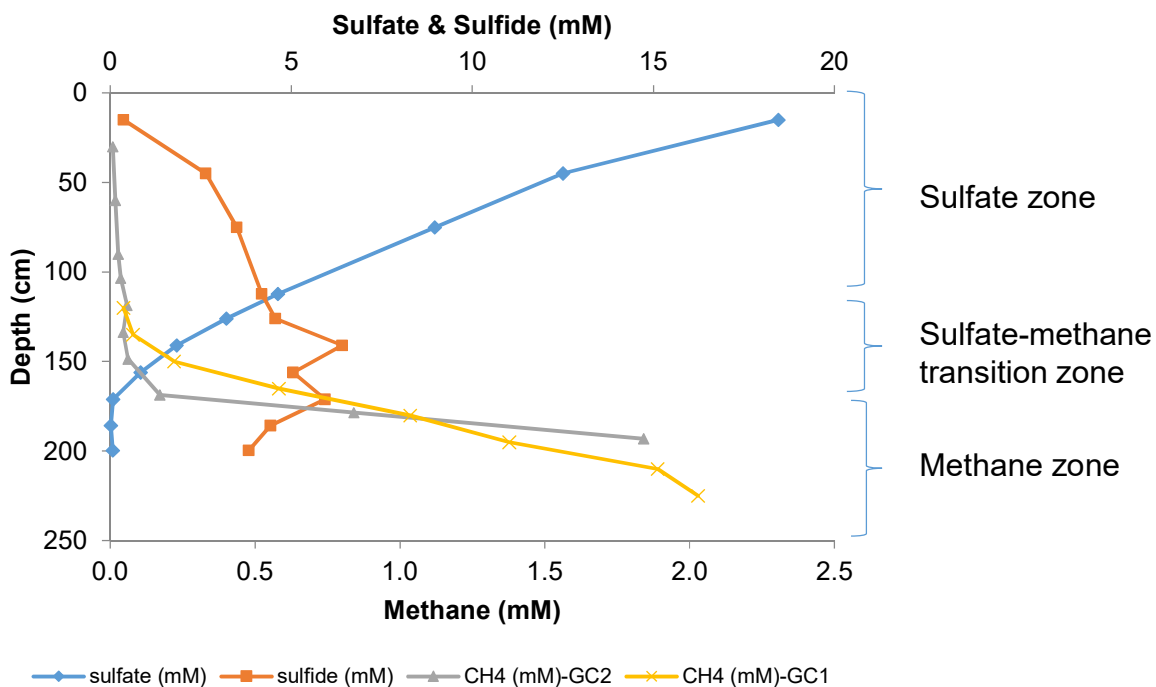
Supplementary data

Table S1. The overview of all the enrichment slurries fed with propionate and the total amounts of the reactants consumed and products formed during the enrichment period. The enrichment slurries were consisted of sediment either from sulfate zone (SZ), sulfate-methane transition zone (SMTZ) or methane zone (MZ) and incubated at 25°C or 10°C, with 3 mM, 20 mM or without (-) sulfate amendments along the study. Slurries with * were presented in the propionate conversion graphs and used for molecular analysis.

Sediment zone	Slurry Code	Treatment	Incubation temperature (°C)	Reactants (μmol/slurry)		Products (μmol/slurry)		
				Butyrate	Sulfate	Acetate	Sulfide	Methane
SZ	B1	-	25	35085	313	37497	717	63347
	B2	-	25	38415	312	29386	508	64830
	B3	20 mM SO ₄ ²⁻	25	36896	37342	109911	39836	1030
	B4	20 mM SO ₄ ²⁻	25	36816	35382	74468	33996	3252
	B5	-	10	22092	351	24613	460	19853
	B6	-	10	24609	319	31487	364	12978
	B7	20 mM SO ₄ ²⁻	10	19587	15551	33563	17064	93
	B8	20 mM SO ₄ ²⁻	10	22414	15282	35718	18012	0
SMTZ	*B1	3 mM SO ₄ ²⁻	25	33451	5500	10151	7479	73569
	B2	3 mM SO ₄ ²⁻	25	33748	8020	30128	9107	69486
	*B3	20 mM SO ₄ ²⁻	25	40754	45716	45255	38991	4183
	B4	20 mM SO ₄ ²⁻	25	41405	47734	46877	42512	3727
	B5	3 mM SO ₄ ²⁻	10	26272	6463	35148	7321	32045
	B6	3 mM SO ₄ ²⁻	10	28158	6531	37574	7268	32483
	B7	20 mM SO ₄ ²⁻	10	29226	35141	31129	36984	35
	B8	20 mM SO ₄ ²⁻	10	33078	31697	41505	32413	1015
MZ	B1	20 mM SO ₄ ²⁻	10	26059	18632	35892	14784	2956
	B2	20 mM SO ₄ ²⁻	10	29488	34963	33448	38500	0
	B3	20 mM SO ₄ ²⁻	25	54945	41587	91742	30618	5792
	B4	20 mM SO ₄ ²⁻	25	56743	54643	84195	39675	587
	B5	-	25	45588	358	43022	261	105926
	B6	-	25	45829	782	29932	487	97903
	B7	-	10	18145	610	12727	380	27090
	B8	-	10	16225	601	29455	424	8417

Table S2. The number of reads per sample generated by Pyrosequencing for Bacteria and HiSeq Illumina sequencing for Archaea.

Origin	Slurry	Bacterial reads	Archaeal reads
Sulfate zone	ENV	8787	9120
	B4	12393	88555
	B1	18687	121246
	B7	12007	61722
	B5	12194	89283
Sulfate-methane transition zone	ENV	3202	18696
	B1	3758	75708
	B3	5167	47520
	B6	5443	42599
	B7	7198	58464
Methane zone	ENV	10903	30848
	B3	15094	39087
	B5	11718	136909
	B2	11686	52551
	B8	10891	94124

Figure S1. Depth profiles of sediment pore water sulfate, sulfide and methane for Station M₁, in Aarhus Bay, Denmark. Methane-GC1 and Methane-GC2 stands for methane concentrations retrieved from two different gravity corers, gravity corer 1 and 2, respectively. SZ; Sulfate zone, SMTZ; sulfate-methane transition zone; MZ, methane zone.

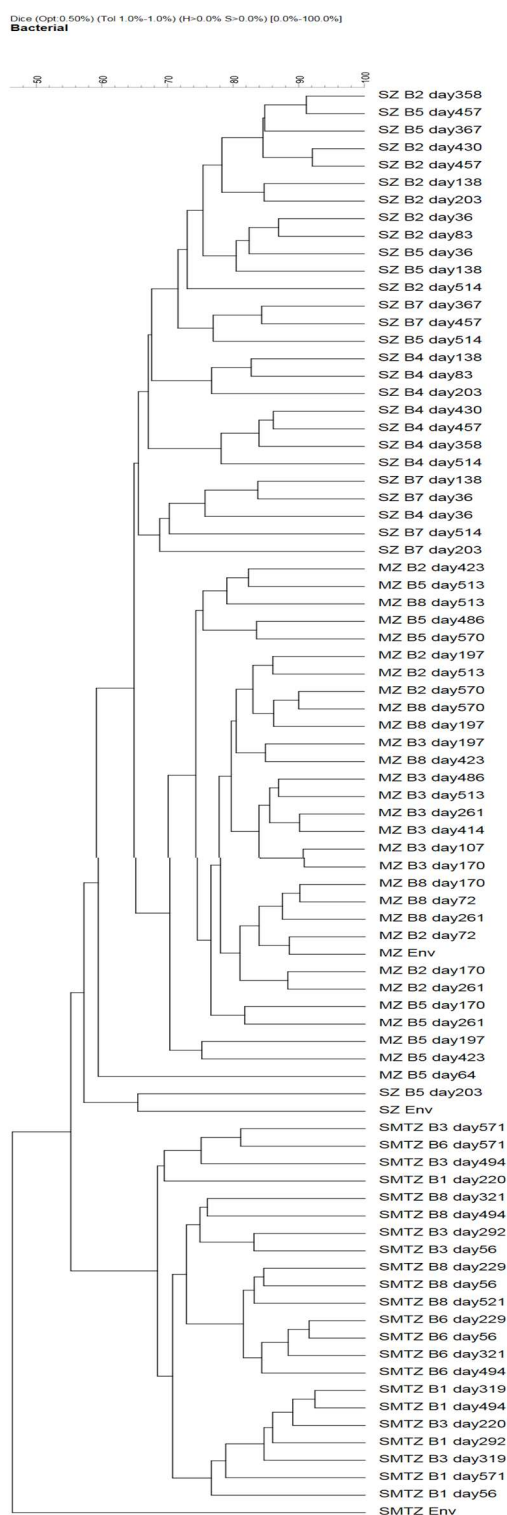


Figure S2. Cluster analysis of bacterial DGGE profiles of sediment samples taken at different biogeochemical zones and samples of enrichment slurries that were taken at different time points. The trees were generated using Dice similarity coefficient and UPGMA clustering algorithm. SZ: Sulfate zone, SMTZ: Sulfate-methane transition zone, MZ: Methane zone.

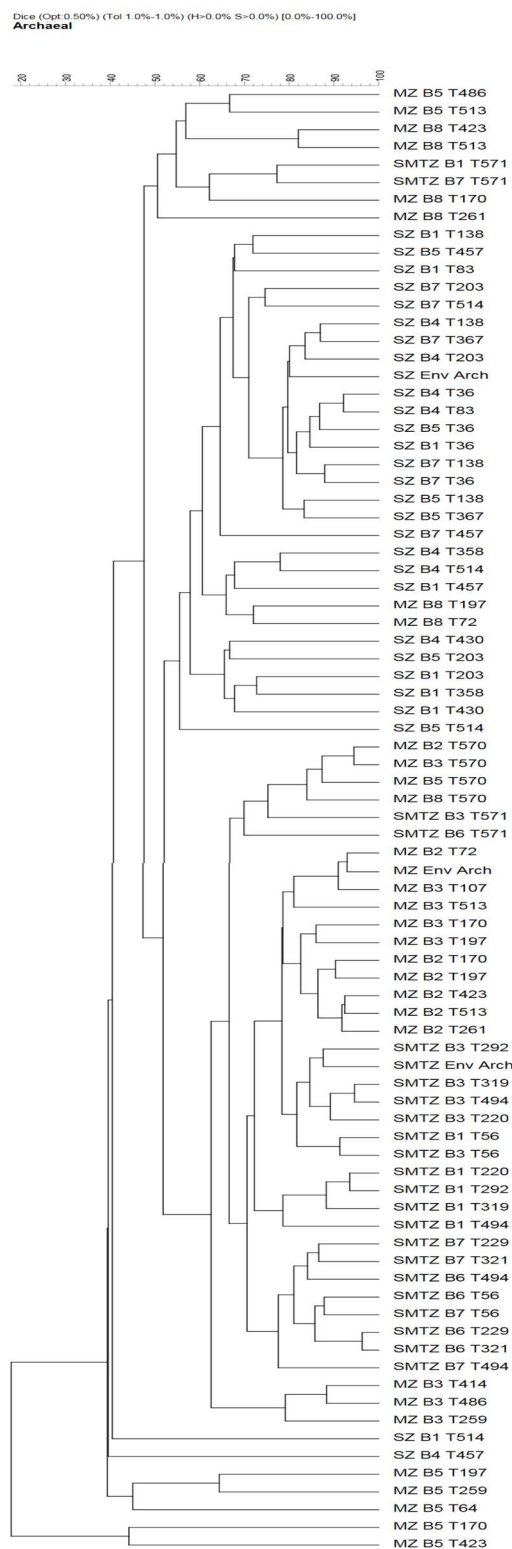


Figure S3. Cluster analysis of archaeal DGGE profiles of sediment samples taken at different biogeochemical zones and samples of enrichment slurries that were taken at different time points. The trees were generated using Dice similarity coefficient and UPGMA clustering algorithm. SZ: Sulfate zone, SMTZ: Sulfate-methane transition zone, MZ: Methane zone.

Figure S4. Relative abundances of the bacterial community in all slurries and environmental samples at family level, normalized to 100%. Only those families that were present at an abundance >1% in at least one sample were included in the graph. SZ: Sulfate zone, SMTZ: Sulfate-methane transition zone; MZ: Methane zone, Env: Sediment sample belonging to the indicated biogeochemical zone. S: 20mM sulfate, 3S:3mM sulfate is used as electron acceptor in slurries. Slurries that were not labeled with 'S' or '3S' were incubated without sulfate. The number of reads of each sample was given in brackets.

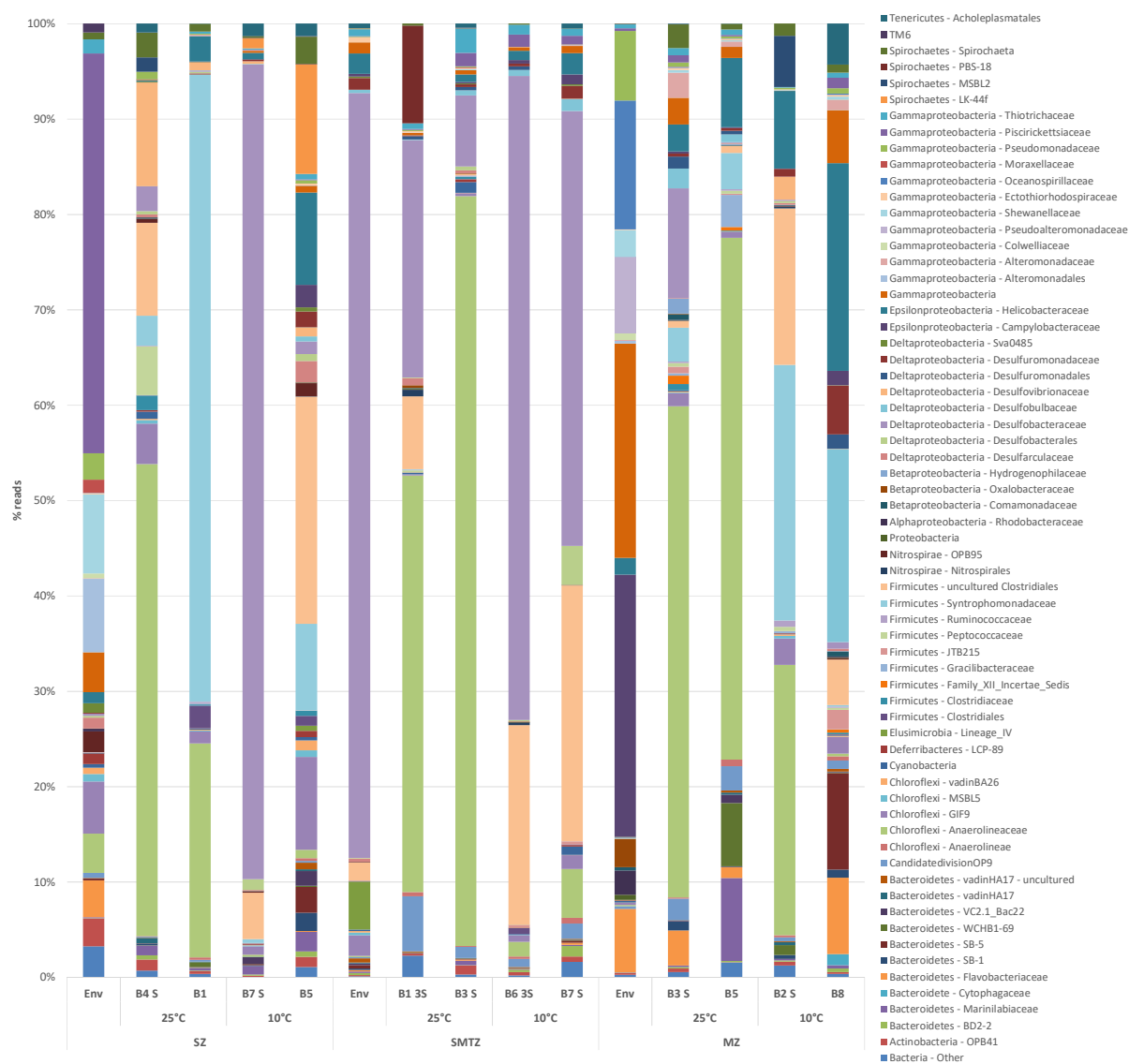


Figure S5. The heatmap depicts the correlation between bacterial orders present at a relative abundance $>1\%$ of total reads across the 12 slurry samples and experimental parameters. Correlations were determined by means of the two tailed Spearman's Rank Order Correlation test. The heatmap colors represent the relative percentage of the microbial order assignments. Square colors shifted towards bright green indicate strong correlation.

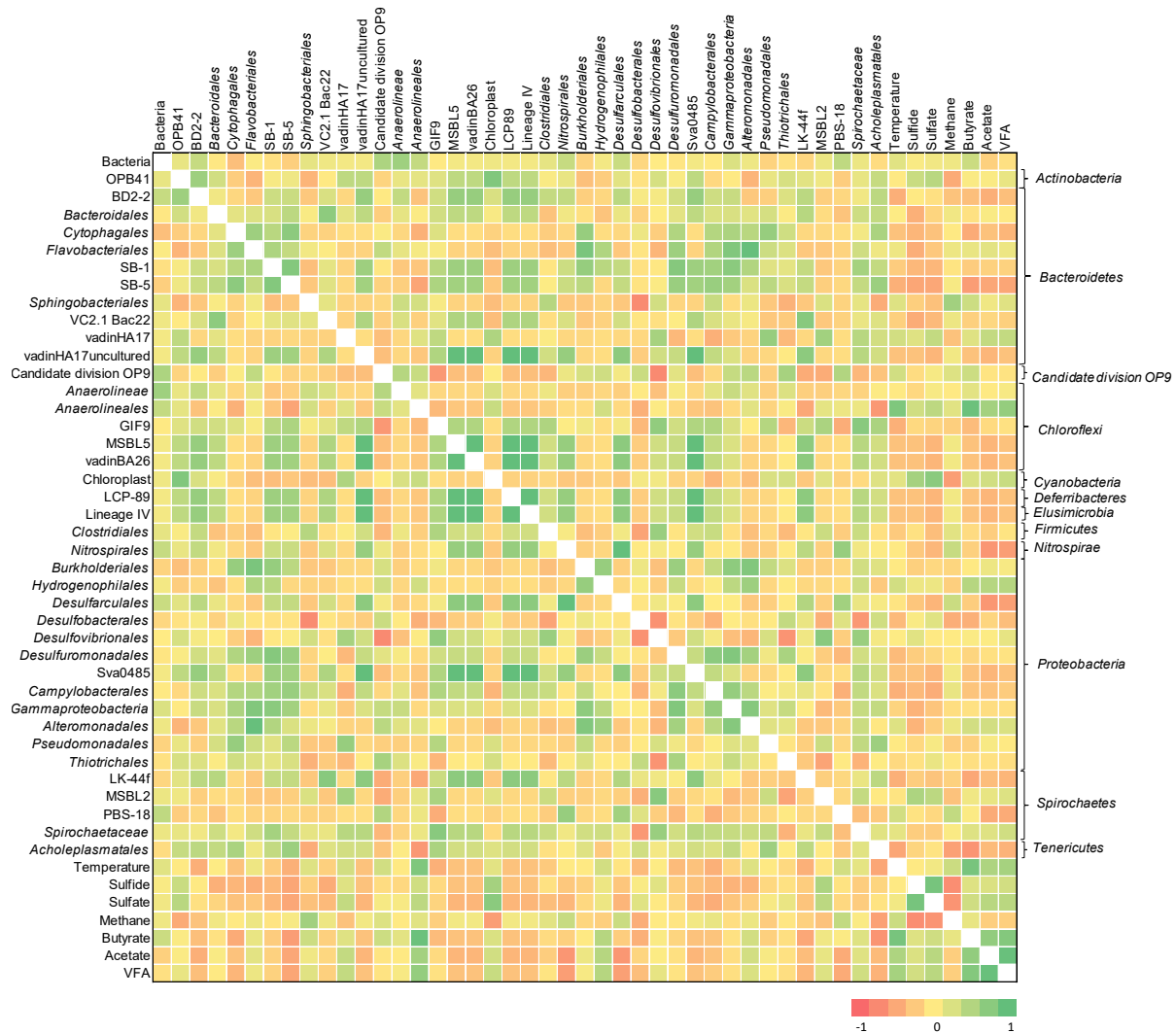


Figure S6. Relative abundances of the archaeal community in all slurries and environmental samples at family level, normalized to 100%. Only those families that were present at an abundance >1% in at least one sample were included in the graph. SZ: Sulfate zone, SMTZ: Sulfate-methane transition zone; MZ: Methane zone. Env: Sediment sample belonging to the indicated biogeochemical zone. S: 20mM sulfate, 3S:3mM sulfate is used as electron acceptor in slurries. Slurries that were not labeled with 'S' or '3S' were incubated without sulfate.

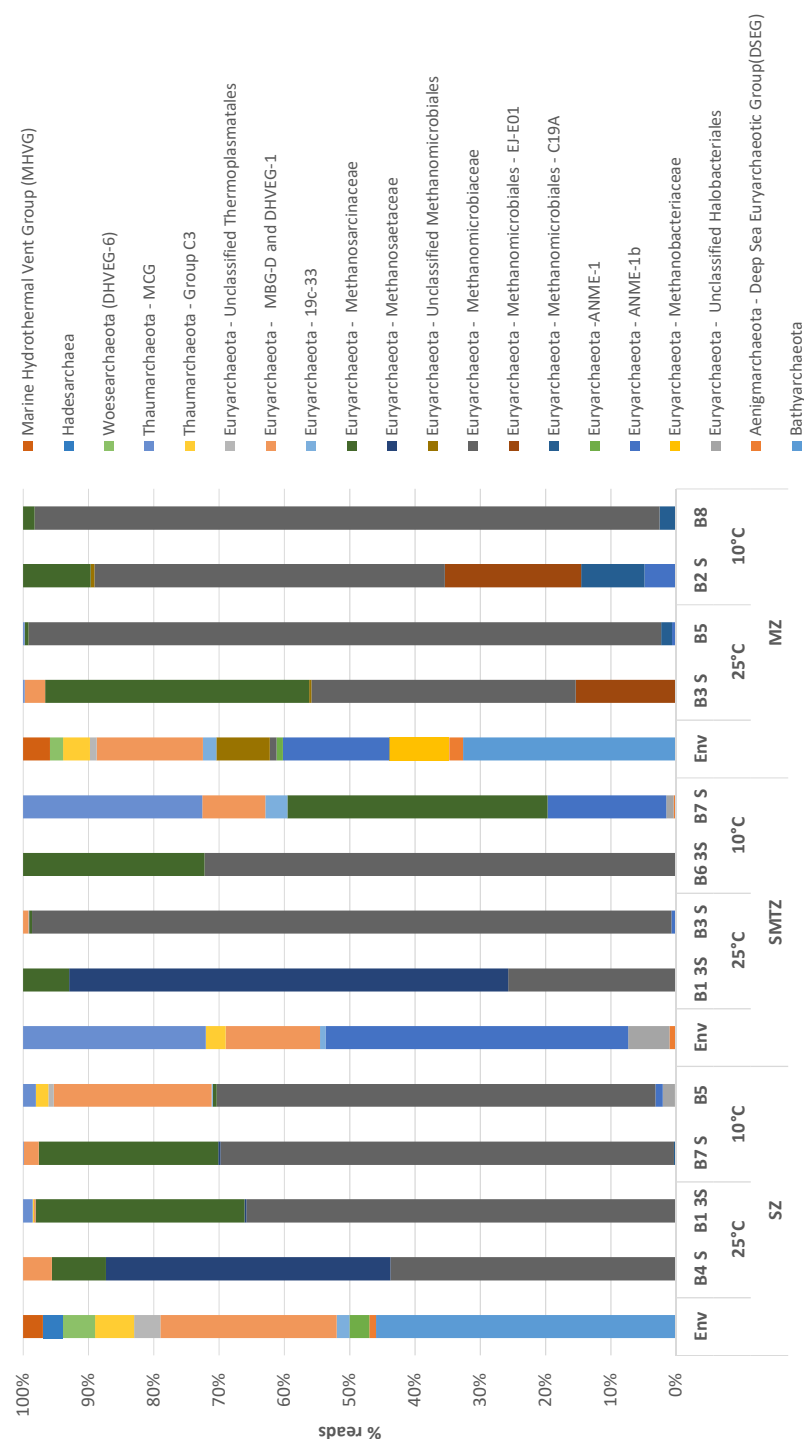
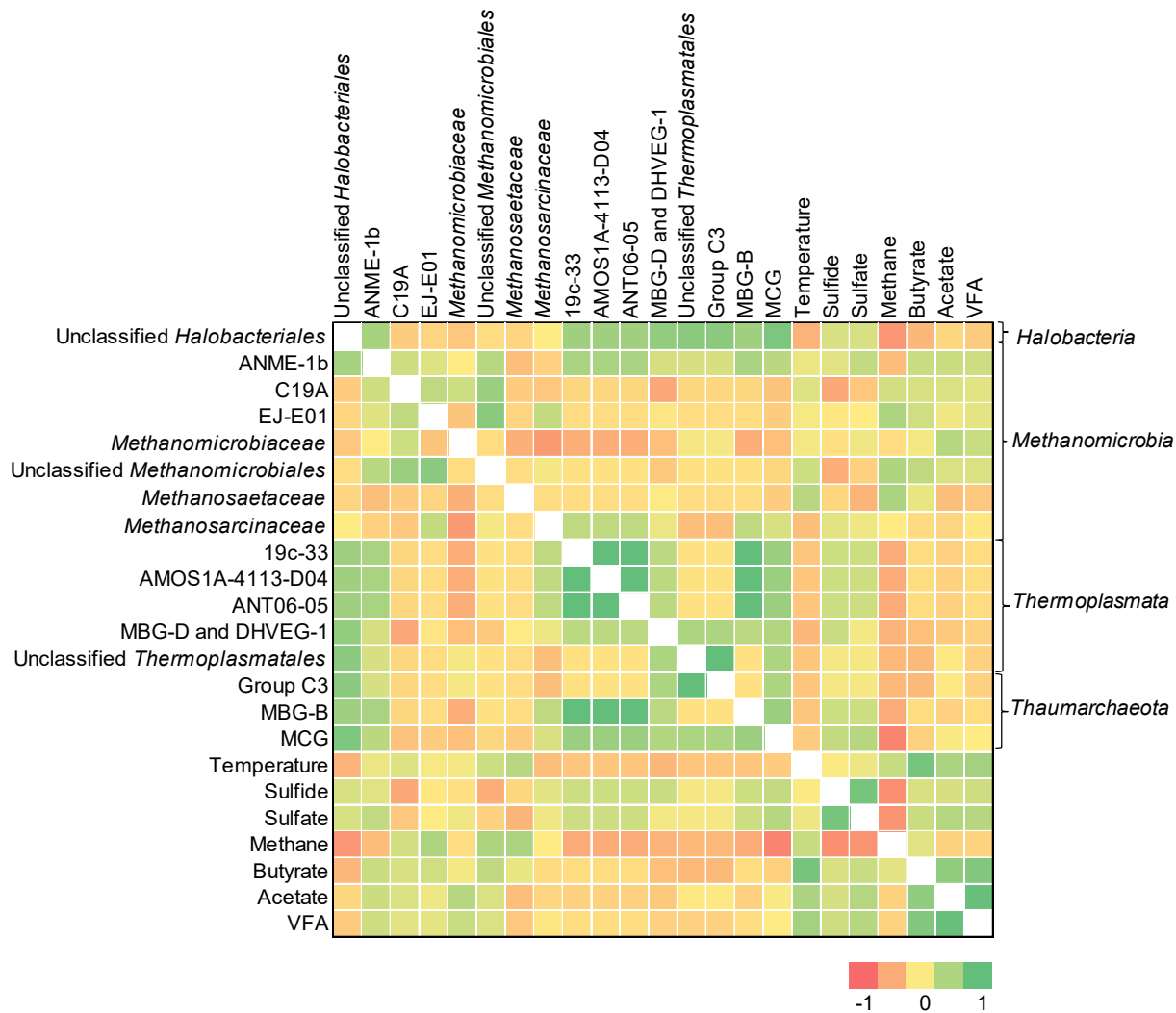


Figure S7. The heatmap depicts the correlation between archaeal families present at a relative abundance >1% of total reads across the 12 slurry samples analyzed and experimental parameters. Correlations were determined by means of the two tailed Spearman's Rank Order Correlation test. The heatmap colors represent the relative percentage of the microbial family assignments. Square colors shifted towards bright green indicate strong correlation.



Chapter 4

Propionate conversion under sulfidogenic and methanogenic conditions in different biogeochemical zones of Aarhus Bay, Denmark

Derya Ozuolmez, Alfons J. M. Stams, Caroline M. Plugge

-Manuscript in preparation for publication-

Abstract

Propionate conversion was analysed in enrichment slurries containing sediment from different biogeochemical zones of Aarhus Bay, Denmark, and the enriched prokaryotic community was determined at the end of the incubation period. Sediment slurries were amended with 3, 20 mM sulfate and without sulfate at 25°C and 10°C. After 514-571 days of incubation, methanogenesis in the sulfate zone and sulfate reduction in the methane zone slurries was observed and both processes occurred simultaneously through the whole sediment. Bacterial community analysis revealed the dominance of *Desulfobacteraceae* and *Desulfobulbaceae* members in sulfidogenic slurries incubated both at 25°C and 10°C. Sulfate-free slurries at 25°C were dominated with the sequences related to *Cryptanaerobacter* belonging to *Peptococcaceae*. Sulfate-free slurries incubated at 10°C consisted of sequences related to *Desulfobacteraceae*. Archaeal community analysis revealed the prevalence of different genera of the *Methanomicrobiales* in slurries incubated at different temperatures and with different sulfate concentrations, and the occurrence of *Methanosarcinaceae* was only observed in the absence of sulfate. In summary, our results show that Aarhus Bay sediment contains sulfate reducers, syntrophs and methanogens throughout the sediment, suggesting teamwork in the conversion of propionate.

4.1 Introduction

The mineralization of organic matter in anoxic marine sediments is a sequential process, in which several intermediates are produced by fermentative bacteria. These intermediates, including acetate, propionate, butyrate, are eventually degraded to carbon dioxide and/or methane. Sulfate reduction and methanogenesis are important terminal electron-accepting processes and controlled mainly by the amount of available sulfate (Jørgensen, 1982; Reeburgh and Heggie, 1977; Winfrey and Zeikus, 1977). In marine sediments, sulfate reduction is considered to be dominant over methanogenesis as the primary terminal electron accepting step in the degradation of organic matter (Kristjansson et al., 1982; Lovley et al., 1982). Propionate is one of the important intermediates in anaerobic degradation process and can be oxidized by several marine sulfate-reducing bacteria either completely to carbon dioxide or incompletely to acetate (Table 1). These SRB belong to the families *Desulfobacteraceae*, *Desulfobulbaceae*, *Syntrophobacteraceae* and *Peptococcaceae* (Rabus et al., 2013; Kuever, 2014b, 2014c; Leloup et al., 2007 and 2009). Incomplete-oxidizing sulfate reducers, such as *Desulfobulbus spp.*, convert propionate to acetate and carbon dioxide (Kuever, 2014c). The end-product acetate is subsequently consumed by other sulfate reducers such as *Desulfobacter spp.* in the presence of sulfate.

In the absence of sulfate, complete propionate conversion to CH₄ takes place and is only possible by cooperation of syntrophic bacteria with methanogens (Schink and Stams, 2013; Stams, 1994) (Table 1). Syntrophic fatty acid metabolism is the rate limiting step of organic carbon degradation, but contributes to the carbon flux significantly in methanogenic environments (Schink, 1997; Schink and Stams, 2013). Despite previous studies, claiming that sulfate reduction and methanogenesis are temporally or spatially separated depending on sulfate concentration (Cappenberg, 1974; Mountfort and Asher, 1979), both processes co-occur in anoxic marine environments in the presence of high organic carbon (Oremland and Taylor, 1978; Oremland et al., 1982; Senior et al., 1982). Therefore, an excessive amount of available organic carbon may lead methanogenic archaea inhabit the habitats rich in sulfate and contribute to organic matter degradation together with syntrophic bacteria.

The relative distribution of sulfate-reducing bacteria in Black Sea and Aarhus Bay sediments shows that SRB are present in the methane zone with a similar high abundance as in the sulfate zone (Leloup et al., 2007 and 2009). It is speculated that SRB and methanogens cooperate for the mineralization of organic matter in Black Sea and Aarhus Bay sediments. Similarly, Kendall and colleagues (2006) described marine propionate- and butyrate-degrading syntrophs and suggested

that syntrophic associations have a great role in the methane reserves in marine sediments. Krylova and Conrad (1998) demonstrated that there are yet uncultured propionate-converting bacteria which act either as SRB or syntrophs depending on sulfate availability. Therefore, it is crucial to understand how sulfate-reducers, syntrophs and methanogens interact during propionate conversion under high and low sulfate conditions in marine sediments.

Table 1. Overview of reactions examined in this study. ΔG values were obtained from Thauer et al., 1977.

No.	Equation		ΔG° (kJ/reaction)*
Acetogenic reactions			
1	$\text{Propionate}^- + 3 \text{H}_2\text{O}$	\rightarrow $\text{Acetate}^- + \text{HCO}_3^- + 3 \text{H}_2 + \text{H}^+$	+76.1
Sulfate-reducing reactions			
2	$\text{Propionate}^- + 0.75 \text{SO}_4^{2-}$	\rightarrow $\text{Acetate}^- + 0.75 \text{HS}^- + \text{HCO}_3^- + 0.25 \text{H}^+$	-37.8
3	$4 \text{H}_2 + \text{SO}_4^{2-} + \text{H}^+$	\rightarrow $\text{HS}^- + 4 \text{H}_2\text{O}$	-151.9
4	$\text{Acetate}^- + \text{SO}_4^{2-}$	\rightarrow $2 \text{HCO}_3^- + \text{HS}^-$	-47.6
Methanogenic reactions			
5	$4 \text{H}_2 + \text{HCO}_3^- + \text{H}^+$	\rightarrow $\text{CH}_4 + 3 \text{H}_2\text{O}$	-135.6
6	$\text{Acetate}^- + \text{H}_2\text{O}$	\rightarrow $\text{CH}_4 + \text{HCO}_3^-$	-31.0
Syntrophic propionate conversion			
1+5	$\text{Propionate}^- + 0.75 \text{H}_2\text{O}$	\rightarrow $\text{Acetate}^- + 0.75 \text{CH}_4 + 0.25 \text{HCO}_3^- + 0.25 \text{H}^+$	-25.6
Complete propionate conversion by SRB			
2+4	$\text{Propionate}^- + 1.75 \text{SO}_4^{2-}$	\rightarrow $1.75 \text{HS}^- + 3 \text{HCO}_3^- + 0.25 \text{H}^+$	-85.4
Complete propionate conversion by syntrophs and methanogens			
1+5+6	$\text{Propionate}^- + 1.75 \text{H}_2\text{O}$	\rightarrow $1.75 \text{CH}_4 + 1.25 \text{HCO}_3^- + 0.25 \text{H}^+$	-56.6

In this study, we aimed to identify the propionate conversion process and the responsible microorganisms in the sulfate, sulfate-methane transition and methane zones of Aarhus Bay, Denmark. We set up batch slurries with and without sulfate additions and incubated them at 10°C and 25°C. In this way, we examined the effect of sulfate concentration, sediment depth and temperature on the ultimate enriched bacterial and archaeal community.

4.2 Materials and methods

The materials and methods section of this chapter is exactly the same as the materials and methods section of the chapter 3. Therefore, please consult Chapter 3.

4.3 Results

4.3.1 Sampling site geochemistry

The geochemistry of the Aarhus Bay sediment was revealed by pore water analysis and biogeochemical zones were defined as sulfate zone between 0 cm and 120 cm, sulfate-methane transition zone (SMTZ) between 120 cm and 170 cm and methane zone between 170 cm and 300 cm (Fig S1).

4.3.2 Sediment slurry enrichments

4.3.2.1 Sulfate zone sediment slurries

Sulfate zone sediment slurries were incubated for 514 days at 25°C and 10°C. In sulfate-amended slurries, propionate conversion started immediately. Acetate and sulfide steadily increased as a result of repeated additions of propionate and sulfate. Slight changes were detected in acetate concentration between days 220 and 430 at 25°C, which is followed by a decrease. After propionate addition, acetate concentration increased again in response to propionate conversion (Fig 1A). In contrast, propionate conversion in 10°C slurries started after 50 days of incubation and was slower along the incubation period (Fig 1B). Several additions of propionate and sulfate yielded acetate and sulfide. Methane formation in sulfidogenic slurries was observed after 309 days at 25°C (Fig 1A), while no methane was detected in slurries incubated at 10°C (Fig 1B) throughout the study.

In sulfate-free sediment slurries, ~1 mM sulfate was detected at the beginning of the incubation, which originated from the sediment (Fig 1C, 1D). In the first 50 days of incubation at 25°C, conversion of propionate was coupled to sulfate reduction (Fig 1C). Several feeds of propionate led to the formation of methane and acetate until day 238. After that day, the acetate concentration fluctuated. Propionate conversion at 10°C was slow. Trace amounts of sulfate were depleted in 70 days and methane formation started after 260 days of incubation (Fig 1D). The total methane produced in 10°C slurries was half the amount of methane that was produced in 25°C slurries in the end of the experiment.

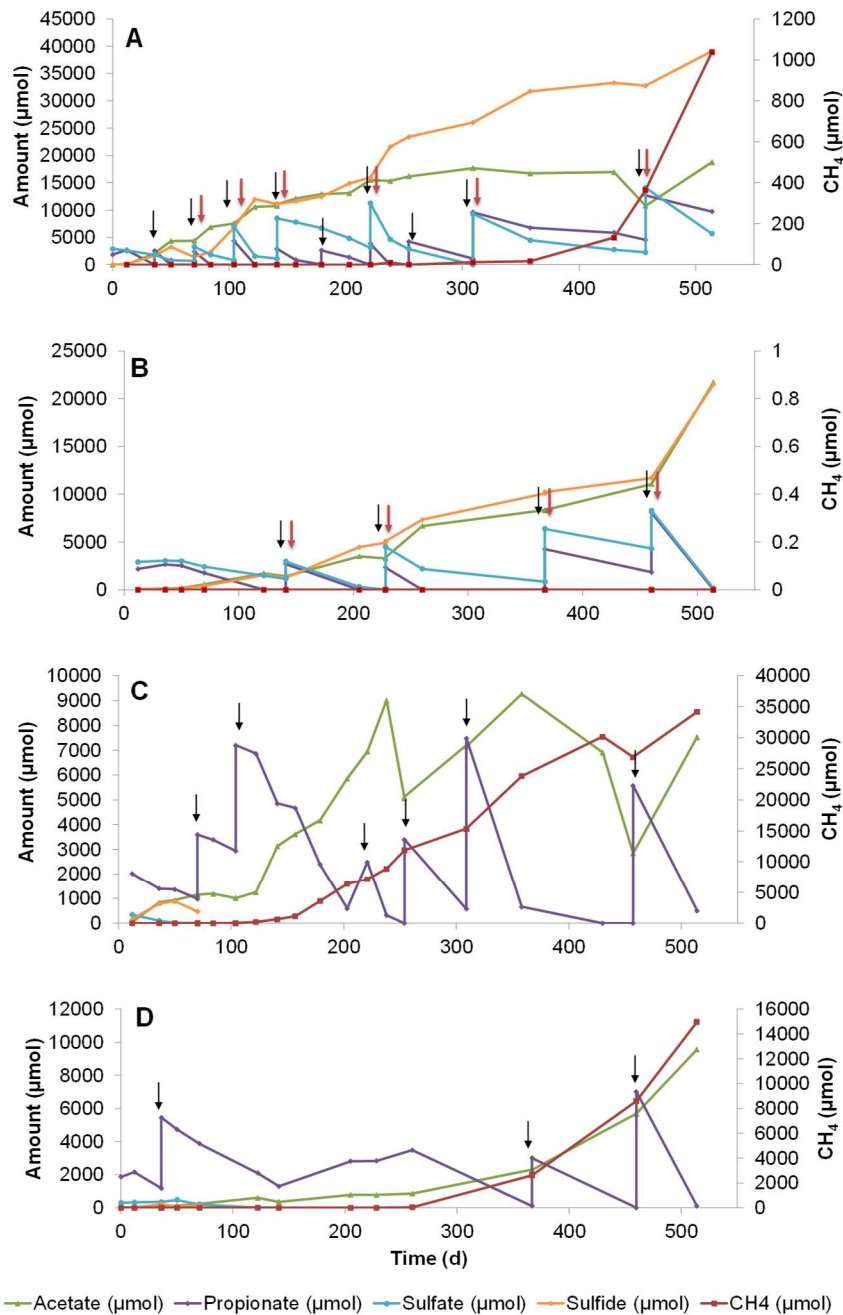


Figure 1. Changes in propionate, sulfate, acetate, sulfide and methane concentrations during 514 days of incubation in sediment slurry enrichments constituted of sulfate zone sediment (A) Slurry P₄, with 20mM sulfate addition at 25°C, (B) Slurry P₈, with 20mM sulfate addition at 10°C, (C) Slurry P₁, without sulfate addition at 25°C, (D) Slurry P₆, without sulfate addition at 10°C. Arrows denote the time points for the additions of sulfate (red) and propionate (black).

4.3.2.2 Sulfate-methane transition zone sediment slurries

SMTZ sediments were treated with low (3 mM) and high (20 mM) concentrations of sulfate for 571 days at 25°C and 10°C. Several re-feeds of propionate and sulfate were performed over the course of the experiment (Fig 2).

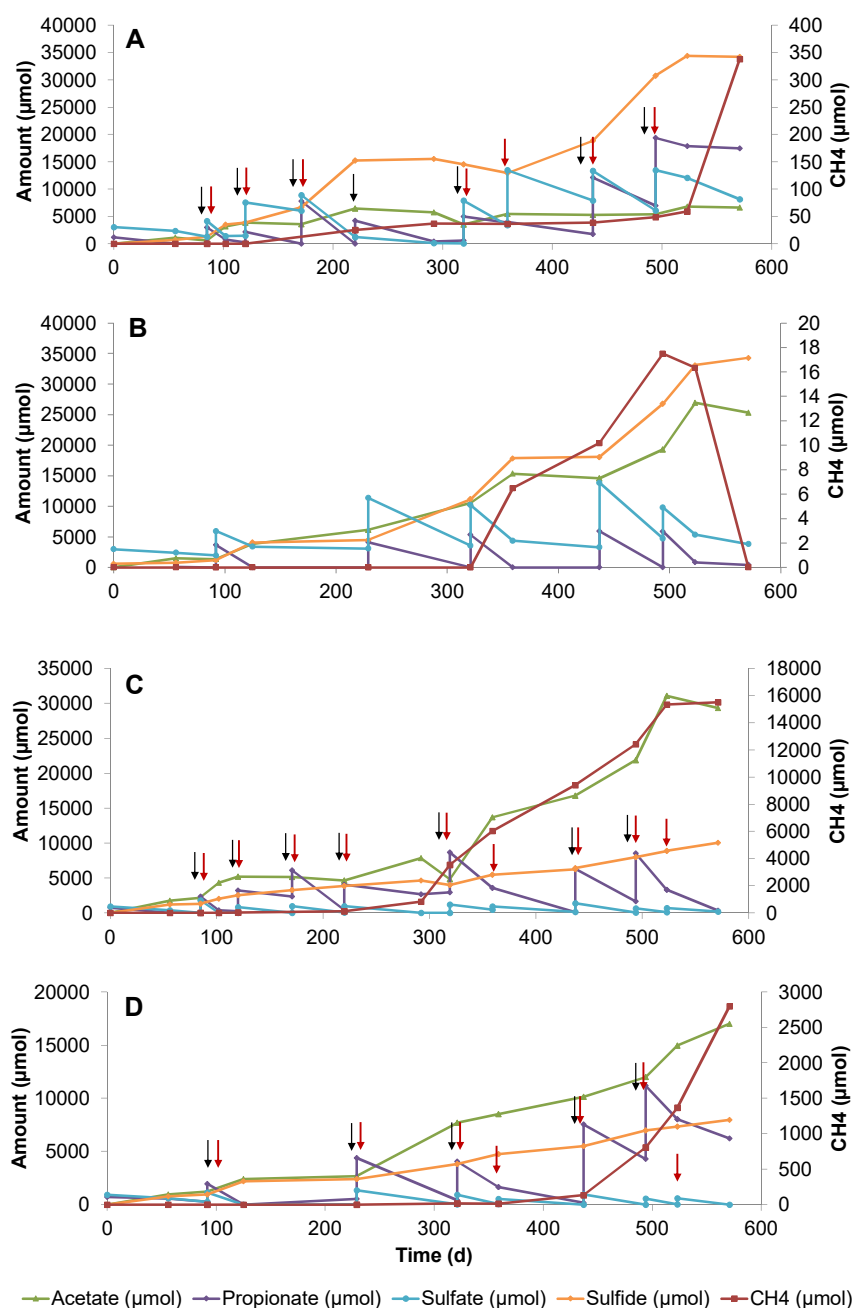


Figure 2. Changes in propionate, sulfate, acetate, sulfide and methane concentrations during 571 days of incubation in sediment slurry enrichments constituted of sulfate-methane transition zone sediment (A) Slurry P3, with 20mM sulfate addition at 25°C, (B) Slurry P7, with 20mM sulfate

addition at 10°C (C) Slurry P2, with 3mM sulfate addition at 25°C, (D) Slurry P5, with 3mM sulfate addition at 10°C. Arrows denote the time points for the additions of sulfate (red) and propionate (black).

In high sulfate treatments, the amount of consumed propionate was similar at both temperatures (Fig 2A, 2B). Propionate conversion coupled to sulfate reduction occurred and consequently the sulfide concentration increased. Acetate accumulated slowly in 25°C slurries (Fig 2A) whereas a steady increase in acetate was observed in 10°C slurries (Fig 2B). Methane in 25°C slurries was first observed on day 220, slightly increased until day 523, and a sudden rise was measured between days 523 and 571. On the other hand, methane formation in 10°C slurries was detected on day 359 and reached to 17 $\mu\text{mol}/\text{bottle}$ by the end of the experiment which was 20 times less than the methane that was produced in 25°C slurries.

The concentrations of propionate consumed and acetate accumulated in low sulfate amended slurries were two times higher at 25°C (Fig 2C) as compared to the slurries incubated at 10°C (Fig 2D). Methane formation started on day 85 at 25°C, gradually increased and reached to a concentration which was more than five times higher than that was measured in 10°C slurries.

4.3.2.3 Methane zone sediment slurries

The fastest propionate conversion in the methane zone slurries occurred under sulfate-amended conditions at 25°C (Fig 3A). Propionate conversion via sulfate reduction started in the beginning of the experiment and continued during the course of the study. Methane formation was observed on day 294 and boosted after day 414. However, the conversion of propionate at 10°C was slow and no methane production occurred during the experiment (Fig 3B).

The highest methane concentration was observed in the sulfate-free slurry at 25°C (Fig 3C). Approximately 1.1 mM sulfate was measured in the slurry at the beginning of the experiment, and propionate conversion coupled to sulfate reduction occurred within the first 50 days. The depletion of sulfate in the slurry was followed by a lag phase where almost no change was observed in propionate and acetate levels. After day 107, propionate conversion started rapidly with concomitant acetate and methane production. Acetate accumulated until day 259 and then was almost completely consumed. Propionate conversion in methanogenic slurries at 10°C occurred via sulfate reduction until the trace amount of sulfate had depleted (Fig 3D). Thereafter a lag phase of 226 days was observed which was followed by rapid propionate conversion accompanied by steep

increase in acetate and methane. In total, 9 times less methane was produced at 10°C as compared to 25°C in sulfate-free slurries.

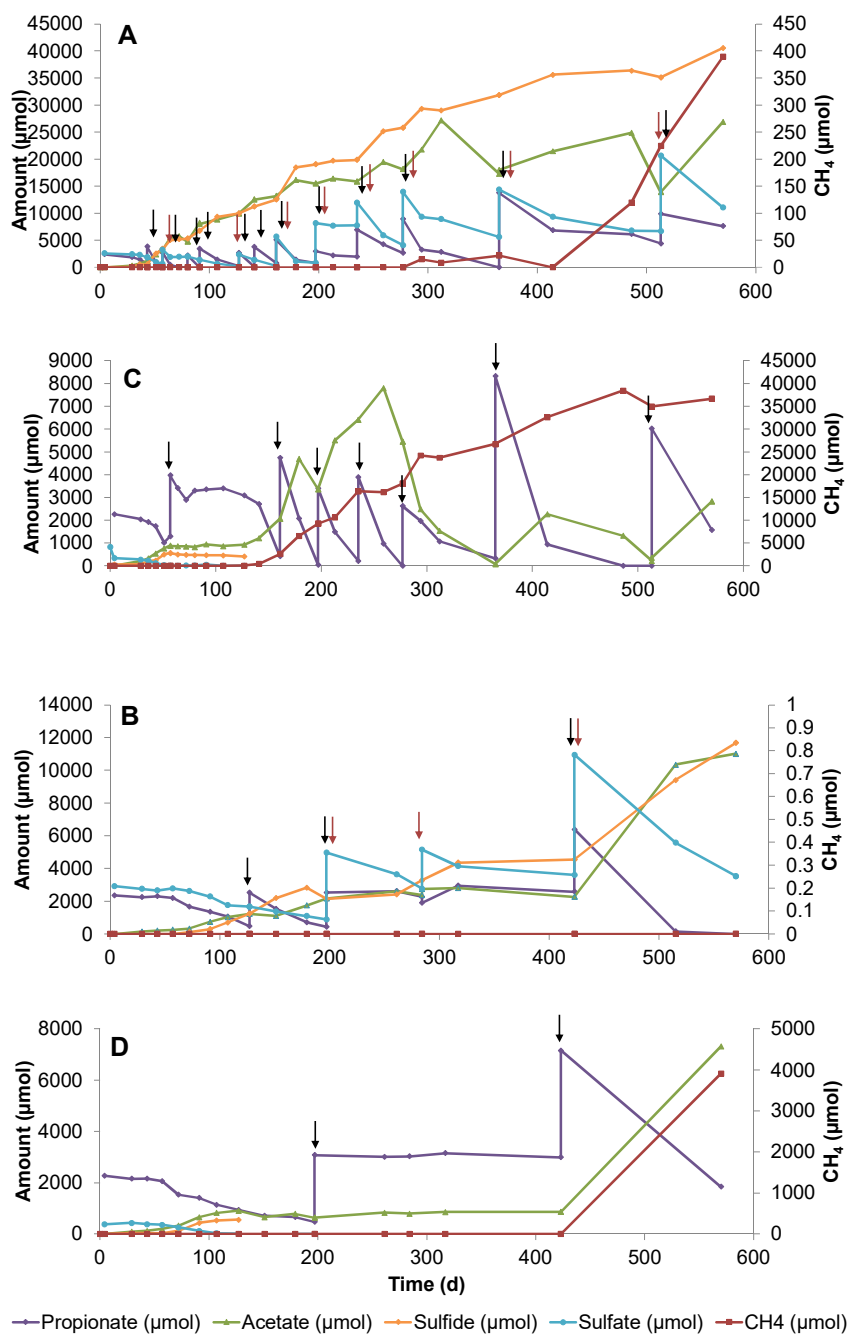


Figure 3. Changes in propionate, sulfate, acetate, sulfide and methane concentrations during 570 days of incubation in sediment slurry enrichments constituted of methane zone sediment (A) Slurry P6, with 20mM sulfate addition at 25°C, (B) Slurry P8, with 20mM sulfate addition at 10°C (C) Slurry P3, without sulfate addition at 25°C, (D) Slurry P1, without sulfate addition at 10°C. Arrows denote the time points for the additions of sulfate (red) and propionate (black).

4.3.3 Distribution of bacterial and archaeal community through PCR-DGGE analysis

Changes in the community structure over time in all slurries were visualized by denaturing gradient gel electrophoresis (DGGE). Bacterial DGGE gels harboured more bands in general compared to the archaeal gels. Some bands were present at all times with the same intensity, some of them disappeared or became fainter and some appeared and get intensified in time; revealing a dynamic bacterial community. In archaeal DGGE gels, most of the bands kept their position throughout the incubation period. Some bands became fainter while new bands appeared in methanogenic slurries especially after 100 days of incubation and thickened (data not shown). These banding patterns were organized in dendrograms by UPGMA clustering analysis (Fig S2, S3).

Clustering analysis of bacterial DGGE banding patterns gave separate clusters for each depth zone (i.e. SZ, SMTZ, MZ) except for the sample SZ P₁ and SZ P₈ which differed from all other samples (Fig S2). Methane zone slurries formed 4 sub-clusters; each slurry under different incubation condition formed a separate sub-cluster. Sulfate zone slurries formed 2 sub-clusters for each slurry, one representing the earlier incubation time samples and the other representing the later incubation time samples. SMTZ slurries formed two main sub-clusters, one representing the 25°C and the other 10°C slurries.

For the Archaeal communities, slurries belonging to each geochemical zone were grouped as one cluster similar to what was observed for Bacteria, except for the sub-clusters of three slurries belonging to the methane zone, MZ P₃, P₆, P₈ (Fig S3). SMTZ slurries grouped based on incubation temperature, and one sub-cluster representing the samples of the last sampling time of each slurry differed from all other SMTZ samples. On the other hand, SZ slurries clustered depending on the sampling time. The slurries formed different sub-clusters as the community in the slurries differed by the enrichment of some metabolic groups.

4.3.4 Bacterial community composition after long-term incubation

PCR amplified partial 16S rRNA gene fragments obtained from the last sampling time of all slurries were sequenced. After filtering and trimming, between 1888 and 27196 high quality reads were found per sample (Table S2) and clustered into 64–131 operational taxonomic units (OTUs) per sample.

OTUs classified into 33 phyla, with 95% of the OTUs belonging to *Proteobacteria* (61.3%), *Firmicutes* (17.5%), *Chloroflexi* (9.8%), *Bacteroidetes* (3.4%), *Spirochaetes* (2.5%) and Candidate division OP9 (1%). The *Desulfobacteraceae* and *Desulfobulbaceae* were the two dominant families in the phylum *Proteobacteria*, having 38.6% and 29.2% of the reads, respectively (Fig S4). The *Firmicutes* phylum was dominated by the *Peptococcaceae* family comprising 86.8% of the reads. Similarly, the *Anaerolinaceae* family dominated the *Chloroflexi* phylum containing 78.1% of the reads (Fig S4). Above mentioned four families were the most dominant in all samples. Despite the overall dominance of these families, a high degree of variation was observed in their relative abundances between different slurries.

The most abundant OTUs in different slurries belonged to the genera *Cryptanaerobacter* (76%) in the phylum *Firmicutes*, *Desulfobulbus* (59%), *Desulfosarcina* (52%), SEEP-SRB₁ (45%) and *Desulforhopalus* (44%) in the phylum *Proteobacteria* (Fig 4). Additionally, the most abundant OTUs (85%) in one slurry (SZ P6) belonged to the family *Desulfobacteraceae* which could not be assigned to any genus (Fig 4).

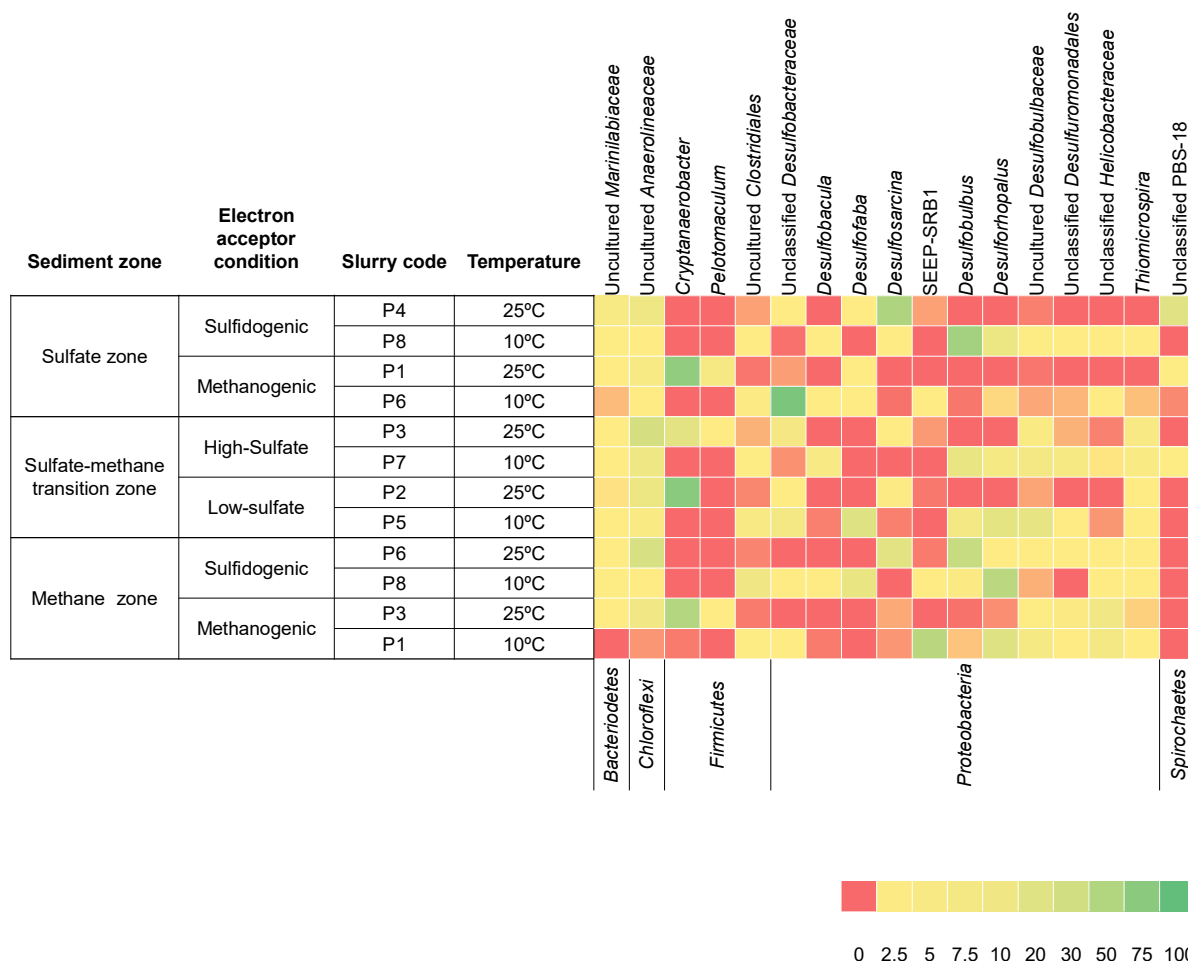


Figure 4. The heatmap depicts the relative percentage of the most common (>5 %) bacterial 16S rRNA gene sequences across the 12 slurries fed with propionate. The heatmap colors represent the relative percentage of the bacterial assignments within each sample. Colors shifted towards dark green indicate higher abundance. Taxonomy is shown at the genus level (unless unclassified) above and at the phylum level below the heatmap.

The microbial community was analysed using redundancy analysis (RDA) (Fig 5). The bacterial community composition in RDA was plotted on the basis of the relative read abundance of OTUs in each sample. The highest read abundance, in decreasing order, belonged to the bacterial orders *Desulfobacterales*, *Clostridiales* and *Anaerolineales* with OTU numbers 26, 19 and 15, respectively (Fig 5).

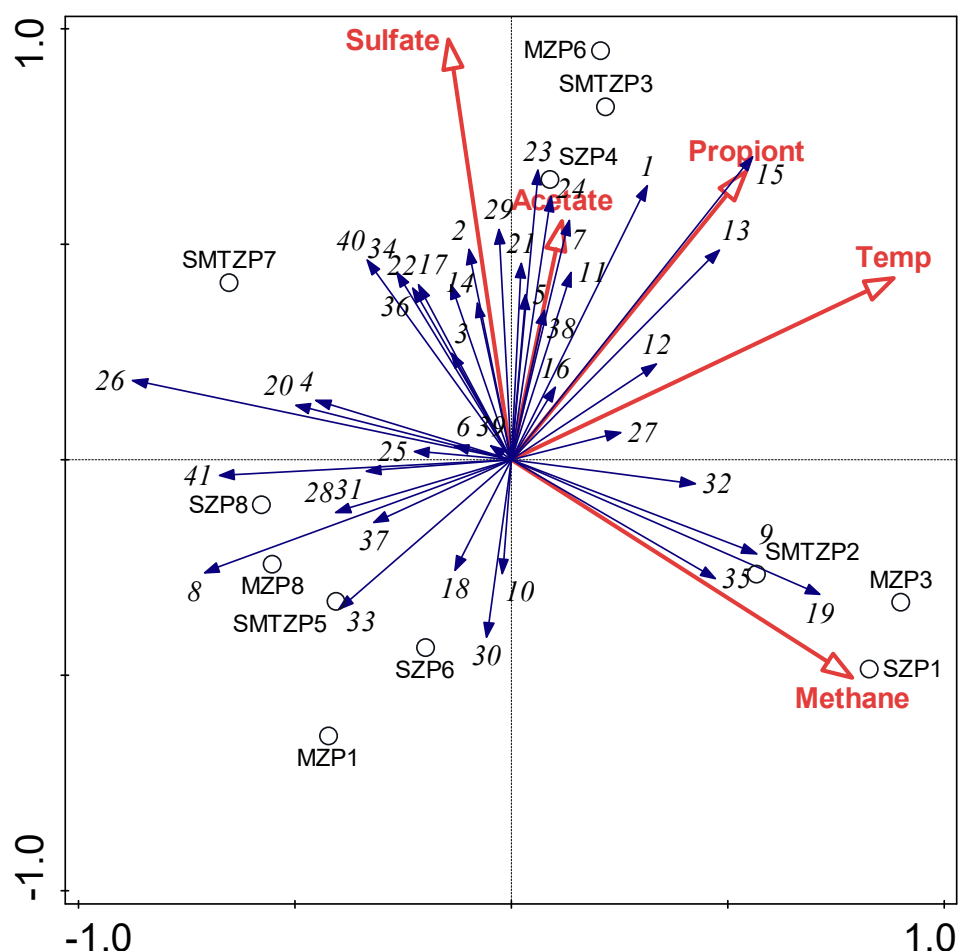


Figure 5. Redundancy analysis triplot showing relationship between bacterial community composition at order level and environmental parameters. Environmental variables are given as red vectors. Blue vectors represent bacterial orders. Orders were included with a relative abundance of at least 1% in any sample. Vector length gives the variance that can be explained by a particular environmental parameter. Perpendicular distance reflects association, with smaller distances indicating a larger association. Temp: Temperature, Propionat: Propionate.

OTU numbers and corresponding taxa are as followed: (1)Bacteria-Other; (2)Actinobacteria-OPB41; (3)Bacteroidetes; (4)Bacteroidetes-BD2-2; (5)Bacteroidetes-Bacteroidales; (6)Bacteroidetes-Flavobacteriales; (7)Bacteroidetes-SB-1; (8)Bacteroidetes-SB-5; (9)Bacteroidetes-Sphingobacteriales; (10)Bacteroidetes-VC2.1.Bac22; (11)Bacteroidetes-vadinHA17; (12)Bacteroidetes-vadinHA17-uncultured bacterium; (13)Candidate division OP9; (14)Chloroflexi-Anaerolineae; (15)Chloroflexi-Anaerolineales; (16)Chloroflexi-GIF9; (17)Cyanobacteria-Chloroplast; (18)Elusimicrobia-Lineage_IV; (19)Firmicutes-Clostridiales; (20)Nitrospirae-Nitrospirales; (21)Planctomycetes-Planctomycetales; (22)Proteobacteria-Rhizobiales; (23)Proteobacteria-Burkholderiales; (24)Proteobacteria-Deltaproteobacteria; (25)Proteobacteria-Desulfarcuiales; (26)Proteobacteria-Desulfobacterales; (27)Proteobacteria-Desulfovibrionales; (28)Proteobacteria-Desulfuromonadales; (29)Proteobacteria-Svao485; (30)Proteobacteria-Campylobacteriales; (31)Proteobacteria-Gammaproteobacteria; (32)Proteobacteria-Alteromonadales; (33)Proteobacteria-Chromatiales; (34)Proteobacteria-Thiotrichales; (35)RF3; (36)RF3-uncultured

bacterium; (37)*Spirochaetes*-LK-44f; (38)*Spirochaetes*-PBS-18; (39)*Spirochaetes*-*Spirochaetaceae*; (40)TM6; (41)*Tenericutes*-*Acholeplasmatales*.

The OTUs affiliating with the order *Desulfobacterales* were associated with the slurries incubated at 10°C in which they were dominant. These slurries showed close clustering towards the bottom left part of the RDA triplot and they were negatively correlated with the temperature. The second most abundant order, *Clostridiales*, showed strong association with methane and was plotted between the slurries SZP₁, SMTZP₂ and MZP₃ in which the highest methane concentration was measured. These three slurries were incubated at 25°C and without or low sulfate which was supported by a negative association to sulfate and a positive association to temperature. Another abundant order, *Anaerolineales*, associated with high sulfate and high temperature conditions clustering in the upper right portion of the graph between temperature and sulfate, adjacent to the slurries SZP₄, MZP₆, SMTZP₃ incubated under these conditions (Fig 5, S4).

4.3.5 Archaeal community composition and structure

PCR amplified partial 16S rRNA gene fragments obtained from the slurries on the last sampling day were sequenced. After filtering and trimming, between 5547 and 108810 high quality reads were found per sample.

The highest percentage of 16S rRNA reads for Archaea clustered within the families *Methanomicrobiaceae* (39.8%), an unclassified *Methanomicrobiales* clone (EJ-Eo1) (21.4%) belonging to *Methanomicrobiales*, Marine Benthic Group D (MBG-D) and DHVEG-1 (10.7%), *Methanosarcinaceae* (10.4%) and unclassified *Methanomicrobiales* (9.7%) (Fig S6). *Methanoculleus* and *Methanogenium* from the family *Methanomicrobiaceae* dominated different slurries (Fig 6). The unclassified *Methanomicrobiales* clone (EJ-Eo1) dominated three slurries where the relative abundances of *Methanoculleus* and *Methanogenium* were low. *Methanosarcina* was observed to be the dominant genus being present in four slurries with read percentages ranging between 14-30%, whereas *Methanococcoides* had less reads in seven slurries. Marine Benthic Group D (MBG-D) and DHVEG-1 from the order *Thermoplasmatales* dominated two methane zone slurries containing sulfate with read percentages 45% and 47% (Fig 6).

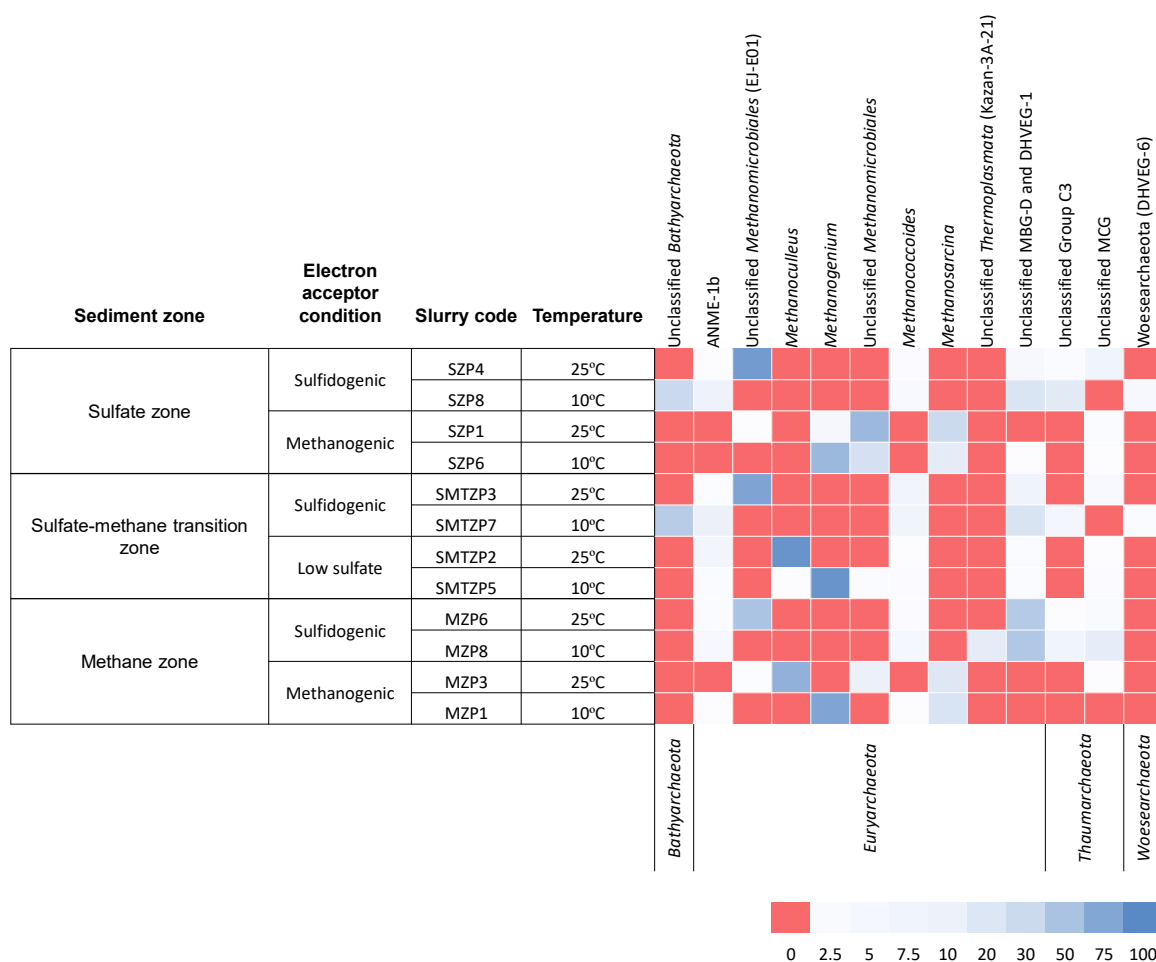


Figure 6. The heatmap depicts the relative abundance of the most common (>5 %) archaeal 16S rRNA gene sequences (unless unclassified) across the 12 slurries fed with propionate. The heatmap colors represent the relative percentage of the archaeal assignments within each sample. Colors shifted towards bright blue indicate higher abundance.

Archaeal RDA triplots showed that the slurries originating from the same biogeochemical zone were not clustered closely which indicated that the community composition changed upon incubation (Fig 7). A strong association was observed between methane and the families *Methanomicrobiaceae*, unclassified *Methanomicrobiales* and *Methanosarcinaceae*, and negative association between sulfate and these taxa. The slurries SZP6, MZP1, SMTZP2 and SMTZP5, which were dominated with *Methanomicrobiaceae*, showed close clustering (Fig 7, S6). The other two slurries, SZP1 and MZP3, were strongly associated with methane and showed close association with other two methanogenic families *Methanosarcinaceae* and unclassified *Methanomicrobiales*. The unclassified *Methanomicrobiales* clone (EJ-E01) was prevalent in the slurries containing sulfate and was plotted between the sulfidogenic slurries SMTZP3, SZP4 and MZP6 (Fig 7, Fig S6). MBG-D and

DHVEG-1 showed a close relation to sulfate and was plotted close to the sulfidogenic slurries MZP6 and MZP8 in which they were dominantly present.

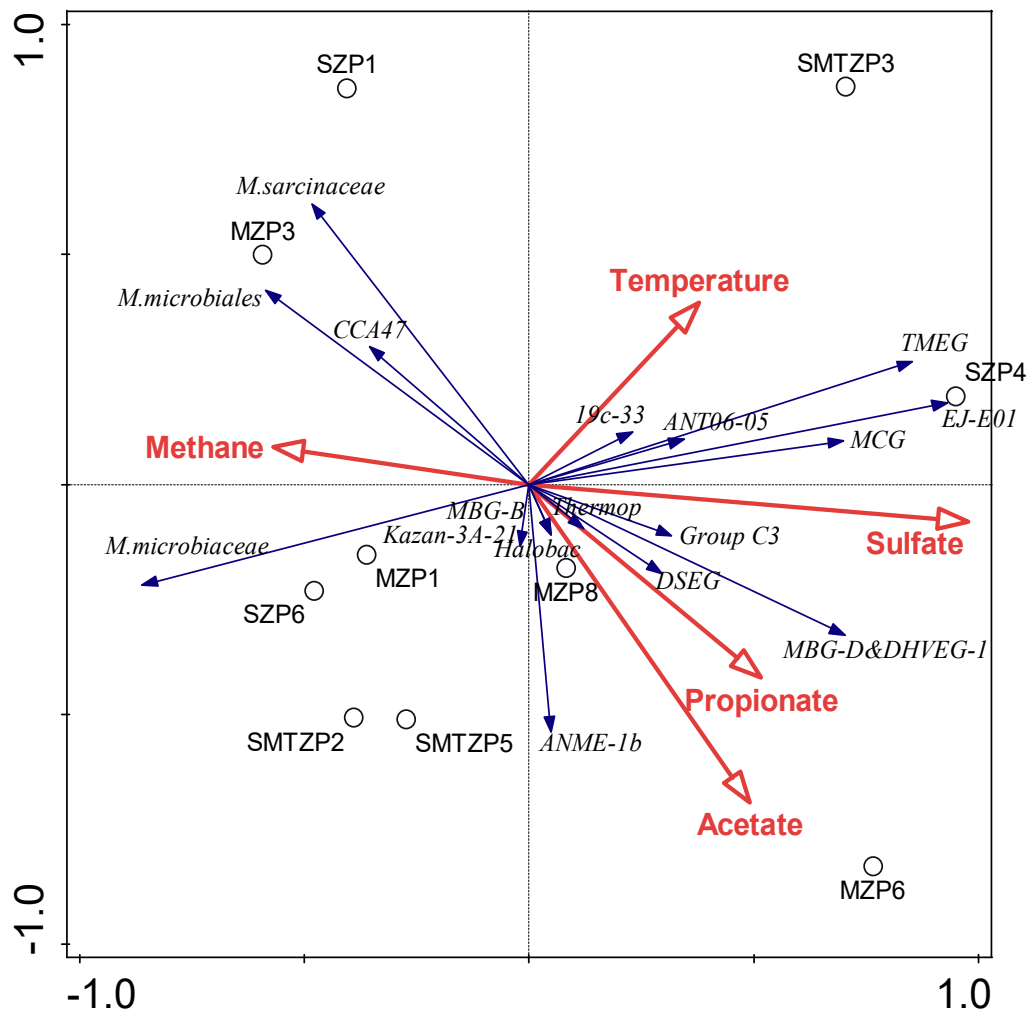


Figure 7. Redundancy Analysis Triplot showing relationship between Archaeal community composition at family level and environmental parameters. Environmental variables are given as red vectors. Blue vectors represent Archaeal families. Families were included with a relative abundance of at least 1% in any sample. Vector length gives the variance that can be explained by a particular environmental parameter. Perpendicular distance reflects association, with smaller distances indicating a larger association. Full names of the phylotypes in the plot are as followed: *M.sarcinaceae*: *Methanosarcinaceae*; *M.microbiales*: *Methanomicrobiales*; *M.microbiaceae*: *Methanomicrobiaceae*; *Halobac*: *Halobacteriales*; *Thermop*: *Thermoplasmatales*.

4.3.6 Correlation within the microbial community and between the microbial community and environmental parameters

Correlation analysis of the sequencing data revealed both positive and negative relations between 34 bacterial orders that were present in different slurries (Fig S5). *Clostridiales* had a strong negative correlation to *Desulfobacterales* order ($P < 0.05$) and to sulfate and sulfide, however showed a positive correlation to temperature and methane. An overall negative correlation was observed between *Desulfobacterales* and the orders *Clostridiales* ($P < 0.05$), *Anaerolineales* ($P < 0.05$), candidate division OP9 ($P < 0.05$), and the incubation temperature ($P < 0.01$). Strong positive correlations were observed between *Anaerolineales* and temperature ($P < 0.01$), VFA ($P < 0.01$), propionate ($P < 0.01$). Unclassified *Deltaproteobacteria* showed positive correlation to the orders SB-1 ($P < 0.01$), *Flavobacteriales*, *Anaerolineales*, candidate division OP9 and to all environmental parameters except for methane (Fig S5).

The hydrogenotrophic methanogenic family *Methanomicrobiaceae* and unclassified *Methanomicrobiales* order showed similar trend in their correlation to other taxa and environmental parameters except for few differences (Fig S7). *Methanomicrobiaceae* family was the only family showing positive correlation to the ANME-1b and strong positive correlation to methane production ($P < 0.05$). On the other hand, unclassified *Methanomicrobiales* was positively correlated to *Methanosarcinaceae*. Differently from other methanogenic groups, the unclassified *Methanomicrobiales* (EJ-Eo1 clone) showed positive correlations to some families belonging to *Thermoplasmata* and *Thaumarchaeota* phyla and all environmental parameters except for methane. MBG-D and DHVEG-1 was positively correlated to most of the taxonomic groups and environmental parameters, whereas strong negative correlations were observed to methane and the methanogenic taxa ($P < 0.05$), except for the unclassified *Methanomicrobiales* (Fig S7).

4.4 Discussion

4.4.1 Sulfate-dependent propionate conversion

Propionate is an important substrate for sulfate reducers in marine sediments, providing about 10% of the reducing equivalents for sulfate reduction (Sørensen et al., 1981). The propionate conversions in sulfate amended SZ and MZ slurries at 25°C were similar in terms of immediate start and conversion rate of propionate (Fig 1A, 3A). The stoichiometry of the propionate conversion in MZ slurries was determined as $\text{CH}_3\text{CH}_2\text{COO}^- + 0.9 \text{SO}_4^{2-} \rightarrow \text{CH}_3\text{COO}^- + 0.8 \text{HS}^-$, and this pointed to

incomplete propionate oxidation (Table 1, reaction 2). On the other hand, the ratio of reduced sulfate to the consumed propionate in SZ slurry ($\text{CH}_3\text{CH}_2\text{COO}^- + 1.6 \text{SO}_4^{2-} \rightarrow \text{CH}_3\text{COO}^- + 1.5 \text{HS}^-$) is close to the theoretical values of complete propionate conversion (Table 1, reactions 2+4) (Table S1). Especially between the days 220 and 430, propionate was completely converted coupled to sulfate reduction and no net acetate increase was observed (Fig 1A). The high concentration of acetate detected at the end of the incubation period might have originated from the metabolism of fermentative bacteria. Yet, simultaneous increase in acetate and methane between the days 457 and 514 suggests syntrophic conversion of propionate by fermentative bacteria and hydrogenotrophic methanogenic archaea, in addition to the ongoing sulfate-dependent propionate conversion (Fig 1A). It was striking to detect rapidly increasing methane in MZ as well as SZ slurry after 414 and 309 days of incubation, respectively (Fig 1A, 3A). The late methane production might be linked to the sulfide inhibition of methanogens which was reported in previous studies (Pender et al., 2004; O'Flaherty et al., 1998; Shin et al., 1995). Despite high sulfidogenic activity, methanogenic archaea might have adapted to the slurry conditions and be involved in the consumption of conversion products.

The ratio of consumed propionate and sulfate in high-sulfate amended SMTZ slurry at 25°C ($\text{CH}_3\text{CH}_2\text{COO}^- + 1.3 \text{SO}_4^{2-} \rightarrow 0.3 \text{CH}_3\text{COO}^- + 1.2 \text{HS}^-$) points to the combination of incomplete and complete propionate oxidation via sulfate reduction. The acetate that was formed as primary product from incomplete conversion was further oxidized by aceticlastic SRB (Table S1, Fig 2A). Propionate in the low sulfate-amended slurry at 25°C was converted by both sulfate reducers and syntrophs in cooperation with methanogens ($\text{CH}_3\text{CH}_2\text{COO}^- + 0.3 \text{SO}_4^{2-} \rightarrow 1.1 \text{CH}_3\text{COO}^- + 0.3 \text{HS}^- + 0.5 \text{CH}_4$) (Table S1, Fig 2C). The low levels of sulfate were not sufficient to support complete propionate conversion through sulfate reduction and consequently syntrophic propionate-degrading communities became active (Muyzer and Stams, 2008).

4.4.2 Sulfate-independent propionate conversion

Propionate conversion in sulfate-free SZ and MZ slurries at 25°C started with the reduction of sulfate originating from the sediment (Fig 1C, 3C). This conversion indicated the existence of metabolically active sulfate-reducing microorganisms in sulfate zone as well as in methane zone. Previous studies reported the presence of active SRB with similar cell numbers in the upper and lower parts of the coastal marine sediments of Limfjorden and Aarhus Bay, Denmark (Jørgensen, 1978; Thomsen et al., 2001; Leloup et al., 2009) and deep-sea sediment (Leloup et al., 2007). The

high abundance of SRB in sulfate-depleted sediments might be due to the acetogenic and fermentative growth characteristics of some SRB in the absence of sulfate (Plugge et al., 2011; Muyzer and Stams, 2008). The fast propionate conversion with concomitant acetate and methane production in both SZ and MZ slurries suggests the activity of syntrophic propionate-converting consortia (Fig 1C, 3C). Under methanogenic conditions, the degradation of propionate to acetate, CO₂, and 3H₂ is highly endergonic process ($\Delta G^\circ = 76.1$ kJ/mol) (Table 1), but it can be accomplished by syntrophic cooperation of propionate-oxidizing bacteria and H₂- or formate-consuming methanogens (Boone and Bryant, 1980; McInerney et al., 2008). Acetate rapidly accumulated in the slurries as a result of propionate conversion, and was utilized only after propionate became depleted (Fig 1C, 3C). Similar conversion dynamics were reported for both methanogenic (Viggi et al., 2014; Stams et al., 1992) and sulfidogenic batch cultures (Laanbroek and Pfennig, 1981). Apparently, acetoclastic methanogens contributed to the conversion process by consuming accumulated acetate after propionate amount became low in both slurries (Fig 1C, 3C). Archaeal DGGE profiles of SZ slurry reflected appearance of new bands on day 138 and 358 (data not shown) after methane production and acetate consumption started, respectively (Fig 1C). Clustering analysis placed these two time samples in different sub-clusters indicating the change in archaeal community structure along the incubation (Fig S3). In MZ slurry, acetate was consumed down to near zero value, showing efficient cooperation of syntrophic bacteria, hydrogenotrophic and acetoclastic methanogenic archaea.

4.4.3 The effect of temperature on propionate conversion

Low incubation temperature have an impact on propionate conversion both in the presence and absence of sulfate in Aarhus Bay sediments. Propionate conversion at 10°C occurred overall slower and methane was not detected in sulfate amended SZ and MZ slurries (Fig 1B, 3B). More acetate accumulated in high-sulfate SMTZ slurry at 10°C as compared to its replicate at 25°C. This might be linked to the low activity of acetoclastic microorganisms. Previous experiments performed with marine sediments in sulfate-amended slurries showed that the rate of sulfate reduction decreased and as a result, organic acid concentration increased at temperatures below 25°C (Weston and Joye, 2005).

In sulfate-free MZ slurry at 10°C, a long lag phase was observed between the consumption of trace amount of sulfate and the start of propionate conversion (Fig 3D). It is known that microorganisms in subsurface environments have low metabolic and growth rate, and can persist

in a dormant state (Jørgensen and Marshall, 2016). On the other hand, the distance between hydrogen-producing and hydrogen-consuming microorganisms during syntrophic degradation of a compound is important (Stams, 1994). Grotenhuis et al. (1991) observed μm range between propionate-oxidizing bacteria and methanogens in propionate-adapted methanogenic granules. Therefore, the slow growth and the establishment of the microbial clusters might have led to a late start of the syntrophic conversion of propionate at low temperature.

4.4.4 Bacteria enriched in sulfate-amended slurries

The most abundant sulfate-reducing genera in sulfate-amended SZ and MZ slurries at 25°C were *Desulfosarcina* belonging to *Desulfobacteraceae* and *Desulfobulbus* belonging to *Desulfobulbaceae* (Fig 4, 4S). The *Desulfobacteraceae* family mainly consist of sulfate reducers that completely oxidize organic substrates (Kuever, 2014b) and is commonly found as the dominant SRB in anoxic marine sediments (Dhillon et al. 2003; Llobet-Brossa et al. 2002; Leloup et al. 2007 and 2009; Jørgensen and Bak, 1991). Leloup et al. (2009) reported that the upper sulfate-rich sediment of Station M₁, Aarhus Bay was dominated by *Desulfosarcina* species. Similar findings on the predominance of *Desulfosarcina*-like *dsrAB* sequences were observed at Station 6 in Aarhus Bay (Sahm et al., 1999), in Kysing Fjord, Denmark, (Thomsen et al., 2001) and Mariager Fjord, Denmark (Wagner et al., 2005). *Desulfosarcina* species are able to use propionate as electron donor (Widdel, 1980). Thus they participated in propionate conversion in sulfate-amended sediment slurry enrichments at 25°C.

Sulfate-amended slurries at 10°C were dominated by *Desulfobulbus* and *Desulforhopalus* (Fig 4, 4S). The relative abundance of *Desulfobulbus* decreased, whereas *Desulforhopalus* increased with increasing depth. Low temperature SMTZ slurries also contained *Desulfofaba*, belonging to *Desulfobacteraceae*. *Desulfofaba* species are known as obligately psychrophilic marine sulfate-reducers capable of propionate oxidation (Kuever, 2014b). Most members of *Desulfobulbaceae* are incomplete oxidizers and specialized in the oxidation of organic acids, including propionate, to acetate (Kuever, 2014c; Muyzer and Stams; 2008; Devereux et al., 1989; Widdel and Bak, 1992). This is in agreement with the observed acetate accumulation in the *Desulfobulbaceae* containing slurries. The higher relative abundance of *Desulfobulbaceae* and some *Desulfobacteraceae* members in low temperature slurries is in line with the statistical analysis showing the negative correlation between the order *Desulfobacterales* and the incubation temperature (Fig S5). Apparently, the

Desulfobulbaceae members had the competitive advantage and dominated over *Desulfobacteraceae* in low temperature slurries.

All sulfidogenic slurries incubated at 25°C contained uncultured *Anaerolineaceae* belonging to the phylum *Chloroflexi* (Fig 4, S4). The cultured representatives of this lineage are known as filamentous, slow-growing and strictly anaerobic chemoorganotrophs decomposing carbohydrates and amino acids (Yamada and Sekiguchi, 2009). It was reported that *Anaerolineaceae* members act as secondary degraders and degrade dead biomass together with acetate and H₂-consuming methanogens (Kleinstuber et al., 2012). Therefore, the uncultured *Anaerolineaceae* in our study might have formed a syntrophic relationship with hydrogenotrophic and/or acetoclastic methanogens and took part in the degradation of organic content and/or dead biomass.

4.4.5 Bacteria enriched in sulfate-free slurries

Sulfate-free and low-sulfate amended slurries composed of sediment from each biogeochemical zone and incubated at 25°C are dominated by *Cryptanaerobacter* and also contain *Pelotomaculum* both of which belong to the family *Peptococcaceae* (Fig 4, Fig S4). Currently known propionate-oxidizing syntrophic species of the genus *Pelotomaculum* are *P. schinkii*, *P. thermopropionicum*, and *P. propionicum* (de Bok et al., 2005; Imachi et al., 2002, 2007). The *Pelotomaculum* enriched in our study apparently takes part in propionate conversion. On the other hand, there is only one cultured species of the genus *Cryptanaerobacter*, namely *C. phenolicus*, and it transforms phenol and 4-hydroxybenzoate (4-OHB) into benzoate (Juteau et al., 2005). Its closest cultured relative is *Pelotomaculum thermopropionicum*. Propionate utilization in the presence of a hydrogenotrophic methanogen by this genus has not been reported. We hypothesize that, *Cryptanaerobacter* might have the capability to convert propionate in syntrophy with hydrogenotrophic methanogens. The idea behind this hypothesis is based on ; i) the isolation of *C. phenolicus* from a methanogenic consortium, ii) the syntrophic lifestyle of its closest cultured relatives and iii) the presence of propionate as a sole carbon source in the slurries. Additionally, the hypothesis is supported with the statistical analysis showing positive correlation of the order *Clostridiales* with methane and temperature (Fig S5).

4.4.6 Sulfate-reducing bacteria enriched in sulfate-free slurries

Bacterial community analysis revealed the dominance of unclassified *Desulfobacteraceae* members constituting 85% of the total reads in low-temperature sulfate-free SZ slurry (Fig 4, S4). Although it was surprising to observe a sulfate-reducing family representing the substantial part of the reads in sulfate-free slurry, there are non-sulfate reducing members of this family, such as the butyrate-utilizing marine syntroph *Algorimarina butyrica* (Kendall et al., 2006). In addition, Ulrich and Edwards (2003) enriched benzene-degrading cultures which were dominated by a phylotype affiliated to *Desulfobacteraceae*, and which were capable of switching from sulfate-reducing to methanogenic life style. Raskin et al. (1996) also reported the presence of *Desulfovibrio spp.* and *Desulfobacterium spp.* in a methanogenic reactor and explained this occurrence by their ability to function as proton-reducing acetogens and/or fermenters. These results illustrate the significance of metabolic flexibility of microorganism under changing conditions such as temperature, electron acceptor availability, the presence/absence of partner organisms.

Similar to the above mentioned SZ slurry, sulfate-free MZ slurry incubated at 10°C contained high numbers of *Desulfobacteraceae*-related reads (Fig 4). These reads were assigned as SEEP-SRB₁, defining *Desulfosarcina/Desulfococcus* branch of *Desulfobacteraceae*. SEEP-SRB₁ clade has been shown to live together with ANME-2 and ANME-1 in a syntrophic consortium in AOM-mediating environments and enrichments (Harrison et al., 2009; Vigneron et al., 2013; Timmers et al., 2015). The members of this group have been reported to have low sequence similarity to the cultivated species which points to new species or genera with unknown physiological properties (Knittel et al., 2003). As this slurry contains ANME-1b related reads, SEEP-SRB₁ might have formed consortia with this archaeal cluster and involved in anaerobic oxidation of methane (Fig 3D, Fig 6).

4.4.7 Archaea involved in propionate conversion

Archaeal community analyses revealed the dominance of the order *Methanomicrobiales* in almost all slurries. The members of *Methanomicrobiales* utilize H₂+CO₂ and most members also use formate as substrate for methanogenesis (Garcia et al., 2006). This suggests that H₂+CO₂ and/or formate was the main substrate used by methanogenic *Archaea* in the slurries (Fig 6, S6). Hydrogenotrophic methanogenesis has been detected in near-surface marine sediments (Parkes et al., 2007; Webster et al., 2009; Sørensen et al. 1981; Blair and Carter 1992). Different genera or groups of *Methanomicrobiales* increased in relative abundance in the slurries based on incubation

temperature and sulfate availability. *Methanoculleus* was observed in the low sulfate-amended SMTZ and sulfate-free MZ slurries incubated at 25°C, whereas *Methanogenium* comprised most of the sequences in SZ, SMTZ and MZ slurries incubated at 10°C without or with low sulfate amendment (Fig 6). The optimum growth temperature of *Methanoculleus* ranges between 25°C and 60°C, whereas *Methanogenium* species grow best between 15-35°C. Therefore, temperature might have been a determining factor for the dominance of different genera. On the other hand, high sulfate-amended slurries incubated at 25°C contained predominantly unclassified *Methanomicrobiales* sequences, termed as EJ-Eo1 (Fig 6, Fig S6). It is obvious that the increased relative abundance of this unclassified hydrogenotrophic methanogenic group was closely related to the presence of sulfate, as was approved by its positive correlation with sulfate and temperature (Fig S7). Hydrogenotrophic methanogenesis in high sulfate containing sediments has also previously been detected in marine sediments (Kendall and Boone, 2006a; Parkes et al., 1990).

Methanosarcina belonging to the *Methanosarcinaceae* that utilize acetate, methylated compounds and $H_2 + CO_2$ detected (Kendall and Boone, 2006b). Since *Methanosarcina* was detected in sulfate-free SZ and MZ slurries, it constituted close relationships with incomplete propionate converters, and carried out acetate consumption (Fig 6, Fig S6). *Methanococcoides* (ANME-3 *Archaea*) increased its relative abundance in the SMTZ and MZ slurries (Fig 6). Lösekann et al. (2007) reported that ANME-3 live syntrophically with *Desulfobulbus spp.*, which were present in the slurries that the relative abundance of *Methanococcoides* increased (Fig 4). The other anaerobic methanotrophic group that increased its relative abundance was ANME-1 (Fig 6). Most probably, anaerobic oxidation of methane occurred not only in the slurries comprised of SMTZ sediment, which was considered as the most common ANME habitat on earth (Thomsen et al., 2001; Niemann et al., 2006; Parkes et al., 2007), but also in SZ and MZ sediment slurries.

Non-methanogenic *Archaea* detected in the slurries included the MBG-D and DHVEG-1 belonging to *Euryarchaeota* and MCG belonging to *Thaumarchaeota* (Fig 6). These groups were previously reported as dominant archaeal groups in deep subsurface sediments in addition to coastal marine surface sediments and that their relative abundance is independent from the major biogeochemical zones, indicating their diverse metabolism (Fry et al., 2008; Teske and Sørensen, 2008; Lloyd et al., 2013; Parkes et al., 2014; Roussel et al., 2009). Webster et al. (2010) detected MCG and MBG-D in sulfate zone sediment slurry enrichments within the active archaeal community incorporating ^{13}C -acetate. As a result, MBG-D were stimulated in acetate-amended slurries. These findings are in line with our observations where both of MCG and MBG-D increased in relative

abundances in slurries containing sulfate and their relative abundances were positively correlated with sulfate and acetate concentrations (Fig 6, S7).

4.5 Conclusions

In this research, we found clear changes in the bacterial and archaeal community in the long-term enrichment slurries depending on the presence/absence of sulfate, incubation temperature and, in some cases the biogeochemical zone. Propionate was converted by both sulfate-reducing and syntrophic communities in the presence of sulfate at all depth zones. The presence of defined microbial communities indicates that syntrophs are not simply out-competed by high sulfidogenic activity, rather they can stay in a dormant state with a low metabolic activity and take part in the conversion as they constitute close relationship with partner organism(s). Members of *Desulfobacteraceae* and *Desulfobulbaceae* were observed in sulfate-amended slurries as well as in sulfate-free slurries at low temperature. This indicates that changing to a syntrophic lifestyle allows sulfate reducers to remain in sulfate-depleted/limited environments and this explains the high relative abundance of SRB in deep marine sediments. The dominance of *Cryptanaerobacter*, without a known propionate-converting metabolism, in sulfate-free slurries at high temperature throughout the sediment brought the possibility that yet uncultured species of *Cryptanaerobacter*, in addition to *Pelotomaculum* sp., utilize propionate as a substrate in syntrophy with hydrogenotrophic methanogens. The dominant syntrophic partners belonged to the hydrogenotrophic methanogenic order *Methanomicrobiales* that enriched in all slurries with different representative genera and unclassified group under different incubation conditions. The *Methanosarcina* enriched only in the absence of sulfate, suggesting a potential competition with acetate-degrading sulfate reducers. Further cultivation studies are currently ongoing to identify the uncultured microorganisms involved in propionate conversion as well as to determine their interaction with other bacterial and archaeal groups during conversion process.

Acknowledgements

We gratefully acknowledge Mark A. Lever (Eidgenössische Technische Hochschule, Zurich, Switzerland), Kasper U. Kjeldsen, Hans Røy (Aarhus University, Aarhus, Denmark) for skillful technical assistance and the captains and crews of sailing vessel Marieje and research vessel Tyra for their help during different cruises. We thank Peer Timmers (Wageningen University &

Research), Martin Liebensteiner and Kivanc Ozuolmez for assistance during sampling, Ton van Gelder (Wageningen University & Research) for technical assistance in the laboratory. This work has been funded by the Wimek Graduate School of Wageningen University & Research and the Darwin Center for Biogeosciences (the Netherlands). Research of Alfons Stams is supported by ERC grant (project 323009) Gravitation grant (project 024.002.002) of the Netherlands Ministry of Education, Culture and Science and the Netherlands Science Foundation (NWO).

Supplementary data

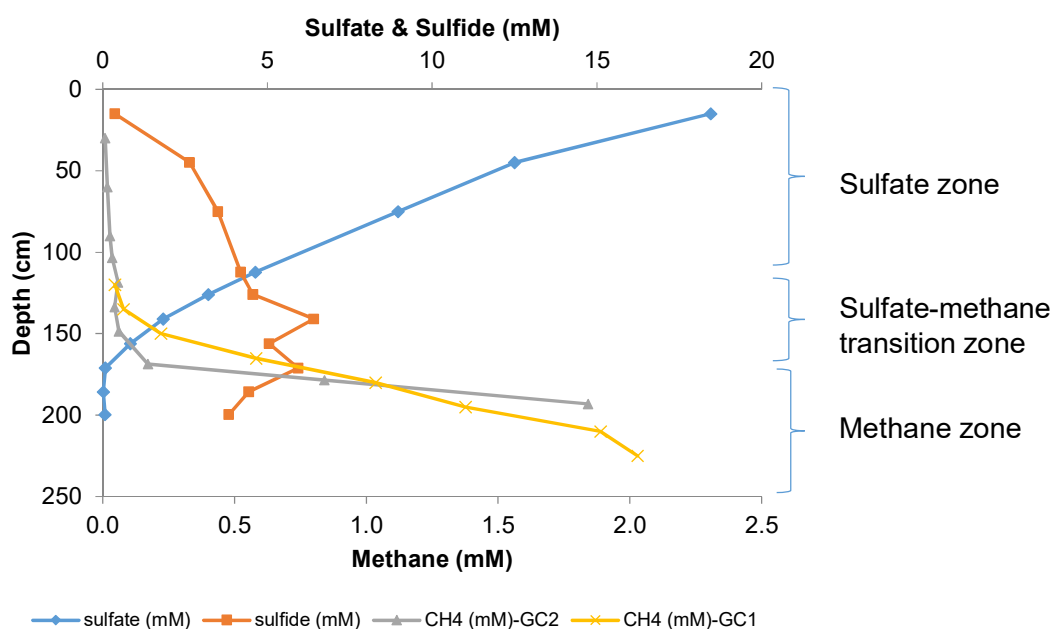
Table S1. The overview of all the enrichment slurries fed with propionate and the total amounts of the reactants consumed and products formed during the enrichment period. The enrichment slurries were consisted of sediment either from sulfate zone (SZ), sulfate-methane transition zone (SMTZ) or methane zone (MZ) and incubated at 25°C or 10°C, with 3 mM, 20 mM or without (-) sulfate amendments along the study. Slurries with * were presented in the propionate conversion graphs and used for molecular analysis.

Sediment zone	Slurry Code	Treatment	Incubation temperature (°C)	Reactants (μmol/slurry)		Products (μmol/slurry)		
				Propionate	Sulfate	Acetate	Sulfide	Methane
SZ	*P1	-	25	26157	336	17905	881	37464
	P2	-	25	2726	159	1183	284	0
	P3	20 mM SO ₄ ²⁻	25	20623	29592	19126	29062	33
	*P4	20 mM SO ₄ ²⁻	25	26681	42456	25677	39089	1038
	P5	-	10	17190	354	13170	151	9083
	*P6	-	10	18414	125	9558	207	14959
	P7	20 mM SO ₄ ²⁻	10	15491	13410	18442	18296	0
	*P8	20 mM SO ₄ ²⁻	10	17679	18592	21716	21495	0
SMTZ	P1	3 mM SO ₄ ²⁻	25	27494	9343	25160	6993	29829
	*P2	3 mM SO ₄ ²⁻	25	32207	9330	34093	8892	15509
	*P3	20 mM SO ₄ ²⁻	25	27819	37381	9246	34439	339
	P4	20 mM SO ₄ ²⁻	25	28694	40125	11250	35587	74
	*P5	3 mM SO ₄ ²⁻	10	18465	6638	16996	7316	2797
	P6	3 mM SO ₄ ²⁻	10	17365	6839	17427	7642	2197
	*P7	20 mM SO ₄ ²⁻	10	26008	33660	27709	34299	17
	P8	20 mM SO ₄ ²⁻	10	27162	35346	26523	36833	34
MZ	*P1	-	10	7204	932	7346	552	3909
	P2	-	10	3897	809	1575	673	926
	*P3	-	25	27472	825	13791	563	38473
	P4	-	25	34576	604	20771	509	43969
	P5	20 mM SO ₄ ²⁻	25	39414	33244	30817	32821	1670
	*P6	20 mM SO ₄ ²⁻	25	49211	45738	49783	40572	418
	P7	20 mM SO ₄ ²⁻	10	16577	20444	15542	15184	0
	*P8	20 mM SO ₄ ²⁻	10	11366	16233	11913	12356	0

Table S2. The number of reads per sample generated by pyrosequencing for Bacteria and HiSeq Illumina sequencing for Archaea.

Origin	Slurry	Bacterial reads	Archaeal reads
Sulfate zone	ENV	8733	9120
	P1	9903	13481
	P4	12305	74345
	P6	27196	67941
	P8	15062	16472
Sulfate-methane transition zone	ENV	3186	18696
	P2	8730	33641
	P3	5653	30858
	P5	5949	79958
	P7	3934	21631
Methane zone	ENV	10824	30848
	P1	14192	78094
	P3	14752	108810
	P6	14171	25156
	P8	1888	5547

Figure S1. Depth profiles of sediment pore water sulfate, sulfide and methane for Station M₁, in Aarhus Bay, Denmark. Methane-GC₁ and Methane-GC₂ stands for methane concentrations retrieved from two different gravity corers, gravity corer 1 and 2, respectively. SZ; Sulfate zone, SMTZ; sulfate-methane transition zone; MZ, methane zone.



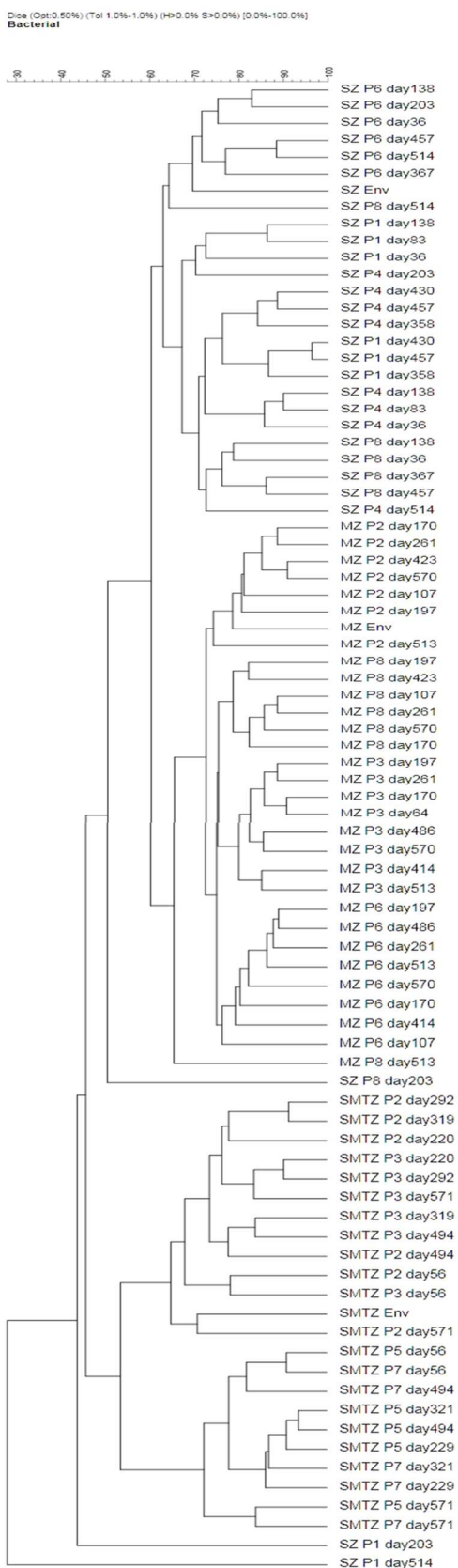


Figure S2. Cluster analysis of bacterial DGGE profiles of sediment samples taken at different biogeochemical zones and samples of enrichment slurries that were taken at different time points. The trees were generated using Dice similarity coefficient and UPGMA clustering algorithm. SZ: Sulfate zone, SMTZ: Sulfate-methane transition zone, MZ: Methane zone.

Propionate conversion under sulfidogenic and methanogenic conditions

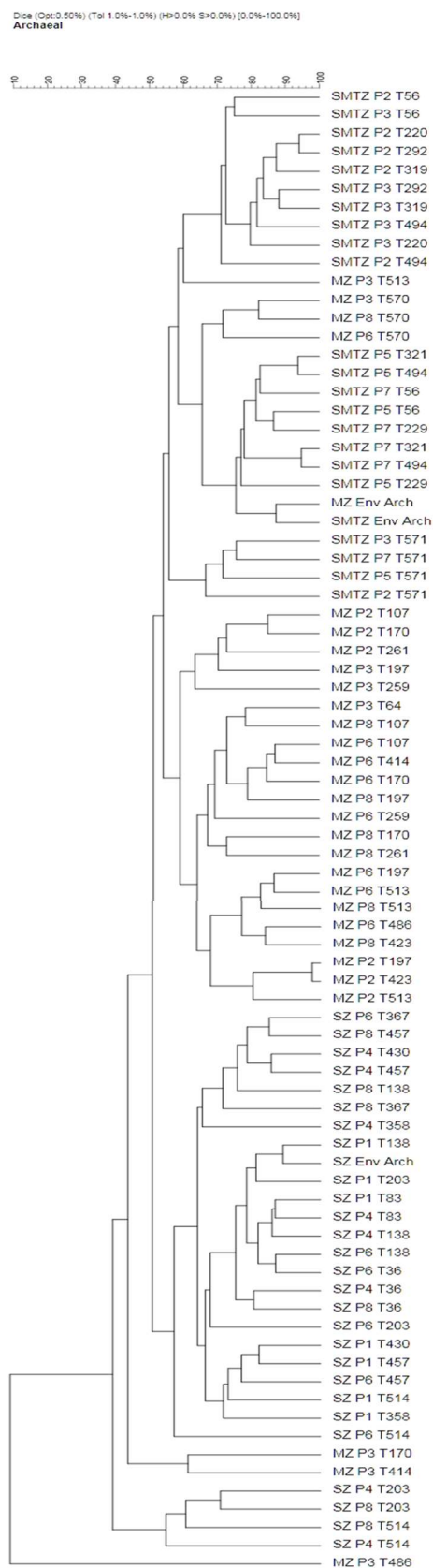


Figure S3. Cluster analysis of archaeal DGGE profiles of sediment samples taken at different biogeochemical zones and samples of enrichment slurries that were taken at different time points. The trees were generated using Dice similarity coefficient and UPGMA clustering algorithm. SZ: Sulfate zone, SMTZ: Sulfate-methane transition zone, MZ: Methane zone.

Figure S4. Relative abundances of the bacterial community in all slurries and environmental samples at family level, normalized to 100%. Only those families that were present at an abundance >1% in at least one sample were included in the graph. SZ: Sulfate zone, SMTZ: Sulfate-methane transition zone; MZ: Methane zone. Env: Sediment sample belonging to the indicated biogeochemical zone. S: 20mM sulfate, 3S: 3mM sulfate is used as electron acceptor in slurries. Slurries that were not labeled with 'S' or '3S' were incubated without sulfate. The number of reads of each sample was given in brackets.

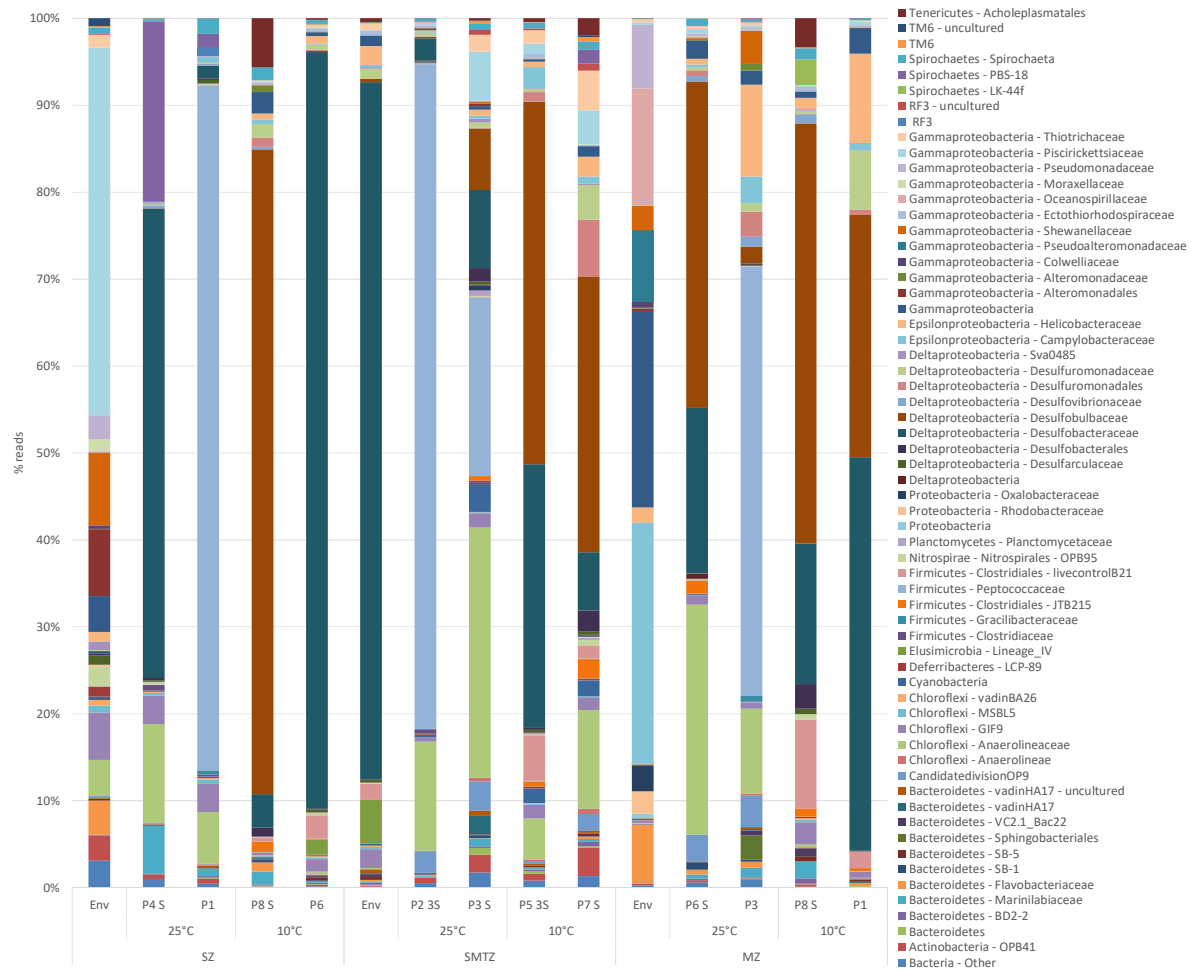


Figure S5. The heatmap depicts the correlation between bacterial orders present at a relative abundance >1% of total reads across the 12 slurry samples analyzed and experimental parameters. Correlations were determined by means of the two tailed Spearman's Rank Order Correlation test. The heatmap colors represent the relative percentage of the microbial order assignments. Square colors shifted towards bright green indicate strong correlation.

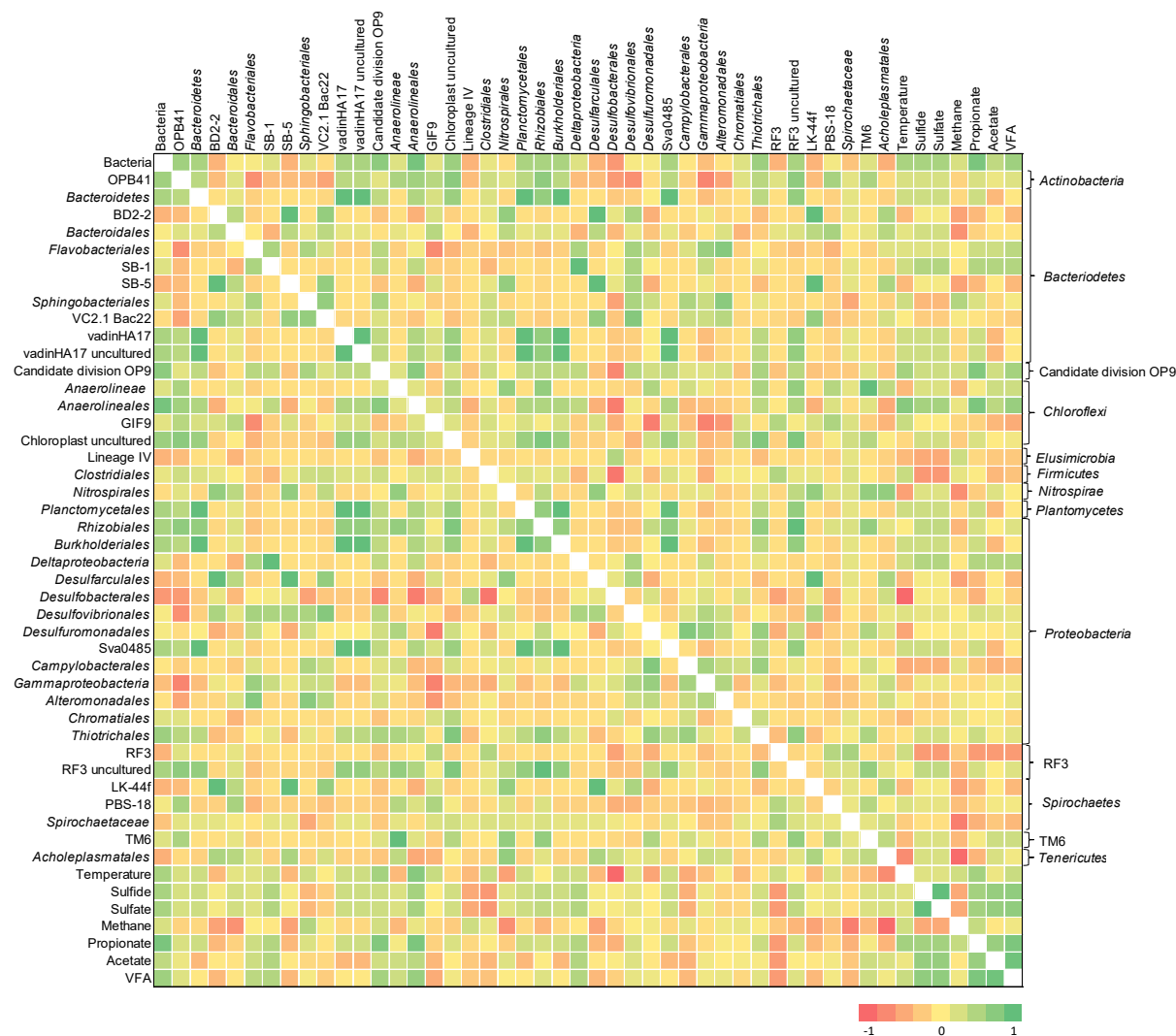


Figure S6. Relative abundances of the archaeal community in all slurries and environmental samples at family level, normalized to 100%. Only those families that were present at an abundance >1% in at least one sample were included in the graph. SZ: Sulfate zone, SMTZ: Sulfate-methane transition zone; MZ: Methane zone. Env: Sediment sample belonging to the indicated biogeochemical zone. S: 20mM sulfate, 3S: 3mM sulfate is used as electron acceptor in slurries. Slurries that were not labeled with 'S' or '3S' were incubated without sulfate.

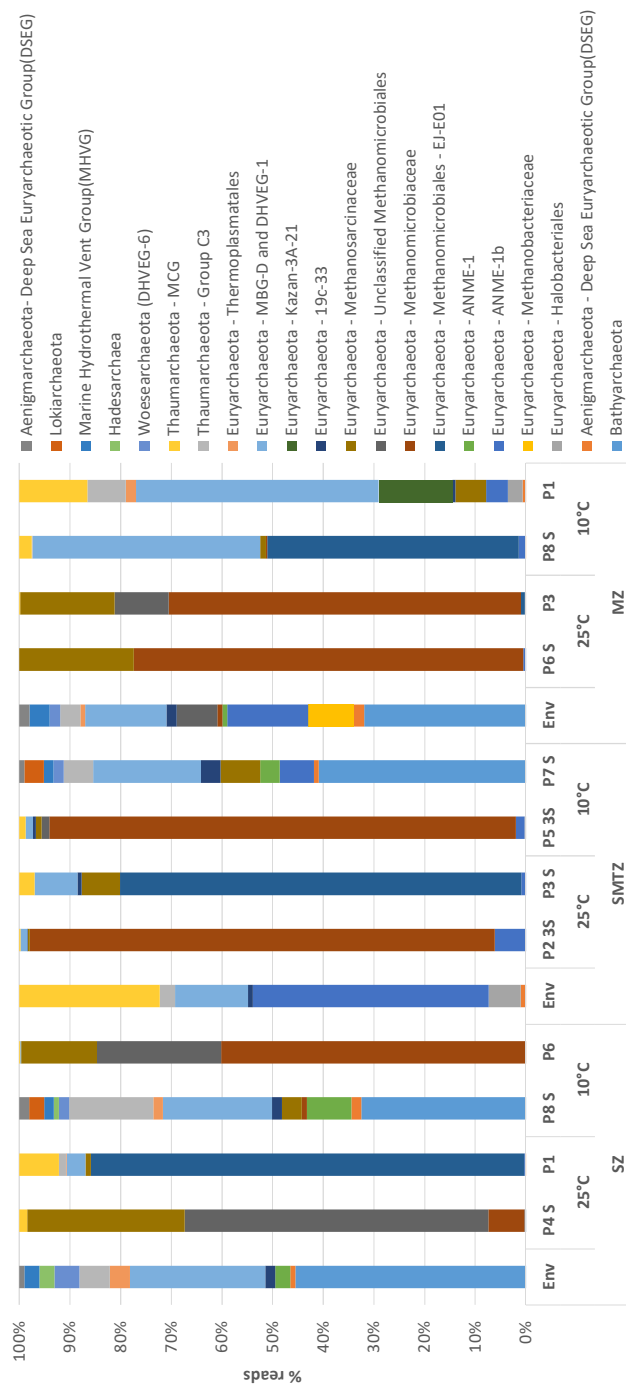
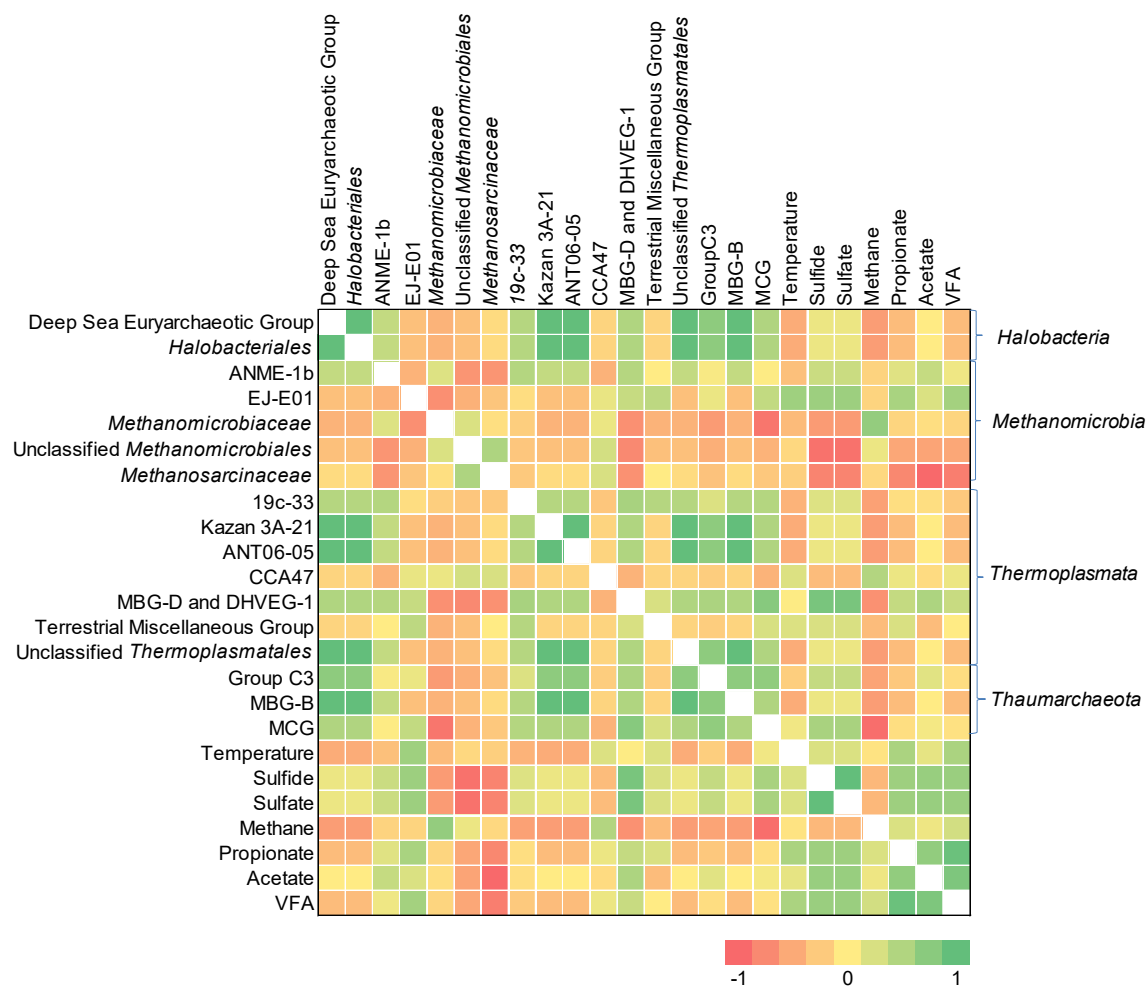


Figure S7. The heatmap depicts the correlation between archaeal families present at a relative abundance >1% of total reads across the 12 slurry samples analyzed and experimental parameters. Correlations were determined by means of the two tailed Spearman's Rank Order Correlation test. The heatmap colors represent the relative percentage of the microbial family assignments. Square colors shifted towards bright green indicate strong correlation.



Chapter 5

Membrane lipid composition in enrichments from the sulfate and methane zones of Aarhus Bay, Denmark

Derya Ozuolmez^{*}, Eli K. Moore^{*}, Ellen C. Hopmans, Caroline M. Plugge, Jaap S.
Sinninghe Damsté (*) Contributed equally

Abstract

Sulfate reduction and methanogenesis are important terminal electron accepting processes contributing to the organic matter (OM) degradation under anoxic conditions in coastal marine sediments. It is not well known which metabolic strategies are used by sulfate reducing bacteria (SRB) in the methane zone and methanogenic archaea in the sulfate zone, or which physiological adaptations are utilized under different metabolic regimes. To understand how the microbial community responds to different growth conditions and substrates, enrichment slurries were developed using sediment taken from sulfate, sulfate-methane transition and methane zones of Aarhus Bay, Denmark. Enrichment slurries were amended with different sulfate concentrations (0, 3, 20 mM) and carbon substrates (propionate and butyrate) and were incubated at two different temperatures (10°C and 25°C). Intact polar membrane lipid (IPL) analysis and next generation sequencing of the 16S rRNA gene were performed on the enrichment slurries at the end of the incubation period. Overall, the distribution of IPLs and microbial community shifted between different sediment zones and growth conditions, with greater IPL diversity found in butyrate-amended cultures as compared to the propionate-amended enrichment slurries. Recently discovered trimethylornithine lipids (TMOs) were identified in three butyrate-amended methane zone slurries. The presence of TMO lipids in these slurries could be linked with the enrichment of methanogenic microbial communities, as TMOs were observed only in methanogenic environments to date. Multivariate analysis showed that *Bacteroidetes* and *Methanomicrobiales* taxa, and sulfate amendments were closely clustered with many IPLs indicating that these taxa contributed to the IPL variation among the enrichment slurries.

5.1 Introduction

Organic matter (OM) degradation in coastal marine sediments is an important process in the global carbon cycle (Henrichs, 1992; Hedges and Keil, 1995; Burdige, 2007). In oxic sediments, OM is degraded ultimately to carbon dioxide and water, whereas under anoxic conditions organic matter is degraded by physiologically different microorganisms employing fermentation or terminal electron accepting processes. In marine sediments, where sulfate concentration is high, sulfate reduction is the predominant pathway for OM degradation, while methanogenesis becomes important in zones where sulfate is low or depleted (Jørgensen, 1982; Holmkvist et al., 2011; Bowles et al., 2014). Yet the diversity and metabolic capabilities of marine anaerobic microbes are largely unexplored (Jørgensen and Boetius, 2007). The characterization of microbial communities involved in sulfate reduction and methanogenesis is essential to understand OM decomposition in coastal marine sediments.

Anaerobic degradation of organic matter in marine sediments is a complex process involving physiologically different microorganisms (Schink and Stams, 2013). The first step is an extracellular hydrolytic conversion of polymers to oligomers and monomers which is followed by fermentation of these compounds to reduced organic compounds such as short chain fatty acids, alcohols, formate, H_2 and CO_2 . Organic acids and alcohols are further degraded to acetate, formate, H_2 and CO_2 . When sulfate concentration is high, SRB can use all fermentation products, and oxidize them to CO_2 by reducing sulfate to sulfide (Schink and Stams, 2013). Sulfate-depleted marine sediments are major sources of biogenic methane. In the absence of sulfate, complex organic material is mineralized exclusively to CO_2 and methane by physiologically diverse microorganisms that are co-operating, including fermentative, acetogenic bacteria, and methanogenic archaea (de Bok et al., 2005; Stams et al., 2005; Dolfing et al., 2008; Plugge et al., 2009; Müller et al., 2010). Propionate and butyrate are important intermediates in anaerobic methanogenic food chain since their complete conversion can be accomplished only by syntrophically (Schink and Stams, 2013; McNerney et al., 2008). The studies showing the presence of sulfate reducers in the methane and methanogens in sulfate zones of marine sediments indicates the importance of hydrogen, that is produced during organic matter mineralization, on the metabolism of methanogenic and the sulfate-reducing microbial populations (Plugge et al., 2011; Finke et al., 2007b; Leloup et al., 2009; Leloup et al., 2007). Further research is needed to determine what type of metabolism sulfate reducers use in the methane zone, and methanogenic archaea in the sulfate zone.

Intact polar membrane lipids (IPL) are the building blocks of cell membranes and representative of living biomass as they rapidly hydrolyze upon cell lysis (White et al., 1979; Harvey et al., 1986). IPLs can also be structurally specific to microbial taxa or may differ depending on the habitat characteristics, thus providing information of the biogeochemistry of an environment (Sturt et al., 2004; Schubotz et al., 2009). Analysis of IPLs by high performance liquid chromatography-electrospray ionization-mass spectrometry (HPLC/ESI/MS) can provide information on the physiological status of microbial communities as the structural composition of lipid membranes is influenced by environmental conditions such as growth temperature, pH, and nutrient limitation (Shimada et al., 2008; Van Mooy et al., 2009; Vences-Guzmán et al., 2011; Moore et al., 2015a). IPL distributions in marine sediments have also been observed to change in accordance with habitat characteristics and inhabiting microbial community (Schubotz et al., 2009; Rossel et al., 2011). In this study, enrichment slurries were established using sulfate zone (SZ), sulfate-methane transition zone (SMTZ) and methane zone (MZ) sediments of Aarhus Bay, Denmark. Propionate and butyrate were used as carbon sources, different sulfate concentrations were applied, and incubated at 10°C and 25°C. IPL analysis and next generation sequencing of the 16S rRNA gene were performed on the last incubation day samples of enrichment slurries and the original sediment to understand the microbial responses to different incubation conditions.

5.2 Materials and Methods

5.2.1 Sediment sampling and enrichment slurry incubations

Sediment cores were collected in May 2011 in Aarhus Bay, Denmark (56°07'066"N, 10°20'793"E). Subsamples representing sulfate zone (SZ, 15-120 cm), sulfate-methane transition zone (SMTZ, 120-170 cm) and methane zone (MZ, 170-300 cm) were mixed in an anaerobic chamber and used as inoculum for sediment slurry enrichments. 100 ml of the homogenized sediment from each zone was mixed with 300 ml of anaerobic mineral salts medium in 1L serum bottles. Media was prepared as was described in Chapter 2. 10 mM propionate or butyrate was used as carbon sources with and without 20 mM sulfate in sulfate zone and methane zone slurries, and with 3 mM and 20 mM sulfate for sulfate-methane transition zone slurries as electron acceptor. One set of the bottles representing each condition in duplicate was incubated at 10°C as *in situ* temperature (Dale et al., 2008) and the other set was kept at 25°C statically throughout the experiment. The overview of enrichment slurries and incubation conditions is given in chapters 3 and 4. At the end of the

enrichment period (514 days for SZ, 571 days for SMTZ, and 570 days for MZ), 1 ml of liquid slurry samples were collected for IPL analysis, freeze dried and stored at -80°C before IPL extraction.

5.2.2 Intact polar lipid extraction

The slurry samples which were used for molecular analysis were used for lipid analysis. Additionally, methane zone slurry samples which were not analysed for molecular analysis were also extracted and analyzed in order to confirm the presence or absence of trimethylornithine lipids (TMOs). Lipids were extracted from ~0.1 g freeze-dried powdered enrichment cultures using a method adapted from Bligh and Dyer (1959) (Rütters et al., 2002a). A solvent mixture (approximately 5 ml g⁻¹ dry weight, dw of methanol (MeOH):dichloromethane (DCM): potassium phosphate buffer at pH 7.4 (2:1:0.8, v/v/v) was added to approximately 0.3–1.3 g dry weight of powdered enrichment culture in a centrifuge tube and placed in an ultrasonic bath for 10 min. After sonication, the powdered enrichment culture-solvent mixture was centrifuged at 2,500 rpm for 2 min and the overlying solvent extract was pipetted off. The extraction was repeated twice and the replicate extracts were combined with the first extract for each sample. DCM and phosphate buffer were added to the combined extracts to yield a ratio of 1:1:0.9 (v/v/v) and achieve separation of a DCM phase and an aqueous MeOH/phosphate buffer phase by centrifugation at 2,500 rpm for 2 min. The DCM phase, containing the IPLs, was pipetted off and passed over extracted cotton wool to remove any remaining particles and collected in a glass tube. The aqueous phase was rinsed twice with DCM, and each DCM rinse also passed over extracted cotton wool and combined with the original DCM phase. The combined DCM samples were dried under a N₂ flow and stored at -20°C until analysis.

5.2.3 HPLC-ESI/IT/MS analysis of IPLs

Extracted IPLs from the sediment enrichment slurries were analyzed by high-performance liquid chromatography–electrospray ionization-ion trap mass spectrometry (HPLC-ESI/IT/MS) according to Sturt et al. (2004), with some modifications (Moore et al., 2013). An Agilent 1200 series high-performance liquid chromatograph (Agilent, San Jose, CA), with thermostatted autoinjector was coupled to a Thermo LTQ XL linear ion trap mass spectrometer with an Ion Max source and ESI probe (Thermo Scientific, Waltham, MA). Chromatographic separation was performed on a Lichrosphere diol column (250 mm by 2.1 mm; 5-µm particles; Grace Alltech Associates Inc.,

Deerfield, IL). The MS scanning mass range of m/z 400 to 2,000 in positive-ion mode, followed by data dependent dual-stage tandem MS (MS^2), in which the four most abundant masses in the mass spectrum were fragmented successively. Each MS^2 was followed by data-dependent, triple-stage tandem MS (MS^3), wherein the base peak of the MS^2 spectrum was fragmented. IPL abundance was assessed by integrating the HPLC-ESI/IT/MS base peak chromatogram area per gram of peat, dry weight. Performance of the HPLC-ESI/IT/MS was monitored by regular injections of platelet-activating factor (PAF) standard (1-*O*-hexadecyl-2-acetyl-*sn*-glycero-3-phosphocholine).

5.2.4 Statistical analyses

Multivariate canonical correspondence analysis (CCA) (McGarigal et al., 2000) was performed to compare the microbial taxa identified in chapters 3 and 4 with the associated distribution of IPLs in each enrichment slurry in order to find phylogenetic groups and IPLs which could correlate with each other or with particular incubation conditions. CCA was executed using R statistical analysis software.

5.3 Results

5.3.1 Microbial community analysis

The microbial diversity varied much between different sediment zones and different incubation conditions as described in chapters 3 and 4. These results are described here briefly for comparison with IPL results. Bacterial taxa *Thiomicrospira*, GIF9 from the phylum *Chloroflexi*, and *Arcobacter* were the most abundant microbial taxa in sediment of the SZ, SMTZ and MZ, respectively. As compared to the original sediment, all three taxa were relatively minor in abundance in both propionate- and butyrate-amended sediment slurries which originated from the corresponding sediment zones. The microbial composition in enrichment slurries representing each sediment zone changed considerably under different incubation conditions. *Cryptanaerobacter* belonging to *Peptococcaceae* was the most abundant phylotype in low or no sulfate-containing propionate-amended enrichment slurries from each sediment zone at 25°C. In butyrate-amended sediment slurries, *Anaerolineaceae* was abundant at 25°C under both high and low sulfate conditions. Other taxa were highly abundant only in one particular enrichment slurry, such as *Desulfobacteraceae* in the 10°C low sulfate propionate-amended sulfate zone slurry, or *Desulfobacterium* in the 10°C high sulfate butyrate-amended sulfate zone slurry. Sulfate zone sediment slurries were dominated by

one phylotype. Five out of eight SZ slurries contained one phylotype accounting for over 50% relative abundance and two other slurries contained one taxa accounting for over 45% relative abundance. Unassigned taxa were generally low in relative abundance.

The archaeal taxa were not as diverse as the bacterial taxa, and it was more common for one phylogenetic group to make up a large majority of the total *Archaea* than for *Bacteria*. In propionate-amended sediment slurries, uncultured *Methanomicrobiales* (EJ-Eo1) was highly abundant in 25°C high sulfate slurries of each sediment zone, and *Methanomicrobiaceae* was highly abundant in all low/no sulfate slurries of each sediment zone at both 10°C and 25°C. In propionate-amended sulfate-containing methane zone slurries, MBG-D and DHVEG-1 belonging to *Thermoplasmatales* was highly abundant. *Methanomicrobiaceae* was the most abundant taxon in all butyrate-amended sediment slurries except for the SMTZ slurries incubated with high sulfate at 10°C and with low sulfate at 25°C. *Methanosarcinaceae* was the second most abundant archaeal taxon in butyrate-amended slurries with *Methanosaetaceae* having high relative abundance in two slurries.

The overall diversity was greater for bacterial and archaeal taxa compared to the diversity of IPL head group classes. There were 380 different bacterial and 17 archaeal taxa identified in propionate-amended sediment slurries, versus 7 different IPL head group classes and 29 different IPL head group core lipid combinations identified in the propionate-amended sediment slurries. Similarly, there were 384 bacterial and 17 archaeal taxa identified in butyrate-amended sediment slurries, versus 14 different IPL head group classes and 55 different IPL head group core lipid combinations identified in the butyrate-amended sediment slurries.

5.3.2 Dominant IPLs in enrichment slurries and original sediment

The most abundant classes of IPLs identified in most of the sediment enrichment slurries were phosphatidylethanolamine (PE), phosphatidylglycerol (PG), phosphatidylcholine (PC), lyso-PC (LPC; PC containing one fatty acid), and dihexose (DH) containing lipids (Fig. 1, 2, Table S1). Other identified IPLs (MH, PA, OL, TMO, PI, DMPE, Betaine, MMPE, GlcA) were found in some enrichment slurries, although some had relatively high abundances in certain slurries, such as monomethylphosphatidylethanolamine (MMPE) in slurry SZP8 (30425552 peak area/g dry weight) or glucuronic acid (GlcA) in culture SMTZB1 (35097613 peak area/g dry weight). Tetraether lipids, which are known to be attributed to archaea (De Rosa and Gambacorta, 1988; Kates, 1993; Koga et al., 1993; Hoefs et al., 1997; Hopmans et al., 2000), were not detected in the sediment slurries. IPL

abundance (per gram dry weight) and diversity were much lower in the original sediment core extracts compared to the enrichment slurries (Fig. 1, 2, Table S1). The IPLs identified in the original sediment extracts were PA, PE, and phosphatidylinositol (PI) with PA and PE being identified in all sediment zones analyzed, and PI was only identified in the SZ (Table S1). The IPL distributions and microbial communities of the enrichment slurries composed of various biogeochemical zones (SZ, SMTZ, MZ) responded differently to different incubation conditions, particularly when they are compared to the IPL distributions and microbial communities in the corresponding sediment zones.

5.3.3 IPL distributions in enrichment slurries

5.3.3.1 Sulfate zone enrichment slurries

PE was identified in all sulfate zone enrichment slurries occurring in moderately high abundances (between 2125058-11455795 peak area/g dry weight) in two 10°C cultures amended with different substrates and sulfate concentrations (Fig. 1, 2, Table S1). PG was detected in 10°C butyrate-amended slurries in the presence of sulfate and 10°C propionate-amended slurries in the presence and absence of sulfate. In propionate-amended sulfate zone slurries, DH was observed only in the absence of sulfate at both temperatures, whereas in butyrate-amended sulfate zone slurries DH occurred both in the absence of sulfate at both temperatures and in the presence of sulfate at 25°C. PC was detected in two butyrate-amended slurries in the presence of sulfate at both temperatures, and LPC was detected in all but one of the sulfate containing slurries amended with butyrate and incubated at 10°C. MMPE was detected only in one slurry which was fed with propionate and sulfate and incubated at 10°C.

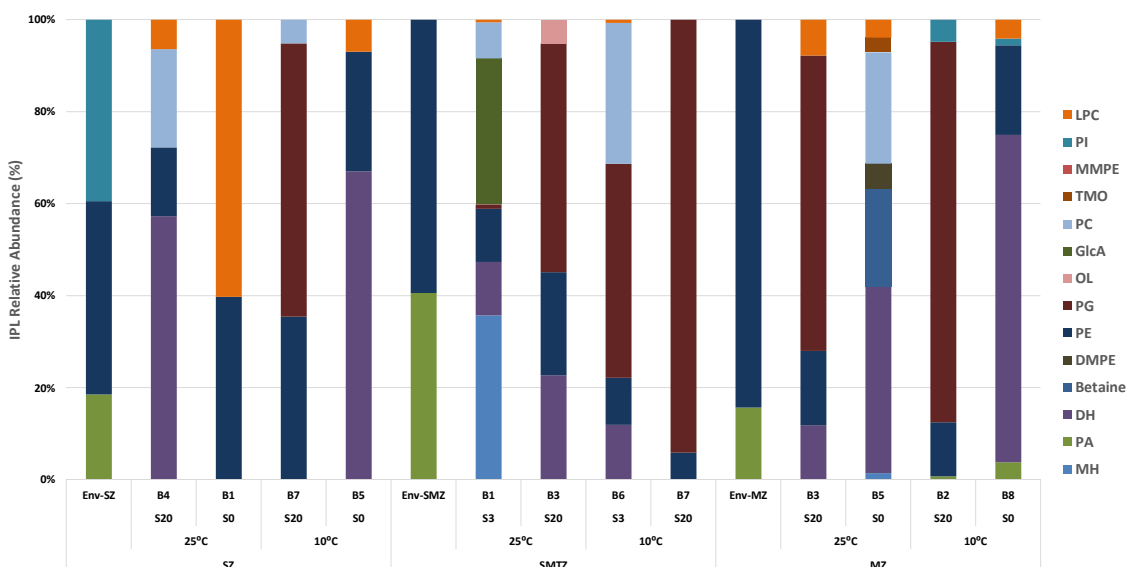


Figure 1: Relative abundance of intact polar lipids (IPLs) in butyrate-amended enrichment slurries. Env = environmental samples, B = slurry code (listed in Table S1 in chapters 3 and 4), S20 = 20 mM sulfate added, S0 = 0 mM sulfate added, S3 = 3 mM sulfate added, °C indicates incubation temperature, SZ = sulfate zone, SMTZ = sulfate-methane transition zone, MZ = methane zone. IPL key: MH = monohexose, PA = phosphatidic acid, DH = dihexose, DMPE = dimethylphosphatidylethanolamine, PE = phosphatidylethanolamine, PG = phosphatidylglycerol, OL = ornithine, GlcA = glucuronic acid, PC = phosphatidylcholine, TMO = trimethylornithine, MMPE = monomethylphosphatidylethanolamine, PI = phosphatidylinositol, LPC = lyso-phosphatidylcholine.

5.3.3.2 Sulfate-methane transition zone slurries

PG was identified in all SMTZ slurries except for the one that contained high sulfate and propionate at 25°C and had higher abundance in butyrate-amended slurries (22801451 peak area/g dry weight on average) than propionate-amended slurries (4355003 peak area/g dry weight on average) (Figs. 1, 2, Table S1). PE occurred in all SMTZ slurries except for the 10°C low sulfate propionate-amended slurry and higher PE abundances were detected on average in butyrate-amended slurries. DH was identified in one propionate-amended slurry (25°C, low sulfate) and three butyrate-amended slurries, with higher abundance than in the propionate-amended slurry. PC was detected only in three butyrate-amended slurries with higher abundance in two 10°C slurries, and LPC was detected in one propionate- and two butyrate-amended slurries all at low abundances (520065-711956 peak area/g dry weight). PI was identified only in three propionate-amended slurries having different sulfate concentrations and incubated at different temperatures. Monohexose (MH), GlcA, and

ornithine lipid (OL) were all detected in two butyrate-amended slurries incubated at 25°C, with MH and GlcA both at low and high sulfate and OL only under high sulfate conditions.

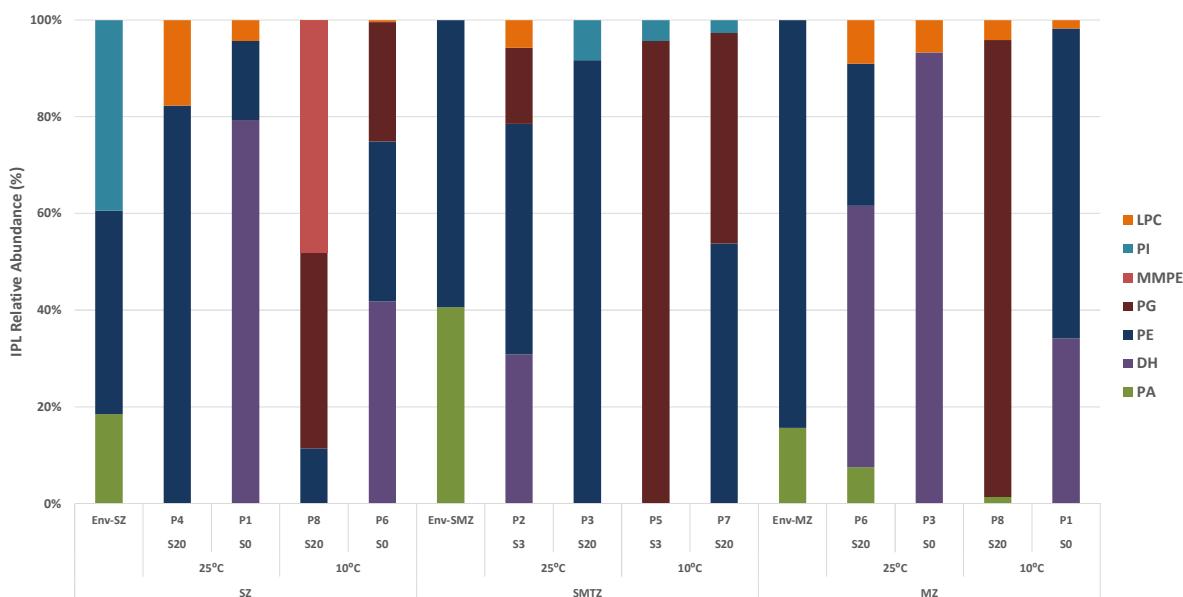


Figure 2: Relative abundance of intact polar lipids (IPLs) in propionate-amended enrichment slurries. Env = environmental samples, B = slurry code (listed in Table S1 in chapters 3 and 4), S20 = 20 mM sulfate added, S0 = 0 mM sulfate added, S3 = 3 mM sulfate added, °C indicates incubation temperature, SZ = sulfate zone, SMTZ = sulfate-methane transition zone, MZ = methane zone. IPL key: PA = phosphatidic acid, DH = dihexose, PE = phosphatidylethanolamine, PG = phosphatidylglycerol, MMPE = monomethylphosphatidylethanolamine, PI = phosphatidylinositol, LPC = lyso-phosphatidylcholine.

5.3.3.3 Methane zone slurries

PC was identified only in three butyrate-amended enrichment slurries, having high abundance in two of them (293717847 peak area/g dry weight on average), which contained sulfate (Fig. 1, 2, 3, Table S1). Trimethylornithine lipid (TMO) was identified in three butyrate slurries in which PC was identified, but at moderate to low abundances (11454294 peak area/g dry weight on average), and was not detected in any of the propionate-amended slurries (Fig. 3). LPC was detected in most of the butyrate- and propionate-amended slurries. The highest LPC abundances were detected in two sulfate containing slurries (23535905 peak area/g dry weight) in which PC and TMO reached to the highest abundance. PE was identified in most of the slurries with higher average abundances in the propionate slurries. DH was identified at moderate to low abundances (between 485170-21381687) in three propionate- and five butyrate-amended slurries incubated at different temperatures with or without sulfate. PG was detected in one propionate- and four butyrate-amended slurries, all five

of which contained sulfate. PI was identified at relatively low abundances (between 101628-801746) in two propionate- and two butyrate-amended slurries, all incubated at 10°C with and without sulfate. MH, betaine, and dimethylphosphatidylethanolamine (DMPE) were all detected at relatively low abundances (737203, 11195317, 2801118 peak area/g dry weight, respectively) in one methane zone slurry that was amended with butyrate and incubated at 25°C without sulfate.

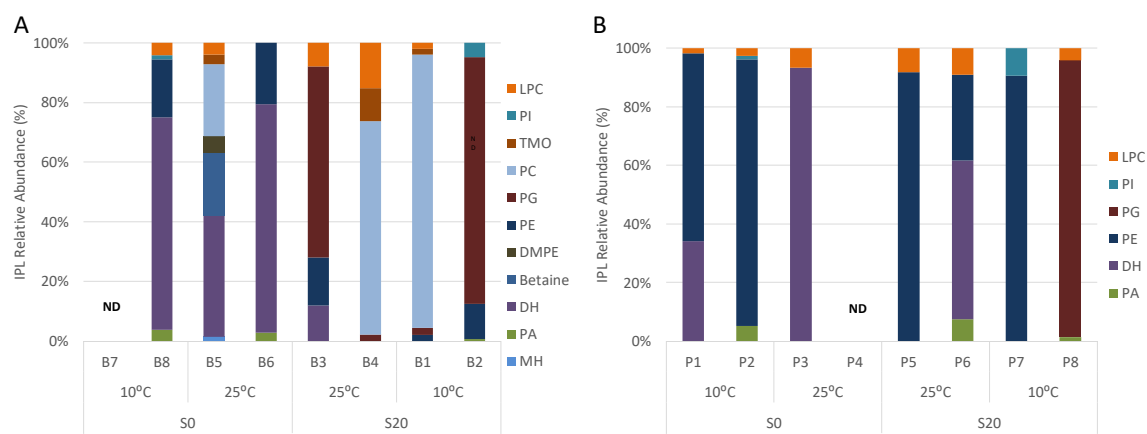


Figure 3: Relative abundance of intact polar lipids (IPLs) in all methane zone enrichment slurries amended with butyrate (A) and propionate (B). IPL relative abundances for cultures B2, B3, B5, B8 from Fig. 1 and P1, P3, P6, P8 from Fig.2 are combined to show full comparison between all methane zone slurries. IPL key: Mhex = monohexose, PA = phosphatidic acid, DH = dihexose, DMPE = dimethylphosphatidylethanolamine, PE = phosphatidylethanolamine, PG = phosphatidylglycerol, PC = phosphatidylcholine, TMO = trimethylornithine, PI = phosphatidylinositol, LPC = lyso-phosphatidylcholine. ND: not determined.

5.3.4 Multivariate analysis

Canonical correspondence analysis components 1 and 2 explained 30% and 23% of variation, respectively, for *Bacteria* in butyrate-amended slurries; 37% and 28% of variation, respectively, for *Archaea* in butyrate-amended slurries; 42% and 21% of variation, respectively, for *Bacteria* in propionate-amended slurries; and 53% and 22% for *Archaea* in propionate-amended slurries.

In butyrate-amended slurries, the observed bacteria and IPLs clustered into three groups (Fig. 4A). These groups are as followed: [1] PE, PA, OL, PG, and PI clustered more closely with *Flavobacteriaceae* (BBF), *Cytophagaceae* (BBC₁), *Bacteroidetes-SB-5* (BBS₅), *Marinilabiaceae* (BBM), *Actinobacteria-OPB₄₁* (BAO), *Bacteroidetes-BD2-2* (BBB), *Bacteroidetes-VC2.1_Bac22* (BBV), and high sulfate conditions; [2] MH and GlcA clustered more closely with *Anaerolineaceae* (BCA₂), Candidate division OP₉ (BCO), Other Bacteria (BO), and low sulfate conditions; [3] PC, LPC, DH, TMO, Betaine, and DMPE clustered more closely with *Bacteroidetes-SB-1* (BBS), *Bacteroidetes-WCHB₁₋₆₉* (BBW), *Bacteroidetes-vadinHA₁* (BBVH), *Chloroflexi-GIF₉* (BCG), and low sulfate



4: (A) Canonical correspondence analysis of intact polar lipid (IPL) distribution, bacterial taxa distribution, and growth conditions for butyrate-amended enrichment slurries. (B) Canonical correspondence analysis of intact polar lipid (IPL) distribution, archaeal taxa distribution, and growth conditions for butyrate-amended enrichment slurries.

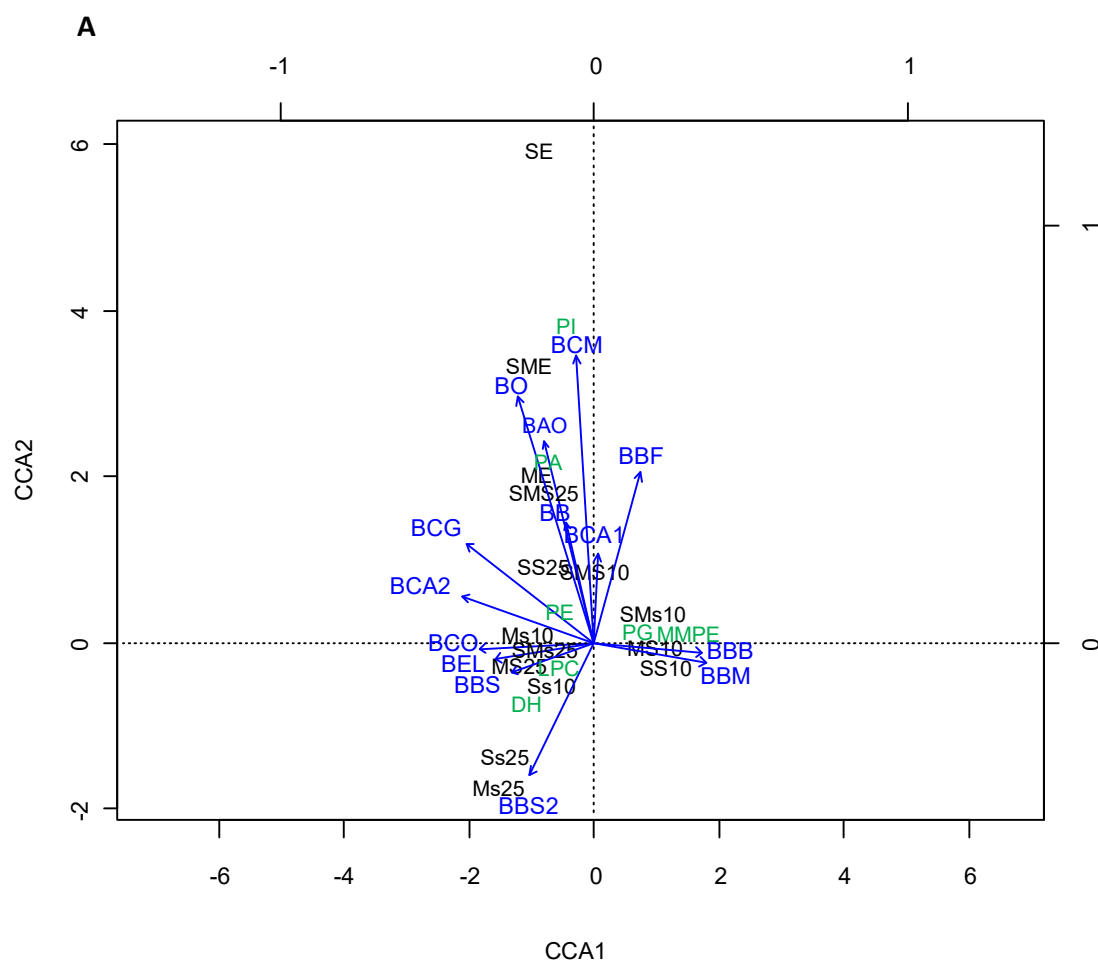
Green text, IPL key: MH = monohexose, PA = phosphatidic acid, DH = dihexose, DMPE = dimethylphosphatidylethanolamine, PE = phosphatidylethanolamine, PG = phosphatidylglycerol, OL = ornithine, GlcA = glucuronic acid, PC = phosphatidylcholine, TMO = trimethylornithine, MMPE = monomethylphosphatidylethanolamine, PI = phosphatidylinositol, LPC = lysophosphatidylcholine.

131

Blue text, archaeal taxa key: EHH = *Euryarchaeota* - *Halobacteria* - *Halobacteriales*; EMA = *Euryarchaeota* - *Methanomicrobia* - ANME-1b; EMM = *Euryarchaeota* - *Methanomicrobia* - *Methanomicrobiales*; EMMC = *Euryarchaeota* - *Methanomicrobia* - *Methanomicrobiales* - C19A; EMME = *Euryarchaeota* - *Methanomicrobia* - *Methanomicrobiales* - EJ-Eo1; EMMM₁ = *Euryarchaeota* - *Methanomicrobia* - *Methanosarcinales* - *Methanosaetaceae*; EMMM₂ = *Euryarchaeota* - *Methanomicrobia* - *Methanomicrobiales* - *Methanomicrobiaceae*; EMMM₃ = *Euryarchaeota* - *Methanomicrobia* - *Methanosarcinales* - *Methanosarcinaceae*; ETTA₁ = *Euryarchaeota* - *Thermoplasmata* - *Thermoplasmatales* - AMOS1A-4113-Do4; ETTM = *Euryarchaeota* - *Thermoplasmata* - *Thermoplasmatales* - Marine Benthic Group D and DHVEG-1; TMC = *Thaumarchaeota* - Miscellaneous Crenarchaeotic Group.

In propionate-amended slurries, bacterial taxa and IPLs were spread out among more groups as compared to the butyrate cultures. PG and MMPE group were positioned closely to *Bacteroidetes*-BD2-2 (BBB), *Marinilabiaceae* (BBM), and 10°C culture conditions; PI was positioned closely to *Chloroflexi*-MSBL5 (BCM); PA was positioned close to *Bacteroidetes* (BB) and *Actinobacteria*-OPB41 (BAO); DH was close to *Bacteroidetes*-SB-1 (BBS); PE and LPC were not positioned near any particular taxon, but clustered closely to low sulfate culture conditions (Fig. 5A). Among archaeal taxa in propionate-amended slurries, PI clustered with *Methanomicrobiaceae* (EMMM₂) and *Thermoplasmatales*-TMEG; PA with *Thermoplasmatales*-CCA47 (ETTC); LPC with *Methanomicrobiales* (EMM); PE with *Methanomicrobiales*-EJ-Eo1 (EMME) and low sulfate culture conditions (Fig. 5B).

Membrane lipids in enrichments from the sulfate and methane zones



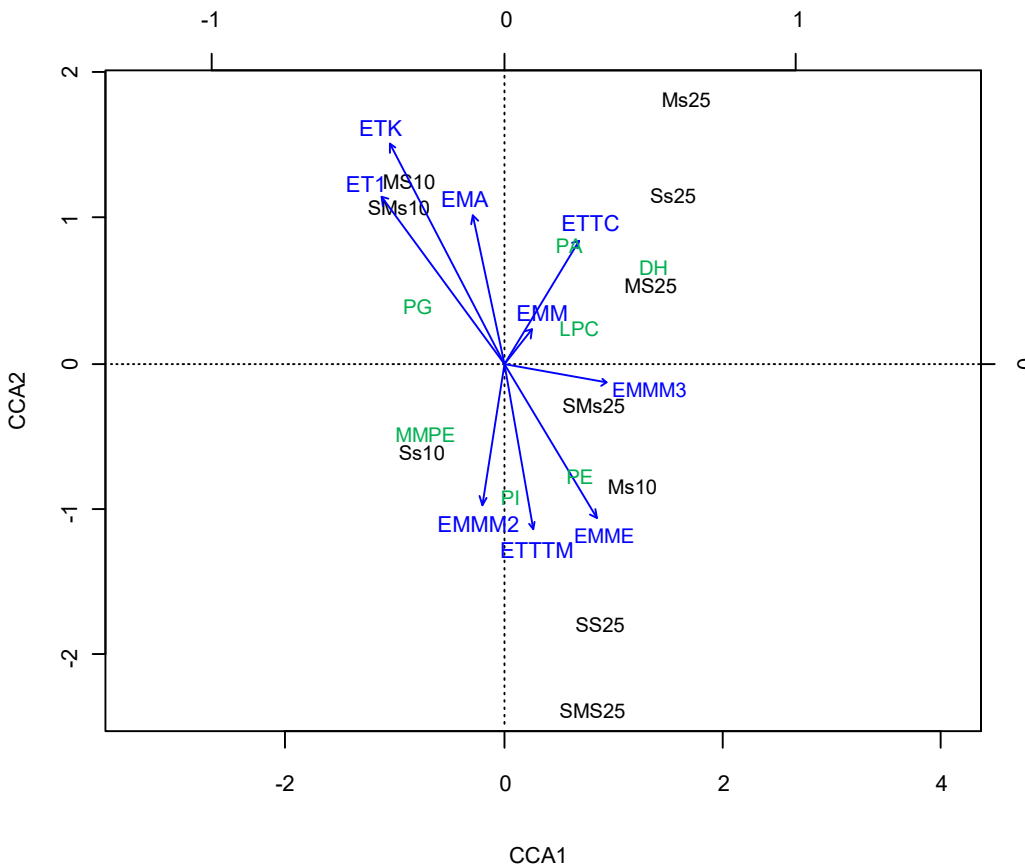
B

Figure 5: (A) Canonical correspondence analysis of intact polar lipid (IPL) distribution, bacterial taxa distribution, and growth conditions for propionate-amended enrichment slurries. (B) Canonical correspondence analysis of intact polar lipid (IPL) distribution, archaeal taxa distribution, and growth conditions for propionate-amended enrichment slurries.

Black text, culture condition key: S = sulfate zone, SM = sulfate-methane transition zone, M = methane zone, S = high amended sulfur, s = low amended sulfur, 25 = 25°C, 10 = 10°C.

Green text, IPL key: PI = phosphatidylinositol, PA = phosphatidic acid, PE = phosphatidylethanolamine, PG = phosphatidylglycerol, MMPE = monomethylphosphatidylethanolamine, DH = dihexose, LPC = lyso-phosphatidylcholine.

Blue text, bacterial taxa key: BAO = Bacteria - *Actinobacteria* - OPB41; BB = Bacteria - *Bacteroidetes*; BBB = Bacteria - *Bacteroidetes* - BD2-2; BBF = Bacteria - *Bacteroidetes* - *Flavobacteriaceae*; BBM = Bacteria - *Bacteroidetes* - *Marinilabiaceae*; BBS = Bacteria - *Bacteroidetes* - SB-1; BBS2 = Bacteria - *Bacteroidetes* - *Sphingobacteriales*; BCA1 = Bacteria - *Chloroflexi* - *Anaerolineae*; BCA2 = Bacteria - *Chloroflexi* - *Anaerolineae*; BCG = Bacteria - *Chloroflexi* - GIF9; BCM = Bacteria - *Chloroflexi* - MSBL5; BCO = Bacteria - Candidate division OP9; BEL = Bacteria - *Elusimicrobia* - Lineage_IV; BO = Bacteria other.

Blue text, archaeal taxa key: EMA = *Euryarchaeota* - *Methanomicrobia* - ANME-1b; EMM = *Euryarchaeota* - *Methanomicrobia* - *Methanomicrobiales*; EMME = *Euryarchaeota* - *Methanomicrobia* - *Methanomicrobiales* - EJ-Eo1; EMMM2 = *Euryarchaeota* - *Methanomicrobia* - *Methanomicrobiales* - *Methanomicrobiaceae*; EMMM3 = *Euryarchaeota* - *Methanomicrobia* -

Methanosarcinales - *Methanosarcinaceae*; ETK = *Euryarchaeota* - *Thermoplasmata* - Kazan-3A-21; ET₁ = *Euryarchaeota* - *Thermoplasmata* - 19c-33; ETTC = *Euryarchaeota* - *Thermoplasmata* - *Thermoplasmatales* - CCA47; ETTM = *Euryarchaeota* - *Thermoplasmata* - *Thermoplasmatales* - Terrestrial Miscellaneous Gp (TMEG).

5.4 Discussion

The greater diversity of microbial taxa versus IPLs agrees with consistent findings that many IPLs with the same head group and/or core lipid structures are produced by a wide range of microbial species (Fang and Barcelona, 1998; Fang et al., 2000; Schouten et al., 2000; Rütters et al. 2002a; 2002b; Sturt et al., 2004; Lipp et al., 2008; Schubotz et al., 2009). The higher concentrations of bacterial IPLs in samples are generally consistent with higher concentrations of sedimentary organic carbon which likely serves as major substrate (Lipp et al., 2008). Both the microbial community and IPL distribution changed much from the sediment samples compared to the sediment slurries inoculated with corresponding sediment samples, indicating that incubation conditions (temperature, sulfate concentration, carbon source) have an impact on the cell membrane composition of different microbial communities. Twice as many IPL head group structures were observed in butyrate-amended sediment slurries than propionate-amended sediment slurries showing that the butyrate degrading community has more diverse membrane composition.

The most abundant IPLs identified in most of the sediment enrichment slurries are phosphatidylethanolamine (PE), which are often found in aquatic environments and sediments and are attributed to sulfate-reducing bacteria (Rossel et al., 2008). The high abundance of SRB in enrichment slurries (Chapters 3 and 4) and the positive correlation between PE and high sulfate condition (Fig 4A) indicates that the occurrence of PE can be linked to the presence of SRB in enrichment slurries. Other IPLs that showed high relative abundance among sediment slurries were PG and PC. PG has been identified as the second most abundant lipid in bacterial membranes (Dowhan, 1997) including cultured representatives of the deep biosphere (Schubotz, 2005). PC has been identified in more than 10% of all bacteria (Sohlenkamp et al., 2003). The higher relative abundance of PC in only butyrate-amended enrichment slurries therefore suggests a specific bacterial group involving in butyrate conversion might possess PC.

The identification of TMO lipids in three butyrate-amended methane zone enrichment slurries (Fig. 3, Table S1) was surprising since these lipids were originally identified in planctomycete isolates from ombrotrophic northern wetlands (Moore et al., 2013), and peaked in

abundance at the oxic-anoxic interface (Moore et al., 2015b). These ombrotrophic wetlands are methanogenic, suggesting TMOs could be linked to the methanogenic microbial communities in different environments. The TMOs identified in the butyrate-amended methane zone sediment slurries contained core lipids C_{18:0}/βOH-C_{18:0}, C_{18:1}/βOH-C_{18:0}, C_{16:0}/βOH-C_{18:0}, and C_{19:1}/βOH-C_{18:0}. TMOs with core lipids C_{18:1}/βOH-C_{18:0}, C_{16:0}/βOH-C_{18:0}, and C_{19:1}/βOH-C_{18:0} were also identified in northern wetland planctomycete isolates (Moore et al., 2013), and TMOs with core lipids C_{18:1}/βOH-C_{18:0} and C_{16:0}/βOH-C_{18:0} were also identified in northern wetland peats (Moore et al., 2015b). No planctomycete phylotypes were identified using pyrosequencing analysis in any of the butyrate-amended methane zone sediment slurries indicating that the observed TMOs were produced by other microbial groups or the relative abundance of the responsible organisms very low. TMOs have also recently been identified in meso-oligotrophic lakes of Minnesota and Iowa, possibly as a response to low phosphorus concentrations (Bale et al., 2016).

Multivariate analysis showed that the *Bacteroidetes* phylum, and to a lesser extent, *Methanomicrobiales* order contributed to the variation in IPL distribution compared to other abundant phylogenetic groups in butyrate-amended slurries. In propionate-amended slurries, *Bacteroidetes* and *Methanomicrobiales* had also greater contributions than various other microbial groups. The sulfate concentrations in butyrate-amended sediment slurries and 10°C as incubation temperature in the propionate-amended slurries contributed to the microbial composition and IPL variation (Fig. 4 and 5). Various *Bacteroidetes* species have been observed to produce a wide range of IPLs including PEs, ornithine lipids, and lysine lipids (LLs) (Moore et al., 2015a; 2016; Singh et al., 2015). Recently, many marine and estuarine *Flavobacteriaceae* related species, were found to produce PEs and amino lipids as their most abundant membrane lipid structures (Yoon and Kasai, 2016; Jung et al., 2016; Liu et al., 2016; Wang et al., 2016; Park et al., 2016; Liu et al., 2016; Song et al., 2015). The *Flavobacteriaceae* family belong to the *Bacteroidetes* phylum and is clustered closely with PEs and OLs (Fig. 4A). This indicates that *Flavobacteriaceae* contributed to the variation in PEs and OLs in cluster 1 (Fig. 4A). Marine sediment and seawater members of *Halobacteriales* have been reported to produce PGs and PEs (Wang et al., 2010a; Yim et al., 2014) indicating that these taxa contributed to the variation of these IPLs in cluster 1.

This study shows that the membrane structures of microbes inhabiting sulfate, sulfate-methane transition and methane zones of marine sediments can be highly variable among different taxa and depending on different incubation conditions, such as temperature, substrate, and

electron acceptor availability. The presence of trimethylornithine lipids (TMOs) in methane zone slurries indicates that these IPLs can be found in a wider range of ecosystems than previously observed. Further study is needed to shed light on how microbial communities in coastal marine sediment respond to changes in environmental and incubation conditions. Such studies will be extremely important given the high level of human impact on coastal ecosystems (Syvitski et al., 2005; Talaue-McManus L. 2010; Deegan et al., 2012; Halpern et al., 2015).

Supplementary data

Table S1. Relative abundance (HPLC/MS base peak area/g sediment dw [dry weight]) of all IPLs identified in Aarhus Bay sediment and the enrichment slurries inoculated with this sediment. 120 cm = sulfate zone, 135-165 cm = sulfate-methane transition zone, 180-300 cm = methane zone.

Sample	Mhex	PA	DH	Betaine	DMPE	PE	PG	OL	GlcA	PC	TMO	MMPE	PI	LPC
SZP1	0	0	10306876	0	0	2125058	0	0	0	0	0	0	0	567541
SZP4	0	0	0	0	0	3932722	0	0	0	0	0	0	0	844881
SZP6	0	0	14475168	0	0	11455795	8540072	0	0	0	0	0	0	167282
SZP8	0	0	0	0	0	7253934	25716826	0	0	0	0	30425552	0	85194
SZB1	0	0	0	0	0	1946176	0	0	0	0	0	0	0	2954044
SZB2	0	0	27195033	0	0	2394770	0	0	0	0	0	0	0	1476664
SZB4	0	0	7594944	0	0	1983971	0	0	0	2832247	0	0	0	849552
SZB5	0	0	11499437	0	0	4455602	0	0	0	0	0	0	0	1204249
SZB7	0	0	0	0	0	10303739	17291589	0	0	1499265	0	0	0	0
SMTZP2	0	0	2791308	0	0	4313418	1425473	0	0	0	0	0	0	520065
SMTZP3	0	0	0	0	0	4361251	0	0	0	0	0	0	395300	0
SMTZP5	0	0	0	0	0	0	6402583	0	0	0	0	0	289450	0
SMTZP7	0	0	0	0	0	6472388	5236955	0	0	0	0	0	326489	0
SMTZB1	39551686	0	12878869	0	0	12799850	1060523	0	35097613	8812082	0	0	0	590925
SMTZB3	0	0	5197585	0	0	5120743	11400411	1174897	0	0	0	0	0	0
SMTZB6	0	0	12235720	0	0	10403673	47667216	0	0	31353022	0	0	0	711956
SMTZB7	0	0	0	0	0	1494608	24104131	0	0	0	0	0	0	0
SMTZB8	0	0	0	0	0	19584619	29774976	0	0	34063439	0	0	0	0
MZP1	0	0	5934192	0	0	11110238	0	0	0	0	0	0	0	304481
MZP2	0	452062	0	0	0	7984413	0	0	0	0	0	0	101628	231587
MZP3	0	0	4325181	0	0	0	0	0	0	0	0	0	0	311242
MZP4	0	0	0	0	0	0	0	0	0	0	0	0	0	0
MZP5	0	0	0	0	0	7937245	0	0	0	0	0	0	0	704338
MZP6	0	715154	5176235	0	0	2812398	0	0	0	0	0	0	0	863567
MZP7	0	0	0	0	0	7741609	0	0	0	0	0	0	0	0
MZP8	0	350711	0	0	0	0	24202780	0	0	0	0	0	801746	0
MZB1	0	0	485170	0	0	17021650	18855340	0	0	757859168	15574565	0	0	1065405
MZB2	0	68529	0	0	0	1153218	8106805	0	0	0	0	0	467142	16962049
MZB3	0	0	1648930	0	0	2230226	8895759	0	0	0	0	0	0	1088251
MZB4	0	0	0	0	0	0	3354888	0	0	110589668	17064261	0	0	23535905
MZB5	737203	0	21381687	11195317	2801118	0	0	0	0	12704704	1724058	0	0	2048403
MZB6	0	613445	16440021	0	0	4403271	0	0	0	0	0	0	0	0
MZB7	0	0	0	0	0	0	0	0	0	0	0	0	0	0
MZB8	0	365393	6954652	0	0	1906084	0	0	0	0	0	0	139512	401081
120	0	531101	0	0	0	1207772	0	0	0	0	0	0	1131887	0
135	0	443604	0	0	0	0	0	0	0	0	0	0	0	0
150	0	552721	0	0	0	808333	0	0	0	0	0	0	0	0
165	0	738732	0	0	0	0	0	0	0	0	0	0	0	0
180	0	1255773	0	0	0	0	0	0	0	0	0	0	0	0
195	0	373889	0	0	0	0	0	0	0	0	0	0	0	0
210	0	473870	0	0	0	2551160	0	0	0	0	0	0	0	0
225	0	247824	0	0	0	0	0	0	0	0	0	0	0	0

Chapter 6

Physiological and molecular characterization of anaerobic marine propionate- and butyrate-converting syntrophic cultures

Derya Ozuolmez, M. Cristina Gagliano, Daan van Vliet, Alfons J.M. Stams,
Caroline M. Plugge

Abstract

Degradation of propionate and butyrate in marine sediments is carried out predominantly by sulfate-reducing bacteria. However in sulfate-depleted zones, these compounds are degraded by methanogenic communities, which have been poorly studied. Here, we studied anaerobic conversion of propionate and butyrate under sulfate-free and low-sulfate conditions by syntrophic communities enriched from different biogeochemical zones of Aarhus Bay. Several transfers from previously enriched sediment slurries were performed. Butyrate conversion after four transfers occurred rapidly and acetate and methane and/or sulfide accumulated in the cultures. On the other hand, propionate conversion proceeded slow enabling enrichment of acetoclastic methanogens and hence the complete conversion of propionate. The addition of low amounts of sulfate to the cultures did not inhibit syntrophic conversion, instead, both sulfate reduction and methanogenesis proceeded concomitantly. The butyrate-converting cultures were dominated by *Syntrophomonas bryantii* and an uncultured *Syntrophomonas* species. The propionate-converting cultures were dominated by bacteria that are phylogenetically similar to *Cryptanaerobacter phenolicus* and different *Pelotomaculum* species (95-96%, 16S rRNA gene based), indicating presence of possible novel species of propionate-converting syntrophs. Low sulfate amended butyrate- and propionate-converting cultures contained *Desulfobacteraceae* members together with uncultured *Syntrophomonas* sp. and *Cryptanaerobacter* sp., respectively. Hydrogenotrophic methanogens were present in all enrichment cultures, whereas acetoclastic methanogens were abundant in sulfate-free cultures but had low abundance in sulfate-amended cultures.

6.1 Introduction

Propionate and butyrate are important intermediates in anaerobic degradation of organic matter in marine sediments. These compounds can be oxidized by a variety of marine sulfate-reducing bacteria (SRB) either completely to CO₂ or incompletely to acetate (Widdel, 1988; Muyzer and Stams, 2008). Bacteria that can couple propionate and butyrate oxidation to sulfate reduction include members of the families *Desulfobacteraceae*, *Desulfobulbaceae*, *Syntrophobacteraceae*, *Peptococcaceae* (Kuever et al., 2014b; Stackebrandt, 2014). In sulfate-depleted sediments, organic matter is degraded through syntrophic interactions of acetogenic bacteria and methanogens. In sulfate-depleted sediments, methanogens consume hydrogen, formate and acetate that are formed as products of organic carbon degradation. Hydrogen and formate consumption allows propionate and butyrate conversion to be energetically favorable (McInerney et al., 1979; Boone and Bryant, 1980). In this way, a syntrophic relationship is established between bacteria and methanogens (Schink and Stams, 2013; McInerney et al., 2008).

Syntrophic propionate-oxidizing bacteria are affiliated with two phylogenetic groups of bacteria. The first group contains Gram-negative genera *Syntrophobacter* and *Smithella*, belonging to the *Deltaproteobacteria*. The second group contains Gram-positive bacteria affiliated to genera *Pelotomaculum* and *Desulfotomaculum*, belonging to the phylum *Firmicutes* (Boone and Bryant, 1980; Harmsen et al., 1998; Wallrabenstein et al., 1995; Imachi et al. 2002; Plugge et al. 2002; de Bok et al. 2005; Chen et al., 2005; Stams et al., 1993). These genera are phylogenetically associated to sulfate-reducing bacteria and some of these syntrophs can couple propionate oxidation to sulfate reduction. On the other hand, there are few species that are obligately syntrophic and hence unable to reduce sulfate; these are *Pelotomaculum schinkii* (de Bok et al., 2005) and *Pelotomaculum propionicicum* (Imachi et al., 2007).

Most syntrophic butyrate-degrading bacteria are classified as low GC Gram-positive bacteria. Organisms capable of syntrophic butyrate metabolism include all species of *Syntrophomonas* (Stieb and Schink, 1985; Zhao et al., 1990; McInerney et al. 1981; Lorowitz et al. 1989; Zhang et al. 2004; Zhang et al. 2005; Roy et al., 1986; Sousa et al. 2007a; Wu et al. 2006a; Wu et al. 2006b; Wu et al. 2007), *Thermosyntropha lipolytica* (Svetlitschnyi et al. 1996), *Syntrophothermus lipocalidus* (Sekiguchi et al. 2000) and the Gram-negative *Syntrophus aciditrophicus* (Jackson et al, 1999). The majority of the *Syntromonadaceae* family members are not obligate syntrophs as they can dismutate crotonate without a syntrophic partner (McInerney et al.,

1979, 1981; Stieb and Schink, 1985; Beaty and McInerney, 1987; Lorowitz et al., 1989; Zhao et al., 1990, 1993; Svetlitsnyi et al., 1996; Sekiguchi et al., 2000; Zhang et al., 2004; Hatamoto et al., 2007). The exceptions to this are *Syntrophomonas sapovorans* and *S. zehnderi*, which degrade all linear saturated fatty acids with 4 to 18 carbon atoms only in coculture with methanogens (Roy et al., 1986; Sousa et al., 2007a). A syntrophic butyrate-degrading bacterium, *Algorimarina butyrica*, was isolated from marine sediments (Kendall et al., 2006). This bacterium is phylogenetically affiliated to *Deltaproteobacteria* and closely related to the sulfate-reducing *Desulfonema magnum*. Yet, it cannot couple butyrate oxidation to sulfate reduction (Kendall et al., 2006). *A. butyrica* is the first and the only marine syntrophic butyrate degrader isolated.

The main goal of this study was to establish marine propionate- and butyrate-degrading syntrophic consortia in enrichment cultures using the sediment slurry enrichments obtained in chapters 3 and 4. Based on this previous research, we proposed that *Cryptanaerobacter/Pelotomaculum* phylotype converts propionate and *Syntrophomonas* and *Desulfobacteraceae* family members convert butyrate in syntrophy with methanogens in Aarhus Bay sediment. In order to further enrich these microorganisms and to confirm the results of our previous study, the enrichment slurries were sub-cultured for four times. Here, propionate and butyrate degradation and product formation was quantified, and the eventual microbial community composition in the fourth sub-cultures was analyzed.

6.2 Materials and Methods

6.2.1 Source of inocula and preparation of sub-cultures

Propionate and butyrate degrading sediment slurries were set up using sediment taken from sulfate zone (SZ), sulfate-methane transition zone (SMTZ) and methane zone (MZ) of Station M1 in Aarhus Bay, Denmark. 1 L glass bottles were used to mix the sediment with marine anoxic mineral salt medium (see Chapter 3) containing 10 mM propionate or butyrate as carbon sources with and without 20 mM sulfate in sulfate zone and methane zone slurries, and with 3 mM and 20 mM sulfate for sulfate-methane transition zone slurries. The overview of all butyrate- and propionate-amended sediment slurries is given in chapter 3 and 4. The slurries were regularly monitored for substrate consumption and product formation and regular additions of propionate, butyrate and/or sulfate were performed. These enrichment slurries have been maintained for 514-571 days. Subsequently, sediment-free transfers were performed from original slurries into culture bottles containing the

same medium as was used to prepare enrichment slurries. The medium content and preparation was described in chapter 3. After three transfers, the culture bottles were without sediment particles and the fourth transfer was used to quantify propionate and butyrate conversion and to analyze the microbial composition of the enrichment cultures.

Enrichment cultures were inoculated in triplicate with 20 ml of original slurry into 250 ml serum vials with 134 ml of anoxic mineral salts medium (including carbon source, reductant, and vitamin solution). 10 mM butyrate or propionate was used as carbon source with 3 mM sulfate as electron acceptor for SMTZ and without sulfate for SZ and MZ cultures. The enrichment cultures were incubated statically in the dark at 25°C with a gas composition of N₂/CO₂ (80:20 v/v) at 1,7 atm pressure.

6.2.2 Analytical methods

Methane in the headspace of the culture bottles was analyzed by gas chromatography with a Shimadzu GC-14B (Shimadzu, Kyoto, Japan) equipped with a packed column (Molsieve 13X, 60-80 mesh, 2 m length, 3 mm internal diameter; Varian, Middelburg, The Netherlands) and a thermal conductivity detector set at 70mA. The oven and the injector temperatures were both 100°C. The detector temperature was 150°C. Argon was the carrier gas at a flow rate of 30 ml min⁻¹.

Propionate, butyrate and acetate were quantified using a Thermo Scientific Spectrasystem HPLC system (Thermo Scientific, Waltham, MA) equipped with a Varian Metacarb 67H 300x6.5 mm column (Agilent, Santa Clara, MA) connected to a UV and Refractive Index (RI) detector. 0.005 M sulfuric acid was used as eluent and 10 mM sodium crotonate as internal standard. The flow rate was 0.8 ml min⁻¹ and analyses were carried out at 30°C. Data analyses were performed using ChromQuest (Thermo Scientific, Waltham, MA) and Chromeleon software (Thermo Scientific, Waltham, MA).

Sulfate and sulfide in SMTZ cultures were measured as described in Chapter 3.

6.2.3 DNA extraction

Genomic DNA was extracted from the propionate and butyrate-amended cultures using Fast DNA Kit for Soil (MP Biomedicals, Santa Ana, CA) according to the manufacturer's instructions. Two 45-second beat beating steps were applied using a Fastprep Instrument (MP Biomedicals, Santa Ana,

CA). The DNA quality was examined on 1% (w/v) agarose gel and the DNA quantity was determined using Nanodrop 1000 spectrophotometer (Thermo Fisher Scientific, Wilmington, DE).

6.2.4 Clone library construction

Extracted DNA was used for a clone library construction. Almost full-length 16S rRNA genes were amplified using primers 27F (5'-AGAGTTTGGATCMTGGCTCAG-3') (Lane, 1991) and 1369R (5'-GCCCCGGAACGTATTCACCG-3') (Iwamoto et al., 2000) for Bacteria, and the primers 25F (5'-CYGGTTGATCCTGCCRG-3') (Dojka et al., 1998) and 1386R (5'-GCGGTGTGTGCAAGGAGC-3') (Skillmann et al., 2004) for Archaea. PCR amplification was carried out using GoTaq DNA Polymerase kit (Promega, Madison, WI, USA). Bacterial 16S rRNA amplification was carried out as described in Sousa et al. (2007b), while archaeal amplicons were obtained following the protocol of Borrel et al. (2012). 16S rRNA gene amplicons' integrity and length was checked on agarose gel and subsequently purified with Zymoclean Gel DNA Recovery Kit (Zymo Research, Orange, CA, USA). Ligation and cloning of the PCR products were performed with the use of a pGEM®-T Easy Vector kit (Promega, Madison, WI, USA) and *E. coli* XL blue competent cells (Agilent Technologies, Santa Clara, USA). White colonies were randomly selected and transferred to a 96 well Masterblock® plate (Greiner Bio-One, the Netherlands). Nearly full-length 16S rRNA genes were sequenced by GATC Biotech (Konstanz, Germany) using the primers T7 and SP6. Sequences were manually trimmed and checked for chimeras using VecScreen (<http://www.ncbi.nlm.nih.gov/tools/vecsreen/>) and Decipher (<http://decipher.cee.wisc.edu/FindChimeras.html>). Sequence similarity was checked using NCBI MegaBlast (<http://blast.ncbi.nlm.nih.gov/Blast.cgi>). Data analysis of amplicons was carried out with the SilvaNGS software pipeline (<https://www.arb-silva.de/ngs>).

6.2.5 Fluorescence in situ hybridization (FISH)

FISH analysis was performed on paraformaldehyde-fixed biomass samples taken from the enrichment cultures, according to the procedure described in Amann et al. (1995). Three samples per each culture condition were analyzed to ensure the complete analysis of the microbial dynamics. Oligonucleotide probes were specific for Bacteria (EUB338mix probes) and Archaea (ARC915 probe) domains. Details of the employed oligonucleotide probes are available at probeBase (Greuter et al., 2016). Probes were labelled with Cy3 or FITC fluorophores. All the hybridizations with specific probes were carried out in combination with DAPI staining, to highlight the probe

coverage versus the total community. Samples were examined by epifluorescence microscopy (Olympus BX41) equipped with Infinity Camera (Lumenera corporation, Canada). FISH images were further modified using the ImageJ software package (version 1.37v, Wayne Rasband, National Institute of Health, Bethesda, MD, USA, available in the public domain at <http://rsb.info.nih.gov/ij/index.html>).

6.3 Results and discussion

6.3.1 Butyrate conversion

The conversion of butyrate was studied under sulfate-reducing and methanogenic conditions in enrichment cultures that were derived from three enrichment slurries prepared with SZ, SMTZ and MZ sediment (Figure 1). Butyrate was completely metabolized within 11 days in all enrichment cultures. In the SZ culture, 18.0 ± 1.37 mM butyrate was converted to 27.3 ± 0.6 mM acetate and 8.8 ± 0.3 mM methane (Table 1, Figure 1a). Acetate and methane were produced in the MZ culture (Figure 1c). The ratios of consumed butyrate to produced acetate and methane in SZ and MZ cultures are 1 : 1.5 : 0.5 and 1 : 1.6 : 0.4, respectively. These values are close to the predicted stoichiometric values of syntrophic butyrate degradation ($\text{Butyrate} + 0.5 \text{HCO}_3^- + 0.5 \text{H}_2\text{O} \rightarrow 2 \text{CH}_3\text{COO}^- + 0.5 \text{CH}_4 + 0.5 \text{H}^+$) (Chapter 3-Table 1, reaction 7).

In low-sulfate amended SMTZ cultures, butyrate conversion was coupled to both sulfate reduction and methanogenesis (Fig 1b, 1e). 15.8 ± 0.4 mM butyrate was degraded and 4.2 ± 0.5 mM sulfate was reduced. Here, 27.3 ± 0.9 mM acetate, 5.1 ± 0.1 mM sulfide and 5.9 ± 0.5 mM methane were produced (Table 1). Two possible routes for butyrate conversion in these enrichments could have occurred: (1) Butyrate oxidation via sulfate reduction (Chapter 3-Table 1, reaction 2) plus concurrent syntrophic butyrate conversion with acetate- and hydrogen-dependent sulfate reduction and/or methanogenesis (Chapter 3-Table 1, reactions 1 + 3, 4, 5 and/or 6), (2) Syntrophic butyrate conversion with acetate- and hydrogen-dependent sulfate reduction and/or methanogenesis (Chapter 3-Table 1, reactions 1 + 3, 4, 5 and/or 6). In case of the first route, both a sulfate reducer and an acetogen convert butyrate.

Table 1. The overview of substrate consumption and product formation in the enrichment cultures. The values represented in the table are the total amounts of the reactants consumed and the products formed along the study. All cultures were prepared in triplicate. The values are the mean of triplicates for butyrate SMTZ and MZ cultures, duplicates for butyrate SZ and propionate SMTZ and MZ. The two replicates of propionate SZ culture did grow slower, thus the values from only one replicate of this culture is presented here. NA: not applicable, NM: not measured. Hydrogen or formate were not detected in any of the incubations.

Substrate	Origin	Time (d)	Reactants (mM)			Products (mM)		
			Butyrate	Propionate	Sulfate	Acetate	Methane	Sulfide
Butyrate	SZ	11	18.0 ± 1.4	NA	NA	27.3 ± 0.6	8.8 ± 0.3	NM
	SMTZ	11	15.8 ± 0.4	NA	4.2 ± 0.5	27.3 ± 0.9	5.9 ± 0.5	5.1 ± 0.1
	MZ	11	15.8 ± 0.4	NA	NA	25.8 ± 0.5	6.2 ± 0.3	NM
Propionate	SZ	70	NA	18.2	NA	0.78	24.5	NM
	SMTZ	297	NA	17.7 ± 0.7	NM	15.1 ± 1.0	10.3 ± 0.4	NM
	MZ	297	NA	17.9 ± 0.0	NA	1.5 ± 0.0	26.4 ± 1.6	NM

In the second, butyrate is converted only by an acetogen to acetate and hydrogen and hydrogen is consumed by a methanogen and part of the acetate is oxidized by a sulfate reducer (Fig 1e).

Previous studies have reported the existence of syntrophic butyrate degradation in sulfate containing ecosystems, such as marine sediments, anaerobic digesters and batch cultures (Kendall et al., 2006; Visser et al., 1993; Struchtemeyer et al., 2011). The results of our study support previous findings and show that under low sulfate concentrations syntrophic butyrate degradation can occur simultaneously with sulfate reduction (Fig 1b, 1e). Methanogenesis can be the dominant pathway for the utilization of the products H₂ and/or formate, whereas acetate is probably utilized via sulfate reduction (Fig 1e, Table 1). This is supported by the absence of aceticlastic methanogens in SMTZ culture as revealed by community analysis (Fig 2e, Table S2).

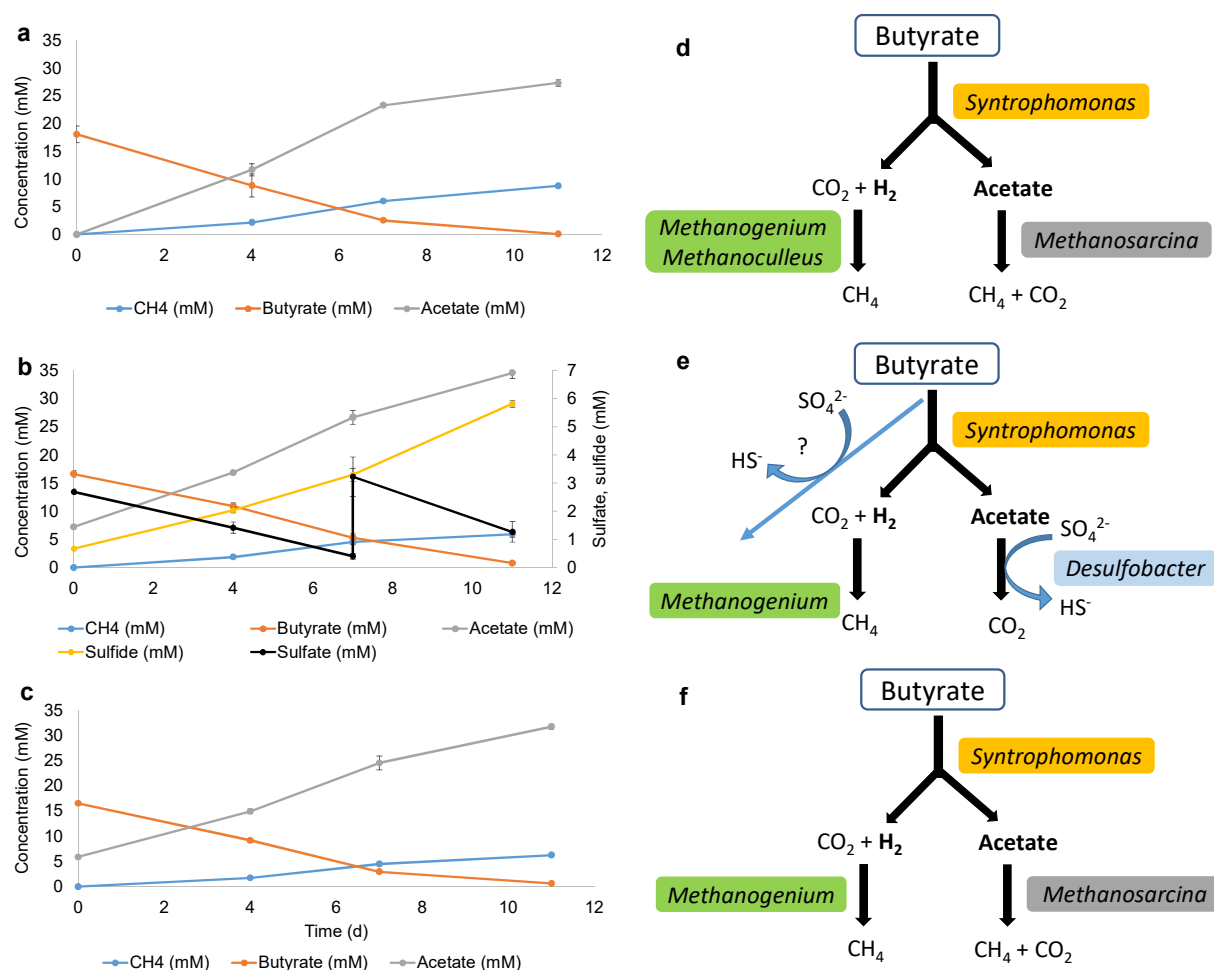


Figure 1. Butyrate conversions (SZ (a), SMTZ (b) and MZ (c)) and proposed butyrate conversion routes (SZ (d), SMTZ (e) and MZ (f)) in the cultures. Butyrate conversion routes are proposed based on microorganisms with high relative abundance and observed butyrate conversion stoichiometries. Values are mean of biological duplicates for SZ and triplicates for SMTZ and MZ. Error bars indicate the standard deviations.

6.3.2 Microbial communities in butyrate enrichments

Bacterial 16S rRNA based clone libraries of butyrate-degrading enrichment cultures after 11 days of incubation revealed dominance of *Syntrophomonas* (Figure 2a, 2b, 2c and Table S1). Within the clone library, 16 clones derived from the SZ culture (53%) and 23 clones derived from the MZ culture (77%) showed 99% similarity to *Syntrophomonas bryantii* (Figures 2a and 2c). *S. bryantii* is a Gram-positive, spore-forming, butyrate degrading syntroph isolated from marine mud (Stieb and Schink, 1985). The ability of *S. bryantii* to form spores can be an advantage to survive under unfavorable conditions in marine sediments. This ability might explain the dominance of *S. bryantii*, a marine

isolate, in both sulfate and methane zone enrichment cultures. 42% of the clones derived from the SMTZ culture affiliated with an uncultured *Syntrophomonas* sp. (95% similarity) (Figure 2b and Table S1). Low sulfate concentration in SMTZ culture might have stimulated *Syntrophomonas* to reach as high relative abundance as in the SZ and MZ cultures. Sulfate-reducing bacteria that directly couple butyrate oxidation to sulfate reduction grow faster than syntrophic butyrate degraders. On the other hand, the growth rates of some syntrophic butyrate degraders were reported to be higher than some butyrate-oxidizing sulfate-reducers (Oude Elferink et al., 1994). This might be due to their similar kinetic properties rather than thermodynamic factors since Gibbs free energy changes for the complete oxidation of butyrate coupled to sulfate reduction (ΔG° of -6.1kJ per electron transferred) or to methane production (ΔG° of -4.1kJ per electron transferred) are in the same range (Chapter 3, Table 1) (McInerney and Beaty, 1988). These reasons may allow syntrophic butyrate degraders to exist in sulfate-reducing ecosystems such as marine sediments and aquifers (Kendall et al., 2006; Struchtemeyer et al., 2011). Similarly, *Syntrophomonas* in our study could take part in butyrate degradation in the presence of sulfate, with both sulfate reducers and methanogens as partner organisms (Fig 1e). The second most abundant phylotype (26%) in the SMTZ culture was affiliated to *Deltaproteobacteria* (99%) and had 98% similarity to *Desulfobacter latus* (Figure 2b and Table S1). A *D. latus* related bacterium was the dominant acetate-degrading organism after several sub-culturing period in low-sulfate amended SMTZ culture (Kuever et al., 2014b) and probably was the syntrophic partner of *Syntrophomonas*. Despite the higher free-energy change associated with acetate oxidation by sulfate (ΔG° of -47.6 kJ/mol) as compared to acetate cleavage to CH_4 and CO_2 (ΔG° of -31 kJ/mol), Schönheit et al. (1982) has explained that the difference in substrate affinities can account for the inhibition of methanogenesis from acetate in sulfate-rich environments. In Chapter 2, we report minor competition between acetate-consuming *D. latus* and *Methanosaeta concilii* for acetate in a mixed coculture. Butyrate in the SMTZ culture was converted solely by *Syntrophomonas* and $\sim 4\text{ mM}$ acetate was consumed (Table 1) by *D. latus* while hydrogen was utilized by *Methanogenium cariaci*, a marine methanogen (Romesser et al., 1979) to produce methane (Fig 1e, 2e). This observation was further supported by FISH analysis on SMTZ culture fixed after 16 days of cultivation, highlighting the presence of one morphotype positive to the ARC915 probe (Fig S2), which is in agreement with the clone library results (Fig 2e). Two morphologies were detected with the bacterial EUB338 probe. These morphotypes most likely correspond to *Syntrophomonas* sp. and *D. latus*. As visible in Figure S2a, there is an association between the bacterial and archaeal morphotypes, in particular between *Syntrophomonas* and

Methanogenium, while *Desulfobacter* clusters were less frequent in all the samples analyzed. DAPI staining observations underline that these three microorganisms are the key players and almost all the cells are active in the SMTZ enrichment culture (Figure S2b). Overall, we can speculate about a syntrophic relationship between these three microorganisms, in which *Syntrophomonas* converts 15.8 mM butyrate to ~32 mM acetate and 30 mM H₂, and *D. latus* consumes ~4 mM acetate coupled to reduction of ~5 mM sulfate and *M. cariaci* consumes ~24 mM H₂ to produce 6 mM CH₄ (Table 1).

The remaining bacterial phylotypes affiliated with *Bacteroidetes*, *Sulfurovum*, *Synergistetes*, *Anaerolineae* (Figure 2 and Table S1). These phylotypes are commonly found in marine sediments (Parkes et al., 2014; Webster et al., 2011; Webster et al., 2010; Fry et al., 2008) and are associated with the decomposition of carbohydrates and proteinaceous substrates (Yamada and Sekiguchi, 2009; Kleinsteuber et al., 2012; Godon et al., 2005). Therefore, the existence of non-butyrate-converting bacteria in all cultures suggests that they either are involved in the degradation of dead biomass or consumption of intermediates of butyrate degradation. FISH with specific probes or DAPI staining didn't highlight any other morphotype within the Bacteria domain.

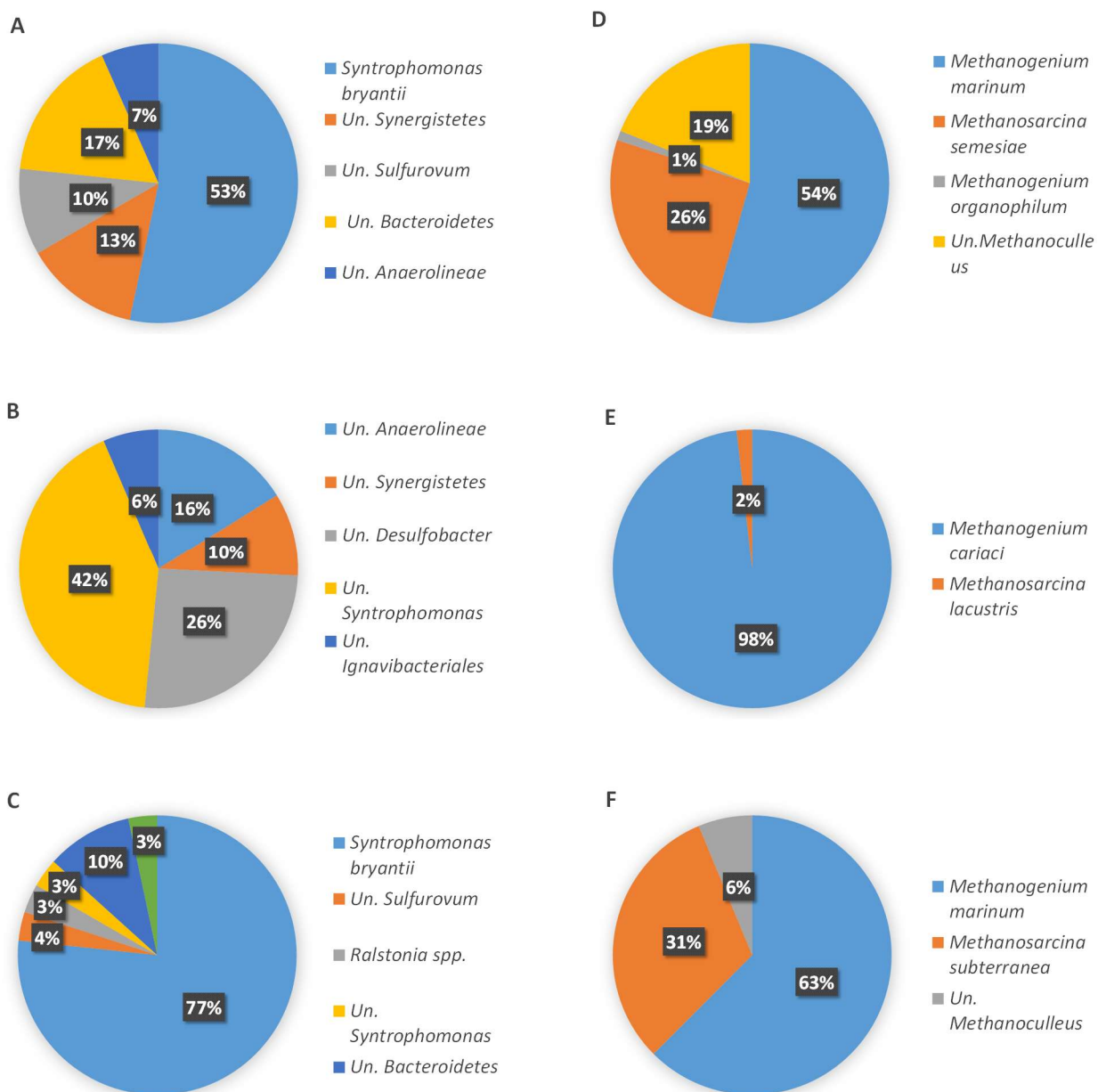


Figure 2. Distribution of bacteria (a, b, c) and archaea (d, e, f) detected in 16S rRNA gene clone libraries derived from butyrate-amended SZ (a, d), SMTZ (b, e) and MZ (c, f) cultures, respectively. Un: Uncultured.

Archaeal clone libraries of the SZ, SMTZ and MZ enrichment cultures show that most of the sequences affiliated with different *Methanomicrobiaceae* species, members of which are specialists in H_2 - and formate-utilization (Garcia et al., 2006) (Figure 2d, 2e, 2f and Table S2). Hydrogenotrophic methanogens are commonly found in near-surface marine sediments (Parkes et al., 2007; Sørensen et al. 1981; Blair and Carter, 1992). In the SMTZ, most clones (110 clones, 98%)

representing *Methanomicrobiaceae* affiliated with *Methanogenium cariaci* (Fig 2e, Table S2). SZ and MZ cultures were dominated by clones affiliated with *Methanogenium marinum* (54%). The other methanogenic phylotype found both in SZ and MZ cultures was an uncultured *Methanoculleus* sp., showing 92-95% similarity to its closest cultured species *Methanoculleus taiwanensis* (Table S2). The fact that this phylotype has low similarity to any cultured species, suggests that it may represent a novel species within the family *Methanomicrobiaceae*. Both *Methanogenium* and *Methanoculleus* species use H₂ and formate for methane production and were isolated from marine sediments (Romesser et al. 1979; Chong et al., 2002; Weng et al., 2015). *Methanogenium* sp. and *Methanoculleus* sp. consumed H₂/formate that was produced by the conversion of butyrate and acted as syntrophic partners of *Syntrophomonas* in the MZ and SZ enrichments (Fig 1d, 1f). This is supported by the amount of methane produced which is close to the stoichiometric values of syntrophic butyrate degradation in SZ and MZ cultures (Table 1). The relationship of *Methanogenium* sp. and *Methanoculleus* sp. with *Syntrophomonas* was reflected in FISH micrographs of SZ and MZ cultures (Figures S1 and S3). Archaeal cells are more abundant than bacterial cells in the SZ culture (Fig S1). The other methanogenic species detected in all butyrate-converting enrichment cultures was *Methanosarcina* sp. with 26%, 2% and 31% of the clones in the SZ, SMTZ and MZ clone libraries, respectively (Figure 2 and Table S2). The closest cultured relative of *Methanosarcina* sp. was *M. semesiae* in the SZ culture, *M. lacustris* in the SMTZ culture and *M. subterranea* in the MZ culture (Table S2). *Methanosarcina* species are metabolically diverse and able to consume methylated compounds, acetate and H₂/CO₂ (Kendall and Boone, 2006b). *M. semesiae* and *M. subterranea* species grow only on methyl compounds, but not on acetate, H₂/CO₂ or formate (Lyimo et al., 2000; Shimizu et al., 2015). However, the enrichment cultures did not contain any methyl group substrates, instead acetate, H₂/CO₂ or formate were the only possible methanogenic substrates. Therefore, *Methanosarcina*-related phylotypes found in these cultures might have consumed these intermediates (Fig 1d, 1f). FISH micrograph of MZ culture showed that *Methanosarcina* sp. cells were clustered with *Syntrophomonas* sp. cells, suggesting that *Methanosarcina* sp. may be syntrophic partners of *Syntrophomonas* sp. (Figure S3). However, this should be clarified with further research employing specific probes.

The initial sediment slurries from which SZ and SMTZ enrichment cultures were derived were dominated by sequences related to *Methanosaetaceae* and contained much less sequences affiliated to *Methanosarcina* (Chapter 3). After 4 sub-culturing steps *Methanosaetaceae*-related sequences were lost and *Methanosarcinaceae*-related methanogens were further enriched in the SZ

culture (Figure 2 and Table S2). In the SMTZ enrichment culture the acetoclastic methanogens were not enriched (Table S2). Instead, an acetotrophic sulfate-reducer (*Desulfobacter*) became the dominant acetate-consuming microorganism.

6.3.3 Propionate conversion

Propionate conversion was studied under methanogenic conditions in a similar manner as butyrate conversion (Table 1, Figure 3). Maintenance of activity in the propionate-converting enrichment cultures was more difficult compared to the butyrate-converting cultures. After each transfer, propionate conversion started after a long lag phase. The only culture in which propionate conversion started immediately was the SZ culture and propionate was consumed faster as compared to the SMTZ and MZ cultures (Figure 3). In the SZ culture, 18.2 mM propionate was completely converted to 24.5 mM methane in 70 days (Table 1). The acetate originating from the inoculum (1.8 mM) was consumed completely by day 35. Thereafter, 0.8 mM acetate was produced at the end of the incubation period and consumed by day 70 (Table 1). Propionate conversion in the MZ cultures was considerably slower than propionate conversion in the SZ culture (Figure 3c). 17.9 ± 0.01 mM propionate was completely, but slowly converted to 26.4 ± 1.6 mM methane within 297 days. The acetate detected in the beginning of the incubation was consumed within the first 36 days. Thereafter, 1.5 ± 0.0 mM acetate was produced and consumed at the end of the incubation period (Table 1). The amount of methane ultimately produced from propionate in the SZ (1.3 mol of methane/propionate) and in the MZ cultures (1.5 mol of methane/propionate) was close to the value predicted from the stoichiometry of the methanogenic propionate conversion pathway ($\text{CH}_3\text{CH}_2\text{COO}^- + 1.75 \text{H}_2\text{O} \rightarrow 1.75 \text{CH}_4 + 1.25 \text{HCO}_3^- + 0.25 \text{H}^+$) (Chapter 4-Table 1, reactions 1+5+6). During the incubation, H_2 and formate were not detected and only traces of acetate were intermediately found. Propionate conversion in methanogenic environments is a rate limiting step and complete propionate conversion can be accomplished only if products are consumed by partner organisms (Schink and Stams, 2013; McInerney et al., 2008). The stoichiometry of propionate conversions in SZ and MZ cultures shows that the formation of the products is in pace with their formation from propionate (Fig 3d, 3f).

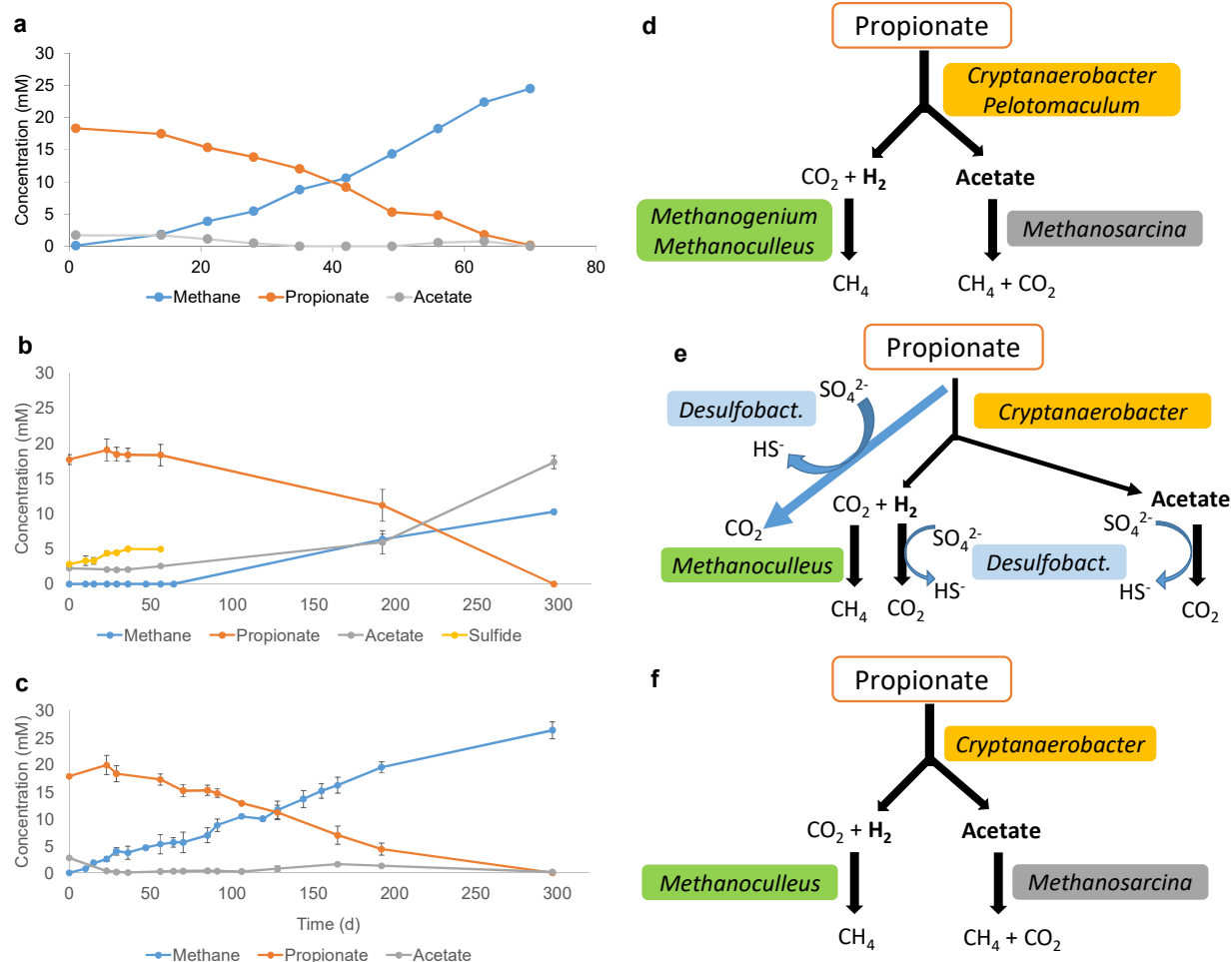


Figure 3. Propionate conversions (SZ (a), SMTZ (b) and MZ (c)) and proposed propionate conversion routes (SZ (d), SMTZ (e) and MZ (f)) in the cultures. Propionate conversion routes are proposed based on microorganisms with high relative abundance and observed propionate conversion stoichiometries. Values are mean of biological duplicates for SMTZ and MZ. As the replicate cultures of SZ grew slow, the values from only one replicate is used in the graph. Error bars indicate the standard deviations. *Desulfobact.* = *Desulfobacterium*.

The propionate conversion rate in SMTZ culture was similar to that in the MZ culture (0.06 mM/day). The conversion dynamics in SMTZ culture differed significantly from the SZ and MZ cultures (Figure 3). After a lag phase of more than 56 days propionate conversion proceeded by concomitant acetate and methane production. Here, 17.7 ± 0.70 mM propionate was converted to 10.3 ± 0.35 mM methane and 15.1 ± 0.95 mM acetate (Figure 3b and Table 1). This indicated that the conversion of propionate occurred by coupling of acetogenesis and hydrogenotrophic methanogenesis processes (Fig 3e). The ratio of consumed propionate to the produced acetate and methane in the SMTZ cultures is 1 : 0.9 : 0.6. As the theoretical ratio is 1: 1: 0.75, this suggests that

aceticlastic methanogenesis did not occur, and a minor part of the hydrogen/formate may have been used by sulfate reducers (Fig 3e).

6.3.4 Microbial community in propionate-degrading enrichments

Bacterial clone library analysis of propionate-amended enrichment cultures carried out on samples taken after 70 days for the SZ culture and 297 days for the SMTZ and MZ cultures, revealed dominance of clones related to *Cryptanaerobacter* sp. in the SZ (54% of all sequences) and MZ (35% of all sequences) cultures (Figure 4a, 4c). *C. phenolicus* is the only cultured species of the genus *Cryptanaerobacter* and it degrades phenol in syntrophic association with hydrogenotrophic methanogens (Juteau et al., 2005). The closest cultured relatives of two clones in the SZ culture affiliated with *Pelotomaculum isophthalicum* (96%), and *Pelotomaculum terephthalicum* (95%), which are phylogenetically closely related to each other and to *C. phenolicus* (Ezaki, 2009). *P. terephthalicum* and *P. isophthalicum* are known syntrophs that metabolize a variety of phthalate isomers and other aromatic compounds (McInerney et al., 2008; Qiu et al., 2006). As the sequence similarities of *Cryptanaerobacter* sp. and *Pelotomaculum* sp. with their closest cultured relatives detected in our study are below the threshold value of novel species status (98.65%) (Kim et al., 2014), these phylotypes seem to be novel species of propionate-converting bacteria within the family *Peptococcaceae*. A recent study suggested that *Cryptanaerobacter* sp. and *Pelotomaculum* sp. were the propionate-oxidizing species in enrichment cultures inoculated with sludge from agricultural biogas plants (Ahlert et al., 2016). Therefore, further research is needed to test the ability of *Cryptanaerobacter* sp. to consume propionate.

The majority of the clones (47% of all sequences) obtained from the SMTZ enrichment culture related to *Desulfobacterium indolicum* (93% similarity) (Figure 4b and Table S3). Additionally, 2 clones in this culture are distantly related to *Desulfosarcina variabilis* (93% similarity). As this value is below the suggested threshold (94.5% 16S rRNA based) for delineating a novel genus (Yarza et al., 2014), this phylotype might be a novel genus with members utilizing propionate and/or acetate within the family *Desulfobacteraceae*. The other phylotype that is affiliated with the *Desulfobacteraceae* family in this culture was assigned as *Desulfobacterium catecholicum* (13% of all sequences) (Table S3). This sulfate-reducing bacterium can utilize H₂+CO₂, formate, acetate and propionate as well as aromatic compounds and alcohols as carbon sources (Szewzyk and Pfennig, 1987).

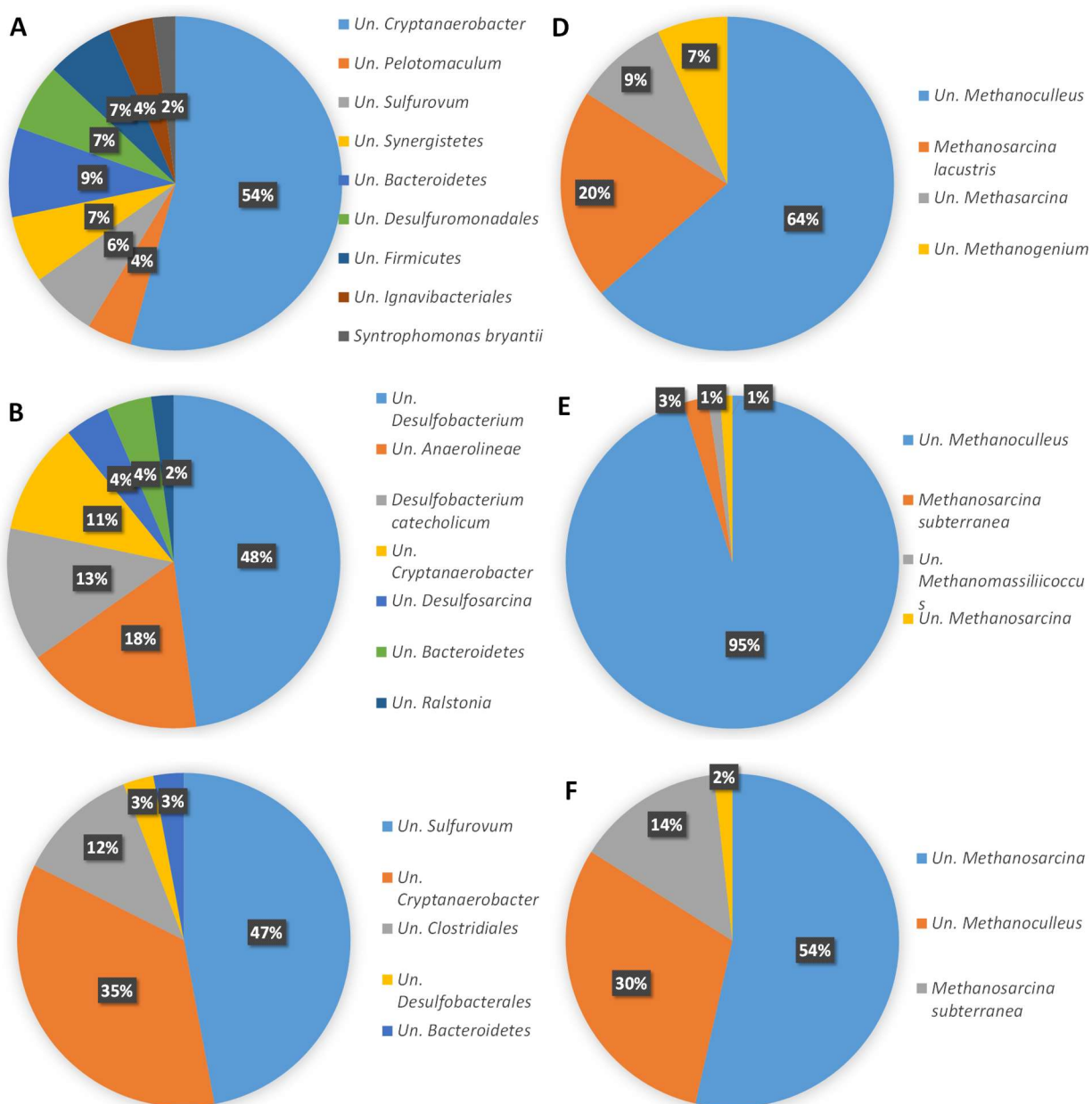


Figure 4. Distribution of bacteria (a, b, c) and archaea (d, e, f) detected in 16S rRNA gene clone libraries derived from propionate-amended SZ (a, d), SMTZ (b, e) and MZ (c, f) cultures, respectively. Un: Uncultured.

Therefore, *D. catecholicum* in the SMTZ enrichment may have degraded propionate and/or contributed to the utilization of H_2/CO_2 , formate or acetate that are formed during incomplete propionate conversion (Fig 3e). The phylotype related to *Cryptanaerobacter phenolicus* comprised

of 11% of all sequences in SMTZ culture. Its existence after several sub-culturing steps suggests that this bacterium is possibly involved in syntrophic propionate conversion (Fig 3e).

The majority of the bacterial clones retrieved from MZ enrichment culture showed 96-97% similarity (16S rRNA based) to *Sulfurovum aggregans*, belonging to *Epsilonproteobacteria*. This is followed by uncultured *Cryptanaerobacter* sp., representing 35% of the clones (Figure 4c and Table S3). *S. aggregans* is a mesophilic chemolithoautotrophic bacterium isolated from a deep-sea hydrothermal vent (Mino et al., 2014). This bacterium uses hydrogen as electron donor, CO₂ as carbon source and sulfur, thiosulfate or nitrate as electron acceptors, the ability to use sulfate as an electron acceptor has not been reported. *Epsilonproteobacteria* have been shown to be widely present in marine and terrestrial environments (Campbell et al., 2006) and detected in anoxic saline sediment incubations fed with different electron donors (Koizumi et al., 2005), suggesting that they can use a wide range of electron donors and acceptors and/or constitute relationships with other metabolic groups of bacteria (Campbell et al., 2006). The function of the *Sulfurovum* sp. in SZ and MZ cultures is hard to define based on the physiological characterization of the closest relative of this phylotype. Nevertheless, we cannot rule out the possibility that the *Epsilonproteobacteria* in our culture might have used hydrogen and acetate as electron donor. Starke et al (2016) have reported that an epsilonproteobacterial *Campylobacteriales* member featured the fastest and highest acetate incorporation in the microbial consortium containing benzene-degrading *Cryptanaerobacter*, *Pelotomaculum* species. Similarly, *Sulfurovum*-like species were suggested to be the hydrogen- or acetate-consuming syntrophic partners of *Pelotomaculum*, *Cryptanaerobacter* phylotypes during the degradation of benzene under sulfate-reducing conditions (Kleinstuber et al., 2008; Hermann et al., 2010). Epsilonproteobacterial species have also been observed in phenol-degrading methanogenic reactors, however their role remained unexplored (Ju and Zhang, 2014; Zhang et al., 2005; Fang et al., 2004). Therefore, *Sulfurovum* sp. in our culture might be responsible for hydrogen and/or acetate consumption. As sulfate reduction by *Sulfurovum* sp. has not been reported, the possible electron acceptor for *Sulfurovum* sp. in MZ culture may be oxidized sulfur compounds (e.g. sulfur, thiosulfate). These compounds might have been formed by the reaction of hydrogen sulfide and traces of oxygen that were possibly introduced into the bottle during sampling.

The majority of all archaeal clones obtained from 3 propionate-amended cultures (125 out of 184) affiliated with an uncultured *Methanoculleus*. 106 clones derived from the SZ and SMTZ cultures have 95-96% 16S rRNA based similarity to *M. taiwanensis* (Figure 4d, 4e and Table S4).

This uncultured *Methanoculleus* phylotype constituted 64% and 95% of the SZ and SMTZ clones, respectively. The MZ culture yielded 16 clones (29% of the MZ archaeal clones) highly related to *Methanoculleus marisnigri* (98% 16S rRNA based). This indicates that *Methanoculleus* formed close relationship with the propionate-converting bacteria in the cultures and consumed H₂ produced during incomplete propionate conversion (Fig 3d, 3e, 3f). The second most prevalent sequences (40 out of 184) in the archaeal clone libraries affiliated with *Methanosarcina* sp. (32 clones) and *Methanosarcina subterranea* (Figure 4 and Table S4). These clones were dominant in the MZ culture (38 out of 56) and in the minority in SMTZ culture (2 out of 84 clones). The observed complete propionate conversion to methane and CO₂ in the MZ culture strongly suggests that *Methanosarcina* sp. has been involved in acetate utilization in the cultures (Fig 3f).

Samples for FISH were collected at the beginning of the incubation period (day 16) only from MZ cultures. In Fig. S4, fluorescence micrographs of samples hybridized with probes specific for Archaea (red) and Bacteria (green) reveal cells with morphology resembling *Methanosarcina* and *Methanoculleus*. For the bacteria, no distinct morphotype could be recognized due to a lack of cultured representatives (Fig 3, Table 1).

6.4 Conclusions

Long term slurry incubations and sub-culturing resulted in highly enriched syntrophic cultures converting propionate and butyrate to methane. Propionate was converted completely by syntrophs, acetoclastic and hydrogenotrophic methanogens under methanogenic conditions, whereas acetate accumulation occurred during butyrate conversion and acetoclasts were not present in the enrichments. Microbial diversity analysis revealed dominance of *Syntrophomonas* sp. in butyrate-amended and *Cryptanaerobacter* sp. in propionate-amended enrichment cultures. The detected *Cryptanaerobacter* sp. may be a novel propionate-converting syntroph within the family *Peptococcaceae*, as it is only distantly related to its closest relatives. Low sulfate-amended butyrate- and propionate-converting SMTZ cultures contained sequences related to *Desulfobacteraceae* family members besides presumed syntrophs. Hydrogenotrophic methanogens *Methanogenium* and *Methanoculleus* acted as the main syntrophic partners in butyrate- and propionate-converting cultures, respectively, and acetoclastic methanogens consumed acetate especially in propionate-converting cultures. Acetate in the sulfate-amended cultures was consumed by sulfate reducers, pointing to a competitive advantage of sulfate reducers over methanogens in the presence of sulfate. Overall, the results of our study indicated the presence of

a functionally competent syntrophic community in the coastal marine sediment of Aarhus Bay, capable to degrade propionate and butyrate to methane under methanogenic conditions at different biogeochemical zones. Further attempts to obtain the novel marine propionate- and butyrate-converting syntrophs, *Syntrophomonas* sp. and *Cryptanaerobacter* sp., in defined cultures are in progress.

Acknowledgments

We gratefully acknowledge Monika Jarzembowska and Ton van Gelder (Wageningen University & Research) for technical assistance. This work has been funded by the Wimek Graduate School of Wageningen University & Research and the Darwin Center for Biogeosciences (the Netherlands).

Supplementary materials

Table S1. Overview of bacterial clones sequenced and their similarity with their closest relatives in butyrate-amended SZ, SMTZ and MZ cultures.

# of clones	%	Affiliation	Closest relative (accession no.)	Similarity (%)	Closest cultured relative (accession no.)	Similarity (%)
16	53	<i>Syntrophomonas bryantii</i>	<i>Syntrophomonas bryantii</i> strain CuCal (NR_104881.1)	99	<i>Syntrophomonas bryantii</i> strain CuCal (NR_104881.1)	99
3	10	Uncultured <i>Synergistetes</i>	Uncultured organism clone SBYC_5692 (JN447925.1)	96	<i>Aminobacterium colombiense</i> strain DSM 12261 (NR_074624.1)	88
1	3	Uncultured <i>Synergistetes</i>	Uncultured <i>Synergistaceae bacterium</i> clone Alk1-11C (HM992535.1)	98	<i>Thermovirga lienii</i> strain Cas60314 (NR_043522.1)	92
2	7	Uncultured <i>Sulfurovum</i>	Uncultured <i>bacterium</i> clone B7_10.3_1 (FJ1717139.1)	99	<i>Sulfurovum</i> sp. NBC37-1 strain NBC37-1 (NR_074503.1)	95
1	3	Uncultured <i>Sulfurovum</i>	Uncultured <i>bacterium</i> clone SW-25 (JX403042.1)	99	<i>Sulfurovum aggregans</i> strain Manchim33 (NR_126188.1)	97
4	13	Uncultured <i>Bacteroidetes</i>	Uncultured organism clone SBZL_705 (JN522195.1)	93	<i>Sunxiuqinia rutila</i> strain HG677 (NR_134207.1)	87
1	3	Uncultured <i>Bacteroidetes</i>	Uncultured organism clone SBZO_6057 (JN532989.1)	95	<i>Cytophaga fermentans</i> strain ATCC 19072 (NR_044696.1)	88
2	7	Uncultured <i>Anaerolineae</i>	Uncultured <i>Chloroflexi bacterium</i> clone RII-AN021 (JQ580400.1)	99	<i>Leptolinea tardivitalis</i> strain YMTK-2 (NR_040971.1)	91
13	42	Uncultured <i>Syntrophomonas</i>	<i>Syntrophomonas</i> sp. TB-6 (AM882624.1)	95	<i>Syntrophomonas</i> sp. TB-6 (AM882624.1)	95
8	26	Uncultured <i>Desulfobacter</i>	Uncultured <i>delta proteobacterium</i> clone 56 EDB2 (AM882624.1)	99	<i>Desulfobacter latus</i> strain DSM 3381 (NR_042142.1)	98
5	16	Uncultured <i>Anaerolineae</i>	Uncultured <i>bacterium</i> clone A6 (AY540497.1)	99	<i>Leptolinea tardivitalis</i> strain YMTK-2 (NR_040971.1)	91
3	10	Uncultured <i>Synergistetes</i>	Uncultured organism clone SBYC_5692 (JN447925.1)	97	<i>Aminobacterium colombiense</i> strain DSM 12261 (NR_074624.1)	88
2	6	Uncultured <i>Ignavibacteriales</i>	<i>Bacterium</i> YC-LK-LK12 (KP174649.1)	99	<i>Meliobacter roseus</i> strain P3M-2 (NR_074796.1)	95
23	77	<i>Syntrophomonas bryantii</i>	<i>Syntrophomonas bryantii</i> strain CuCal (NR_104881.1)	99	<i>Syntrophomonas bryantii</i> strain CuCal (NR_104881.1)	99
1	3	Uncultured <i>Syntrophomonas</i>	<i>Syntrophomonas</i> sp. TB-6 (AM882624.1)	95	<i>Syntrophomonas</i> sp. TB-6 (AM882624.1)	95
2	7	Uncultured <i>Bacteroidetes/Chlorobi</i>	Uncultured <i>bacterium</i> clone NF033 (JX391652.1)	96	<i>Owenweeksia hongkongensis</i> strain DSM 17368 (NR_074100.1)	88
1	3	Uncultured <i>Sulfurovum</i>	Uncultured <i>bacterium</i> clone B7_10.3_1 (FJ1717139.1)	99	<i>Sulfurovum aggregans</i> strain Manchim33 (NR_126188.1)	97
1	3	Uncultured <i>Ralstonia</i>	Uncultured <i>Ralstonia</i> sp. clone AtlantisII_d (HQ530524.1)	99	<i>Ralstonia insidiosa</i> strain AU2944 (NR_025242.1)	99
1	3	Uncultured <i>Bacteroidetes</i>	Uncultured <i>Cytophagales bacterium</i> clone TDNP_USbc97_180_1_43 (FJ516910.1)	99	<i>Mariniphaga anaerophila</i> strain Fu11-5 (NR_134076.1)	90

Table S2. Overview of archaeal clones sequenced and their similarity with their closest relatives in butyrate-amended SZ, SMTZ and MZ cultures.

	# of clones	%	Affiliation	Closest relative (accession no.)	Similarity (%)	Closest cultured relative (accession no.)	Similarity (%)
SZ	49	54	Methanogenium marinum	Methanogenium marinum strain AK-1 (NR_028225.1)	99	Methanogenium marinum strain AK-1 (NR_028225.1)	99
	23	26	Methanosarcina semesiae	Methanosarcina sp. MTP4 (CP009505.1)	99	Methanosarcina semesiae strain MD1 (NR_028182.1)	99
				Methanogenium organophilum strain DSM 3597 (NR_044721.1)	98	Methanogenium organophilum strain DSM 3597 (NR_044721.1)	98
	1	1	Methanogenium organophilum				
	16	18	Uncultured Methanoculleus	Uncultured archaeon clone MCSArc_B6 16S (EU591669.1)	94-96	Methanoculleus taiwanensis strain CYW4 (KM111599.1)	93-96
SMTZ	1	1	Uncultured Methanoculleus	Uncultured archaeon clone LGH02-C3-9-A-70	94	Methanoculleus taiwanensis strain CYW4 (KM111599.1)	92
	110	98	Methanogenium cariaci	Methanogenium cariaci (M59130.1)	99	Methanogenium cariaci (M59130.1)	99
	2	2	Methanosarcina lacustris	Methanosarcina sp. WH1 (CP009504.1)	100	Methanosarcina lacustris Z-7289 (CP009515.1)	99
MZ	20	63	Methanogenium marinum	Methanogenium marinum strain AK-1 (NR_028225.1)	99	Methanogenium marinum strain AK-1 (NR_028225.1)	99
	10	31	Methanosarcina subterranea	Methanosarcina sp. WH1 (CP009504.1)	100	Methanosarcina subterranea strain HC-2 (NR_134763.1)	99
	2	6	Uncultured Methanoculleus	Uncultured archaeon clone MCSArc_B6 16S (EU591669.1)	95	Methanoculleus taiwanensis strain CYW4 (KM111599.1)	95

Table S3. Overview of bacterial clones sequenced and their similarity with their closest relatives in propionate-amended SZ, SMTZ and MZ cultures.

# of clones	%	Affiliation	Closest relative (accession no.)	Similarity (%)	Closest cultured relative (accession no.)	Similarity (%)
SZ P1	10	Uncultured <i>Cryptanaerobacter</i>	Uncultured bacterium clone PLAB4 (AB701662.1)	98	<i>Cryptanaerobacter phenolicus</i> strain LR7.2 16S (NR_025757.1)	96
	6	Uncultured <i>Cryptanaerobacter</i>	Uncultured bacterium clone ARWH-BF05 (AB546032.1)	98	<i>Cryptanaerobacter phenolicus</i> strain LR7.2 16S (NR_025757.1)	92-96
	4	Uncultured <i>Cryptanaerobacter</i>	Uncultured bacterium clone A_Lac-1_35 (EU307089.1)	98	<i>Cryptanaerobacter phenolicus</i> strain LR7.2 16S (NR_025757.1)	95
	5	Uncultured <i>Cryptanaerobacter</i>	Uncultured <i>Firmicutes</i> bacterium clone NPA01 (AB853918.1)	98	<i>Cryptanaerobacter phenolicus</i> strain LR7.2 16S (NR_025757.1)	96
	3	Uncultured <i>Sulfurovum</i>	Uncultured bacterium clone B7_10.3_1 (FJ1717139.1)	99	<i>Sulfurovum aggregans</i> strain Monchim33 (NR_126188.1)	97
	3	Uncultured <i>Synergistetes</i>	Uncultured organism clone SBXZ_3880 (JN433166.1)	91	<i>Aminobacterium colombiense</i> strain DSM 12261 (NR_074624.1)	91
	3	Uncultured <i>Desulfuromonadales</i>	<i>Desulfuromusa bakii</i> strain Gyprop (NR_026175.1)	99	<i>Desulfuromusa bakii</i> strain Gyprop (NR_026175.1)	99
	2	Uncultured <i>Bacteroidetes</i>	Uncultured bacterium clone b49 (KJ578036.1)	99	<i>Cytophaga fermentans</i> strain ATCC 19072 (NR_044696.1)	90
	2	Uncultured <i>Bacteroidetes</i>	Uncultured bacterium clone Er-MLAYS-71 (EU542481.1)	99	<i>Prolixibacter bellariivorans</i> strain JCM 13498 (NR_113041.1)	89
	1	Uncultured <i>Firmicutes</i>	Uncultured <i>Gracilbacter</i> sp. clone 2_100_B10_b (JQ087078.1)	97	<i>Gracilbacter thermotolerans</i> strain JW/YIL-S1 (NR_115692.1)	97
	1	Uncultured <i>Firmicutes</i>	Uncultured bacterium clone B19CH1_61_65 (HF558553.1)	97	<i>Proteiniborus ethanologenes</i> strain GW (NR_044093.1)	87
	1	Uncultured <i>Firmicutes</i>	Uncultured bacterium clone HS006 (JX391342.1)	99	<i>Tissierella creatinini</i> strain BN11 (NR_104805.1)	94
	1	Uncultured <i>Pelotomaculum</i>	Uncultured bacterium clone 347_TC26_111 (KM251003.1)	99	<i>Pelotomaculum terephthalicum</i> strain JT (NR_040948.1)	95
	1	Uncultured <i>Pelotomaculum</i>	Uncultured bacterium clone JI (AB091325.1)	96	<i>Pelotomaculum isophthalicum</i> strain JI (NR_041320.1)	96
	1	Uncultured <i>Ignavibacteriales</i>	Uncultured <i>Ignavibacteriales</i> bacterium clone HYH151_Bac16s_AQDS01_01_B01 (KU324269.1)	96	<i>Melioribacter roseus</i> strain P3M-2 (NR_074796.1)	84
	1	Uncultured <i>Ignavibacteriales</i>	Uncultured <i>Chlorobi</i> bacterium clone FI-ANO13_1 (JQ579954.1)	99	<i>Melioribacter roseus</i> strain P3M-2 (NR_074796.1)	0.9
	1	Uncultured <i>Syntrophomonas bryantii</i>	<i>Syntrophomonas bryantii</i> strain CuCal (NR_104881.1)	99	<i>Syntrophomonas bryantii</i> strain CuCal (NR_104881.1)	99
SMTZ P2	22	Uncultured <i>Desulfobacterium</i>	Uncultured <i>Desulfobacteraceae</i> clone TDNP_USbc97_20_4_80 (FJ516922.1)	99	<i>Desulfobacterium indolicum</i> strain In04 (NR_028897.1)	93-94
	7	Uncultured <i>Anaerolineae</i>	Uncultured <i>Chloroflexi</i> bacterium clone RII-ANO21 (JQ580400.1)	99	<i>Leptolinea tardivitalis</i> strain YMTK-2 (NR_040971.1)	91
	6	Uncultured <i>Desulfobacterium catecholicum</i>	[<i>Desulfobacterium</i>] <i>catecholicum</i> strain NZva20 (NR_028895.1)	99	[<i>Desulfobacterium</i>] <i>catecholicum</i> strain NZva20 (NR_028895.1)	99
	5	Uncultured <i>Cryptanaerobacter</i>	Uncultured bacterium clone A_Lac-1_35 (EU307089.1)	98	<i>Cryptanaerobacter phenolicus</i> strain LR7.2 (NR_025757.1)	95
	2	Uncultured <i>Bacteroidetes</i>	Uncultured bacterium clone Er-MLAYS-71 (EU542481.1)	99	<i>Prolixibacter denitrificans</i> strain MIC1-1 (NR_137212.1)	89
	1	Uncultured <i>Desulfosarcina</i>	Uncultured delta proteobacterium clone 81 EDB3 (AM882635.1)	99	<i>Desulfosarcina variabilis</i> strain Montpellier (NR_044680.1)	93
	1	Uncultured <i>Desulfosarcina</i>	Uncultured delta proteobacterium clone 19 EDB1 (AM882602.1)	99	<i>Desulfosarcina variabilis</i> strain Montpellier (NR_044680.1)	98
	1	Uncultured <i>Anaerolineae</i>	Uncultured <i>Chloroflexi</i> bacterium clone RII-ANO43 (JQ580422.1)	99	<i>Leptolinea tardivitalis</i> strain YMTK-2 (NR_040971.1)	91
	1	Uncultured <i>Desulfuromonadales</i>	<i>Pelobacter</i> sp. SF893, complete genome (CP015519.1)	96	<i>Pelobacter</i> sp. SF893, complete genome (CP015519.1)	96
	1	Uncultured <i>Ralstonia</i>	Uncultured <i>Ralstonia</i> sp. clone AtlantisII_d (HQ530524.1)	99	<i>Ralstonia insidiosa</i> strain ATCC 49129 (CP016023.1)	99
MZ P3	14	Uncultured <i>Sulfurovum</i>	Uncultured bacterium clone B7_10.3_1 (FJ1717139.1)	99	<i>Sulfurovum aggregans</i> strain Monchim33 (NR_126188.1)	96-97
	7	Uncultured <i>Cryptanaerobacter</i>	Uncultured bacterium clone A_Lac-1_35 (EU307089.1)	98	<i>Cryptanaerobacter phenolicus</i> strain LR7.2 (NR_025757.1)	95
	3	Uncultured <i>Cryptanaerobacter</i>	Uncultured bacterium clone: PLAB4 (AB701662.1)	98	<i>Cryptanaerobacter phenolicus</i> strain LR7.2 (NR_025757.1)	96
	2	Uncultured <i>Clostridiales</i>	Uncultured bacterium clone 300_TC38_31 (KM250983.1)	98	<i>Gracilbacter thermotolerans</i> strain JW/YIL-S1 (NR_115692.1)	97
	2	Uncultured <i>Cryptanaerobacter</i>	Uncultured bacterium clone: ARWH-BF05 (AB546032.1)	98	<i>Cryptanaerobacter phenolicus</i> strain LR7.2 (NR_025757.1)	96
	1	Uncultured <i>Sulfurovum</i>	Uncultured bacterium clone B1_10.3_2 (FJ1717148.1)	99	<i>Sulfurovum aggregans</i> strain Monchim33 (NR_126188.1)	97
	1	Uncultured <i>Sulfurovum</i>	Uncultured bacterium clone T3-1_246 (KX097819.1)	99	<i>Sulfurovum aggregans</i> strain Monchim33 (NR_126188.1)	98
	1	Uncultured <i>Bacteroidetes</i>	Uncultured bacterium clone N0047 (JX391483.1)	94	<i>Tangfeifania diversioriginum</i> strain G22 (NR_134211.1)	93
	1	Uncultured <i>Desulfobacteriales</i>	Uncultured bacterium zdt-33i5 clone zdt-33i5 (AC150251.1)	96	<i>Desulfatiferula olefinivorans</i> strain LM2801 (NR_043971.1)	86
	1	Uncultured <i>Clostridiales</i>	Uncultured bacterium clone B19CH1_61_65 (HF558553.1)	97	<i>Acetomicrobium faecale</i> strain DSM 20678 (NR_117173.1)	87
	1	Uncultured <i>Clostridiales</i>	Uncultured bacterium clone LJ142-3i10 (FJ672228.1)	98	<i>Garcilla nitratireducens</i> strain Met 79 (NR_025688.1)	91

Table S4. Overview of archaeal clones sequenced and their similarity with their closest relatives in propionate-amended SZ, SMTZ and MZ cultures.

# of clones	%	Affiliation	Closest relative (accession no.)	Similarity (%)	Closest cultured relative (accession no.)	Similarity (%)
SZ P1	25	57	Uncultured <i>Methanoculleus</i>		<i>Methanoculleus taiwanensis</i> strain CYW4 (NR_134762.1)	96
	9	20	<i>Methanosarcina lacustris</i>		<i>Methanosarcina lacustris</i> Z-7289 (CP009515.1)	99
	3	7	Uncultured <i>Methanogenium</i>		<i>Methanogenium cariaci</i> 16S ribosomal RNA (M59130.1)	98
	2	5	Uncultured <i>Methanosarcina</i>		<i>Methanosarcina lacustris</i> Z-7289 (CP009515.1)	99
	1	2	Uncultured <i>Methanosarcina</i>		<i>Methanosarcina lacustris</i> Z-7289 (CP009515.1)	91
	1	2	Uncultured <i>Methanosarcina</i>		<i>Methanosarcina lacustris</i> Z-7289 (CP009515.1)	92
	1	2	Uncultured <i>Methanoculleus</i>		<i>Methanoculleus taiwanensis</i> strain CYW4 (NR_134762.1)	96
	1	2	Uncultured <i>Methanoculleus</i>		<i>Methanoculleus taiwanensis</i> strain CYW4 (NR_134762.1)	95
	1	2	Uncultured <i>Methanoculleus</i>		<i>Methanoculleus taiwanensis</i> strain CYW4 (NR_134762.1)	95
			Uncultured archaeon clone Zolletone_Spring_Propane_48 (GU453565.1)	99		
SMTZ P2	78	93	Uncultured <i>Methanoculleus</i>		<i>Methanoculleus</i> sp. 1H2c2 strain: 1H2c2 (LC183829.1)	95-96
	2	2	Uncultured <i>Methanoculleus</i>		Uncultured <i>Methanoculleus</i> sp. clone D059111C04 (GU179436.1)	98
	2	2	<i>Methanosarcina subterranea</i>		<i>Methanosarcina</i> sp. WH1, complete genome (CP009504.1)	99
	1	1	Uncultured <i>Methanomassiliicoccus</i>		Uncultured archaeon clone MD-178-10-3261_T2-P_5900_06A08 (JQ817907.1)	93
	1	1	Uncultured <i>Methanosarcina</i>		<i>Methanosarcina</i> sp. M15 (KT799840.1)	96
					<i>Methanoculleus</i> sp. 1H2c2 strain: 1H2c2 (LC183829.1)	99
MZ P3	30	54	Uncultured <i>Methanosarcina</i>		<i>Methanosarcina</i> sp. WH (CP009504.1)	99
	12	21	Uncultured <i>Methanoculleus</i>		Uncultured <i>Methanoculleus</i> sp. clone D059111C04 (GU179436.1)	98
	8	14	<i>Methanosarcina subterranea</i>		<i>Methanosarcina subterranea</i> strain HC-2 (NR_134763.1)	99
	3	5	Uncultured <i>Methanoculleus</i>		<i>Methanoculleus marisnigri</i> strain JR1 (NR_074174.1)	98
	1	2	Uncultured <i>Methanoculleus</i>		Uncultured archaeon clone PL-9A5 (AY570665.1)	97
	1	2	Uncultured <i>Methanoculleus</i>		<i>Methanoculleus palmolei</i> strain DSM 4273 (NR_028253.1)	98
	1	2	Uncultured <i>Methanomassiliicoccus</i>		Uncultured archaeon clone SAT_386 (FJ655657.1)	83
					<i>Methanosarcina subterranea</i> strain HC-2 (NR_134763.1)	99
					<i>Methanoculleus marisnigri</i> strain JR1 (NR_074174.1)	98
					<i>Methanosarcina subterranea</i> strain HC-2 (NR_134763.1)	99

Figure S1. FISH images with probes EUB338 mix (green, Bacteria) and ARC915 (red, Archaea), from the butyrate-amended SZ culture after 16 days of cultivation. In (a), arrows indicate the morphologies possibly related with the clonal analysis data. Cells of *Methanoculleus* sp. are little coccoids, *Methanogenium* sp. are big irregular cocci and *Synthrophomonas* sp. are rods. In (b) DAPI staining of the same microscopic field demonstrates the probes coverage of total cells. Scale bar is 5 μ m.

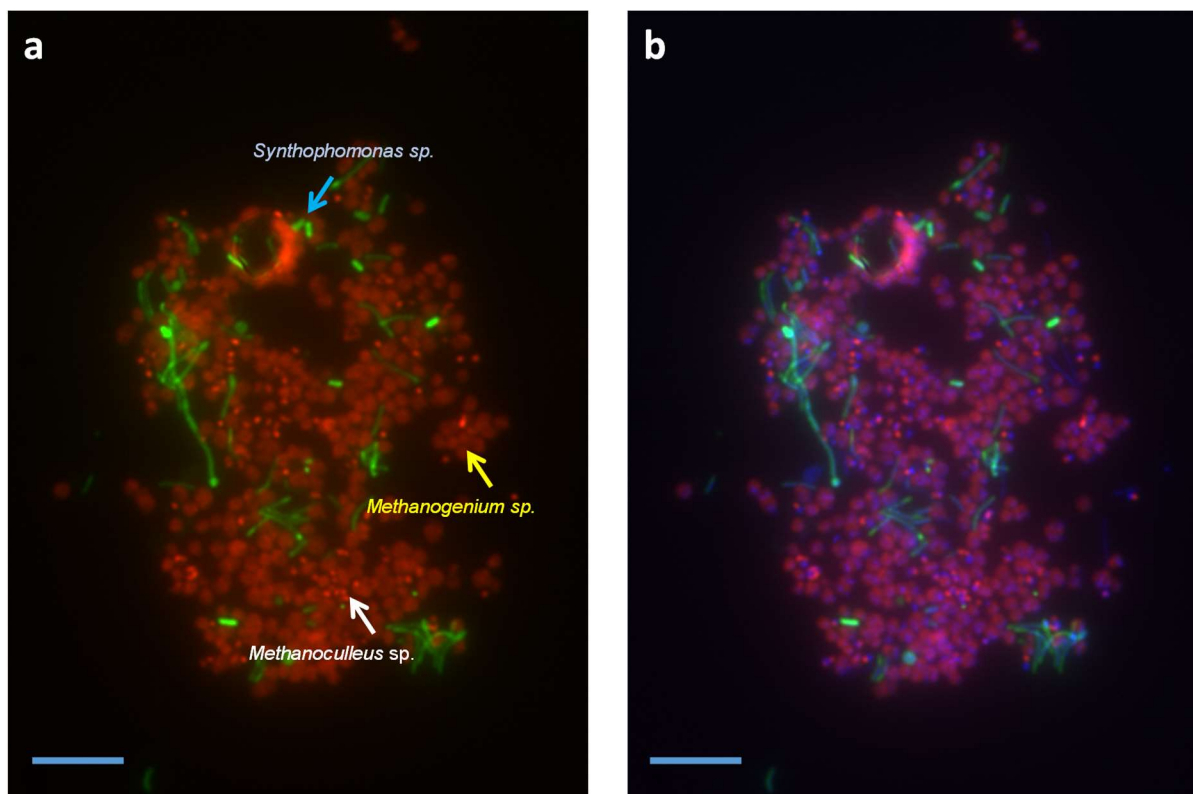


Figure S2. FISH images with probes EUB338 mix (green, Bacteria) and ARC915 (red, Archaea), from the butyrate-amended SMTZ culture after 16 days of cultivation. In (a), arrows indicate morphologies possibly related with the clonal analysis data. In (b), DAPI staining of the same microscopic field demonstrates the probes coverage of total cells. Scale bar is 5 μm .

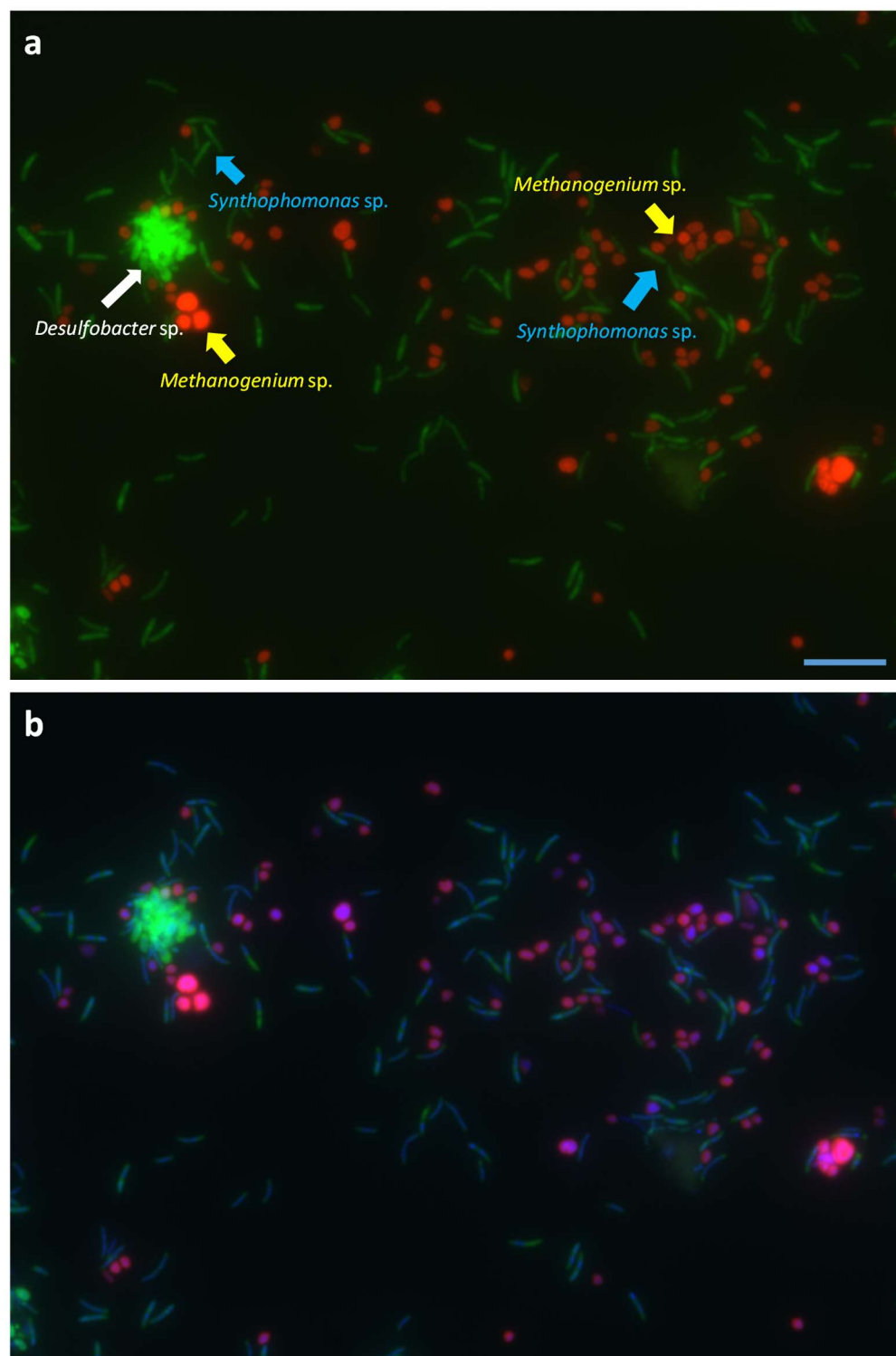


Figure S3. FISH images with probes EUB338 mix (green, Bacteria) and ARC915 (red, Archaea), from the butyrate-amended MZ culture after 16 days of cultivation. In all the images, arrows indicate the morphologies possibly related with the clonal analysis data. In (a) a general overview of the culture, (b) a cluster of *Syntrophomonas* and *Methanosarcina* cells, (c) close association between *Syntrophomonas* and *Methanogenium* cells, (d) DAPI staining of the same microscopic field shown in figure S3c. Scale bar 5 μ m.

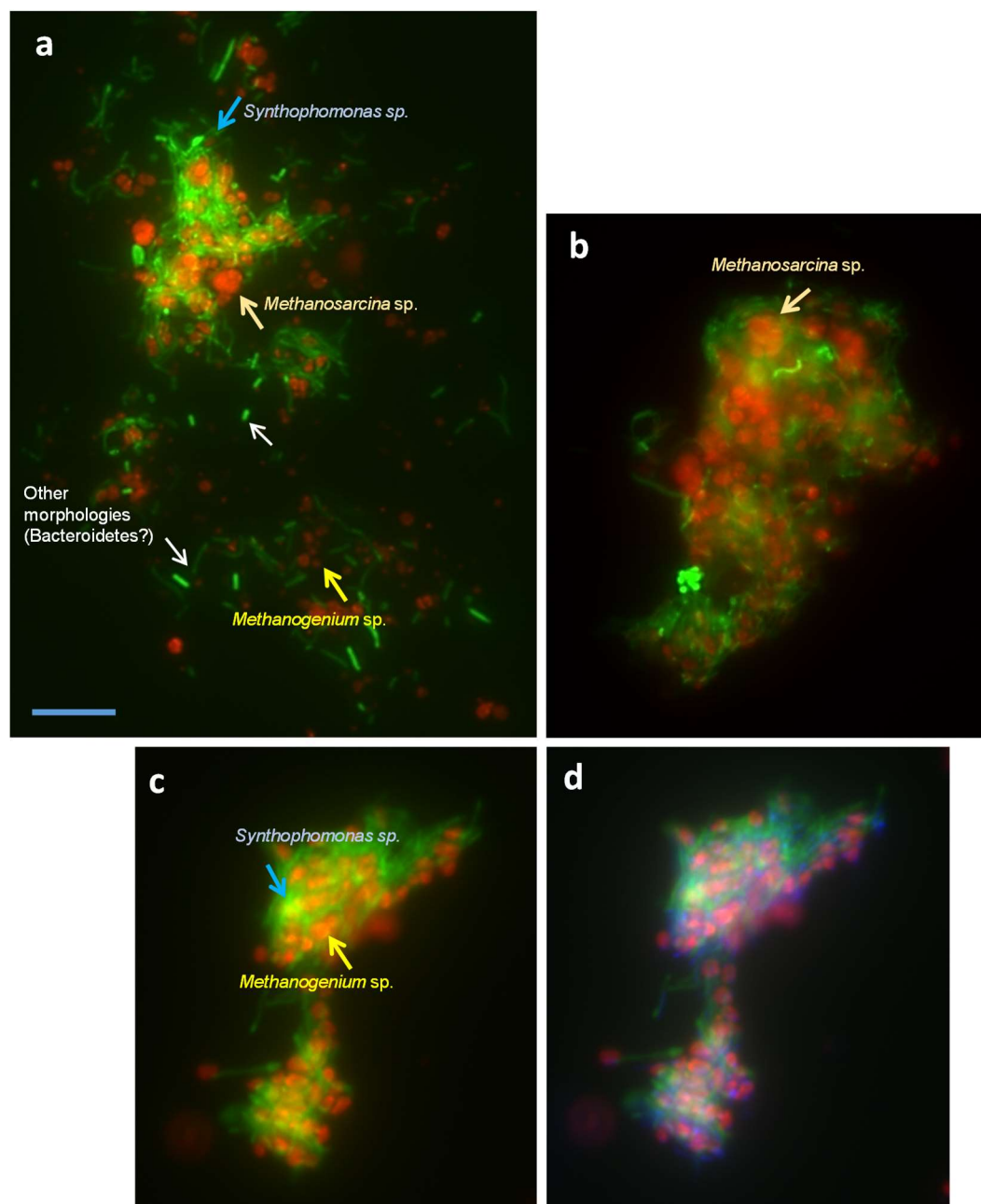
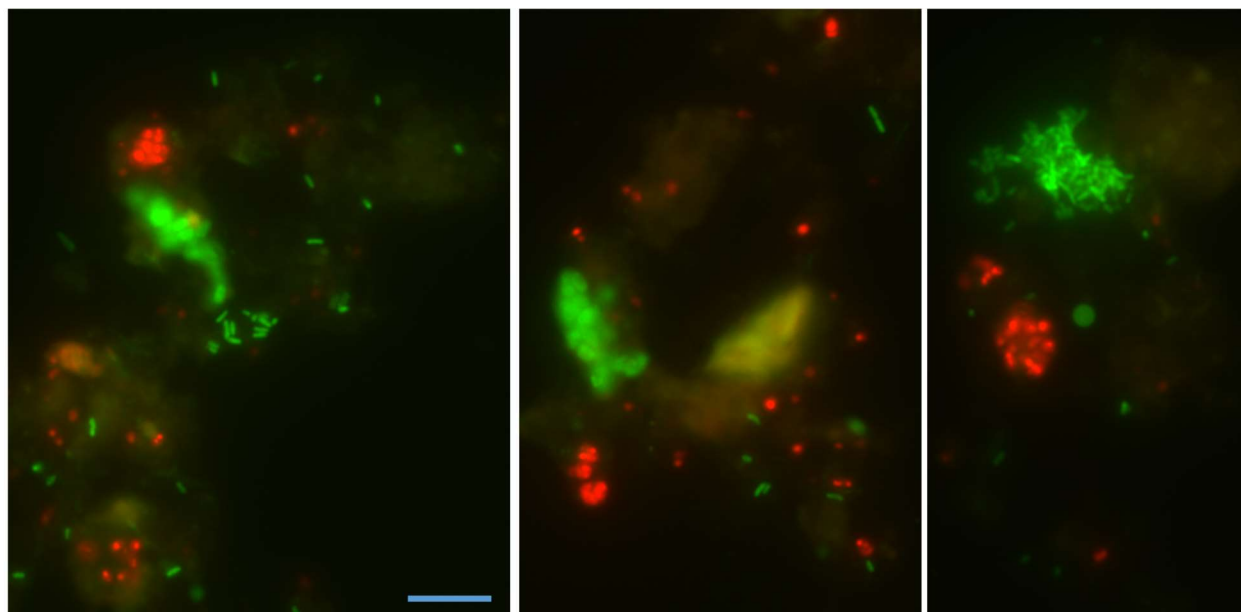


Figure S4. FISH images with probes EUB338 mix (green, Bacteria) and ARC915 (red, Archaea), from the propionate-amended MZ culture after 16 days of cultivation. Scale bar 5 μ m.



Chapter 7

General Discussion

Derya Özüölmez

Coastal marine ecosystems receive regular inputs of organic matter and nutrients from primary production of phytoplanktons, rivers, coastal erosion, and the atmosphere (Jørgensen, 1982). In coastal marine sediments, the oxic zone is a thin layer (few mm or cm) due to the rapid aerobic mineralization and therefore oxygen is limited. Because of that the major part of the organic matter is degraded in the anoxic part of the sediment involving physiologically different microbes. Decomposition of organic matter is carried out by combined action of different metabolic groups of bacteria, including primary fermenters, secondary fermenters, bacteria that reduce different electron acceptors such as nitrate, iron, sulfate or carbon dioxide and at least two types of methanogenic archaea. Major intermediates of anaerobic decomposition of organic matter such as acetate, propionate, butyrate and H_2 are the most important electron donors for sulfate-reduction in marine environments. Thus sulfate-reducing bacteria (SRB) contribute significantly to the mineralization of organic matter as well as to the Earth's sulfur cycle (Jørgensen, 1982; Sørensen et al., 1981). It is estimated that 25-50% of the organic carbon is mineralized through sulfate reduction, which makes sulfate an important electron acceptor in anoxic part of the marine sediments (Jørgensen, 1982). The conversion of propionate and butyrate in deep sulfate-depleted sediments is critical due to the lack of electron acceptors other than CO_2 . For complete degradation of propionate or butyrate, syntrophic cooperation of one acetogenic bacteria and two methanogenic archaea is required (Schink and Stams, 2013) (**Chapter 1**). Syntrophic associations between propionate- or butyrate-degrading bacteria and methanogens contribute substantially to methane production in marine sediments (Kendall et al., 2006). Previous studies have shown SRB predominance in high-sulfate and methanogen predominance in low-sulfate environments (Ward and Winfrey, 1985; Widdel, 1988; Cappenberg, 1974; Mountfort and Asher, 1979). However, several other studies demonstrated that methanogenesis occurs simultaneously with sulfate reduction in sulfate-containing anoxic sediments (Oremland and Taylor, 1978; Oremland and Polcin, 1982; Oremland et al., 1982a, 1982b, 1987; Kiene et al., 1986; Oremland et al., 1988; Wang and Lee, 1995) and active SRB in methane-rich anoxic sediments (Jørgensen, 1978; Thomsen et al., 2001; Leloup et al., 2007, 2009).

7.1 Conversion of propionate and butyrate in marine sediments

7.1.1 Propionate and butyrate conversion coupled to sulfate reduction

The effect of sulfate on butyrate and propionate conversion was studied in **chapter 3** and **4**. The sulfate in all slurries was rapidly consumed showing that sulfate reduction is a dominant process

for butyrate and propionate conversion in Aarhus Bay sediments. Rapid sulfate reduction in methane zone sediment slurries indicates an active sulfate-reducing community in the sulfate-depleted sediments (Jørgensen, 1978; Thomsen et al., 2001; Leloup et al., 2007, 2009). These findings confirm findings of previous studies showing the presence of active SRB at similar cell numbers in the upper and lower parts of the coastal marine sediments of Limfjorden and Aarhus Bay, Denmark (Leloup et al., 2009; Thomsen et al., 2001; Jørgensen, 1978) and deep-sea sediment (Leloup et al., 2007).

Butyrate and propionate can only be metabolized by syntrophic associations of acetogenic bacteria and hydrogen- and acetate-consuming methanogens in the absence of sulfate (Muyzer and Stams, 2008). The results obtained in the **chapter 3 and 4** show that the absence of sulfate causes a delay in butyrate and propionate conversion, which requires cooperation of different microorganisms (McInerney et al., 2008). Acetate, which was accumulated by syntrophic conversion of propionate and butyrate, was consumed rapidly and methane was produced concomitantly. This suggests the presence of active syntrophic propionate- and butyrate-converting microorganisms and their ability to form consortia with hydrogen and acetate utilizing methanogens throughout the sediment column. Our results are consistent with previous studies that showed evidence of butyrate- and propionate-converting syntrophs in sulfate-containing marine sediments (Kendall et al., 2006; Kendall and Boone, 2006a).

The trend of product formation and consumption during butyrate and propionate conversions was considerably different in high (20 mM) and low (3 mM) sulfate amended SMTZ slurries at 25°C. High concentration of sulfate caused low and stable methane yields despite a sudden methane increase at the end of the incubation period (**Chapter 3 and 4**). Lower methane concentrations (339-4183 $\mu\text{mol/slurry}$) in high sulfate amended slurries as compared to low sulfate amended slurries (15509-73569 $\mu\text{mol/slurry}$) along slurry incubations indicates possible sulfide inhibition on methanogenesis (Pender et al., 2004; O'Flaherty et al., 1998; Shin et al., 1995). Under low sulfate condition, however, methane concentrations were relatively high, especially during butyrate conversion. The results obtained from the **chapters 3 and 4** indicate that low sulfate concentration stimulates the whole microbiome; both sulfate reduction and methanogenesis occur in Aarhus Bay sediments.

7.1.2 The effect of temperature on propionate and butyrate conversion

Different temperatures have an impact on butyrate and propionate conversion in Aarhus Bay sediments. The results of **chapter 3 and 4** show that at low incubation temperature (10°C) butyrate and propionate conversion is very slow, with low sulfate consumption and high acetate accumulation. This result is in line with previous experiments showing decreased sulfate reduction rates at temperatures below 25°C in sulfate-amended sediment slurries (Weston and Joye, 2005). On the other hand, efficient acetate consumption with simultaneous methane production in sulfate-free slurries at 25°C has also been shown by Roussel et al (2015).

Sulfate-methane transition zone is located between sulfate and methane zones and characterized by low sulfate and methane concentrations. In this sediment zone, methane and sulfate are mutually depleted by the microbial anaerobic oxidation of methane (AOM) (Sultan et al., 2016; Iversen and Jørgensen, 1985). Methanogenesis during butyrate and propionate conversion at 10°C in high-sulfate amended SMTZ slurries was relatively low and fluctuating (**Chapter 3 and 4**). Although high sulfate and sulfide concentrations can be the reason of low methane yields, the fluctuating methane production during butyrate conversion and total methane consumption during propionate conversion can be related to anaerobic oxidation of methane (AOM). AOM has been reported to occur in SMT zone of Aarhus Bay (Webster et al., 2011; Aquilina et al., 2010; Thomsen et al., 2001; Dale et al., 2008). Since the incubation temperature (10°C) resembles the *in situ* temperature of Aarhus Bay (Dale et al., 2008) the microbial communities residing in SMTZ might be involved in oxidation of the produced methane.

7.2 Microbial community dynamics in propionate and butyrate conversion

Microbial communities in the butyrate and propionate converting enrichment slurries show different dynamics throughout the several biogeochemical zones (SZ, SMTZ, MZ).

7.2.1 Bacterial community at different sulfate concentrations

The sulfate concentrations caused a variation of presence of intact polar membrane lipids (IPL), which are the building blocks of cell membranes and representative of living biomass, in butyrate-converting slurries (**Chapter 5**), although the microbial composition changed considerably both in propionate and butyrate-converting slurries (**Chapter 3 and 4**). The enriched bacteria in the incubations with sulfate were similar when butyrate and propionate were used as substrate. These

were mainly the sulfate reducers belonging to *Desulfobacteraceae* and *Desulfobulbaceae* (Figure 1 and 2). *Desulfosarcina* and *Desulfobacterium* dominated the butyrate-converting slurries, whereas *Desulfosarcina*, *Desulfobulbus* and *Desulforhopalus* were the main SRB in propionate-converting slurries. The increase in the relative abundance of *Desulfobacteraceae* and *Desulfobulbaceae* in SZ, SMTZ and MZ sediment slurries suggests the presence of sulfate reducers throughout the anoxic sediment column. Our findings confirm the reports showing the abundance and the activity of sulfate-reducing bacteria in Aarhus Bay sediments at Station 1 (Leloup et al. 2009) and Station 6 (Sahm et al., 1999), in Kysing Fjord, Denmark, (Thomsen et al., 2001) and Mariager Fjord, Denmark (Wagner et al., 2005). The ability of some SRB to grow fermentatively may explain their abundance in sulfate-depleted sediments and the sudden increase in their relative abundance in sulfate-amended methane zone slurries.

The absence of sulfate causes a change in the enriched microbial community. *Syntrophomonas* increased in relative abundance in the butyrate-converting sediment slurries, whereas *Cryptanaerobacter* dominated the propionate-converting sediment slurries. *Syntrophomonas* is a known butyrate-degrading syntrophic specialist that grows in close association with methanogens and other hydrogen- and/or formate-utilizing microorganisms (Plugge et al., 2011; Sousa et al., 2009; Oude Elferink et al., 1994). The fact that the relative abundance of *Syntrophomonas* was also high in some sulfate-containing slurries and kept the high abundance after several transfers (**Chapter 6**), lead us to speculate that the presence of sulfate can prevent *Syntrophomonas* species to be the dominant bacterial group, but does not inhibit their involvement in butyrate conversion, suggesting a role of syntrophic butyrate conversion even in the presence of sulfate. Coexistence of *Syntrophomonas* spp. and sulfate reducers were reported during butyrate (Struchtemeyer et al., 2011; Visser et al., 1993) and oleate and palmitate (Sousa et al., 2009) degradation in the presence of sulfate.

The genus *Cryptanaerobacter* belongs to the family *Peptococcaceae*. As *Cryptanaerobacter* dominated the slurries that contain low or no sulfate (**Chapter 4**) (Figure 7.2) and the enrichment cultures after subculturing process (**Chapter 6**), we hypothesize that a novel species of this bacterium might have the capability to convert propionate in syntrophy with hydrogenotrophic methanogens. The idea behind this hypothesis is based on ; i) the isolation of *C. phenolicus* from a methanogenic consortium, ii) the syntrophic lifestyle of its closest cultured relatives and iii) the presence of propionate as a sole carbon source in the slurries.

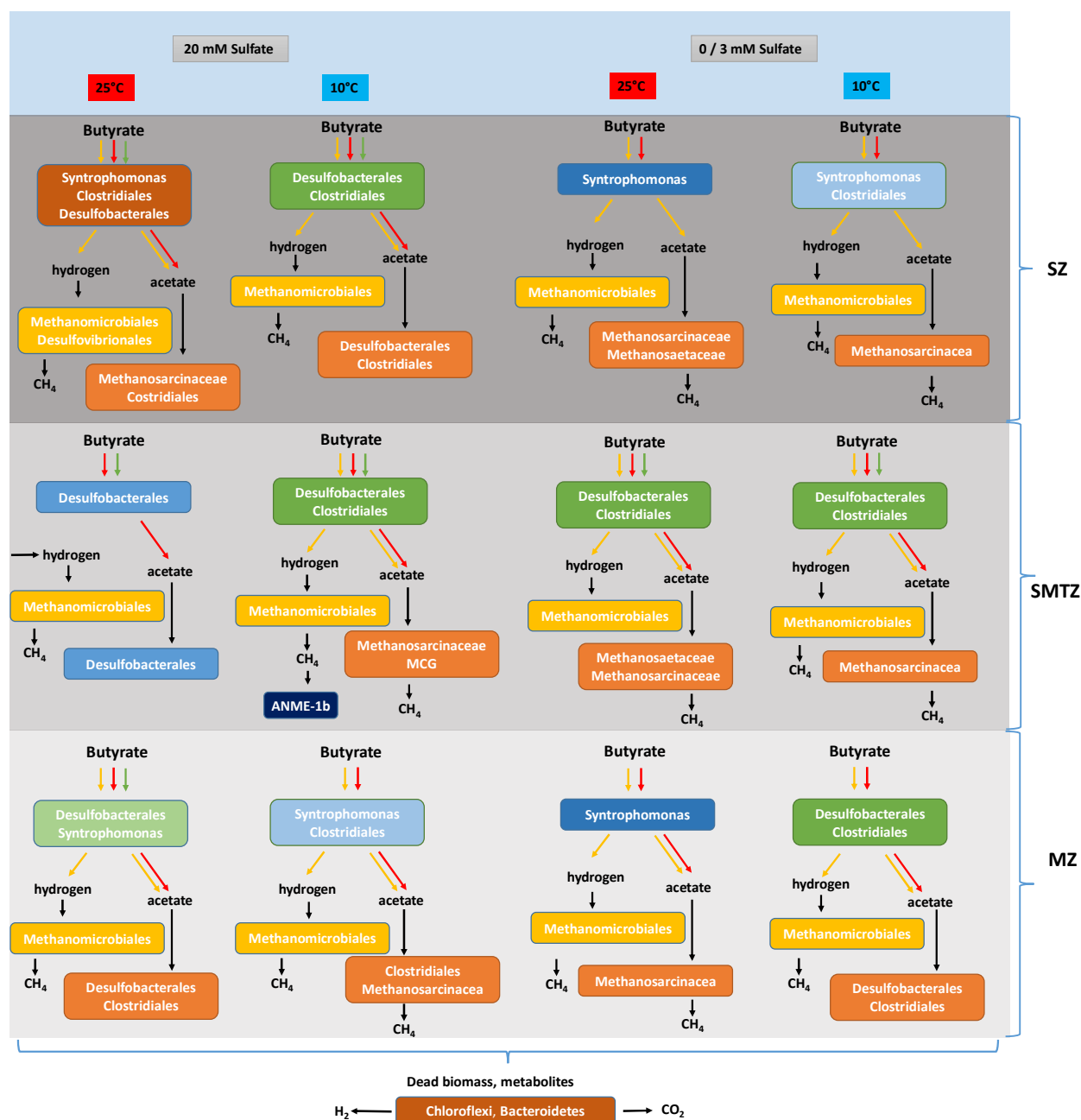


Figure 1. Overview of butyrate conversion and the proposed responsible microbial community at different temperatures and sulfate concentrations in enrichment slurries of sulfate, sulfate-methane transition and methane zone sediment of Aarhus Bay. Possible butyrate conversion pathways are shown with different coloured arrows; red arrows represent incomplete butyrate conversion coupled to sulfate reduction, green arrows represent complete butyrate conversion coupled to sulfate reduction, yellow arrows represent syntrophic butyrate conversion. Horizontal arrow represents the substrates originate from fermentation, decomposition of dead biomass and/or metabolites.

Additionally, the hypothesis is supported with the statistical analysis showing positive correlation of the order *Clostridiales* with methane production and temperature. *Desulfobacteraceae* was dominant under sulfate-free and low-sulfate conditions during butyrate and propionate conversion (**Chapter 4**). This result agrees with the previous studies reporting that non-sulfate reducing, syntrophic members of *Desulfobacteraceae* involve in butyrate (Kendall et al., 2006) and benzene degradation (Ulrich and Edwards, 2003). Despite the importance of *Syntrophobacter* in syntrophic propionate conversion (Plugge et al., 2011) in shallow methanogenic sediments (Lloyd et al., 2006; McInerney et al., 2008), we did not detect *Syntrophobacter* in Aarhus Bay sediment or in the sediment slurries. Similarly, Leloup et al. (2009) reported only very low abundance of *Syntrophobacter*-like sequences at Station 1 in Aarhus Bay. The results of this thesis illustrate the significance of metabolic flexibility of microorganisms under changing conditions such as temperature, electron acceptor availability, the presence/absence of partner organisms.

7.2.2 Bacterial community at different temperatures

The most obvious difference in the microbial community composition at high and low temperature is the dominance of *Cryptanaerobacter* at 25°C, and *Desulfobacteraceae* (*Desulfofaba*), especially *Desulfobulbaceae* members (*Desulfobulbus*, *Desulforhopalus*) at 10°C during propionate conversion. Likewise, *Desulfobulbaceae* and some *Desulfobacteraceae* members are negatively correlated with temperature (**Chapter 4**). Incubation at low temperature had also an impact on IPL composition in propionate-converting slurries (**Chapter 5**). In butyrate-converting slurries, there is no clear difference in microbial community between different temperatures. However, *Clostridiales* had higher relative abundance at 10°C regardless of the sulfate concentration and the sediment depth. *Clostridiales* are commonly found in surface and deep marine sediments, soils and methanogenic environments (Fry et al., 2008; Parkes et al., 2014). As 10°C resembles the *in situ* temperature, our results provide support for possible involvement of *Clostridiales* in butyrate conversion in marine sediments.

7.2.3 Bacterial community at different sediment depth

Pyrosequencing of 16S rRNA gene amplicons of Aarhus Bay sediment revealed the dominance of the *Desulfobacteraceae* in the SMTZ, accounting for 79% of the sequences (**Chapter 3 and 4**) in the original sediment. This result shows that the microbial community in the SMTZ is distinct from the

microbial community in the SZ and MZ. This is in accordance with previous studies documenting the high abundance of *Desulfobacteraceae* in SMTZ of marine sediments (Wagner et al., 2005).

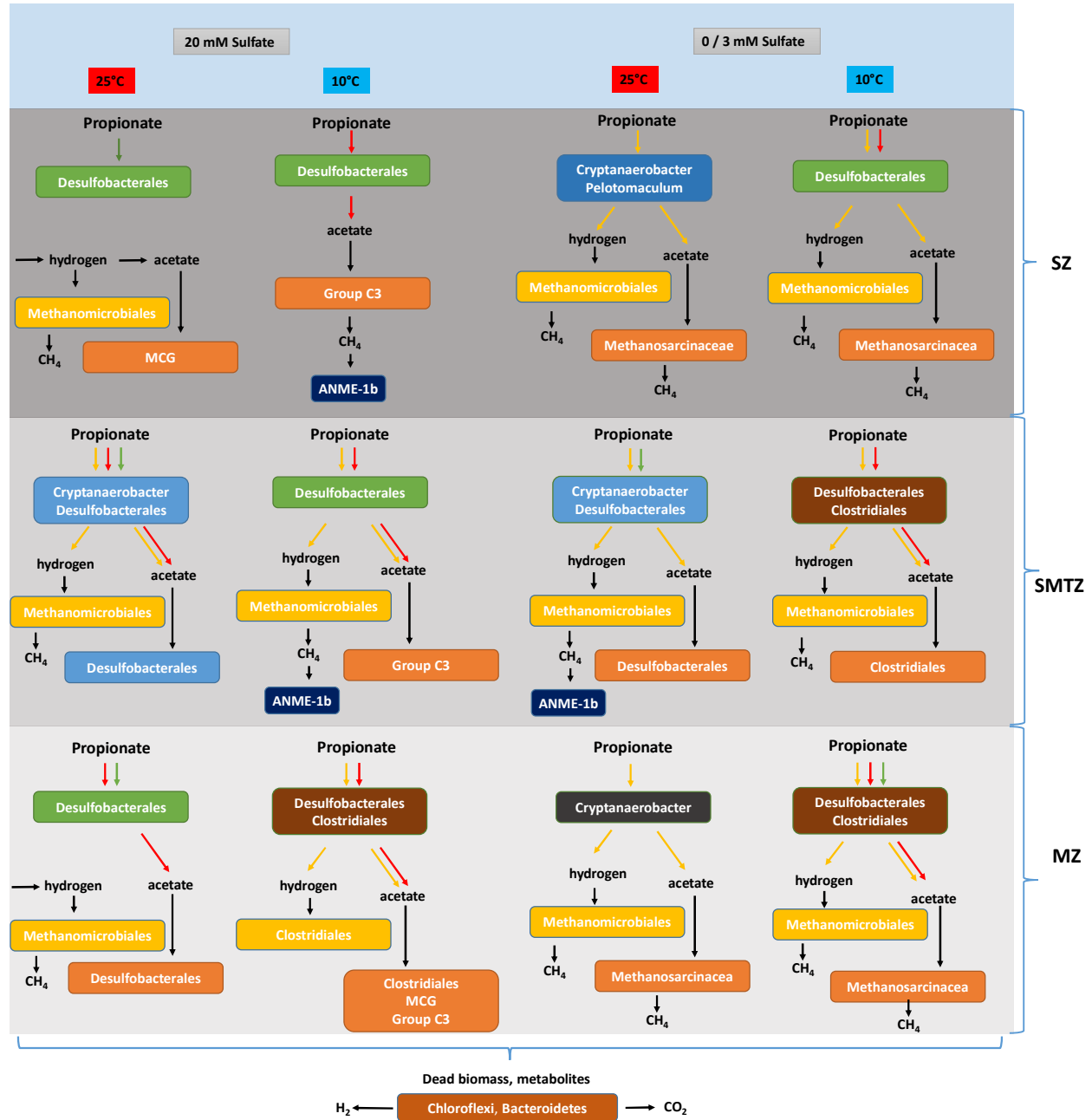


Figure 2. Overview of propionate conversion and the proposed responsible microbial community at different temperatures and sulfate concentrations in enrichment slurries of sulfate, sulfate-methane transition and methane zone sediment of Aarhus Bay. Possible propionate conversion pathways are shown with different coloured arrows; red arrows represent incomplete propionate conversion coupled to sulfate reduction, green arrows represent complete propionate conversion coupled to sulfate reduction, yellow arrows represent syntrophic propionate conversion. Horizontal arrow represents the substrates originate from fermentation, decomposition of dead biomass and/or metabolites.

Pyrosequencing showed that *Desulfobacteraceae* was still present in the SMTZ enrichment slurries after long term incubation and therefore might have involved in propionate and butyrate conversion at high and low sulfate concentrations. In **Chapter 6**, *Syntrophomonas* became dominant in the low sulfate containing SMTZ slurry at 25°C after several transfers, and *Desulfobacter latus*, belonging to *Desulfobacteraceae*, was the syntrophic partner of *Syntrophomonas*. On the other hand, the dominant propionate-converting organism at the same incubation condition was still a member of *Desulfobacteraceae* (**Chapter 6**). This suggests that *Syntrophomonas* can effectively compete with sulfate reducers for butyrate in the presence of sulfate.

The presence of *Desulfobacteraceae*, including acetate-degrading sulfate reducers, at 10°C might be associated with their syntrophic interaction with methane-oxidizing archaea, similar to the *in situ* condition (Knittel and Boetius, 2009; Boetius et al., 2000). This result is consistent with low and fluctuating methane concentrations in high sulfate-amended butyrate- and propionate-converting SMTZ slurries in which the abundance of ANME-1b (methane oxidizing archaea, ANME) is relatively high (**Chapter 3 and 4**).

7.2.4 Archaea as syntrophic partners

Methanomicrobiales was the dominant archaeal order in both butyrate- and propionate-converting slurries regardless of the origin of the sediment, the incubation temperature and the sulfate concentration (**Chapter 3 and 4**). This finding is supported by the statistical analysis showing that *Methanomicrobiales* clustered with various IPLs that were abundant at different temperatures and sulfate concentrations in the butyrate- and propionate-converting slurries (**Chapter 5**). Similarly, different genera of *Methanomicrobiaceae* were dominant in the enrichment cultures after several transfers (**Chapter 6**). They were the main syntrophic partners of butyrate and propionate degraders responsible for H₂ and/or formate consumption. In addition, the FISH micrographs of butyrate-converting enrichment cultures visualize the close relationship of syntrophic bacteria and methanogenic archaea (**Chapter 6**). The predominance of hydrogenotrophic methanogens has been observed in near-surface and sulfate-rich marine sediments (Webster et al., 2009; Parkes et al., 2007; Kendall and Boone, 2006a; Parkes et al., 1990; Blair and Carter 1992; Sørensen et al. 1981) which explains the high abundance of *Methanomicrobiales* under sulfidogenic as well as methanogenic conditions in our incubations.

The other syntrophic partner organisms belonged to the aceticlastic methanogenic families, *Methanosarcinaceae* and *Methanosaetaeaceae*. *Methanosarcina*, belonging to *Methanosarcinaceae*, was present in sulfate-amended and sulfate-free slurries whereas *Methanosaetaeaceae* was enriched only in slurries with low or free of sulfate (**Chapter 3**). After subculturing, however, *Methanosaetaeaceae*-related methanogens were replaced by *Methanosarcinaceae*-related methanogens in SZ and by *Desulfobacter latus* in SMTZ cultures (**Chapter 6**).

In addition to the methane-producing archaea, methane-oxidizing archaea (ANME-1b) were also detected in propionate and butyrate slurries (**Chapter 3 and 4**), but they were not enriched further, due to their slow growth (**Chapter 6**). Low methane and high sulfide amounts in SMTZ slurries support the findings of Timmers et al. (2015) where ANME-1b was enriched in batch incubations with Baltic Sea sediments. The enrichment of both ANME-1 and *Desulfobacteraceae* in SMTZ slurries at low temperature is in accordance with previous findings documenting that SMTZ sediments are dominated by the members of *Desulfobacteraceae* and ANME clusters, forming close associations and involving in anaerobic oxidation of methane (Harrison et al., 2009; Knittel and Boetius, 2009). The other methane-oxidizing archaeal genera detected in the same slurries with ANME-1b were *Methanococcoides* and *Methanlobus* which are defined as ANME-3 *Archaea* (Knittel and Boetius, 2009, Lösekann et al., 2007, Niemann et al., 2006). Apparently, the incubation condition, inhabiting microbial community and the amounts of sulfate, sulfide and methane in the slurries favoured the enrichment of ANME-3 group.

7.3 H₂ and acetate: substrates for syntrophy or competition?

The competition mechanism of sulfate reducers and methanogens for hydrogen has been explained by Hoehler et al. (1998). SRB can consume as low as 1-2 nM H₂, while hydrogenotrophic methanogens require a minimum of 10-20 nM H₂. However, methanogens can coexist with sulfate reducers in sulfate zone of marine sediments by utilizing methylated compounds such as methanol, methylated amines and methylated sulfides. Nanomolar concentrations of H₂ may leak from methanogens which can subsequently be scavenged by sulfate reducers in the methane zone sediments (Finke et al., 2007b). The leaked H₂ controls the metabolic processes between different physiological types of organisms.

Energy yields from acetate in sulfate-reducing marine sediment are often sufficiently high to allow several potentially competing microbial processes to co-occur. The main reason is that acetate exists in much higher concentrations than H₂, in micromolar concentrations compared to

nanomolar concentrations of H_2 (Albert and Martens 1997; Jørgensen and Parkes 2010), making it theoretically possible for aceticlastic methanogens to co-occur with energetically more favourable acetate-oxidizing sulfate reduction in the sulfate zone (Finke et al., 2007b; Wang et al. 2010b). However, almost all acetate in the sulfate zone is converted to CO_2 , not to CH_4 (Jørgensen and Parkes, 2010), suggesting the predominance of aceticlastic sulfate reduction. Finke et al. (2007b) reported increasing sulfate and decreasing H_2 concentrations in marine sediments incubated with methylamine and methanol. They concluded that the H_2 production from methanogens becomes favorable under sulfate-reducing conditions and interspecies transfer of leaked H_2 during acetate oxidation might occur which provides a mechanism for survival of aceticlastic methanogens in sulfate-reducing sediments (Finke et al., 2007b). The importance of H_2 leakage was described for the first time by Phelps et al. (1985) using mixed pure cultures grown on acetate or methanol. They showed sulfate-dependent H_2 transfer from *Methanosarcina barkeri* to *Desulfovibrio vulgaris*, resulting in less methane production and more CO_2 and sulfide production. The methanogens started to produce H_2/CO_2 instead of CH_4 upon sulfate addition and the sulfate-reducing partner scavenged the produced hydrogen efficiently and kept the concentration low enough for the methanogens to continue producing H_2/CO_2 . Achtnich et al. (1995) showed that hydrogen-utilizing sulfate reducers influence aceticlastic methanogenesis in anoxic paddy soils leading to oxidation of the methyl carbon. King et al. (1983) reported a decreasing % CO_2 after inhibition of sulfate reduction, thus inhibition of the H_2 scavenging partner in marine sediments for non-competitive substrates such as methylamine and trimethylamine. We performed a similar experiment to the study of Phelps et al. (1985) and showed interspecies hydrogen transfer between aceticlastic *Methanosaeta concilii* and hydrogenotrophic microorganisms, *Desulfovibrio vulgaris* or *Methanococcus maripaludis*, using acetate as electron donor (**Chapter 2**). Our results showed that *D. vulgaris* could reduce sulfate and grow on leaked hydrogen from *M. concilii*, and the cell increase of *M. maripaludis* was synchronized with the growth of *M. concilii*. The switch from methanogenesis to hydrogen production shows cooperation rather than competition between methanogens and sulfate reducers. Hydrogen production from *Methanosaeta* was demonstrated for *Methanosaeta thermophila* when growing on acetate (Valentine et al., 2000), and we reported for the first time hydrogen leakage from a mesophilic halotolerant *Methanosaeta*. In addition to hydrogen leakage, we tested coexistence of *M. concilii* with *Desulfobacter latus* on acetate under sulfidogenic conditions in mixed pure cultures (**Chapter 2**). The results showed that acetate conversion by aceticlastic methanogens in the presence of high sulfate and active aceticlastic sulfate reducers is

possible. Butyrate and propionate conversion at high sulfate concentration occurred by syntrophic interactions of acetogenic bacteria with acetate- and hydrogen-consuming sulfate reducers and methanogens. This was revealed by consumption of accumulated acetate with simultaneous methane production both in sulfate and methane zone slurries (**Chapter 3 and 4**). Despite cooperative interactions of sulfate reducers and methanogens, we still observed competition between them for acetate. *Methanosaetaceae*, which was dominant aceticlastic methanogen in enrichment slurries (**Chapter 3**), was washed out after several transfers and replaced by *Methanosarcinaceae* in sulfate zone (SZ) cultures and by acetate-consuming *D. latus* in sulfate-methane transition zone (SMTZ) cultures (**Chapter 6**). High acetate concentration resulting from incomplete butyrate conversion during sub-culturing process can be the reason of high relative abundance of *Methanosarcinaceae*, whose members are known to be more successful at high acetate concentrations (Jetten et al., 1992). Additionally, *D. latus* grew faster in SMTZ cultures, thus gained competitive advantage over methanogens (Muyzer and Stams, 2008).

7.4 Concluding remarks and future perspectives

Sulfate reduction and methanogenesis are important terminal electron-accepting processes in coastal marine sediments, and propionate, butyrate, acetate, and H_2 /formate are major end-products of organic matter degradation in these ecosystems. Since the conversion of propionate and butyrate is critical in sulfate-depleted sediments and acetate and H_2 /formate play an important role during their degradation, it is important to know which populations of microorganisms are involved in their degradation in the upper and lower parts of the marine sediments and how they interact with each other during degradation.

In this thesis, we demonstrated that sulfate reducers were more competitive than methanogens in high-sulfate environments and thus sulfate reduction is the dominant pathway for butyrate and propionate conversions in Aarhus Bay sediment. *Desulfosarcina* and *Desulfobacterium* are involved in butyrate conversion, whereas *Desulfosarcina*, *Desulfobulbus* and *Desulforhopalus* are involved in propionate conversion. We also determined that the presence of SRB, especially *Desulfobacteraceae* and *Desulfobulbaceae*, was independent of the presence of sulfate. We observed that *Desulforhopalus*, SEEP-SRB₁ group, unclassified *Desulfobacteraceae* were more competitive in environments without sulfate and *Desulfobulbaceae* were more successful at low temperature as compared to *Desulfobacteraceae*. The fact that many sulfate reducers have both sulfidogenic and acetogenic type of metabolism, increases the chance of survival in environments lacking sulfate.

The syntrophic butyrate-converting genus *Syntrophomonas* was detected under sulfate-free as well as low-sulfate conditions, whereas syntrophic conversion of propionate was likely performed by an unknown species of *Cryptanaerobacter* throughout the sediment. *Methanomicrobiales* were the major competitors for hydrogen in high and low-sulfate environments. In the presence of sulfate, *Methanosarcinaceae* and *Desulfobacteraceae* became the most competitive acetate consumers, whereas *Methanosaetaceae* could outcompete these groups at low acetate and sulfate concentrations. On the other hand, mixed pure cultures of *Methanosaeta concilii* with hydrogenotrophic *D. vulgaris* and *M. maripaludis* indicated hydrogen leakage from *M. concilii*, which allowed *D. vulgaris* to grow and *M. maripaludis* to sustain itself. Hydrogen leakage provides an explanation for biogeochemical zonation for non-competitive and competitive substrates in marine sediments. This thesis provided insight into the relationship between sulfidogenic and methanogenic propionate and butyrate conversion at different depths of marine sediments, the role of H_2 /formate and acetate during conversion and the responsible microbial community. It is apparent that several factors influence the interspecies interactions and conversion dynamics, such as temperature, sulfate availability, sulfide and methane concentrations, sediment depth and the syntrophic microbial community. Novel *Syntrophomonas* and *Cryptanaerobacter* species detected by 16S rRNA gene sequencing analysis are likely involved in butyrate and propionate conversions, respectively, at different depths in marine sediments. Further attempts are necessary to isolate and characterize these microorganisms. As it is difficult to obtain syntrophs in pure or defined mixed cultures, different incubation conditions should be applied. These can include different substrates and substrate concentration, electron acceptor concentration, incubation temperatures and prolonged incubation time. The isolates can further be co-cultured with the organisms that are competitive or cooperative to get insight about interspecies interactions and their role in propionate and butyrate conversions in marine sediments.

While it is advantageous to monitor metabolic products and identify the metabolic pathways during incubation in batch systems, homogenization of sediment destroys the spatial structure of the microbial community. Continuous flow-through reactors can be used to cultivate microorganisms while maintaining low substrate concentrations comparable to *in situ* or to measure reaction rates without disrupting the porous structure in the sediment or spatial arrangements of microorganisms. However, long-term incubation is difficult with continuous flow-through reactors as it is laborious to maintain the system steady for long periods. Intact sediment core incubation is another method that is used to mimic *in situ* conditions. Here, only the

concentrations of carbon based substrates can be controlled while the pore-water constituents can be kept similar to *in situ* concentrations. Incubation with ^{13}C -labelled substrates (e.g. acetate, propionate and butyrate) and subsequent ^{13}C -labelled RNA/DNA/PLFA analysis can give information on the microorganisms using the labeled substrate, hence involving in the cycling of these substrates.

As the numerically rare community members may have important ecological and metabolic functions within marine sediments, the combination of single-cell methodologies with different FISH techniques can be applied for the analysis of less-abundant and more informative target microorganisms and their interactions within mixed populations. In this respect, after incubation with labeled substrates under *in situ* or near *in situ* conditions, subsamples can be chemically fixed for FISH and the cells can subsequently be visualized by nanoSIMS (Secondary Ion Mass Spectrometry). Simultaneous imaging of identity and the quantification of metabolic activity by nanoSIMS will provide insights into the physiology of microorganisms obtained both in axenic cultures and enrichments, as well as the ecophysiology in their natural environment. Proteins may also be considered as suitable targets for the direct identification of key enzymes involved in the uptake of particular labeled compounds.

Appendices

References

- Achtnich C, Schuhmann A, Wind T, Conrad R (1995) Role of interspecies H₂ transfer to sulfate and ferric iron-reducing bacteria in acetate consumption in anoxic paddy soil. *FEMS Microbiol Ecol* 16:61–69.
- Ahlert S, Zimmermann R, Ebling J, König H (2016) Analysis of propionate-degrading consortia from agricultural biogas plants. *Microbiologyopen* 5: 1027–1037.
- Albert DB, Martens CS (1997) Determination of low-molecular-weight organic acid concentrations in seawater and pore-water samples via HPLC. *Mar Chem* 56:27–37.
- Alperin MJ, Reeburgh WS, Whitaker MJ (1988) Carbon and hydrogen isotope fractionation resulting from anaerobic methane oxidation. *Glob Biochem Cycles* 2: 279–288.
- Alphenaar PA, Visser A, Lettinga G (1993) The effect of liquid upward velocity and hydraulic retention time on granulation in UASB reactors treating wastewater with a high sulphate content. *Bioresour Technol* 43(3):249–258.
- Amann RI, Ludwig W, Schleifer KH, Amann RI, Ludwig W (1995) Phylogenetic identification and in situ detection of individual microbial cells without cultivation. *Microbiol Rev* 59:143–169.
- Amend JP, Shock EL (2001) Energetics of overall metabolic reactions of thermophilic and hyperthermophilic Archaea and Bacteria. *FEMS Microbiol Rev* 25:175–243.
- Aquilina A, Knab NJ, Knittel K, Kaur G, Geissler A, Kelly SP, Fossing H, Boot CS, Parkes RJ, Mills RA, Boetius A, Lloyd JR, Pancost RD (2010) Biomarker indicators for anaerobic oxidizers of methane in brackish-marine sediments with diffusive methane fluxes. *Org Geochem* 41:414–426.
- Bale NJ, Hopmans EC, Schoon PL, de Kluijver A, Downing JA, Middelburg JJ, Sinninghe Damsté JS, Schouten S (2016) Impact of trophic state on the distribution of intact polar lipids in surface waters of lakes. *Limnol Oceanogr* 61:1065–1077.
- Banat IM, Nedwell DB (1983) Mechanisms of turnover of C₂–C₄ fatty acids in high-sulphate and low-sulphate anaerobic sediments. *FEMS Microbiol Lett* 17:107–110.
- Barker HA (1936) On the biochemistry of the methane fermentation. *Arch Mikrobiol* 7:404–419.
- Barnes RO, Goldberg ED (1976) Methane production and consumption in anoxic marine sediments. *Geology* 4:297–300.
- Beatty PS, McInerney MJ (1987) Growth of *Syntrophomonas wolfei* in pure culture on crotonate. *Arch Microbiol* 147:389–393.

- Beck M, Riedel T, Graue J, Köster J, Kowalski N, Wu CS, Wegener G, Lipsewiers Y, Freund H, Böttcher ME, Brumsack HJ, Cypionka H, Rullkötter J, Engelen B (2011) Imprint of past and present environmental conditions on microbiology and biogeochemistry of coastal Quaternary sediments. *Biogeosciences* 8:55–68.
- Berry D, Mahfoudh K Ben, Wagner M, Loy A (2011) Barcoded primers used in multiplex amplicon pyrosequencing bias amplification. *Appl Environ Microbiol* 77:7846–7849.
- Biddle JF, Fitz-Gibbon S, Schuster SC, Brenchley JE, House CH (2008) Metagenomic signatures of the Peru Margin seafloor biosphere show a genetically distinct environment. *Proc Natl Acad Sci* 105:10583–10588.
- Blair NE, Carter WD (1992) The carbon isotope biogeochemistry of acetate from a methanogenic marine sediment. *Geochim Cosmochim Acta* 56:1247–1258.
- Bligh EG, Dyer WJ (1959) A rapid method of total lipid extraction and purification. *Canad J of Biochem and Physiol* 37:911–917.
- Boetius A, Ravensschlag K, Schubert CJ, Rickert D, Widdel F, Gieseke A, Amann R, Jørgensen BB, Witte U, Pfannkuche O (2000) A marine microbial consortium apparently mediating anaerobic oxidation of methane. *Nature* 407:623–626.
- Boone DR, Johnson RL, Liu Y (1989) Diffusion of the interspecies electron carriers H₂ and formate in methanogenic ecosystems and its implications in the measurement of K_m for H₂ or formate uptake. *Appl Environ Microbiol* 55:1735–1741.
- Boonnet DR, Bryant MP (1980) Propionate-degrading bacterium, *Syntrophobacter wolinii* sp. nov. gen. nov., from methanogenic ecosystems. 40:626–632.
- Borowski WS, Paull CK, Ussler W (1999) Global and local variations of interstitial sulphate gradients in the deep-water, continental margin sediments: Sensitivity to underlying methane and gas hydrates. *Mar Geol* 159:131–154.
- Borrel G, Lehours AC, Crouzet O, Jézéquel D, Rockne K, Kulczak A, Duffaud E, Joblin K, Fonty G (2012) Stratification of Archaea in the deep sediments of a freshwater meromictic lake: vertical shift from methanogenic to uncultured Archaeal lineages. *PLoS One*. 7:e43346.
- Bowles MW, Mogollon JM, Kasten S, Zabel M, Hinrichs K-U (2014) Global rates of marine sulfate reduction and implications for sub-sea-floor metabolic activities. *Science* 344:889–891.
- Bragg L, Stone G, Imelfort M, Hugenholtz P, Tyson GW (2012) Fast, accurate error-correction of amplicon pyrosequences using Acacia. *Nat Methods* 9:425–426.
- Burdige DJ (2007) Preservation of organic matter in marine sediments : controls, mechanisms, and an imbalance in sediment organic carbon budgets? *Chem Rev* 107:467–485.

- Callaghan AV, Morris BEL, Pereira IAC, McNerney MJ, Austin RN, Groves JT, Kukor JJ, Suflita JM, Young LY, Zylstra GJ, Wawrik B (2012) The genome sequence of *Desulfatibacillum alkenivorans* AK-01: a blueprint for anaerobic alkane oxidation. *Environ Microbiol* 14:101–113.
- Campbell BJ, Engel AS, Porter ML, Takai K (2006) The versatile ϵ -proteobacteria: key players in sulphidic habitats. *Nat Rev Microbiol* 4:458–468.
- Canfield DE (1993) Organic matter oxidation in marine sediments. In: Interactions of C, N, P, and S biogeochemical cycles and global change. Wollast, R, Chou, L, and Mackenzie, F, (eds) Springer-Verlag, Berlin Heidelberg pp 333–363.
- Canfield D, Thamdrup B, Kristensen E (2005) Heterotrophic carbon metabolism. In: Aquatic Geomicrobiology. Southward, A., Tyler, P., Young, C., and Fuiman, L. (eds). Elsevier, Academic Press, pp 129–166.
- Canfield DE, Thamdrup B, Kristensen E. (2006) Heterotrophic carbon metabolism. In: Aquatic geomicrobiology. Southward A. Tyler P, Young C, Fuiman, L, (eds) Elsevier, Academic Press, pp 129–166. F
- Caporaso JG, Kuczynski J, Stombaugh J, Bittinger K, Bushman FD, Costello EK, Fierer N, Peña AG, Goodrich JK, Gordon JI, Huttley G, Kelley ST, Knights D, Koenig JE, Ley RE, Lozupone C, McDonald D, Muegge BD, Pirrung M, Reeder J, Sevinsky JR, Turnbaugh PJ, Walters W, Widmann J, Yatsunenko T, Zaneveld J, Knight R (2010) QIIME allows analysis of high-throughput community sequencing data. *Nat Methods* 7:335–336.
- Cappenberg, TE (1974) Interrelations between sulfate-reducing and methane-producing bacteria in bottom deposits of a fresh-water lake. I. Field observations. *Antonie Van Leeuwenhoek* 40:285–295.
- Cappenberg TE, Prins RA (1974) Interrelations between sulfate-reducing and methane-producing bacteria in bottom deposits of a fresh-water lake. III. Experiments with ^{14}C -labeled substrates. *Antonie Van Leeuwenhoek* 40:457–469.
- Chabrière E, Charon MH, Volbeda A, Pieulle L, Hatchikian EC, Fontecilla-Camps JC (1999) Crystal structures of the key anaerobic enzyme pyruvate:ferredoxin oxidoreductase, free and in complex with pyruvate. *Nat Struct Biol* 6:182–190.
- Chapelle F, Lovley D. (1992) Competitive exclusion of sulfate reduction by Fe (III)-reducing bacteria: a mechanism for producing discrete zones of high-iron ground water. *Ground Water* 30: 29–36.
- Chen S, Liu X, Dong X (2005) *Syntrophobacter sulfatireducens* sp. nov., a novel syntrophic, propionate-oxidizing bacterium isolated from UASB reactors. *Int J Syst Evol Microbiol* 55:1319–1324.
- Chong SC, Liu Y, Cummins M, Valentine DL, Boone DR (2002) *Methanogenium marium* sp. nov., a H_2 -using methanogen from Skan Bay, Alaska, and kinetics of H_2 utilization. *Antonie van Leeuwenhoek* 81:263–270.

- Christensen D, Blackburn TH (1982) Turnover of ^{14}C -labelled acetate in marine sediments. *Mar Biol* 71:113–119.
- Christensen D (1984) Determination of substrates oxidized by sulfate reduction in intact cores of marine sediments. *Limnol Oceanogr* 29, 189–192.
- Claypool GE, Kvenvolden KA (1983) Methane and other hydrocarbon gases in marine sediment. *Annu Rev Earth Planet Sci* 11:299–327.
- Claypool GE (2004) Ventilation of marine sediments indicated by depth profiles of pore water sulfate and $\delta^{34}\text{S}$. *Geochemical Soc Spec Publ* 9:59–65.
- Claypool GE, Kvenvolden KA (1983) Methane and other hydrocarbon gases in marine sediment. *Annu Rev Earth Pl Sc* 11(1): 299–327.
- Cline JJD (1969) Spectrophotometric determination of hydrogen sulfide in natural waters¹. *Limnol Oceanogr* 14:454–458.
- Conklin A, Stensel HD, Ferguson J (2006) Growth kinetics and competition between *Methanosarcina* and *Methanosaeta* in mesophilic anaerobic digestion. *Water Environ Res* 78:486–496.
- Conrad R (1996) Soil microorganisms as controllers of atmospheric trace gases (H_2 , CO , CH_4 , OCS , N_2O , and NO). *Microbiol Rev* 60:609–640.
- Cord-Ruwisch R, Seitz HJ, Conrad R (1988) The capacity of hydrogenotrophic anaerobic bacteria to compete for traces of hydrogen depends on the redox potential of the terminal electron acceptor. *Arch Microbiol* 149:350–357.
- Crill PM, Martens CS (1986) Methane production from bicarbonate and acetate in an anoxic marine sediment. *Geochim. Cosmochim. Acta* 50:2089–2097.
- Daims H, Brühl A, Amann R, Schleifer K-H, Wagner M (1999) The domain-specific probe EUB338 is insufficient for the detection of all Bacteria: Development and evaluation of a more comprehensive probe set. *Syst Appl Microbiol* 22:434–444.
- Dale AW, Aguilera DR, Regnier P, Fossing H, Knab NJ, Jørgensen BB (2008) Seasonal dynamics of the depth and rate of anaerobic oxidation of methane in Aarhus Bay (Denmark) sediments. *J Mar Res* 66:127–155.
- Dar SA, Kleerebezem R, Stams AJM, Kuenen JG, Muyzer G (2008) Competition and coexistence of sulfate-reducing bacteria, acetogens and methanogens in a lab-scale anaerobic bioreactor as affected by changing substrate to sulfate ratio. *Appl Microbiol Biotechnol* 78:1045–1055.
- Dar SA, Kuenen JG, Muyzer G (2005) Nested PCR-denaturing gradient gel electrophoresis approach to determine the diversity of sulfate-reducing bacteria in complex microbial communities. *Appl Environ Microbiol* 71:2325–2330. de Bok FAM, Stams AJM, Dijkema C, Boone DR (2001)

- Pathway of propionate oxidation by a syntrophic culture of *Smithella propionica* and *Methanospirillum hungatei*. Appl Environ Microbiol 67: 1800-1804.
- de Bok FA, Roze EHA, Stams AJM (2002a) Hydrogenases and formate dehydrogenases of *Syntrophobacter fumaroxidans*. Antonie van Leeuwenhoek 81:283-291.
- de Bok FAM, Luijten MLGC, Stams AJM (2002b) Biochemical evidence for formate transfer in syntrophic propionate-oxidizing cocultures of *Syntrophobacter fumaroxidans* and *Methanospirillum hungatei*. Appl Environ Microbiol 68:4247-4252.
- de Bok FAM, Hagedoorn PL, Silva PJ, Hagen WR, Schiltz E, Fritsche K, Stams AJM (2003) Two W-containing formate dehydrogenases (CO₂-reductases) involved in syntrophic propionate oxidation by *Syntrophobacter fumaroxidans*. Eur J Biochem 270:2476-2485.
- de Bok FAM, Plugge CM, Stams AJM (2004) Interspecies electron transfer in methanogenic propionate degrading consortia. Water Res 38:1368-1375.
- de Bok FAM, Harmsen HJM, Plugge CM, de Vries MC, Akkermans ADL, de Vos WM, Stams AJM (2005) The first true obligately syntrophic propionate-oxidizing bacterium, *Pelotomaculum schinkii* sp. nov., co-cultured with *Methanospirillum hungatei*, and emended description of the genus *Pelotomaculum*. Int J Syst Evol Microbiol 55:1697-1703.
- De Rosa M and Gambacorta A (1988) The lipids of archaebacteria. Prog Lipid Res 27:153-75.
- Deegan LA, Johnson DS, Warren RS, Peterson BJ, Fleeger JW, Fagherazzi S, Wollheim WM (2012) Coastal eutrophication as a driver of salt marsh loss. Nature 490:388-392.
- Delong EF (1992) Archaea in coastal marine environments. Proc Natl Acad Sci USA 89:5685-5689.
- DeSantis TZ, Hugenholtz P, Keller K, Brodie EL, Larsen N, Piceno YM, Phan R, Andersen GL (2006) NAST: a multiple sequence alignment server for comparative analysis of 16S rRNA genes. Nucleic Acids Res 34:394-399.
- Devereux R, Delaney M, Widdel F, Stahl DA (1989) Natural relationships among sulfate-reducing Eubacteria. J Bacteriol 171:6689-6695.
- Dojka MA, Hugenholtz P, Haack SK, Pace NR (1998) Microbial diversity in a hydrocarbon-and chlorinated-solvent-contaminated aquifer undergoing intrinsic bioremediation. Appl Environ Microbiol 64:3869-3877.
- Dolfing J, Jiang B, Henstra AM, Stams AJM, Plugge CM (2008) Syntrophic growth on formate: a new microbial niche in anoxic environments. Appl Environ Microbiol 74:6126-6131.
- Dong X, Plugge CM, Stams AJM (1994) Anaerobic degradation of propionate by a mesophilic acetogenic bacterium in coculture and triculture with different methanogens. Appl Environ Microbiol 60:2834-2838.

- Dowhan W (1997) Molecular basis for membrane phospholipid diversity: why are there so many lipids? *Ann Rev Biochem* 66(1):199-232.
- Edgar RC (2010) Search and clustering orders of magnitude faster than BLAST. *Bioinformatics* 26:2460-2461.
- Ezaki T (2009) *Peptococcaceae*. In: Bergey's Manual of Systematic Bacteriology. De Vos P, Garrity G, Jones D, Krieg N, Ludwig W, Rainey F, Schleifer K.-H, Whitman W (eds). Springer-Verlag New York, USA pp 969-971.
- Fang J, Barcelona MJ (1998) Structural determination and quantitative analysis of bacterial phospholipids using liquid chromatography/electrospray ionization/mass spectrometry. *J Microbiol Methods* 33:23-35.
- Fang J, Barcelona MJ, Alvarez PJJ (2000) A direct comparison between fatty acid analysis and intact phospholipid profiling for microbial identification. *Org Geochem* 31:881-887.
- Fang HHP, Liu Y, Ke SZ, Zhang T (2004) Anaerobic degradation of phenol in wastewater at ambient temperature. *Water Sci Technol* 49:95-102.
- Fasham MJR, Balino BM, Bowles MC, Anderson R, Archer D, Bathmann U, Boyd P, Buesseler K, Burkil P, Bychkov A, Carlson C, Chen CTA, Doney S, Ducklow H, Emerson S, Feely R, Feldman G, Garcon V, Hansell D, Hanson R, Harrison P, Honjo S, Jeandel C, Karl D, Le Borgne R, Liu KK, Lochte K, Louanchi F, Lowry R, Michaels A, Monfray P, Murray J, Oschlies A, Platt T, Priddle J, Quinones R, Ruiz-Pino D, Saino T, Sakshaug E, Shimmield G, Smith S, Smith W, Takahashi T, Treguer P, Wallace D, Wanninkhof R, Watson A, Willebrand J, Wong CS (2001) A new vision of ocean biogeochemistry after a decade of the Joint Global Ocean Flux Study (JGOFS). *Ambio* 10: 4-31.
- Finke N, Vandieken V, Jørgensen BB (2007a) Acetate, lactate, propionate, and isobutyrate as electron donors for iron and sulfate reduction in Arctic marine sediments, Svalbard. *FEMS Microbiol Ecol* 59:10-22.
- Finke N, Hoehler TM, Jørgensen BB (2007b) Hydrogen 'leakage' during methanogenesis from methanol and methylamine: Implications for anaerobic carbon degradation pathways in aquatic sediments. *Environ Microbiol* 9:1060-1071.
- Fry JC, Parkes RJ, Cragg BA, Weightman AJ, Webster G (2008) Prokaryotic biodiversity and activity in the deep seafloor biosphere. *FEMS Microbiol Ecol* 66:181-196.
- Garcia J-L, Ollivier B, Whitman WB (2006) The Order *Methanomicrobiales*. In: The Prokaryotes. Dworkin M, Falkow S, Rosenberg E, Schleifer K-H, Stackebrandt H (eds) Springer-Verlag, New York pp 208-230.
- Glud RN, Gundersen JK, Røy H, Jørgensen BB (2003) Seasonal dynamics of benthic O₂ uptake in a semienclosed bay: Importance of diffusion and faunal activity. *Limnol Oceanogr* 48:1265-1276.

- Godon JJ, Morinière J, Moletta M, Gaillac M, Bru V, Delgènes JP (2005) Rarity associated with specific ecological niches in the bacterial world: the “Synergistes” example. *Environ Microbiol* 7:213–224.
- Greuter D, Loy A, Horn M, Rattei T (2016) ProbeBase-an online resource for rRNA-targeted oligonucleotide probes and primers: new features 2016. *Nucleic Acids Res* 44:586–589.
- Grotenhuis JTC, Smit M, Plugge CM, Xu YS, van Lammeren AA, Stams AJM, Zehnder AJ (1991) Bacteriological composition and structure of granular sludge adapted to different substrates. *Appl Environ Microbiol* 57:1942–1949.
- Gustafson WG, Feinberg BA, McFarland JT (1986) Energetics of beta-oxidation. Reduction potentials of general fatty acyl-CoA dehydrogenase, electron transfer flavoprotein, and fatty acyl-CoA substrates. *J Biol Chem* 261:7733–7741.
- Halpern BS, Frazier M, Potapenko J, Casey KS, Koenig K, Longo C, Lowndes JS, Rockwood RC, Seliger ER, Selkoe KA, Walbridge S (2015) Spatial and temporal changes in cumulative human impacts on the world’s ocean. *Nat Commun* 6:7615.
- Hamady M, Walker JJ, Harris JK, Gold NJ, Knight R (2008) Error-correcting barcoded primers for pyrosequencing hundreds of samples in multiplex. *Nat Methods* 5(3): 235–237.
- Harmsen HJM, van Kuijk BLM, Plugge CM, Akkermans ADL, de Vos WM, Stams AJM (1998) *Syntrophobacter fumaroxidans* sp. nov., a syntrophic propionate-degrading sulfate-reducing bacterium *Int J Syst Bacteriol* 1383–1388.
- Harrison BK, Zhang H, Berelson W, Orphan VJ (2009) Variations in archaeal and bacterial diversity associated with the sulfate-methane transition zone in continental margin sediments (Santa Barbara Basin, California). *Appl Environ Microbiol* 75:1487–1499.
- Harvey HR, Fallon RD, Patton JS (1986) The effect of organic matter and oxygen on the degradation of bacterial membrane lipids in marine sediments. *Geochim Cosmochim Acta* 50:795–804.
- Harvey HR (2006) Sources and cycling of organic matter in the marine water column. In: *Marine Organic Matter: Biomarkers, Isotopes and DNA*. Volkman JK (ed) Springer Heidelberg, Berlin, pp 1–25.
- Hatamoto M, Imachi H, Fukayo S, Ohashi A, Harada H (2007) *Syntrophomonas palmitatica* sp. nov., an anaerobic syntrophic, long-chain fatty-acid-oxidizing bacterium isolated from methanogenic sludge. *Int J Syst Evol Microbiol* 57:2137–2142.
- Hattori S, Kamagata Y, Hanada S, Shoun H (2000) *Thermacetogenium phaeum* gen. nov., sp. nov., a strictly anaerobic, thermophilic, syntrophic acetate-oxidizing bacterium. *Int J Syst Evol Microbiol* 50(4): 1601–1609.
- Hedges JJ, Keil RG (1995) Sedimentary organic matter preservation: an assessment and speculative synthesis. *Mar Chem* 49:81–115.

- Henrichs SM (1992) Early diagenesis of organic matter in marine sediments: progress and perplexity. *Mar Chem* 39:119–149.
- Herrmann S, Kleinsteuber S, Chatzinotas A, Kuppardt S, Lueders T, Richnow HH, Vogt C (2010) Functional characterization of an anaerobic benzene-degrading enrichment culture by DNA stable isotope probing. *Environ Microbiol* 12:401–411.
- Hinrichs KU, Hayes JM, Sylva SP, Brewer PG, DeLong EF (1999) Methane-consuming archaeobacteria in marine sediments. *Nature* 398:802–805.
- Hoefs M, Schouten S, De Leeuw JW, King LL, Wakeham SG, Sinninghe Damsté JS (1997) Ether lipids of planktonic archaea in the marine water column. *Appl Environ Microbiol* 63:3090–3095.
- Hoehler T, Alperin M, Albert D, Martens C (1998) Thermodynamic control on hydrogen concentrations in anoxic sediments. *Geochim Cosmochim Acta* 62: 1745–1756.
- Hoehler TM, Alperin MJ, Albert DB, Martens CS (2001) Apparent minimum free energy requirements for methanogenic Archaea and sulfate-reducing bacteria in an anoxic marine sediment. *FEMS Microbiol Ecol* 38:33–41.
- Holmer M, Kristensen E (1994) Coexistence of sulfate reduction and methane production in an organic-rich sediment. *Mar Ecol Prog Ser* 107:177–184.
- Holmkvist L, Kamyshny A, Vogt C, Vamvakopoulos K, Ferdelman TG, Jørgensen BB (2011) Sulfate reduction below the sulfate-methane transition in Black Sea sediments. *Deep Sea Res Part I Oceanogr Res Pap* 58:493–504.
- Hopmans EC, Schouten S, Pancost RD, van der Meer MTJ, Sinninghe Damsté JS (2000) Analysis of intact tetraether lipids in archaeal cell material and sediments by high performance liquid chromatography/atmospheric pressure chemical ionization mass spectrometry. *Rapid Commun Mass Spectrom* 14:585–589.
- Imachi H, Sakai S, Ohashi A, Harada H, Hanada S, Kamagata Y, Sekiguchi Y (2007) *Pelotomaculum propionicicum* sp. nov., an anaerobic, mesophilic, obligately syntrophic, propionate-oxidizing bacterium. *Int J Syst Evol Microbiol* 57:1487–1492.
- Imachi H, Sekiguchi Y, Kamagata Y, Hanada S, Ohashi A, Harada H (2002) *Pelotomaculum thermopropionicum* gen. nov., an anaerobic, thermophilic, syntrophic propionate-oxidizing bacterium. *Int J Syst Evol Microbiol* 52: 1729–1735.
- Iversen N, Jørgensen BB (1985) Anaerobic methane oxidation rates at the sulfate-methane transition in marine sediments from Kattegat and Skagerrak (Denmark). *Limnol Oceanogr* 30:944–955.
- Iwamoto TK, Tani K, Nakamura K, Suzuki Y, Kitagawa M, Eguchi M, Nasu M (2000) Monitoring impact of in situ biostimulation treatment on groundwater bacterial community by DGGE. *FEMS Microbiol Ecol* 32:129–141.

- Jackson BE, Bhupathiraju VK, Tanner RS, Woese CR, McInerney MJ (1999) *Syntrophus aciditrophicus* sp. nov., a new anaerobic bacterium that degrades fatty acids and benzoate in syntrophic association with hydrogen- using microorganisms. Arch Microbiol 171:107–114.
- Jetten MSM, Stams AJM, Zehnder AJB (1992) Methanogenesis from acetate: a comparison of the acetate metabolism in *Methanothrix soehngenii* and *Methanosarcina* spp. FEMS Microbiol Lett 88:181–197.
- Jones WJ, Paynter M, Gupta R (1983) Characterization of *Methanococcus maripaludis* sp. nov., a new methanogen isolated from salt marsh sediment. Arch Microbiol 135:91–97.
- Jørgensen BB (1978) A comparison of methods for the quantification of bacterial sulfate reduction in coastal marine sediments. I. Measurement with radiotracer techniques. Geomicrobiol J 1: 11–28.
- Jørgensen BB (1982) Mineralization of organic matter in the sea bed – the role of sulphate reduction. Nature 296:643–645.
- Jørgensen BB (1983) Processes at the sediment water interface. In: The major biogeochemical cycles and their interactions. Bolin B, Cook R (eds.) pp 477–515.
- Jørgensen BB, Bak F (1991) Pathways and microbiology of thiosulphate transformations and sulfate reduction in a marine sediment (Kattegat, Denmark). Appl Environ Microbiol 57:847–856.
- Jørgensen BB (2006) Bacteria and marine biogeochemistry. In: Marine Geochemistry. Schulz H, Zabel M (eds) (Vol. 2) Springer, Berlin pp 169–206.
- Jørgensen BB, Kasten S (2006) Sulfur cycling and methane oxidation. In: Marine Geochemistry. Springer Heidelberg, Berlin pp 271–309.
- Jørgensen BB, Boetius A (2007) Feast and famine — microbial life in the deep-sea bed. Nat Rev Microbiol 5:770–781.
- Jørgensen BB, Parkes RJ (2010) Role of sulfate reduction and methane production by organic carbon degradation in eutrophic fjord sediments (Limfjorden, Denmark). Limnol Oceanogr 55:1338–1352.
- Jørgensen BB, Marshall IPG (2016) Slow microbial life in the seabed. Ann Rev Mar Sci 8:311–332.
- Jung YT, Lee JS, Yoon JH (2016) *Gaetbulibacter aquiaggeris* sp nov., a member of the *Flavobacteriaceae* isolated from seawater. Int J Syst Evol Micr 66:1131–1137.
- Juretschko S, Timmermann G, Schmid M, Schleifer KH, Pommerening-Röser A, Koops HP, Wagner M (1998) Combined molecular and conventional analyses of nitrifying bacterium diversity in activated sludge: *Nitrosococcus mobilis* and *Nitrospira*-like bacteria as dominant populations. Appl Environ Microbiol 64:3042–3051.

- Juteau P, Côté V, Duckett MF, Beaudet R, Lépine F, Villemur R, Bisailon JG (2005) *Cryptanaerobacter phenolicus* gen. nov., sp. nov., an anaerobe that transforms phenol into benzoate via 4-hydroxybenzoate. *Int J Syst Evol Microbiol* 55:245–250.
- Kate M (1993) Membrane lipids of Archaea. In: *The Biochemistry of Archaea (Archaeobacteria)*. Kates M, Kushner DJ, Matheson AT (eds) Elsevier Science, Amsterdam pp 261–295.
- Kato S, Kosaka T, Watanabe K (2009) Substrate-dependent transcriptomic shifts in *Pelotomaculum thermopropionicum* grown in syntrophic co-culture with *Methanothermobacter thermautotrophicus*. *Microb Biotechnol* 2:575–584.
- Kendall MM, Liu Y, Boone DR (2006) Butyrate- and propionate-degrading syntrophs from permanently cold marine sediments in Skan Bay, Alaska, and description of *Algorimarina butyrica* gen. nov., sp. nov. *FEMS Microbiol Lett* 262:107–114.
- Kendall MM, Boone DR (2006a) Cultivation of methanogens from shallow marine sediments at Hydrate Ridge, Oregon. *Archaea* 2:31–38.
- Kendall MM, Boone DR (2006b) The Order *Methanosarcinales*. In: *The Prokaryotes*. Dworkin M, Falkow S, Rosenberg E, Schleifer K-H, Stackebrandt H (eds) Springer-Verlag, New York pp 244–256.
- Kiene RP, Oremland RS, Catena A, Miller LG, Capone DG (1986) Metabolism of reduced methylated sulfur compounds in anaerobic sediments and by a pure culture of an estuarine methanogen. *Appl Environ Microbiol* 52:1037–1045.
- Kim M, Oh HS, Park SC, Chun J (2014) Towards a taxonomic coherence between average nucleotide identity and 16S rRNA gene sequence similarity for species demarcation of prokaryotes. *Int J Syst Evol Microbiol* 64:346–351.
- King GM, Klug MJ, Lovley DR (1983) Metabolism of acetate, methanol, and methylated amines in intertidal sediments of Lowes Cove, Maine. *Appl Environ Microbiol* 45:1848–1853.
- Kleikemper J, Schroth MH, Sigler W V., Schmucki M, Bernasconi SM, Zeyer J (2002) Activity and diversity of sulfate-reducing bacteria in a petroleum hydrocarbon-contaminated aquifer. *Appl Environ Microbiol* 68:1516–1523.
- Kleinstaub S, Schleinitz KM, Breithfeld J, Harms H, Richnow HH, Vogt C (2008) Molecular characterization of bacterial communities mineralizing benzene under sulfate-reducing conditions. *FEMS Microbiol Ecol* 66:143–157.
- Kleinstaub S, Schleinitz KM, Vogt C (2012) Key players and team play: anaerobic microbial communities in hydrocarbon-contaminated aquifers. *Appl Microbiol Biotechnol* 94:851–873.
- Knittel K, Boetius A (2009) Anaerobic oxidation of methane: progress with an unknown process. *Annu Rev Microbiol* 63:311–334.

- Knittel K, Boetius A, Lemke A, Eilers H, Lochte K, Pfannkuche O, Linke P, Amann R (2003) Activity, distribution, and diversity of sulfate reducers and other bacteria in sediments above gas hydrate (Cascadia Margin, Oregon). *Geomicrobiol J* 20:269–294.
- Koga Y, Nishihara M, Morii H, Akagawa-Matsushita M (1993) Ether polar lipids of methanogenic bacteria: structures, comparative aspects, and biosyntheses. *Microbiol Rev* 57:164–182.
- Koizumi Y, Kojima H, Fukui M (2005) Potential sulfur metabolisms and associated bacteria within anoxic surface sediment from saline meromictic Lake Kaiike (Japan). *FEMS Microbiol Ecol* 52:297–305.
- Kristensen E, Holmer M (2001) Decomposition of plant materials in marine sediment exposed to different electron acceptors (O_2 , NO_3^- and SO_4^{2-}), with emphasis on substrate origin, degradation kinetics, and the role of bioturbation. *Geochim Cosmochim Acta* 65:419–433.
- Kristjansson JK, Schönheit P, Thauer RK (1982) Different K_s values for hydrogen of methanogenic bacteria and sulfate reducing bacteria: an explanation for the apparent inhibition of methanogenesis by sulfate. *Arch Microbiol* 131: 278–282.
- Krylova NI, Conrad R (1998) Thermodynamics of propionate degradation in methanogenic paddy soil. *FEMS Microbiol Ecol* 26:281–288.
- Kuever J (2014a) The family *Desulfovibrionaceae*. In: The Prokaryotes. Rosenberg E, DeLong EF, Lory S, Stackebrandt E, Thompson F (eds). Springer Berlin-Heidelberg Verlag, Berlin pp 107–133
- Kuever J (2014b) The family *Desulfobacteraceae*. In: The Prokaryotes. Rosenberg E, DeLong EF, Lory S, Stackebrandt E, Thompson F (eds). Springer Berlin-Heidelberg Verlag, Berlin pp 45–73.
- Kuever, J. (2014c) The Family *Desulfobulbaceae*. In: The Prokaryotes. Rosenberg E, DeLong EF, Lory S, Stackebrandt E, Thompson F (eds). Springer Berlin-Heidelberg Verlag, Berlin pp 75–86.
- Kvist T, Ahring BK, Westermann P (2007) Archaeal diversity in Icelandic hot springs. *FEMS Microbiol Ecol* 59:71–80.
- Laanbroek HJ, Pfennig N (1981) Oxidation of short-chain fatty acids by sulfate-reducing bacteria in freshwater and in marine sediments. *Arch Microbiol* 128(3): 330–335.
- Lagesen K, Hallin P, Rødland EA, Stærfeldt HH, Rognes T, Ussery DW (2007) RNAmmer: consistent and rapid annotation of ribosomal RNA genes. *Nucleic Acids Res* 35:3100–3108.
- Lane DJ (1991) 16S/23S rRNA sequencing. In: Nucleic acid techniques in bacterial systematics. Stackebrandt E, Goodfellow M (eds). Wiley & Sons, Chichester, United Kingdom pp 115–175.
- Leloup J, Fossing H, Kohls K, Holmkvist L, Borowski C, Jørgensen BB (2009) Sulfate-reducing bacteria in marine sediment (Aarhus Bay, Denmark): abundance and diversity related to geochemical zonation. *Environ Microbiol* 11:1278–1291.

- Leloup J, Loy A, Knab NJ, Borowski C, Wagner M, Jørgensen BB (2007) Diversity and abundance of sulfate-reducing microorganisms in the sulfate and methane zones of a marine sediment, Black Sea. *Environ Microbiol* 9:131–142.
- Lever MA (2012) Acetogenesis in the energy-starved deep biosphere-a paradox? *Front Microbiol* 2:1–18.
- Li F, Hinderberger J, Seedorf H, Zhang J, Buckel W, Thauer RK (2008) Coupled ferredoxin and crotonyl coenzyme A (CoA) reduction with NADH catalyzed by the butyryl-CoA dehydrogenase/Etf complex from *Clostridium kluyveri*. *J Bacteriol* 190:843–850.
- Lipp JS, Morono Y, Inagaki F, Hinrichs K-U (2008) Significant contribution of Archaea to extant biomass in marine subsurface sediments. *Nature* 454:991–994.
- Liu C, Zhang XY, Wen XR, Shi M, Chen XL, Su HN (2016) *Arcticiflavibacter luteus* gen. nov., nov., sp. nov., a member of the family *Flavobacteriaceae* isolated from intertidal sand. *Int J Syst Evol Microbiol* 66:144–149.
- Liu Q, Li J, Wei B, Zhang X, Zhang L, Zhang Y, Fang J (2016) *Leeuwenhoekiella nanhaiensis* sp. nov., isolated from deep-sea water. *Int J Syst Evol Microbiol* 66:1352–1357.
- Liu Y, Balkwill DL, Aldrich HC, Drake GR, Boone DR (1999) Characterization of the anaerobic propionate- degrading syntrophs *Smithella propionica* gen. nov., sp. nov. and *Syntrophobacter wolinii*. *Int J Syst Bacteriol* 49:545–556.
- Liu Y, Whitman WB (2008) Metabolic, phylogenetic, and ecological diversity of the methanogenic archaea. *Ann N Y Acad Sci* 1125:171–189.
- Llobet-Brossa E, Rabus R, Böttcher ME, Könneke M, Finke N, Schramm A, Meyer RL, Grötzschel S, Rosselló-Mora R, Amann R (2002) Community structure and activity of sulfate-reducing bacteria in an intertidal surface sediment: a multi-method approach. *Aquat Microb Ecol* 29:211–226.
- Lloyd KG, Lapham L, Teske A (2006) An anaerobic methane-oxidizing community of ANME-1b archaea in hypersaline gulf of Mexico sediments. *Appl Environ Microbiol* 72:7218–7230.
- Lloyd KG, Schreiber L, Petersen DG, Kjeldsen KU, Lever MA, Steen AD, Stepanauskas R, Richter M, Kleindienst S, Lenk S, Schramm A, Jørgensen BB (2013) Predominant archaea in marine sediments degrade detrital proteins. *Nature* 496:215–218.
- Lohner ST, Deutzmann JS, Logan BE, Leigh J, Spormann AM (2014) Hydrogenase-independent uptake and metabolism of electrons by the archaeon *Methanococcus maripaludis*. *ISME J* 8:1673–1681.
- Lorowitz WH, Zhao H, Bryant MP (1989) *Syntrophomonas wolfei* subsp. *saponavida* subsp. nov., a long-chain fatty-acid degrading, anaerobic, syntrophic bacterium; *Syntrophomonas wolfei*

- subsp. *wolfei* supsp. nov.; and emended descriptions of the genus and species. Int J Syst Bacteriol 39:122–126.
- Lösekan T, Knittel K, Nadalig T, Fuchs B, Niemann H, Boetius A, Amann R (2007) Diversity and abundance of aerobic and anaerobic methane oxidizers at the Haakon Mosby Mud Volcano, Barents Sea. Appl Environ Microbiol 73:3348–3362.
- Lovley DR, Ferry JG (1985) Production and consumption of hydrogen during growth of *Methanosarcina* spp. on acetate. Appl Environ Microbiol 49:247–249.
- Lovley DR (1985) Minimum threshold for hydrogen metabolism in methanogenic bacteria. Appl Environ Microbiol 49:1530–1531.
- Lovley DR, Dwyer DF, Klug MJ (1982) Kinetic analysis of competition between sulfate reducers and methanogens for hydrogen in sediments. Appl Environ Microbiol 43:1373–1379.
- Lovley D, Goodwin S (1988) Hydrogen concentrations as an indicator of the predominant terminal electron-accepting reactions in aquatic sediments. Geochim Cosmochim Acta 52: 2993–3003.
- Lyimo TJ, Pol A, Op den Camp HJM, Harhangi HR, Vogels GD (2000) *Methanosarcina semesiae* sp. nov., a dimethylsulfide-utilizing methanogen from mangrove sediment. Int J Syst Evol Microbiol 50:171–178.
- Maltby J, Sommer S, Dale AW, Treude T (2016) Microbial methanogenesis in the sulfate-reducing zone of surface sediments traversing the Peruvian margin. Biogeosciences 13:283–299.
- Martens CS, Berner RA (1977) Interstitial water chemistry of anoxic Long Island Sound sediments 1. Dissolved-gases. Limnol Oceanogr 22:10–25.
- Martens CS, Berner RA (1974) Methane production in the interstitial waters of sulfate-depleted marine sediments. Science (80-) 185:1167–1169.
- McGarigal K, Cushman S, Stafford S (2000) Multivariate statistics for wildlife and ecology research. New York, New York, USA: Springer.
- McInerney MJ, Bryant MP, Pfennig N (1979) Anaerobic bacterium that degrades fatty acids in syntrophic association with methanogens. Arch Microbiol 122:129–135.
- McInerney MJ, Bryant MP, Hespell RB, Costerton JW (1981) *Syntrophomonas wolfei* gen. nov. sp. nov., an anaerobic, syntrophic, fatty acid-oxidizing bacterium. Appl Environ Microbiol 41:1029–39.
- McInerney MJ, Bryant MP (1981) Anaerobic degradation of lactate by syntrophic associations of *Methanosarcina barkeri* and *Desulfovibrio* species and effect of H₂ on acetate degradation. Appl Environ Microbiol 41:346–354.

- McInerney MJ, Beaty PS (1988) Anaerobic community structure from a nonequilibrium thermodynamic perspective. *Can J Microbiol* 34:487–493.
- McInerney MJ, Stams AJM, Boone DR (2005) Genus *Syntrophobacter*. In: Bergey's Manual of Systematic Bacteriology, second edition, vol 2. Staley JT, Boone DR, Brenner DJ, de Vos P, Garrity GM, Goodfellow M, Krieg NR, Rainey FA, Schleifer KH (eds). Springer, New York pp 1021–1027.
- McInerney MJ, Rohlin L, Mouttaki H, Kim U, Krupp RS, Rios-Hernandez L, Sieber J, Struchtemeyer CG, Bhattacharyya A, Campbell JW, Gunsalus RP (2007) The genome of *Syntrophus aciditrophicus*: Life at the thermodynamic limit of microbial growth. *Proc Natl Acad Sci USA* 104:7600–7605.
- McInerney MJ, Struchtemeyer CG, Sieber J, Mouttaki H, Stams AJM, Schink B, Rohlin L, Gunsalus RP (2008) Physiology, ecology, phylogeny, and genomics of microorganisms capable of syntrophic metabolism. *Ann NY Acad Sci* 1125: 58–72.
- McInerney MJ, Sieber JR, Gunsalus RP (2009) Syntrophy in anaerobic global carbon cycles. *Curr Opin Biotechnol* 20: 623–32.
- Millero FJ, Schreiber DR (1982) Use of the ion pairing model to estimate activity coefficients of the ionic components of natural waters. *Am. J. Sci.* 282:1508–1540.
- Mino S, Kudo H, Arai T, Sawabe T, Takai K, Nakagawa S (2014) *Sulfurovum aggregans* sp. nov., a hydrogen-oxidizing, thiosulfate-reducing chemolithoautotroph within the *Epsilonproteobacteria* isolated from a deep-sea hydrothermal vent chimney, and an emended description of the genus *Sulfurovum*. *Int J Syst Evol Microbiol* 64:3195–3201.
- Mitterer RM (2010) Methanogenesis and sulfate reduction in marine sediments: a new model. *Earth Planet Sci Lett* 295:358–366.
- Moore EK, Hopmans EC, Rijpstra WIC, Villanueva L, Sinninghe Damsté JS (2016) Elucidation and identification of amino acid containing membrane lipids using liquid chromatography/high-resolution mass spectrometry. *Rapid Commun Mass Spectrom* 30:739–750.
- Moore EK, Hopmans EC, Rijpstra WIC, Sánchez-Andrea I, Villanueva L, Wienk H, Schoutsen F, Stams AJM, Sinninghe Damsté JS (2015a) Lysine and novel hydroxylysine lipids in soil bacteria: amino acid membrane lipid response to temperature and pH in *Pseudopedobacter saltans*. *Front Microbiol* 6:637.
- Moore EK, Villanueva L, Hopmans EC, Rijpstra WIC, Mets A, Dedysh SN, Sinninghe Damsté JS (2015b) Abundant trimethylornithine lipids and specific gene sequences are indicative of Planctomycete importance at the oxic/anoxic interface in *Sphagnum*-dominated northern wetlands. *Appl Environ Microbiol* 81:6333–6344.
- Moore EK, Hopmans EC, Rijpstra WIC, Villanueva L, Dedysh SN, Kulichevskaya IS, Wienk H, Schoutsen F, Sinninghe Damsté JS (2013) Novel mono-, di-, and trimethylornithine membrane lipids in northern wetland Planctomycetes. *Appl Environ Microbiol* 79:6874–6884.

- Mori K, Iino T, Suzuki KI, Yamaguchi K, Kamagata Y (2012) Aceticlastic and NaCl-requiring methanogen "*Methanosaeta pelagica*" sp. nov., isolated from marine tidal flat sediment. *Appl Environ Microbiol* 78:3416–3423.
- Morris BEL, Henneberger R, Huber H, Moissl-Eichinger C (2013) Microbial syntrophy: interaction for the common good. *FEMS Microbiol Rev* 37:384–406.
- Mountfort DO, Asher RA (1979) Effect of inorganic sulfide on the growth and metabolism of *Methanosarcina barkeri* strain DM. *Appl Environ Microbiol* 37:670–675.
- Mountfort DO, Asher RA (1981) Role of sulfate reduction versus methanogenesis in terminal carbon flow in polluted intertidal sediment of Waimea Inlet, Nelson, New Zealand. *Appl Environ Microbiol* 42:252–258.
- Müller N, Schleheck D, Schink B (2009) Involvement of NADH:acceptor oxidoreductase and butyryl coenzymeA dehydrogenase in reversed electron transport during syntrophic butyrate oxidation by *Syntrophomonas wolfei*. *J Bacteriol* 191:6167–6177.
- Müller N, Worm P, Schink B, Stams AJM, Plugge CM (2010) Syntrophic butyrate and propionate oxidation processes: from genomes to reaction mechanisms. *Environ Microbiol Rep* 2:489–499.
- Murray JW, Grundmanis V, Smethie WM (1978) Interstitial water chemistry in the sediments of Saanich Inlet. *Geochim Cosmochim Acta* 42:1011–1026.
- Muyzer G, de Waal EC, Uitterlinden AG (1993) Profiling of complex microbial populations by denaturing gradient gel electrophoresis analysis of polymerase chain reaction-amplified genes coding for 16S rRNA. *Appl Environ Microbiol* 59: 695–700.
- Muyzer G, Stams AJM (2008) The ecology and biotechnology of sulphate-reducing bacteria. *Nat Rev Microbiol* 6:441–454.
- Nauhaus K, Boetius a, Kruger M, Widdel F (2002) In vitro demonstration of anaerobic oxidation of methane coupled to sulphate reduction in sediment from a marine gas hydrate area. *Environ Microbiol* 4:296–305.
- Nauhaus K, Treude T, Boetius A, Krüger M (2005) Environmental regulation of the anaerobic oxidation of methane: a comparison of ANME-I and ANME-II communities. *Environ Microbiol* 7:98–106.
- Niemann H, Losekann T, de Beer D, Elvert M, Nadalig T, Knittel K, Amann R, Sauter EJ, Schluter M, Klages M, Foucher JP, Boetius A (2006) Novel microbial communities of the Haakon Mosby mud volcano and their role as a methane sink. *Nature* 443:854–858.
- Nübel U, Engelen B, Felske A, Snaird J, Wieshuber A, Amann RI, Ludwig W, Backhaus H (1996) Sequence heterogeneities of genes encoding 16S rRNAs in *Paenibacillus polymyxa* detected by temperature gradient gel electrophoresis. *J Bacteriol* 178:5636–5643.

- O'Flaherty V, Mahony T, O'Kennedy R, Colleran E (1998) Effect of pH on growth kinetics and sulphide toxicity thresholds of a range of methanogenic, syntrophic and sulphate-reducing bacteria. *Process Biochem* 33:555–569.
- O'Sullivan LA, Sass AM, Webster G, Fry JC, Parkes RJ, Weightman AJ (2013) Contrasting relationships between biogeochemistry and prokaryotic diversity depth profiles along an estuarine sediment gradient. *FEMS Microbiol Ecol* 85:143–157.
- Oremland RS, Taylor BF (1978) Sulfate reduction and methanogenesis in marine sediments. *Geochim Cosmochim Acta* 42:209–214.
- Oremland RS, Marsh L, DesMarais DJ (1982a) Methanogenesis in Big Soda Lake, Nevada: an alkaline, moderately hypersaline desert lake. *Appl Environ Microbiol* 43:462–468.
- Oremland RS, Marsh LM, Polcin S (1982b) Methane production and simultaneous sulphate reduction in anoxic, salt marsh sediments. *Nature* 296:143–145.
- Oremland RS, Polcin S (1982) Methanogenesis and sulfate reduction: competitive and noncompetitive substrates in estuarine sediments. *Appl Environ Microbiol* 44:1270–1276.
- Oremland RS, Miller LG, Whiticar MJ (1987) Sources and flux of natural gasses from Mono Lake, California. *Geochim Cosmochim Acta* 51:2915–2929.
- Oremland RS, Whiticar MJ, Strohmaier FE, Kiene RP (1988) Bacterial ethane formation from reduced, ethylated sulfur compounds in anoxic sediments. *Geochim Cosmochim Acta* 52:1895–1904.
- Oude Elferink SJWH, Visser A, Hulshoff Pol LW, Stams AJM (1994) Sulfate reduction in methanogenic bioreactors. *FEMS Microbiol Rev* 15:119–136.
- Oude Elferink SJWH, Vorstman WJC, Sopjes A, Stams AJM (1998) Characterization of the sulfate-reducing and syntrophic population in granular sludge from a full-scale anaerobic reactor treating papermill wastewater. *FEMS Microbiol Ecol* 27:185–194.
- Ozuolmez D, Na H, Lever MA, Kjeldsen KU, Jørgensen BB, Plugge CM (2015) Methanogenic archaea and sulfate reducing bacteria co-cultured on acetate: teamwork or coexistence? *Front Microbiol* 6:1–12.
- Park S, Kim S, Jung YT, Park JM, Yoon JH (2016) *Confluentibacter lentus* gen. nov., sp. nov., isolated from the junction between the ocean and a freshwater lake. *Int J Syst Evol Microbiol* 66:868–873.
- Parkes RJ, Gibson GR, Mueller-Harvey I, Buckingham WJ, Herbert RA (1989) Determination of the substrates for sulphate-reducing bacteria within marine and estuarine sediments with different rates of sulphate reduction. *J Gen Microbiol* 135:175–187.

- Parkes RJ, Cragg BA, Fry JC, Herbert RA, Wimpenny JWT, Allen JA, Whitfield M (1990) Bacterial biomass and activity in deep sediment layers from the Peru Margin. *Philos Trans R Soc London Ser A, Math Phys Sci* 331:139–153.
- Parkes RJ, Webster G, Cragg BA, Weightman AJ, Newberry CJ, Ferdelman TG, Kallmeyer J, Jørgensen BB, Aiello IW, Fry JC (2005) Deep sub-seafloor prokaryotes stimulated at interfaces over geological time. *Nature* 436:390–394.
- Parkes RJ, Cragg BA, Banning N, Brock F, Webster G, Fry JC, Hornibrook E, Pancost RD, Kelly S, Knab N, Jørgensen BB, Rinna J, Weightman AJ (2007) Biogeochemistry and biodiversity of methane cycling in subsurface marine sediments (Skagerrak, Denmark). *Environ Microbiol* 9:1146–1161.
- Parkes RJ, Cragg B, Roussel E, Webster G, Weightman A, Sass H (2014) A review of prokaryotic populations and processes in sub-seafloor sediments, including biosphere:geosphere interactions. *Mar Geol* 352:409–425.
- Pender S, Toomey M, Carton M, Eardly D, Patching JW, Collieran E, O'Flaherty V (2004) Long-term effects of operating temperature and sulphate addition on the methanogenic community structure of anaerobic hybrid reactors. *Water Res* 38:619–630.
- Phelps TJ, Conrad R, Zeikus JG (1985) Sulfate-dependent interspecies H₂ transfer between *Methanosarcina barkeri* and *Desulfovibrio vulgaris* during coculture metabolism of acetate or methanol. *Appl Environ Microbiol* 50:589–594.
- Pidwirny M (2012) Carbon cycle. In: Encyclopedia of Earth. Gullledge J (ed) (Washington D.C., Environmental information coalition, national council for science and the environment). http://editors.eol.org/eoearth/wiki/Carbon_cycle
- Plugge CM, Jiang B, de Bok FAM, Tsai C, Stams AJM (2009) Effect of tungsten and molybdenum on growth of a syntrophic coculture of *Syntrophobacter fumaroxidans* and *Methanospirillum hungatei*. *Arch Microbiol* 191:55–61.
- Plugge CM, Zhang W, Scholten JCM, Stams AJM (2011) Metabolic flexibility of sulfate-reducing bacteria. *Front Microbiol* 2:81.
- Plugge CM, Balk M, Stams AJM (2002) *Desulfotomaculum thermobenzoicum* subsp. *thermosyntrophicum* subsp. nov., a thermophilic, syntrophic, propionate-oxidizing, spore-forming bacterium. *Int J Syst Evol Micr* 52:391–399.
- Pruesse E, Quast C, Knittel K, Fuchs BM, Ludwig W, Peplies J, Glöckner FO (2007) SILVA: a comprehensive online resource for quality checked and aligned ribosomal RNA sequence data compatible with ARB. *Nucleic Acids Res* 35:7188–7196.
- Qiu YL, Sekiguchi Y, Hanada S, Imachi H, Tseng I-C, Cheng S-S, Ohashi A, Harada H, Kamagata Y (2006) *Pelotomaculum terephthalicum* sp. nov. and *Pelotomaculum isophthalicum* sp. nov.:

- two anaerobic bacteria that degrade phthalate isomers in syntrophic association with hydrogenotrophic methanogens. *Arch Microbiol* 185:172–182.
- Quast C, Pruesse E, Yilmaz P, Gerken J, Schweer T, Yarza P, Peplies J, Glöckner FO (2013) The SILVA ribosomal RNA gene database project: improved data processing and web-based tools. *Nucleic Acids Res* 41:590–596.
- Rabus R, Hansen TA Widdel F (2013) Dissimilatory sulfate- and sulfur-reducing prokaryotes. In: *The Prokaryotes – Prokaryotic Physiology and Biochemistry*. Rosenberg E, DeLong EF, Lory S, Stackebrandt E, Thompson F (eds). Springer-Verlag Heidelberg, Berlin pp 309–404.
- Ramiro-Garcia J, Hermes GDA, Giatsis C, Sipkema D, Zoetendal EG, Schaap PJ, Smidt H (2016) NG-Tax, a highly accurate and validated pipeline for analysis of 16S rRNA amplicons from complex biomes. *F1000Research* 5:1791.
- Raskin L, Rittmann BE, Stahl DA (1996) Competition and coexistence of sulfate-reducing and methanogenic populations in anaerobic biofilms. *Appl Environ Microbiol* 62:3847–3857.
- Rasmussen H, Jørgensen BB (1992) Microelectrode studies of seasonal oxygen uptake in a coastal sediment: Role of molecular diffusion. *Mar Ecol Prog Ser* 81:289–303.
- Rebac S, Visser A, Gerbens S, van Lier JB, Stams AJM, Lettinga G (1996) The Effect of sulphate on propionate and butyrate degradation in a psychrophilic anaerobic expanded granular sludge bed (EGSB) reactor. *Environ Technol* 17:997–1005.
- Reeburgh WS (1980) Anaerobic methane oxidation: rate depth distributions in Skan Bay sediments. *Earth Planet Sci Lett* 47:345–352.
- Reeburgh, W.S., Heggie, D.T. (1977) Microbial methane consumption reactions and their effects on methane distributions on freshwater and marine environments. *Limnol Oceanogr* 22: 1–9.
- Roest K, Heilig HGHJ, Smidt H, de Vos WM, Stams AJM, Akkermans ADL (2005) Community analysis of a full-scale anaerobic bioreactor treating paper mill wastewater. *Syst Appl Microbiol* 28:175–185.
- Romesser JA, Wolfe RS, Mayer F, Spiess E, Walther-Mauruschat A (1979) *Methanogenium*, a new genus of marine methanogenic bacteria and characterization of *Methanogenium cariaci* sp. nov. and *Methanogenium marisnigri* sp. nov. *Arch Microbiol* 121:147–153.
- Rossel PE, Elvert M, Ramette A, Boetius A, Hinrichs KU (2011) Factors controlling the distribution of anaerobic methanotrophic communities in marine environments: evidence from intact polar membrane lipids. *Geochim Cosmochim Acta* 75:164–184.
- Rossel PE, Lipp JS, Fredricks HF, Arnds J, Boetius A, Elvert M, Hinrichs KU (2008) Intact polar lipids of anaerobic methanotrophic archaea and associated bacteria. *Org Geochem* 39:992–999.

- Rotaru A-E, Shrestha PM, Liu F, Shrestha M, Shrestha D, Embree M, Zengler K, Wardman C, Nevin KP, Lovley DR (2014) A new model for electron flow during anaerobic digestion: direct interspecies electron transfer to *Methanosaeta* for the reduction of carbon dioxide to methane. *Energy Environ Sci* 7:408–415.
- Roussel EG, Cragg BA, Webster G, Sass H, Tang X, Williams AS, Gorra R, Weightman AJ, Parkes RJ (2015) Complex coupled metabolic and prokaryotic community responses to increasing temperatures in anaerobic marine sediments: critical temperatures and substrate changes. *FEMS Microbiol Ecol* 91:1–16.
- Roussel EG, Sauvadet A-L, Allard J, Chaduteau C, Richard P, Bonavita M-AC, Chaumillon E (2009) Archaeal methane cycling communities associated with gassy subsurface sediments of Marennes-Oléron Bay (France). *Geomicrobiol J* 26:31–43.
- Roy F, Samain E, Dubourguier HC, Albagnac G (1986) *Synthrophomonas sapovorans* sp. nov., a new obligately proton reducing anaerobe oxidizing saturated and unsaturated long chain fatty acids. *Arch Microbiol* 145:142–147.
- Rütters H, Sass H, Cypionka H, Rullkötter J (2002a) Phospholipid analysis as a tool to study complex microbial communities in marine sediments. *J Microbiol Methods* 48:149–160.
- Rütters H, Sass H, Cypionka H, Rullkötter J (2002b) Microbial communities in a Wadden Sea sediment core - clues from analyses of intact glyceride lipids, and related fatty acids. *Org Geochem* 33:803–816.
- Sahm K, MacGregor BJ, Jørgensen BB, Stahl DA (1999) Sulphate reduction and vertical distribution of sulphate-reducing bacteria quantified by rRNA slot-blot hybridization in a coastal marine sediment. *Environ Microbiol* 1:65–74.
- Sanguinetti CJ, Dias Neto E, Simpson AJG (1994) Rapid silver staining and recovery of PCR products separated on polyacrylamide gels. *Biotechniques* 17:915–919.
- Schink B (1997) Energetics of syntrophic cooperation in methanogenic degradation. *Microbiol Mol Biol Rev* 61:262–280.
- Schink B, Stams AJM (2013) Syntrophism among prokaryotes. In: The Prokaryotes. Rosenberg E, DeLong EF, Lory S, Stackebrandt E, Thompson F (eds) Springer Berlin-Heidelberg Verlag, Berlin pp 309–335.
- Schippers A, Kock D, Höft C, Köweker G, Siegert M (2012) Quantification of microbial communities in subsurface marine sediments of the Black Sea and off Namibia. *Front Microbiol* 3:1–11.
- Schirawski J, Uden G (1998) Menaquinone-dependent succinate dehydrogenase of bacteria catalyzes reversed electron transport driven by the proton potential. *Eur J Biochem* 257:210–215.

- Schnurer A, Schink B, Svensson BH (1996) *Clostridium ultunense* sp. nov., a mesophilic bacterium oxidizing acetate in syntrophic association with a hydrogenotrophic methanogenic bacterium. *Int J Syst Bacteriol* 46:1145–1152.
- Schönheit P, Kristjansson JK, Thauer RK (1982) Kinetic mechanism for the ability of sulfate reducers to out-compete methanogens for acetate. *Arch Microbiol* 132:285–288.
- Schouten S, Hopmans EC, Pancost RD, Sinninghe Damste JS (2000) Widespread occurrence of structurally diverse tetraether membrane lipids: Evidence for the ubiquitous presence of low-temperature relatives of hyperthermophiles. *Proc Natl Acad Sci* 97:14421–14426.
- Schubotz F, Wakeham SG, Lipp JS, Fredricks HF, Hinrichs KU (2009) Detection of microbial biomass by intact polar membrane lipid analysis in the water column and surface sediments of the Black Sea. *Environ Microbiol* 11:2720–2734.
- Schubotz, F (2005) Investigation of intact polar lipids of bacteria isolated from deep marine subsurface (MSc Thesis. University of Bremen, Bremen, Germany).
- Schut GJ, Adams MWW (2009) The iron-hydrogenase of *Thermotoga maritima* utilizes ferredoxin and NADH synergistically: a new perspective on anaerobic hydrogen production. *J Bacteriol* 191:4451–4457.
- Sekiguchi Y, Kamagata Y, Nakamura K, Ohashi A, Harada H (2000) *Syntrophothermus lipocalidus* gen. nov., sp. nov., a novel thermophilic, syntrophic, fatty-acid-oxidizing anaerobe which utilizes isobutyrate. *Int J Syst Evol Micro* 50:771–779.
- Senior E, Lindström EB, Banat IM, Nedwell DB (1982) Sulfate reduction and methanogenesis in the sediment of a saltmarsh on the East coast of the United Kingdom. *Appl Environ Microbiol* 43:987–996.
- Shaw DG, McIntosh DJ (1990) Acetate in recent anoxic sediments: direct and indirect measurements of concentration and turnover rates. *Estuar Coast Shelf Sci* 31:775–788.
- Shimada H, Nemoto N, Shida Y, Oshima T, Yamagishi A (2008) Effects of pH and temperature on the composition of polar lipids in *Thermoplasma acidophilum* HO-62. *J Bacteriol* 190:5404–5411.
- Shimizu S, Ueno A, Naganuma T, Kaneko K (2015) *Methanosarcina subterranea* sp. nov., a methanogenic archaeon isolated from a deep subsurface diatomaceous shale formation. *Int J Syst Evol Microbiol* 65:1167–1171.
- Shin HS, Jung JY, Bae BU, Paik BC (1995) Phase-separated anaerobic toxicity assays for sulfate and sulfide. *Water Environ Res* 67:802–806.
- Shock EL, Helgeson HC (1990) Calculation of the thermodynamic and transport properties of aqueous species at high pressures and temperatures: standard partial molal properties of organic species. *Geochim Cosmochim Acta* 54:915–945.

- Shock EL, Sassani DC, Willis M, Sverjensky DA (1997) Inorganic species in geologic fluids: correlations among standard molal thermodynamic properties of aqueous ions and hydroxide complexes. *Geochim Cosmochim Acta* 61:907-950.
- Sieber JR, Le HM, McInerney MJ (2014) The importance of hydrogen and formate transfer for syntrophic fatty, aromatic and alicyclic metabolism. *Environ Microbiol* 16:177-188.
- Sieber JR, McInerney MJ, Gunsalus RP (2012) Genomic insights into syntrophy: the paradigm for anaerobic metabolic cooperation. *Annu Rev Microbiol* 66:429-452.
- Sieber JR, Sims DR, Han C, Kim E, Lykidis A, Lapidus AL, McDonnald E, Rohlin L, Culley DE, Gunsalus R, McInerney MJ (2010) The genome of *Syntrophomonas wolfei*: new insights into syntrophic metabolism and biohydrogen production. *Environ Microbiol* 12:2289-2301.
- Singh H, Du J, Ngo HTT, Won KH, Kim KY, Yi TH (2015) *Pedobacter edaphicus* sp. nov. isolated from forest soil in South Korea. *Arch Microbiol* 197:781-787.
- Skillman LC, Evans PN, Naylor GE, Morvan B, Jarvis GN, Joblin KN (2004) 16S ribosomal DNA-directed PCR primers for ruminal methanogens and identification of methanogens colonising young lambs. *Anaerobe* 10:277-285.
- Smith KS, Ingram-Smith C (2007) *Methanosaeta*, the forgotten methanogen? *Trends Microbiol* 15:150-155.
- Sohlenkamp C, López-Lara IM, Geiger O (2003) Biosynthesis of phosphatidylcholine in bacteria. *Prog Lipid Res* 42:115-162.
- Song J, Choi A, Im M, Joung Y, Yoshizawa S, Cho JC, Kogure K (2015) *Aurantivirga profunda* gen. nov., sp nov., isolated from deep-seawater, a novel member of the family *Flavobacteriaceae*. *Int J Syst Evol Micro* 65:144-149.
- Sørensen J, Christensen D, Jørgensen BB (1981) Volatile fatty acids and hydrogen as substrates for sulfate-reducing bacteria in anaerobic marine sediment. *Appl Environ Microbiol* 42:5-11.
- Sousa DZ, Smidt H, Alves MM, Stams AJM (2007a) *Syntrophomonas zehnderi* sp. nov., an anaerobe that degrades long-chain fatty acids in co-culture with *Methanobacterium formicicum*. *Int J Syst Evol Microbiol* 57:609-615.
- Sousa DZ, Pereira MA, Smidt H, Stams AJM, Alves MM (2007b) Molecular assessment of complex microbial communities degrading long chain fatty acids in methanogenic bioreactors. *FEMS Microbiol Ecol* 60:252-265.
- Sousa DZ, Alves JI, Alves MM, Smidt H, Stams AJM (2009) Effect of sulfate on methanogenic communities that degrade unsaturated and saturated long-chain fatty acids (LCFA). *Environ Microbiol* 11:68-80.

- Stackebrandt E (2014) The emended family *Peptococcaceae* and description of the families *Desulfitobacteriaceae*, *Desulfotomaculaceae*, and *Thermincolaceae*. In: The Prokaryotes. Rosenberg E, DeLong EF, Lory S, Stackebrandt E, Thompson F (eds). Springer-Verlag Heidelberg, Berlin pp 285-290.
- Stams AJM, Grolle KCF, Frijters CTM, Van Lier JB (1992) Enrichment of thermophilic propionate-oxidizing bacteria in syntrophy with *Methanobacterium thermoautotrophicum* or *Methanobacterium thermoformicum*. Appl Environ Microbiol 58:346-352.
- Stams AJM, Van Dijk JB, Dijkema C, Plugge CM (1993) Growth of syntrophic propionate-oxidizing bacteria with fumarate in the absence of methanogenic bacteria. Appl Environ Microbiol 59:1114-1119.
- Stams AJM (1994) Metabolic interactions between anaerobic bacteria in methanogenic environments. Antonie Van Leeuwenhoek 66:271-294.
- Stams AJM, Oude Elferink SWJH, Westermann P (2003) Metabolic interactions between methanogenic consortia and anaerobic respiring bacteria. In: Biomethanation I. T Scheper (eds.) Springer Berlin Heidelberg pp 31-56.
- Stams AJM, Plugge CM, de Bok FAM, van Houten BHGW, Lens P, Dijkman H, Weijma J (2005) Metabolic interactions in methanogenic and sulfate-reducing bioreactors. Water Sci Technol 52:13-20.
- Stams AJM, Plugge CM (2009) Electron transfer in syntrophic communities of anaerobic bacteria and archaea. Nat Rev Microbiol 7:568-577.
- Starke R, Keller A, Jehmlich N, Vogt C, Richnow HH, Kleinstaub S, von Bergen M, Seifert J (2016) Pulsed $^{13}\text{C}_2$ -acetate protein-SIP unveils *Epsilonproteobacteria* as dominant acetate utilizers in a sulfate-reducing microbial community mineralizing benzene. Microb Ecol 71:901-911.
- Stieb M, Schink B (1985) Anaerobic oxidation of fatty acids by *Clostridium bryantii* sp. nov., a spore-forming, obligately syntrophic bacterium. Arch Microbiol 140:387-390.
- Struchtemeyer CG, Elshahed MS, Duncan KE, McInerney MJ (2005) Evidence for aceticlastic methanogenesis in the presence of sulfate in a gas condensate-contaminated aquifer. Appl Environ Microbiol 71:5348-5353.
- Struchtemeyer CG, Duncan KE, McInerney MJ (2011) Evidence for syntrophic butyrate metabolism under sulfate-reducing conditions in a hydrocarbon-contaminated aquifer. FEMS Microbiol Ecol 76:289-300.
- Sturt HF, Summons RE, Smith K, Elvert M, Hinrichs K-U (2004) Intact polar membrane lipids in prokaryotes and sediments deciphered by high-performance liquid chromatography/electrospray ionization multistage mass spectrometry—new biomarkers for biogeochemistry and microbial ecology. Rapid Commun Mass Spectrom 18:617-628.

- Suess E (1980) Particulate organic carbon flux in the oceans-surface productivity and oxygen utilization. *Nature* 288:260–263.
- Sultan N, Garziglia S, Ruffine L (2016) New insights into the transport processes controlling the sulfate-methane-transition-zone near methane vents. *Sci Rep* 6:26701.
- Summers ZM, Fogarty HE, Leang C, Franks AE, Malvankar NS, Lovley DR (2010) Direct exchange of electrons within aggregates of an evolved syntrophic coculture of anaerobic bacteria. *Science* 330:1413–1415.
- Svetlitschny V, Rainey F, Wiegel J (1996) *Thermosyntropho lipolytica* gen. nov., sp. nov., a lipolytic, anaerobic, alkalitolerant, thermophilic bacterium utilizing short-and long-chain fatty acids in syntrophic coculture with a methanogenic archaeum. *Int J Syst Evol Micr* 46(4): 1131–1137.
- Syvitski JPM, Vorosmarty CJ, Kettner AJ, Green P (2005) Impact of humans on the flux of terrestrial sediment to the global coastal ocean. *Science* 308: 376–380.
- Szewzyk R, Pfennig N (1987) Complete oxidation of catechol by the strictly anaerobic sulfate-reducing *Desulfobacterium catecholicum* sp. nov. *Arch Microbiol* 147:163–168.
- Takahashi T, Feely R a, Weiss RF, Wanninkhof RH, Chipman DW, Sutherland SC, Takahashi TT (1997) Global air-sea flux of CO₂: an estimate based on measurements of sea-air pCO₂ difference. *Proc Natl Acad Sci U S A* 94:8292–8299.
- Takai K, Horikoshi K (2000) Rapid detection and quantification of members of the archaeal community by quantitative PCR using fluorogenic probes. *Appl Environ Microbiol* 66:5066–5072.
- Talaue-McManus L (2010) Examining human impacts on global biogeochemical cycling via the coastal zone and ocean margins. In: Carbon and nutrient fluxes in continental margins: A global synthesis. Liu KK, Atkinson L, Quinones R, Talaue-McManus L (eds) Springer-Verlag Berlin Heidelberg pp 497–514.
- Teske AP (2006) Microbial community composition in deep marine subsurface sediments of ODP Leg 201: sequencing surveys and cultivations. In: Proc Ocean Drill Prog, Sci Res. Jørgensen BB, D'Hondt SL, Miller DJ (eds). Ocean Drilling Program, College Station, TX. 201: 1–19.
- Teske A, Sørensen KB (2008) Uncultured archaea in deep marine subsurface sediments: have we caught them all? *ISME J* 2:3–18.
- Thamdrup B, Rossello-Mora R, Amann R (2000) Microbial manganese and sulfate reduction in Black Sea shelf sediments. *Appl Environ Microbiol* 66:2888–2897.
- Thauer RK, Jungermann K, Decker K (1977) Energy conservation in chemotrophic anaerobic bacteria. *Bacteriol Rev* 41:100–180.
- Thomsen T (2001) Biogeochemical and molecular signatures of anaerobic methane oxidation in a marine sediment. *Appl Environ Microbiol* 67:1646–1656.

- Thomsen TR, Finster K, Ramsing NB (2001) Biogeochemical and molecular signatures of anaerobic methane oxidation in a marine sediment. *Appl Environ Microbiol* 67(4): 1646-1656.
- Timmers PHA, Widjaja-Greefkes HCA, Ramiro-Garcia J, Plugge CM, Stams AJM (2015) Growth and activity of ANME clades with different sulfate and sulfide concentrations in the presence of methane. *Front Microbiol*.
- Timmers PH, Suarez-Zuluaga DA, van Rossem M, Diender M, Stams AJM, Plugge CM (2016) Anaerobic oxidation of methane associated with sulfate reduction in a natural freshwater gas source. *ISME J* 10:1400–1412.
- Ulrich AC, Edwards EA (2003) Physiological and molecular characterization of anaerobic benzene-degrading mixed cultures. *Environ Microbiol* 5(2): 92-102.
- Valentine DL, Blanton DC, Reeburgh WS (2000) Hydrogen production by methanogens under low-hydrogen conditions. *Arch Microbiol* 174:415–421.
- van den Bogert B, de Vos WM, Zoetendal EG, Kleerebezem M (2011) Microarray analysis and barcoded pyrosequencing provide consistent microbial profiles depending on the source of human intestinal samples. *Appl Environ Microbiol* 77:2071–2080.
- van Kuijk BLM, Stams AJM (1996) Purification and characterization of malate dehydrogenase from the syntrophic propionate-oxidizing bacterium strain MPOB. *FEMS Microbiol Lett* 144:141–144.
- van Kuijk BLM, Stams AJM (1995) Sulfate reduction by a syntrophic propionate-oxidizing bacterium. *Antonie van Leeuwenhoek* 68:293–296.
- van Mooy BAS, Fredricks HF, Pedler BE, Dyhrman ST, Karl DM, Koblížek M, Lomas MW, Mincer TJ, Moore LR, Moutin T, Rappé MS, Webb EA (2009) Phytoplankton in the ocean use non-phosphorus lipids in response to phosphorus scarcity. *Nature* 458:69–72.
- Vences-Guzmán MÁ, Guan Z, Ormeño-Orrillo E, González-Silva N, López-Lara IM, Martínez-Romero E, Geiger O, Sohlenkamp C (2011) Hydroxylated ornithine lipids increase stress tolerance in *Rhizobium tropici* CIAT899. *Mol Microbiol* 79:1496–1514.
- Viggi C, Rossetti S, Fazi S, Paiano P, Majone M, Aulenta F (2014) Magnetite particles triggering a faster and more robust syntrophic pathway of methanogenic propionate degradation. *Environ Sci Technol* 48(13): 7536-7543.
- Vigneron A, Cruaud P, Pignet P, Caprais JC, Gayet N, Cambon-Bonavita MA, Godfroy A, Toffin L (2014) Bacterial communities and syntrophic associations involved in anaerobic oxidation of methane process of the sonora margin cold seeps, Guaymas basin. *Environ Microbiol* 16:2777–2790.

- Visser PT, Baumgartner LK, Buckley DH, Rogers DR, Hogan ME, Raleigh CD, Turk KA, Des Marais DJ (2003) Dimethyl sulphide and methanethiol formation in microbial mats: potential pathways for biogenic signatures. *Environ Microbiol* 5:296–308.
- Visser A, Beeksmma I, van der Zee F, Stams AJM, Lettinga G (1993) Anaerobic degradation of volatile fatty acids at different sulphate concentrations. *Appl Microbiol Biotechnol* 40(4): 549–556.
- Wagman DD, Evans WH, Parker VB, Schumm RH, Halow I, Bailey SM, Churney KL, Nuttall RL (1982) The NBS tables of chemical thermodynamic properties: selected values for inorganic and C₁ and C₂ organic substances in SI units. *J. Phys. Chem. Ref. Data* 11:392.
- Wagner M, Loy A, Klein M, Lee N, Ramsing NB, Stahl DA, Friedrich MW (2005) Functional marker genes for identification of sulfate-reducing prokaryotes. *Methods Enzymol* 397:469–489.
- Wallrabenstein C, Hauschild E, Schink B (1994) Pure culture and cytological properties of ‘*Syntrophobacter wolinii*’. *FEMS Microbiol Lett* 123:249–254.
- Wallrabenstein C, Hauschild E, Schink B (1995) *Syntrophobacter pfennigii* sp. nov., new syntrophically propionate-oxidizing anaerobe growing in pure culture with propionate and sulfate. *Arch Microbiol* 164:346–352.
- Wang G, Spivack AJ, D’Hondt S (2010) Gibbs energies of reaction and microbial mutualism in anaerobic deep seafloor sediments of ODP Site 1226. *Geochim Cosmochim Acta* 74:3938–3947.
- Wang XC, Lee C (1995) Decomposition of aliphatic amines and amino acids in anoxic salt marsh sediment. *Geochim Cosmochim Acta* 59:1787–1797.
- Wang Y, Wang H, Liu JW, Lai QL, Shao ZZ, Austin B, Zhang XH (2010) *Aestuariusbacter aggregatus* sp. nov., a moderately halophilic bacterium isolated from seawater of the Yellow Sea. *FEMS Microbiol Lett* 309:48–54.
- Wang Y, Zhou CY, Ming H, Kang J, Chen HL, Jing CQ, Feng H, Chang Y, Guo Z, Wang L (2016) *Pseudofulvibacter marinus* sp. nov., isolated from seawater. *Int J Syst Evol Microbiol* 66:1301–1305.
- Wang Y, Qian PY (2009) Conservative fragments in bacterial 16S rRNA genes and primer design for 16S ribosomal DNA amplicons in metagenomic studies. *PLoS One* 4(10): p.e7401.
- Ward DM, Winfrey MR (1985) Interactions between methanogenic and sulfate-reducing bacteria in sediments. In: *Advances in microbial ecology*. Jannasch HW and Williams PJL (eds.) Plenum Press, New York pp 219–286.
- Webster G, Parkes RJ, Fry JC, Weightman J, Weightman AJ (2004) Widespread occurrence of a novel division of bacteria identified by 16S rRNA gene sequences originally found in deep marine sediments. *Appl Environ Microbiol* 70:5708–5713.

- Webster G, Parkes RJ, Cragg BA, Newberry CJ, Weightman AJ, Fry JC (2006) Prokaryotic community composition and biogeochemical processes in deep seafloor sediments from the Peru Margin. *FEMS Microbiol Ecol* 58(1): 65-85.
- Webster G, Blazejak A, Cragg BA, Schippers A, Sass H, Rinna J, Tang X, Mathes F, Ferdelman TG, Fry JC, Weightman AJ, Parkes RJ (2009) Subsurface microbiology and biogeochemistry of a deep, cold-water carbonate mound from the Porcupine Seabight (IODP Expedition 307). *Environ Microbiol* 11:239-257.
- Webster G, Rinna J, Roussel EG, Fry JC, Weightman AJ, Parkes RJ (2010) Prokaryotic functional diversity in different biogeochemical depth zones in tidal sediments of the Severn Estuary, UK, revealed by stable-isotope probing. *FEMS Microbiol Ecol* 72:179-197.
- Webster G, Sass H, Cragg BA, Gorra R, Knab NJ, Green CJ, Mathes F, Fry JC, Weightman AJ, Parkes RJ (2011) Enrichment and cultivation of prokaryotes associated with the sulphate-methane transition zone of diffusion-controlled sediments of Aarhus Bay, Denmark, under heterotrophic conditions. *FEMS Microbiol Ecol* 77:248-263.
- Wellsbury P, Mather I, Parkes RJ (2002) Geomicrobiology of deep, low organic carbon sediments in the Woodlark Basin, Pacific Ocean. *FEMS Microbiol Ecol* 42:59-70.
- Wellsbury P, Parkes RJ (1995) Acetate bioavailability and turnover in an estuarine sediment. *FEMS Microbiol Ecol* 17:85-94.
- Weng CY, Chen SC, Lai MC, Wu SY, Lin S, Yang TF, Chen PC (2015) *Methanoculleus taiwanensis* sp. nov., a methanogen isolated from deep marine sediment at the deformation front area near Taiwan. *Int J Syst Evol Microbiol* 65:1044-1049.
- Weston NB, Joye SB (2005) Temperature-driven decoupling of key phases of organic matter degradation in marine sediments. *Proc Natl Acad Sci U S A* 102:17036-17040.
- White DC, Davis WM, Nickels JS, King JD, Bobbie RJ (1979) Determination of the sedimentary microbial biomass by extractible lipid phosphate. *Oecologia* 40:51-62.
- Whiticar MJ (1999) Carbon and hydrogen isotope systematics of bacterial formation and oxidation of methane. *Chem Geol* 161:291-314.
- Widdel F (1980) Anaerober Abbau von Fettsäuren und Benzoesäure durch neu isolierte Arten sulfatreduzierender Bakterien. Thesis, Göttingen Univ.
- Widdel F (1988) Microbiology and ecology of sulfate- and sulfur-reducing bacteria. In: *Biology of Anaerobic Microorganisms*. Zehnder AJB (ed). John Wiley and Sons Inc. New York pp 469-585.
- Widdel F, Bak F (1992) Gram-negative mesophilic sulfate-reducing bacteria. In: *The prokaryotes. A handbook on the biology of bacteria: ecophysiology, isolation, identification, applications*. 2nd

- edn. Balows A, Truper HG, Dworkin M, Harder W, Schleifer K-H (eds) Springer Verlag, New York, USA pp 3353–3378.
- Wilms R, Sass H, Köpke B, Cypionka H, Engelen B (2007) Methane and sulfate profiles within the subsurface of a tidal flat are reflected by the distribution of sulfate-reducing bacteria and methanogenic archaea. *FEMS Microbiol Ecol* 59:611–621.
- Winderl C, Anneser B, Griebler C, Meckenstock RU, Lueders T (2008) Depth-resolved quantification of anaerobic toluene degraders and aquifer microbial community patterns in distinct redox zones of a tar oil contaminant plume. *Appl Environ Microbiol* 74:792–801.
- Winfrey MR, Zeikus JG (1977) Effect of sulfate on carbon and electron flow during microbial methanogenesis in freshwater sediments. *Appl Environ Microbiol* 33:275–281.
- Wofford NQ, Beaty PS, McInerney MJ (1986) Preparation of cell-free-extracts and the enzymes involved in fatty acid metabolism in *Syntrophomonas wolfei*. *J Bacteriol* 167:179–185.
- Worm P, Stams AJM, Cheng X, Plugge CM (2011) Growth- and substrate-dependent transcription of formate dehydrogenase and hydrogenase coding genes in *Syntrophobacter fumaroxidans* and *Methanospirillum hungatei*. *Microbiology* 157:280–289.
- Wu C, Dong X, Liu X (2007) *Syntrophomonas wolfei* subsp. *methylbutyratica* subsp. nov., and assignment of *Syntrophomonas wolfei* subsp. *saponavida* to *Syntrophomonas saponavida* sp. nov. comb. nov. *Syst Appl Microbiol* 30:376–380.
- Wu C, Liu X, Dong X (2006a) *Syntrophomonas cellicola* sp. nov., a spore-forming syntrophic bacterium isolated from a distilled-spirit-fermenting cellar, and assignment of *Syntrophospora bryantii* to *Syntrophomonas bryantii* comb. nov. *Int J Syst Evol Microbiol* 56:2331–2335.
- Wu C, Liu X, Dong X (2006b) *Syntrophomonas erecta* subsp. *sporosyntropha* subsp. nov., a spore-forming bacterium that degrades short chain fatty acids in co-culture with methanogens. *Syst Appl Microbiol* 29:457–462.
- Yamada T, Sekiguchi Y (2009) Cultivation of uncultured *Chloroflexi* subphyla: significance and ecophysiology of formerly uncultured *Chloroflexi* “subphylum I” with natural and biotechnological relevance. *Microbes Environ* 24:205–216.
- Yarza P, Yilmaz P, Pruesse E, Glöckner FO, Ludwig W, Schleifer K-H, Whitman WB, Euzéby J, Amann R, Rosselló-Móra R (2014) Uniting the classification of cultured and uncultured bacteria and archaea using 16S rRNA gene sequences. *Nat Rev Microbiol* 12:635–645.
- Yim KJ, Cha I-T, Whon TW, Lee H-W, Song HS, Kim K-N, Nam Y-D, Lee S-J, Bae J-W, Rhee S-K, Choi J-S, Seo M-J, Roh SW, Kim D (2014) *Halococcus sediminicola* sp. nov., an extremely halophilic archaeon isolated from a marine sediment. *Antonie Van Leeuwenhoek* 105:73–79.
- Yoon J, Kasai H (2016) *Wenyngzhuangia aestuarii* sp. nov., a marine bacterium of the family *Flavobacteriaceae* isolated from an estuary. *Curr Microbiol* 72:397–403.

- Yu Y, Lee C, Kim J, Hwang S (2005) Group-specific primer and probe sets to detect methanogenic communities using quantitative real-time polymerase chain reaction. *Biotechnol Bioeng* 89:670–679.
- Yu ZT, García-González R, Schanbacher FL, Morrison M (2008) Evaluations of different hypervariable regions of archaeal 16S rRNA genes in profiling of methanogens by Archaea-specific PCR and denaturing gradient gel electrophoresis. *Appl Environ Microbiol* 74:889–893.
- Zhang C, Liu X, Dong X (2004) *Syntrophomonas curvata* sp. nov., an anaerobe that degrades fatty acids in co-culture with methanogens. *Int J Syst Evol Microbiol* 54:969–973.
- Zhang C, Liu X, Dong X (2005) *Syntrophomonas erecta* sp. nov., a novel anaerobe that syntrophically degrades short-chain fatty acids. *Int J Syst Evol Microbiol* 55:799–803.
- Zhang T, Ke SZ, Liu Y, Fang HP (2005) Microbial characteristics of a methanogenic phenol-degrading sludge. *Water Sci Technol* 52:73–78.
- Zhao H, Yang D, Woese CR, Bryant MP (1990) Assignment of *Clostridium bryantii* to *Syntrophospora bryantii* gen. nov., comb. nov. on the basis of a 16S rRNA sequence analysis of its crotonate-grown pure culture. *Int J Syst Evol Micr* 40:40–44.
- Zhao H, Yang D, Woese CR, Bryant MP (1993) Assignment of fatty acid- β -oxidizing syntrophic bacteria to *Syntrophomonadaceae* fam. nov. on the basis of 16S rRNA sequence analyses. *Int J Syst Bacteriol* 43:278–286.
- Zhao H, Yang D, Woese CR, Bryant MP (1990) Assignment of *Clostridium bryantii* to *Syntrophospora bryantii* gen. nov., com. nov. on the basis of a 16S rRNA sequence analysis of its crotonate-grown pure culture. *Int J Syst Bacteriol* 40: 40–44.
- Zinder SH, Koch M (1984) Non-aceticlastic methanogenesis from acetate: acetate oxidation by a thermophilic syntrophic coculture. *Arch Microbiol* 138:263–272.

Summary

Propionate, butyrate, acetate, hydrogen and formate are the major intermediates of organic matter degradation. Sulfate-reducing bacteria (SRB) contribute significantly to the consumption of these substrates in sulfate-rich marine sediments. In sulfate-depleted sediments, however, complete degradation of propionate or butyrate is only possible via syntrophic cooperation of acetogenic bacteria and methanogenic archaea. Despite that the predominance of SRB in sulfate-rich and methanogens in sulfate-depleted sediments was reported, recent studies showed that both types of microorganism could be present in upper and lower parts of marine sediments. In this thesis, propionate and butyrate conversions and the involved microbial community in sulfate, sulfate-methane transition and methane zone sediment of Aarhus Bay, Denmark were studied using sediment slurry incubations. Interspecies hydrogen transfer and coexistence during acetate degradation were investigated in mixed pure cultures.

In **Chapter 2**, interspecies hydrogen transfer between aceticlastic *Methanosaeta concilii* and hydrogenotrophic microorganisms, *Desulfovibrio vulgaris* or *Methanococcus maripaludis*, was investigated. Additionally, coexistence of *M. concilii* and *Desulfobacter latus* growing on acetate under sulfidogenic conditions was studied. The results of **Chapter 2** showed that *D. vulgaris* could reduce sulfate and grow on leaked hydrogen from *M. concilii*. Hydrogen leakage from *M. concilii* provides an explanation for biogeochemical zonation both for competitive (e.g. acetate) and non-competitive substrates (methyl compounds), and this indicates the possible coexistence of SRB and methanogens in sulfate-rich environments.

In **chapter 3 and 4**, long term incubations were examined focusing on butyrate and propionate conversion and the microbial community dynamics in sediment slurry enrichments at different sulfate (0, 3 and 20 mM) concentrations and incubation temperatures (10°C and 25°C). Sulfate reduction is the dominant process for butyrate and propionate conversion in Aarhus Bay sediments. In the absence of sulfate, both propionate and butyrate can be converted efficiently, indicating the presence of syntrophic communities throughout the sediment. The fluctuating methane concentrations and the enrichment of anaerobic methanotrophic archaea (ANME) in butyrate and propionate slurries at 10°C suggest the occurrence of anaerobic oxidation of methane (AOM) in sulfate-methane transition zone (SMTZ) of Aarhus Bay.

The microbial community involved in butyrate and propionate conversion was investigated using next generation sequencing (NGS) 16S rRNA amplicon sequencing. The enriched sulfate-reducing bacteria at high sulfate concentration (20 mM) were different when butyrate and

propionate were used as substrate: *Desulfosarcina* and *Desulfobacterium* dominate the butyrate-converting slurries (**Chapter 3**), whereas *Desulfosarcina*, *Desulfobulbus* and *Desulforhopalus* are the main SRB in propionate-converting slurries (**Chapter 4**). The increase in the relative abundance of *Desulfobacteraceae* and *Desulfobulbaceae* in SZ, SMTZ and MZ sediment slurries suggests the presence of sulfate reducers throughout the anoxic sediment column. In the absence of sulfate, *Syntrophomonas* and *Cryptanaerobacter* become dominant which suggests their role in syntrophic butyrate and propionate conversion, respectively. These results were further supported in **Chapter 6**. The increase in the relative abundance of *Syntrophomonas* in the presence of sulfate (**Chapter 3**) and some members of *Desulfobacteraceae* (**Chapter 4**) in the absence of sulfate shows the metabolic flexibility of the microorganisms at different sulfate concentrations. Temperature has an impact on the microbial community (**Chapter 4**) and IPL composition (**Chapter 5**) in enrichment slurries. *Cryptanaerobacter* is dominant at 25°C, and, *Desulfobacteraceae* (*Desulfobulbus*), especially *Desulfobulbaceae* members (*Desulfobulbus*, *Desulforhopalus*) become dominant at 10°C at 0 and 3 mM sulfate concentrations in propionate-amended enrichment slurries. In butyrate-amended slurries, *Clostridiales* have higher relative abundance at 10°C regardless of the sulfate concentration and the sediment depth which supports important role of *Clostridiales* in butyrate conversion in marine sediments. Archaeal community analyses revealed the dominance of hydrogenotrophic methanogens belonging to *Methanomicrobiales* in both butyrate- and propionate-converting slurries (**Chapter 3 and 4**) and enrichment cultures (**Chapter 6**) regardless of the sediment depth, the incubation temperature and the presence of sulfate, which indicate that they are the main syntrophic partners of butyrate and propionate degraders. The other syntrophic partner organisms are the acetoclastic methanogenic families: *Methanosarcinaceae* and *Methanosaetaeaceae*. The presence of methane-oxidizing archaea (ANME-1b) in low temperature SMTZ slurries together with *Desulfobacteraceae* (**Chapter 3 and 4**) suggests the occurrence of anaerobic oxidation of methane (AOM) in SMTZ of Aarhus Bay.

In conclusion, this thesis confirms the presence and activity of methanogens in sulfate-rich, and SRB in sulfate-depleted marine sediments and their involvement in butyrate, propionate and acetate conversion. Novel bacterial and archaeal members enriched in the sediment slurries are likely involved in propionate, butyrate and acetate conversions at different depths of marine sediments in addition to known the cultured species.

Samenvatting

Propionaat, butyraat, acetaat, waterstof en formiaat zijn de voornaamste tussenproducten van afbraak van organisch materiaal. Sulfaat reducerende bacteriën (SRB) dragen significant bij aan de consumptie van deze substraten in sulfaat-rijke marine sedimenten. Echter, in sulfaat-arme sedimenten is complete afbraak van propionaat en butyraat alleen mogelijk via syntrofe interactie met acetogene bacteriën of methanogene archaea. Ondanks dat literatuur de dominantie van SRB in sulfaat-rijke, en methanogenen in sulfaat-arme sedimenten beschrijft, tonen recente studies aan dat beide typen micro-organismen aanwezig zijn in beide soorten sediment. In deze thesis worden propionaat en butyraat omzetting en de daarbij betrokken microbiële groepen in sulfaat-rijke zone (SZ), sulfaat-arme zone (MZ) en de sulfaat-methaan transitie zone (SMTZ) in het sediment van de Baai van Aarhus, Denemarken besproken aan de hand van sediment slurrie incubaties. Uitwisseling van waterstof en samenleving van micro-organismen gedurende acetaat afbraak zijn onderzocht gebruikmakende van gemixte pure cultures.

In **hoofdstuk 2** wordt waterstof overdracht tussen de aceticlastische methanogeen *Methanosaeta concilii* en hydrotrofe microorganismen, *Desulfovibrio vulgaris* of *Methanococcus maripaludis* besproken. Ook de samenwerking tussen *M. concilii* en *Desulfobacter latus* groeiend op acetaat in sulfaat reducerende condities is bestudeerd. De resultaten van **hoofdstuk 2** laten zien dat *D. vulgaris* sulfaat kan reduceren en groeien met waterstof gelect uit *M. concilii*. Waterstof lekkage van *M. concilii* kan verklaren waarom er biogeochemisch een zonatie is van competitieve (b.v. acetaat) en niet-competitieve (b.v. gemethyleerde stoffen) substraten, en geeft indicatie dat SRB en methanogenen mogelijk samenleven in sulfaat-rijke omgeving.

In **hoofdstuk 3 en 4** worden lange termijn incubaties besproken met focus op butyraat en propionaat omzetting, en de populatie dynamiek daarachter, bij sediment incubaties met verschillende sulfaat concentraties (0, 3 en 20 mM) en incubatie temperatuur (10 °C en 20 °C). Sulfaatreductie is het overheersende proces voor butyraat en propionaat omzetting in sedimenten van de Baai van Aarhus. In afwezigheid van sulfaat worden beide substraten efficiënt omgezet, wat aangeeft dat er syntrofe groepen aanwezig zijn in het sediment. Fluctuerende gehalten van methaan en de verrijking van anaerobe methaan oxiderende archaea (ANME) gedurende butyraat en propionaat omzetting bij 10 °C suggereren dat er anaerobe oxidatie van methaan (AOM) plaatsvindt in de sulfaat-methaan transitie zone van de Baai van Aarhus.

De microben betrokken bij butyraat en propionaat omzetting zijn bestudeerd met next-generation sequencing (NGS) van het 16S rRNA amplicon. De verrijkte sulfaat-reducerende bacteriën bij hoge sulfaat concentraties (20 mM) verschilden wanneer butyraat of propionaat werden gebruikt als substraat. *Desulfosarcina* en *Desulfobacterium* domineerde de butyraat-consumerende slurries (**hoofdstuk 3**), terwijl *Desulfosarcina*, *Desulfobulbus* en *Desulforhopalus* de voornaamste SRB zijn in propionaat-verbruikende slurries (**Hoofdstuk 4**). De toename in relatieve aanwezigheid van *Desulfobacteraceae* en *Desulfobulbaceae* in de SZ, SMTZ en MZ sediment incubaties suggereert de aanwezigheid van sulfaat reduceerders door de gehele anoxische sediment kolom. In de afwezigheid van sulfaat worden *Syntrophomonas* en *Cryptanaerobacter* de dominante organismen, wat hun syntrofe rol in respectievelijk butyraat en propionaat omzetting suggereert. Deze resultaten zijn verder onderbouwt in **Hoofdstuk 6**. De toename in relatieve aanwezigheid van *Syntrophomonas* in de aanwezigheid van sulfaat (**Hoofdstuk 3**) en sommige leden van de *Desulfobacteraceae* (**hoofdstuk 4**) in afwezigheid van sulfaat laat de metabole flexibiliteit van micro-organismen bij verschillende sulfaat concentraties zien.

Temperatuur had effect op de samenstelling (**hoofdstuk 4**) en IPL compositie (**hoofdstuk 5**) van de microbiële groepen in de incubaties. *Cryptanaerobacter* is dominant bij 25 graden Celsius. *Desulfobacteraceae* (*Desulfobulbus*), vooral *Desulfobulbaceae* (*Desulfobulbus*, *Desulforhopalus*), worden dominant bij 10 graden Celsius bij 0 en 3 mM sulfaat in propionaat-verrijkte slurries. In incubaties met butyraat zijn *Clostridiales* relatief meer aanwezig bij 10 °C ongeacht de sulfaatconcentratie en de sedimentdiepte, wat de belangrijke rol van *Clostridiales* in butyraat omzetting in marine sedimenten benadrukt. Analyse op de samenstelling van Archaea liet de dominatie zien van hydrogenotrofe methanogenen behorend tot de *Methanomicrobiales* in zowel butyraat en propionaat omzettende incubaties (**hoofdstuk 3 en 4**) als in verrijkte cultures (**hoofdstuk 6**) ongeacht sedimentdiepte, incubatietemperatuur en aanwezigheid van sulfaat. Dit geeft aan dat zij de voornaamste syntrofe partners zijn van butyraat en propionaat afbrekende micro-organismen. Andere syntrofe partner organismen zijn de aceticlastische methanogene families: *Methanosarcinaceae* en de *Methanosaetaeaceae*. De aanwezigheid van methaan-oxiderende archaea (ANME-1b) bij lage temperatuur SMTZ incubaties, samen met de aanwezigheid van *Desulfobacteraceae* (**hoofdstuk 3 en 4**), suggereren dat anaerobe oxidatie van methaan in SMTZ van de Baai van Aarhus plaatsvindt.

Deze thesis bevestigt de aanwezigheid en activiteit van methanogenen in sulfaat-rijke, en SRB in de sulfaat-arme marine sedimenten; en hun betrokkenheid bij butyraat, propionaat en acetaat omzetting. Nieuwe bacteriële en archaea soorten zijn opgehoopt in de sediment slurrie incubaties en zijn waarschijnlijk betrokken bij propionaat, butyraat en acetaat omzetting in verschillende dieptes van het marine sedimenten en zijn een additie aan de al bekende soorten.

Author affiliations

Alfons J. M. Stams, Caroline M. Plugge, M. Cristina Gagliano, Daan van Vliet, Derya Ozuolmez

Laboratory of Microbiology, Wageningen University & Research, Stippeneng 4, 6708 WE Wageningen, The Netherlands.

Alfons J. M. Stams

Centre for Biological Engineering, University of Minho, Braga, Portugal

Hyunsoo Na

Division of Microbial Ecology, Department of Microbiology and Ecosystem Science, University of Vienna, Vienna, Austria.

Mark A. Lever

Institute of Biogeochemistry and Pollutant Dynamics, Department of Environmental Sciences, Eidgenössische Technische Hochschule Zurich, Zürich, Switzerland.

Kasper U. Kjeldsen, Bo Barker Jørgensen

Center for Geomicrobiology, Department of Bioscience, Aarhus University, Ny Munkegade 114-116, DK-8000 Aarhus, Denmark.

Eli K. Moore

School of Environmental and Biological sciences, Department of Marine and Coastal Sciences, 71 Dudley Rd, New Brunswick, NJ 08901, USA.

Ellen C. Hopmans, Jaap S. Sinninghe Damsté

Royal Netherlands Institute for Sea Research (NIOZ), Department of Marine Organic Biogeochemistry, 1790 AB Den Burg, Texel, The Netherlands

Jaap S. Sinninghe Damsté

Utrecht University, Faculty of Geosciences, 3584 CD, Utrecht, The Netherlands

Acknowledgements

My PhD journey lasted longer than expected, but each and every day was full of memories and experiences which contributed to me to be 'myself'. Not only happy, exciting, cheerful, but also sad, disappointing, difficult moments had to be experienced to grow up. Those times were meaningful when shared with people who helped, encouraged, inspired and gave peace. I would like to thank all those who helped me complete my role in this journey.

First I would like to thank my promoter Fons and co-promoter Caroline. Caroline, thanks for believing in me, encouraging me to reach my goals, reminding me that I have the power to achieve them and teaching to be more critical. I appreciate your all-time availability, help, support, advices. I enjoyed our long meetings with discussions about the thesis as well as life. Fons, I appreciate your modesty while having an extensive scientific knowledge, your availability for discussions, constructive criticism, guidance and positivity. Our first interview was so much fun and joyful. I don't think I will have such kind of positive interview ever in my life. I am very much grateful to you for giving me the opportunity to be a PhD student in your research group.

I would like to thank everyone I collaborated with. Hyunsoo, it has been a great pleasure to meet and work with you. We were lucky to have chance to work together at our laboratory on our project for a month. Thanks for your positive attitude, friendship and contribution to my thesis. Mark and Kasper, I was lucky having you as collaborators of one of the most difficult part of my thesis. Your quick and valuable feedback, advices, guidance for practical and writing part of our paper added so much to my knowledge and writing skills. I also appreciate your help before, during and after our sampling cruise. It was impossible to have such a smooth sampling cruise without your guidance and help. Bo Barker Jørgensen, I am pleased to meet and learned from you. Thanks for your support along our collaboration. Eli, thanks for being such a nice person to work with and for your significant help with lipid analysis and chapter. Jaap Sinninghe Damsté, thanks for your support and feedback for the chapter we worked on. Jan Gerritse, thank you for helping me with hydrogen measurements at Deltares.

I had the chance to participate in Hopkins Microbiology Course at Hopkins Marine Station of Stanford University, California. I am so grateful first to my co-promoter Caroline for pioneering me to apply for the course and to Alfred Spormann, Chris Francis and Paul Rainey for giving me the opportunity, not only once but twice. The four weeks I spent in Monterey added so much exciting

experiences to my PhD journey, teaching me so many new things about marine microbiology. I am happy to have met all the people involved in and participated to this course.

Anja and Carolien, thanks for your enormous help in administrative part of my thesis, always answering my questions and being so kind. Ton, many thanks for your valuable technical help and cheerful chats in the lab. My journey has been very smooth and joyful with your help in the lab. Wim, thank you for your availability and help for all the practical problem in and around the lab.

I would like to thank all my former and current colleagues for the nice and pleasant environment. Many thanks to Ahmad, Ana, Anna, Audrey, Catalina, Cristina, Daan, Detmer, Diana, Edze, Florian, Gerben, Gianina, Irene, Jing, Joana, Juanan, Jueeli, Lara, Marjet, Martin, Martijn, Mauricio, Michael, Monika, Monir, Naiara, Naim, Nam, Nico, Nikolas, Odette, Oylum, Peer, Petra, Pierpaolo, Rozelin, Siavash, Sidnei, Susakul, Teun, Teresita, Thomas, Tian, Vicente, Yuan. I am happy having each of you as colleagues and friends. Thank you for all the funny, philosophical and scientific chats we had along the years! Patrick, I am grateful to have you as Master's student. Thanks for everything.

Samet, any word would be insufficient to express my pleasure to have you as a friend more than a colleague throughout years. I enjoyed not only our lunch/coffee breaks and Dreijen trips that were full of fun chats but also our concept dinners where we discussed the meaning of life. Even your presence meant too much to me, as I knew one day our PhD journeys would come to an end. I learned a lot from you about life and science. I appreciate every bit of time we spent together. Thanks very much for all your help and your true friendship!

Maria, although I met you later in time and could not spend much time together in the lab, you became one of my dearests! Your positivity and sweetest smiles always made me talk to you about anything and this has built a great friendship between us. I thank you not only for being such a great friend to me but also for being the first music teacher of my precious daughter, caring, loving her. I feel so lucky having you around me and my family, and hope we share joyful moments for long years as very good friends.

Cristina, you have joined MicFys when I just need! It was very nice to meet you, have your cheerful voice around and thanks very much for your great help and contribution to my thesis! Hope to keep in touch.

Rozelin, my dear pinky, you were my first friend in Wageningen! What a relief and happiness it was when I met you on my first day in the lab. You have been a good guide while I need a lot of help

Appendices

and advice in the very first months. Later, we spend so much lovely time, chats both in the lab and at your place in Wageningen. Thanks for your warm friendship!

Ana, Joana, my time with you was full of laughter. I really enjoyed having you as colleagues. Thanks for making our time unforgettable. Nam, it was so nice to have long and relieving chats with you, especially about family life and PhD issues. Oylum, I enjoyed preparing and giving practical courses with you and sharing nice moments during our PhD trip. Your positive and calm attitude always made me feel good, which in turn brought a smile on my face. Monika, you crazy girl! I admire your energy, positivity, laughs. Hope you keep it up! Martijn, thanks so much for helping me out with the preparation of the Dutch summary! Susakul, Teresita, you always cheered me up with your warm smiles and joyful chats. Teresita, I hear you calling me 'Mamaaa!'.

Many thanks to my office mates Martin, Teun, Samet, Monika, Sidnei, Florian for turning our working environment into peaceful, funny, cheerful atmosphere. I appreciate your company and joyful chats! Martin, Peer thanks for joining me for sampling cruise in Aarhus. I appreciate your help especially when I was seasick! Ana, Michael, Peer it was a lot of fun to organize the Sense symposium with you. Thanks for sharing the experience with me.

Benim canim ailem, annem babam abilerim, büyük ve kosulsuz sevginizi ve desteginizi kendimi bildim bileli hissettim. Bana hep inandiniz, mutlu olmam için elinizden gelen herseyi yaptınız. Bana kattığınız hersey için, sonsuz sevginiz ve desteginiz için minnettarım! Sizi çok seviyorum, iyi ki varsınız! İzmir'deki güzel ailem, ailem olduğunuz için oyle sansliyim ki! Bana olan sevginizi, desteginizi ve inancinizi hep hissettim. Hersey için çok teşekkürler!

Mia Luna'm, bebegim, birgun ansizin cikageldin, hosgeldin! Senin gelisinle hersey o kadar degisti ki... Bir ogrenciydim, anne oldum; seni buyuturken ben de buyudum. Senden alip, teze ayirdigim vakitler için uzgunum. Bu hayatta edindigim en güzel, en saf, en derin tecrube oldun. Su yasima kadar ogrenemedigim seyleri ogrettin, biliyorum, daha çok sey ogreteceksin. Seni çok seviyorum!

Kivanc, esim, yol arkadasim, bu uzun ve zorlu yola girmemi en az benim kadar istedin, bu surecte hep yanımdaydin, hep destek oldun! Bugun bu yolun sonuna geldiysem senin de emeginle, yardiminla, sevginledir. Yazma sureci boylesi yavas ve zorken gosterdigin hosgoru, yarattigin huzurlu ev ortamı, yaptigin nefis yemekler, verdigin tavsiyeler ve sonsuz sevgin için minnettarım! İyi ki varsin. Seni çok seviyoruz!

About the author

Derya Ozuolmez was born on January 20th, 1984 in Famagusta, Cyprus. She studied Biology at Gazi University, Ankara between 2001 and 2005. After receiving her BSc degree, she started her MSc study at the Department of Fundamental and Industrial Microbiology, Istanbul University. Within the scope of her MSc thesis research, she enriched for and isolated sulfate reducing bacteria from several cooling towers' water and investigated their impact on microbial corrosion of galvanized steel structures using lab-scale systems. She pursued her MSc internship at the Biotechnology Department of Delft University of Technology, Netherlands. After she obtained her MSc degree in 2009, she moved to the Netherlands and worked for 6 months as researcher at the same laboratory as she did her internship. Thereafter, she joined the Microbial Physiology group at the Laboratory of Microbiology of Wageningen University. During her PhD, she studied acetate, propionate and butyrate converting microorganisms in marine anoxic sediments. The work was done under the supervision of Dr Caroline M. Plugge and Prof. Dr Fons Stams and the results of the PhD research are presented in this thesis.



List of Publications

Ozuolmez, D., Na, H., Lever, M.A., Kjeldsen, K.U., Jørgensen, B.B. and Plugge, C.M. (2015) Methanogenic archaea and sulfate reducing bacteria co-cultured on acetate: teamwork or coexistence?. *Front Microbiol*, 6(492): 1-12.

Ozuolmez D., Stams A.J.M., Plugge C.M. Butyrate degradation by sulfate-reducing and methanogenic communities in anoxic sediments of Aarhus Bay, Denmark (In preparation).

Ozuolmez D., Stams A.J.M., Plugge C.M. Propionate conversion under sulfidogenic and methanogenic conditions in different biogeochemical zones of Aarhus Bay, Denmark (In preparation).

Ozuolmez D., Gagliano M.C., van Vliet D., Plugge C.M. Physiological and molecular characterization of anaerobic marine propionate- and butyrate-converting syntrophic cultures (In preparation).

Ilhan-Sungur, E., **Ozuolmez, D.**, Çotuk, A., Cansever, N. and Muyzer, G., 2017. Isolation of a sulfide-producing bacterial consortium from cooling-tower water: Evaluation of corrosive effects on galvanized steel. *Anaerobe*, 43: 27-34.

Ozuolmez, D. and Çotuk, A., 2011. Biofilm formation on galvanized steel by SRB isolate obtained from cooling tower water. *IUFS Journal of Biology*, 70(2): 35-42.



*Netherlands Research School for the
Socio-Economic and Natural Sciences of the Environment*

D I P L O M A

For specialised PhD training

The Netherlands Research School for the
Socio-Economic and Natural Sciences of the Environment
(SENSE) declares that

Derya Özüölmez

born on 20 January 1984 in Famagusta, Cyprus

has successfully fulfilled all requirements of the
Educational Programme of SENSE.

Wageningen, 12 September 2017

the Chairman of the SENSE board

Prof. dr. Huub Rijnaarts

the SENSE Director of Education

Dr. Ad van Dommelen

The SENSE Research School has been accredited by the Royal Netherlands Academy of Arts and Sciences (KNAW)



K O N I N K L I J K E N E D E R L A N D S E
A K A D E M I E V A N W E T E N S C H A P P E N



The SENSE Research School declares that **Ms Derya Özüölmez** has successfully fulfilled all requirements of the Educational PhD Programme of SENSE with a work load of 40 EC, including the following activities:

SENSE PhD Courses

- o Environmental research in context (2011)
- o Principles of Ecological Genomics (2011)
- o Research in context activity: Co-organising SENSE Symposium 'Microbes for Sustainability' Wageningen (2012)

Other PhD and Advanced MSc Courses

- o Teaching and supervising thesis students, Wageningen University (2011)
- o Hopkins Microbiology Course, Stanford University (2012)
- o Scientific Writing, Wageningen University (2013)
- o Project and Time Management, Wageningen University (2014)
- o Career perspectives, Wageningen University (2014)
- o Mobilising your scientific network, Wageningen University (2014)
- o Basic training in ARB – a software environment for sequence data, Wageningen University (2014)

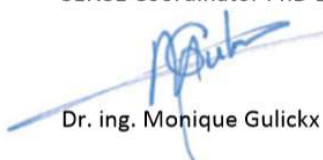
Management and Didactic Skills Training

- o Member of the SENSE PhD Council (2011-2012)
- o Assisting practicals of the BSc course 'Microbial physiology' (2011-2012)
- o Supervising internship of MSc student with thesis entitled 'Enrichment and isolation of butyrate degrading microbes from marine methanogenic sediments' (2013)
- o Assisting practicals of the MSc course 'Research methods microbiology' (2013-2014)

Oral Presentations

- o *Microbial interactions in marine anoxic sediments: competition or teamwork?* The Laboratory of Microbiology PhD trip 'Microbiology in China and Japan', 15 April - 1 May 2011, Beijing, China and Shanghai, Japan
- o *Butyrate conversion in marine sediments.* The Darwin Days: Annual Biogeoscience Conference – by the Darwin Center for Biogeosciences, 18 April 2013, Utrecht, The Netherlands
- o *Enrichment of propionate converting consortia from marine sediments.* The Darwin Days: Annual Biogeoscience Conference – by the Darwin Center for Biogeosciences, 20-21 November 2014, Noordwijkerhout, The Netherlands

SENSE Coordinator PhD Education



Dr. ing. Monique Gulickx

This research was supported by the Wimek Graduate School of Wageningen University & Research and Darwin Center for Biogeosciences, the Netherlands.

Cover design: Derya Özüölmez and Fenna Schaap

Thesis layout: Derya Özüölmez

Printed by: Proefschriftmaken.nl || Digiforce Vianen

Financial support from the Laboratory of Microbiology (Wageningen University) for printing this thesis is gratefully acknowledged.